



Universiteit
Leiden

The Netherlands

Travelling waves on trees and square lattices

Jukic, M.

Citation

Jukic, M. (2022, September 22). *Travelling waves on trees and square lattices*. Retrieved from <https://hdl.handle.net/1887/3463735>

Version: Publisher's Version

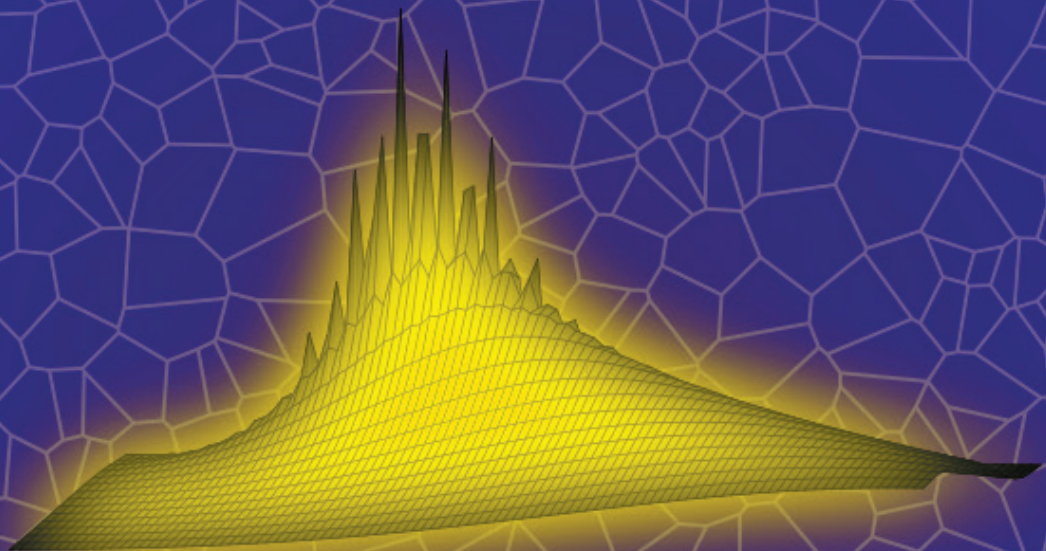
License: [Licence agreement concerning inclusion of doctoral thesis in the Institutional Repository of the University of Leiden](#)

Downloaded from: <https://hdl.handle.net/1887/3463735>

Note: To cite this publication please use the final published version (if applicable).

Travelling Waves on Trees and Square Lattices

Mia Jukić



Travelling Waves on Trees and Square Lattices

Proefschrift

ter verkrijging van
de graad van doctor aan de Universiteit Leiden,
op gezag van rector magnificus prof.dr.ir. H. Bijl,
volgens besluit van het college voor promoties
te verdedigen op donderdag 22 september 2022
klokke 13.45 uur

door

Mia Jukić
geboren te Zagreb, Kroatië
in 1993

Promotores:

Prof. dr. H.J. Hupkes

Prof. dr. A. Doelman

Promotiecommissie:

Prof. dr. F.A.J. de Haas

Prof. dr. R.M.H. Merks

Prof. dr. A. Scheel (University of Minnesota)

Prof. dr. A. Vainchtein (University of Pittsburgh)

Prof. dr. E.S. Van Vleck (University of Kansas)

Cover: © 2022 Mia Jukić

This research was funded by Netherlands Organization for Scientific Research (NWO) through the grant 639.032.612.

*To the loving memory of my father Tado,
Who first showed me the magic of numbers.*

CONTENTS

1	Introduction	5
1.1	Reaction equation	6
1.2	Diffusion equation	8
1.3	Travelling waves on \mathbb{R}	8
1.4	Travelling waves on lattice domains	10
1.5	Integer lattice \mathbb{Z}	11
1.5.1	Fundamental solution of the discrete heat equation	11
1.5.2	Wave-fronts on \mathbb{Z}	12
1.5.3	Pinning on lattices	13
1.6	Infinite k -ary trees	16
1.7	Two-dimensional lattice \mathbb{Z}^2	19
1.7.1	Stability of travelling waves on \mathbb{Z}^2	20
1.8	Graphs and lattices	21
1.8.1	Graph Laplacian	21
1.9	Overview of the thesis	23
2	Dynamics of curved travelling fronts for the discrete Allen-Cahn equation on a two-dimensional lattice	25
2.1	Introduction	25
2.2	Main results	35
2.2.1	Interface formation	36
2.2.2	Interface evolution	37
2.3	Omega limit points	38
2.4	Trapped entire solutions	43
2.5	Large time behaviour of u	46
2.5.1	Proof of Proposition 2.5.1 and Theorem 2.2.2	47
2.5.2	Phase asymptotics	50
2.6	Discrete heat equation	52
2.6.1	Discrete heat kernel	53
2.6.2	Gradient bounds	56
2.7	Construction of super- and sub-solutions	57
2.8	Phase approximation	63

2.8.1	Approximating γ by V	63
2.8.2	Tracking V with Γ	65
2.8.3	Proof of Theorem 2.2.3	69
2.9	Stability results	70
2.9.1	Spatial asymptotics	72
2.9.2	Phase asymptotics	74
3	Curvature-driven front propagation through planar lattices in oblique directions	77
3.1	Introduction	77
3.2	Main results	85
3.2.1	Travelling waves	86
3.2.2	Interface formation	92
3.2.3	Interface asymptotics	94
3.2.4	Numerical results	95
3.3	Omega limit points	98
3.3.1	Construction of ω	99
3.3.2	Trapped entire solutions	100
3.4	Large time behaviour of u	103
3.4.1	Phase construction	104
3.4.2	Phase asymptotics	106
3.5	Linearized phase evolution	107
3.5.1	Strategy	109
3.5.2	Contour deformation	113
3.5.3	Global and outer bounds	118
3.5.4	Core bounds	119
3.6	Phase approximation strategies	122
3.6.1	Coefficient identities	125
3.6.2	Quadratic comparisons	128
3.6.3	Cole-Hopf transformation	132
3.7	Construction of super- and sub-solutions	134
3.7.1	Preliminaries	135
3.7.2	Analysis of \mathcal{J}_Φ	136
3.7.3	Analysis of $\mathcal{J}_{p_\nu^\diamond}$	137
3.7.4	Analysis of $\mathcal{J}_{p_{\nu\nu'}^\diamond}$ and $\mathcal{J}_{q_{\nu\nu'}^\diamond}$	139
3.7.5	Final splitting	141
3.7.6	Proof of Proposition 3.7.1	145
3.8	Phase approximation and stability results	147
4	Propagation reversal for bistable differential equations on trees	149
4.1	Introduction	149
4.2	Main results	154
4.2.1	Cubic nonlinearity	159
4.3	Comparison principles	162
4.4	Pinned monotonic waves	163
4.5	Small d regime	165

4.6	Large d regime	169
4.6.1	Proof of Proposition 4.6.3	172
4.7	Cubic nonlinearity	173
4.7.1	Proof of Lemma 4.7.3	177
4.8	Spatial chaos	179
4.8.1	The Moser theorem	180
4.9	Numerics	184
Bibliography		186
Samenvatting		199
Acknowledgements		201
Curriculum Vitae		203

INTRODUCTION

In this thesis we study bistable reaction-diffusion equations on (multidimensional) lattice domains. The power of reaction-diffusion equations is that they can successfully model various natural and social phenomena with their intuitive and relatively simple (mathematical) representation. In mathematical notation, a lattice reaction-diffusion differential equation is any lattice differential equation (LDE) of the following form

$$\dot{u}_\mu(t) = d \underbrace{[\Delta u(t)]_\mu}_{\text{diffusion}} + \underbrace{g(u_\mu(t))}_{\text{reaction}}, \quad \mu \in \Lambda, \quad (1.0.1)$$

where $\Delta : \ell^\infty(\Lambda) \rightarrow \ell^\infty(\Lambda)$ represents a diffusion operator on a lattice $\Lambda \subset \mathbb{Z}^n$ and $d > 0$ is a diffusion constant. We call $g : \mathbb{R} \rightarrow \mathbb{R}$ the reaction function. One example of such a lattice differential equation on the integer lattice \mathbb{Z} is given by

$$\dot{u}_i(t) = u_{i-1}(t) - 2u_i(t) + u_{i+1}(t) + g(u_i(t)),$$

with $i \in \mathbb{Z}$ and $t \in \mathbb{R}$ or $t > 0$. Lattice equations are closely related to their continuous counterparts

$$u_t(x, t) = d\Delta_x u(x, t) + g(u(x, t)), \quad (1.0.2)$$

where x belongs to some open subset of \mathbb{R}^n and Δ_x is the standard Laplace operator on \mathbb{R}^n . One of the main features of reaction-diffusion equations, both on discrete and continuous domains, is that they admit special solutions, so-called ‘travelling waves’, which we can describe as fixed profiles $\Phi : \mathbb{R} \rightarrow \mathbb{R}$ that move in a particular direction with some speed c . Depending on their shape, we can roughly divide waves into three categories:

- pulses or solitons, which can be described as local perturbations 
- periodic pulses (wave trains) 
- monotone wave fronts that connect two constant states 

In this thesis we focus on the latter type of wave and we study their existence, propagation and long term behaviour on two type of discrete domains - the two-dimensional lattice \mathbb{Z}^2 , and infinite trees.

To guide the reader through the mechanism behind the formation of travelling waves, we will first take a separate look into the phenomena of reaction and diffusion to discover how they work together to form moving solutions. We will explain basic concepts on continuous domains and gradually extend them to the lattice domains treated in this thesis. By \dot{u} we always denote a time-derivative of the function u .

1.1 Reaction equation

In this section we explore various types of reaction equations and explain how do they influence the long-term behaviour of solutions $u(t)$ to (1.0.2) when $d = 0$. In the absence of diffusion, this PDE turns into a pure ODE and therefore we can drop the variable x .

Exponential growth, $g(u) = ru$

One of the simplest reaction equations is given by

$$\dot{u} = ru, \tag{1.1.1}$$

whose solution is given by $u(t) = Ce^{rt}$, for any $C \in \mathbb{R}$. For $C = 0$ we have an *equilibrium solution* $\bar{u} = 0$ that does not change in time.

For $r < 0$ we say that $\bar{u} = 0$ is a *stable* equilibrium since the solution $u(t)$ approaches \bar{u} as $t \rightarrow \infty$. For $r > 0$, $\bar{u} = 0$ is an *unstable* equilibrium since the solution $u(t)$ diverges away from \bar{u} as $t \rightarrow \infty$.

Logistic growth, $g(u) = ru(1 - u)$

The logistic growth equation was first proposed by Pierre-François Verhulst in [92] to model the population growth of the species u . Namely, provided that the growth rate and maximum capacity of the population are given by the positive constants r and K respectively, we have

$$\dot{u} = ru\left(1 - \frac{u}{K}\right). \tag{1.1.2}$$

In words, when the population u is very small, it grows exponentially with some rate $r > 0$, i.e., $\dot{u} \approx ru$. However, as it grows and reaches its maximum capacity K , its growth rate is approaching 0 and we have $\dot{u} \approx 0$. The explicit solution to this equation is given by

$$u(t) = \frac{K}{1 + (K/C - 1)e^{-rt}} \tag{1.1.3}$$

where $C > 0$ is the initial population number at time $t = 0$. This equation has two equilibrium points $\bar{u} = 0$ and $\bar{u} = K$, with the later being stable since the limit $\lim_{t \rightarrow \infty} u(t) = K$ holds.

The logistic growth equation has found numerous applications beyond population growth models. One example is the **SIS epidemiological model** [59] that models diseases like common cold or influenza that do not provide long-term immunity. Namely, individuals in a population are divided into two categories, I (infected) and S (susceptible). We assume that the population size is constant in time and equal to N , i.e., $I(t) + S(t) = N$ for all $t \geq 0$. Moreover, by $\beta > 0$ we denote the average number

of contacts between individuals, multiplied by the probability of a transmission in a contact. The recovery rate of infected individuals is given by γ . These assumptions lead to the following ODEs for I and S

$$\dot{I} = \frac{\beta S}{N}I - \gamma I, \quad \dot{S} = -\frac{\beta S}{N}I + \gamma I.$$

Together with our assumption $I + S = N$, and setting $R_0 := \frac{\beta}{\gamma}$ we arrive at

$$\dot{I} = \gamma(R_0 - 1)I\left(1 - \frac{I}{(1 - 1/R_0)N}\right),$$

which is of the same form as (1.1.2). If $R_0 > 1$, then the number of infected people will grow to

$$\lim_{t \rightarrow \infty} I(t) = \left(1 - \frac{1}{R_0}\right)N,$$

which one often refers to as the *herd immunity threshold*. For $R_0 < 1$, the point $\bar{I} = 0$ is a stable equilibrium since we have $\lim_{t \rightarrow \infty} I(t) = 0$ which implies that the disease is eradicated.

Bistable reaction, $g(u) = u(1 - u)(u - a)$

In many physical systems two stable equilibria compete for dominance. For example, in contrast to the logistic growth equation in which the population size always grows towards its carrying capacity, for some species undercrowding or a low density limits its growth and leads to extinction. This principle is called the Allee effect.

To model this effect, we assume that the maximum capacity is rescaled to 1 and that there exists a critical parameter $a \in (0, 1)$ such that $u < a$ implies that the population is dying out and $u > a$ implies that the population grows. Then the equation for the density $u(t)$ is given by

$$\dot{u} = u(1 - u)(u - a). \tag{1.1.4}$$

We have three equilibria $\bar{u} \in \{0, a, 1\}$, with 0 and 1 being the stable points, in the sense that $u(0) < a$ implies $\lim_{t \rightarrow \infty} u(t) = 0$ and $u(0) > a$ implies $\lim_{t \rightarrow \infty} u(t) = 1$. To justify this conclusion, it is enough to observe that $g(u) < 0$ for $u \in (0, a)$ and $g(u) > 0$ for $u \in (a, 1)$. Indeed, if $u(0) < a$, then we have $\dot{u}(t) < 0$ for small t and the population is decreasing towards 0. On the contrary, for $u(0) > a$, we have $\dot{u}(t) > 0$, which suggests that u is increasing towards 1.

We also point out that the cubic nonlinearity (1.1.4) is only one of the numerous possibilities for modelling bistable reaction effects. As its name suggests, a bistable reaction term can be any function that has two stable equilibria with one unstable equilibrium point a in between. This is equivalent to the following basic assumptions we use in all chapters of this thesis, namely

$$g(u) < 0, \text{ for } u \in (0, a), \quad g(u) > 0, \text{ for } u \in (a, 1),$$

with

$$g'(0) < 0, \quad g'(1) < 0, \quad g'(a) > 0.$$

To emphasize this dependence of the nonlinearity g on the bistable parameter a in the rest of this text we denote $g = g(\cdot; a)$.

1.2 Diffusion equation

In this section we study the equation (1.0.2) in the absence of reaction. For simplicity we take $d = 1$. The diffusion equation, more commonly known as the *heat equation* is one of the most studied partial differential equations. It takes the form

$$u_t(x, t) = \Delta_x u(x, t) \quad (1.2.1)$$

where $x \in \mathbb{R}^n$, $t > 0$ and Δ_x is the standard Laplace operator on \mathbb{R}^n , namely

$$\Delta_x u(x, t) = \sum_{i=1}^n u_{x_i x_i}(x, t).$$

Heat equation on \mathbb{R} In the case of only one spatial variable, the heat equation is simply

$$u_t(x, t) = u_{xx}(x, t), \quad x \in \mathbb{R}, t > 0. \quad (1.2.2)$$

Provided that we have $u(\cdot, 0) = u_0 \in L^\infty(\mathbb{R})$, an explicit formula for the solution $u(x, t)$ is readily available, namely

$$\begin{aligned} u(x, t) &= \frac{1}{\sqrt{4\pi t}} \int_{\mathbb{R}} e^{-\frac{(x-y)^2}{4t}} u_0(y) dy \\ &= [H(\cdot, t) * u_0](x). \end{aligned} \quad (1.2.3)$$

Here the function $H : \mathbb{R} \times (0, \infty) \rightarrow (0, \infty)$, defined by

$$H(x, t) = \frac{1}{\sqrt{4\pi t}} e^{-\frac{x^2}{4t}}$$

is called the *fundamental solution* or the *heat kernel*. Taking derivatives in (1.2.3), and evaluating them either on H or u_0 results in the estimate

$$\sup_{x \in \mathbb{R}} |u_x(x, t)| \leq C \min\{\|u_0\|_{L^\infty} t^{-\frac{1}{2}}, \|u_{0,x}\|_{L^\infty}\}. \quad (1.2.4)$$

This formula shows that the heat equation on \mathbb{R} averages solutions, in the sense that their derivatives converge to 0 as $t \rightarrow \infty$.

1.3 Travelling waves on \mathbb{R}

Combining the bistable reaction function $g(u; a)$ and the diffusion operator results in an interplay between the harsh reaction jumps and the smoothening effect of diffusion. As a result, we have a special solution of (1.0.2) that we call a travelling wave, see Figure 1.1.

To find such a wave profile Φ , we assume that $u(x, t) = \Phi(x - ct)$ and we plug this Ansatz into (1.0.2). Upon substituting $\xi = x - ct$ we arrive at the second-order ODE

$$-c\Phi'(\xi) = d\Phi''(\xi) + g(\Phi(\xi); a), \quad (1.3.1)$$

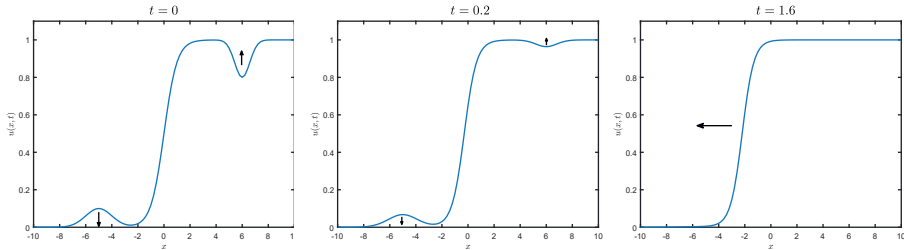


Figure 1.1: Travelling wave on \mathbb{R} . Under the influence of the bistable reaction term, the initial small perturbations are first pushed to either 0 or 1.

which we couple to the boundary conditions

$$\Phi(-\infty) = 0, \quad \Phi(\infty) = 1, \quad (1.3.2)$$

since we want to connect two stable points of the nonlinearity g . The existence of a (unique up to translation) solution (Φ, c) to (1.3.1)-(1.3.2) is shown in [33] via phase-plane analysis. In particular, the authors introduce an additional function $P = \Phi'$ that transforms the second-order ODE (1.3.1) into a system of two first-order ODEs

$$\begin{cases} \Phi'(\xi) &= P(\xi), \\ P'(\xi) &= -\frac{c}{d}\Phi'(\xi) - \frac{1}{d}g(\Phi(\xi); a), \end{cases}$$

to which we add the boundary conditions $P(-\infty) = 0$, $P(\infty) = 0$. A short computation shows that $(0, 0)$ and $(1, 0)$ are two saddle equilibrium points of this system. Therefore, the solution (Φ, P) corresponds to an orbit lying in the intersection of the unstable manifold of $(0, 0)$ and the stable manifold of $(1, 0)$. As Fife shows using a geometric argument in [33], there exists a unique speed c such that these manifolds intersect in the first quadrant of the (Φ, P) plane. This result automatically shows that the wave is monotonically increasing, i.e., $\Phi' > 0$.

In the case of the standard cubic nonlinearity

$$g(u; a) = u(1 - u)(u - a) \quad (1.3.3)$$

one can check that the explicit solution to (1.3.1) is given by

$$\Phi(\xi) = \frac{1}{2} + \frac{1}{2} \tanh \frac{\sqrt{2}\xi}{4}, \quad c = \sqrt{2d}\left(a - \frac{1}{2}\right). \quad (1.3.4)$$

We can read off two important properties from the second formula.

1. The speed satisfies $c = 0$ if and only if $a = 1/2$;
2. Up to the sign change, the speed c is symmetric around $a = 1/2$.

This symmetry result is expected since diffusion operator does not prefer neither of the equilibrium points 0 and 1, which means that the propagation direction is in general determined by the reaction function, or more precisely, by the sign of its integral

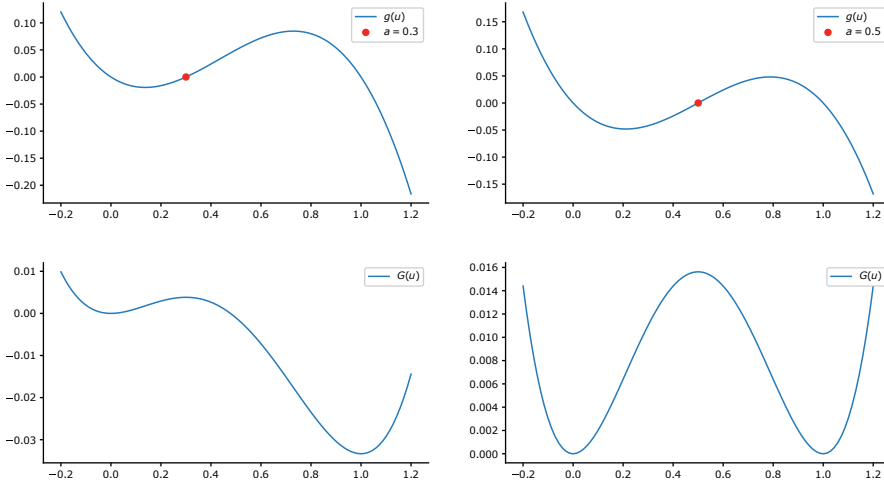


Figure 1.2: The cubic nonlinearity $g(u; a) = u(1 - u)(u - a)$ with its double-well potential $G(u; a)$. On the left we have $a = 0.35$, and we observe that $G(0; a) > G(1; a)$. On the right we have $a = 0.5$ and the system is in balance as the equality $G(0; a) = G(1; a)$ holds.

$G(u; a) = -\int_0^u g(u; a) du$. The function G is often called the *double-well potential*, see Figure 1.2.

To give a visual interpretation, when $a < 1/2$, the equilibrium point 1 with the lower potential energy invades the point 0 with the higher potential energy and the wave moves to the left. If $a > 1/2$, the role of the stable states 0 and 1 is reversed, and the wave propagates to the right with speed $c > 0$. For $a = 1/2$, the wave speed c is equal to 0 as a consequence of both states being in balance due to the equality $G(0; a) = G(1; a)$.

1.4 Travelling waves on lattice domains

In what follows we transfer the familiar concepts from §1.2 and §1.3 to lattice domains. In the absence of the diffusion operator, both equations (1.0.1) and (1.0.2) are systems of decoupled first order ODEs that we have already covered in §1.1.

Therefore, the first obvious difference between these two type of equations comes from the diffusion operator Δ . On the continuous domain \mathbb{R}^n , the Laplace operator Δ_x is a local operator, i.e., to evaluate $\Delta_x u(x_0)$ one needs to know the values of the function u in an arbitrarily small neighborhood around some point x_0 . On the contrary, the discrete diffusion operator is a nonlocal operator on the lattice Λ since it couples multiple points on a lattice. Moreover, its definition differs per type of lattice that we study. We explain these concepts further in the following subsection by studying three kinds of lattice domains - the integers \mathbb{Z} , the two-dimensional domain \mathbb{Z}^2 and infinite k -ary trees \mathcal{T}_k .

1.5 Integer lattice \mathbb{Z}

On the integer domain \mathbb{Z} , one example of a discrete diffusion operator is given by

$$[\Delta u]_i = u_{i+1} - 2u_i + u_{i-1}, \quad (1.5.1)$$

which is considered as the standard discretization of the continuous Laplace operator. The full bistable lattice reaction-diffusion equation on \mathbb{Z} now reads

$$\dot{u}_i(t) = d(u_{i+1}(t) - 2u_i(t) + u_{i-1}(t)) + g(u_i(t); a), \quad i \in \mathbb{Z}, t > 0. \quad (1.5.2)$$

1.5.1 Fundamental solution of the discrete heat equation

The main goal of this subsection is to draw parallels between the discrete heat equation associated to (1.5.1), namely

$$\dot{u}_i(t) = u_{i+1}(t) - 2u_i(t) + u_{i-1}(t), \quad i \in \mathbb{Z}, t > 0, \quad (1.5.3)$$

and the continuous heat equation (1.2.2). We tackle (1.5.3) by applying the Fourier transform which results in the simple ODE in the Fourier space

$$\frac{d}{dt} \hat{u}(\xi) = e^{2t(\cos \omega - 1)} \hat{u}(\xi),$$

whose solution is given by

$$\hat{u}(\xi) = e^{2t(\cos \omega - 1)} \hat{u}^0(\xi),$$

where $u^0 = u(0) \in \ell^2(\mathbb{Z})$. By applying the inverse Fourier transform we derive the explicit formula for the solution

$$u_i(t) = \frac{1}{2\pi} \sum_{k \in \mathbb{Z}} u_k^0 \int_{-\pi}^{\pi} \cos((i-k)\omega) e^{2t(\cos \omega - 1)} d\omega. \quad (1.5.4)$$

In this formula we recognize the integral representation

$$I_k(t) = \frac{1}{2\pi} \int_{-\pi}^{\pi} \cos(k\omega) e^{t \cos \omega} d\omega,$$

of the modified Bessel functions of the first kind $I_k(t)$ for $t > 0$ and $k \in \mathbb{Z}$, see Figure 1.5.1.

Setting $G_k(t) := e^{-2t} I_k(2t)$, the solution (1.5.4) can hence be written as the convolution between the sequence G and the initial condition u^0 , i.e.,

$$u(t) = G * u^0.$$

This is in line with the continuous heat equation where the solution is obtained by convolving between the Gaussian kernel with the initial state, see equation (1.2.3). Our analysis in §2.6 shows that the first differences of solutions decay as

$$\sup_{i \in \mathbb{Z}} |u_{i+1}(t) - u_i(t)| = O(t^{-1/2}).$$

Therefore, the discrete heat equation on \mathbb{Z} averages out its solutions, in the sense that their first differences converge to 0 as $t \rightarrow \infty$, with the same decay rate as the solutions of the continuous heat equation. We summarize the similarities between the discrete and continuous heat kernels in Table 1.1.

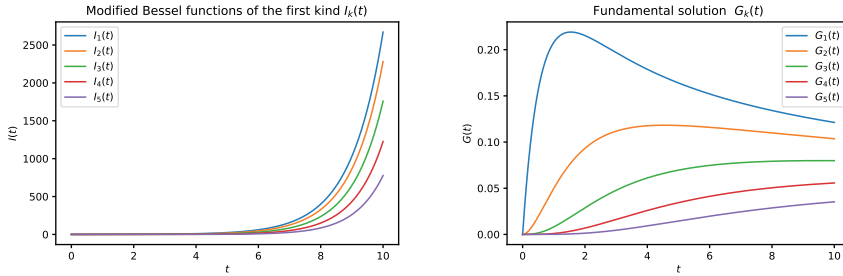


Figure 1.3: On the left we plot modified Bessel functions of the first kind for $k \in \{1, 2, 3, 4, 5\}$ and on the right we plot the corresponding fundamental solution $G_k(t) = e^{-t} I_k(t)$.

1.5.2 Wave-fronts on \mathbb{Z}

Similarities between the fundamental solutions of the continuous and discrete heat equation suggest that the discrete reaction-diffusion equation (1.5.2) also admits travelling wave solutions. To find such solutions, we mimic the procedure from §1.3 and we plug the Ansatz $u_i(t) = \Phi(i - ct)$ into (1.5.2). Upon substituting $\xi = i - ct$, this approach results in the following differential equation for Φ and c

$$-c\Phi'(\xi) = d(\Phi(\xi + 1) - 2\Phi(\xi) + \Phi(\xi - 1)) + g(\Phi(\xi); a). \quad (1.5.5)$$

As before, we couple it to the boundary conditions that connect two stable points of the nonlinearity g , namely

$$\Phi(-\infty) = 0, \quad \Phi(\infty) = 1. \quad (1.5.6)$$

Already at this point we can observe the first difference between the lattice and continuous equations. Namely, the differential equation (1.5.5) involves both past and future values. We call this type of differential equation a mixed functional differential equation (MFDE). Using Brouwer's fixed point theorem, Zinner [97] was the first to show that there exists a travelling wave solution provided that the diffusion parameter d is big enough. In the seminal paper [67] Mallet-Paret gives detailed existence and uniqueness results for a much more general class of MFDEs. In particular, for every $a \in (0, 1)$ and $d > 0$ there exists a speed $c \in \mathbb{R}$ and non-decreasing profile $\Phi : \mathbb{R} \rightarrow \mathbb{R}$ that satisfy (1.5.5)-(1.5.6). In case $c \neq 0$ this wave-pair is unique upon fixing $\Phi(0) = 1/2$. Moreover, in this case both the speed c and profile $\Phi \in C^1(\mathbb{R})$ depend smoothly on the parameters a and d , and the strict inequality $\Phi' > 0$ holds. When we want to emphasize this dependence of the speed c on parameters a and d we write $c(a, d)$.

Provided that the nonlinearity g is the standard cubic we have just as in (1.3.4) the symmetry relation

$$c(1/2 + a, d) = -c(1/2 - a, d),$$

for every $a \in (0, 1/2)$ and $d > 0$. This relation shows that the speed c is, up to the sign change, symmetrical around the axis $a = 1/2$. Moreover, we have $c(1/2, d) = 0$ for every $d > 0$.

Heat equation on \mathbb{R} and \mathbb{Z}

Domain	Continuous domain \mathbb{R}	Discrete domain \mathbb{Z}
Fundamental solution	$H(x, t) = \frac{1}{\sqrt{4\pi t}} e^{-\frac{x^2}{4t}}$	$G_k(t) = e^{-2t} I_k(2t)$
Singularity at $t = 0$	$\lim_{t \rightarrow 0} H(0, t) = \infty$	$G_0(0) = 0$
Integral of the kernel	$\frac{1}{\sqrt{4\pi t}} \int_{\mathbb{R}} e^{-\frac{x^2}{4t}} dx = 1$	$\sum_{k \in \mathbb{Z}} e^{-2t} I_k(2t) = 1$
Decay rate of solutions	$\sup_{x \in \mathbb{R}} u_x(x, t) \leq Ct^{-1/2}$	$\sup_{i \in \mathbb{Z}} u_{i+1}(t) - u_i(t) \leq Ct^{-1/2}$

Table 1.1: In this table we draw some parallels between the (fundamental) solutions of the continuous and discrete heat equations.

Before we delve into the further analysis of waves on lattices, we want to point out some crucial differences between equation (1.5.5) and its counterpart on a continuous domain.

1.5.3 Pinning on lattices

Turning back to lattice domains, we point out one of the key differences between the MFDE (1.5.5) and ODE (1.3.1). In particular, setting $c = 0$ in (1.5.5) results in a difference equation

$$0 = d(\Phi_{i+1} - 2\Phi_i + \Phi_{i-1}) + g(\Phi_i; a), \quad (1.5.7)$$

to which we add the boundary conditions

$$\lim_{i \rightarrow -\infty} \Phi_i = 0, \quad \lim_{i \rightarrow \infty} \Phi_i = 1. \quad (1.5.8)$$

This change from a differential to a difference equation is an underlying mechanism that causes the pinning of waves. Namely, we say that *pinning* or *propagation failure* occurs when the equality $c = 0$ holds for a range of bistable parameters a in some nontrivial interval $[a_-, a_+]$. This is in stark contrast with the continuous reaction-diffusion equation, in which we have $c = 0$ for only one value of the bistable parameter a , see Figure 1.4. The first systematic study of this phenomenon was performed by Keener in [55]. In this paper, Keener embeds the difference equation (1.5.7) into the framework set up by Moser in [71] to show the existence of infinitely many chaotic solutions that block the propagation of waves. Since we also employ this theory in Chapter 4, we give this construction some attention here.

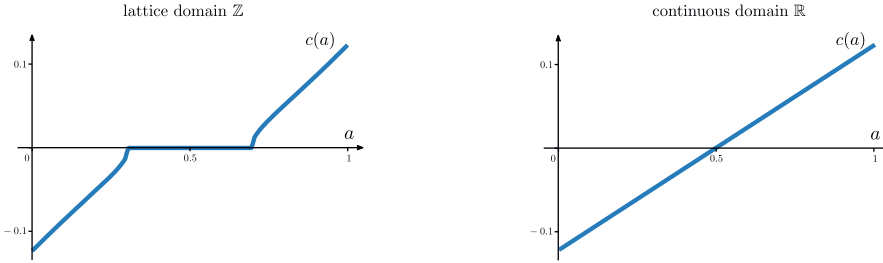


Figure 1.4: Speed c as the function of a . In this example we take $d = 0.025$ and the standard cubic nonlinearity (1.3.3). On the left we plot numerical solutions of the MFDE (1.5.5), and on the right we plot the analytical solution $c(a)$ for the ODE (1.3.1).

Spatial chaos The substitution $P_i := \Phi_{i-1}$ transforms the difference equation (1.5.7) into the two-dimensional recurrence relation

$$\begin{cases} \Phi_{i+1} &= 2\Phi_i - P_i - \frac{1}{d}g(\Phi_i; a), \\ P_{i+1} &= \Phi_i, \end{cases} \quad (1.5.9)$$

for $i \in \mathbb{Z}$. We define a mapping $\phi: \mathbb{R}^2 \rightarrow \mathbb{R}^2$ by

$$\phi(u, v) = \left(2u - v - \frac{1}{d}g(u; a), u \right),$$

together with its inverse

$$\phi^{-1}(u, v) = \left(v, 2v - u - \frac{1}{d}g(v; a) \right).$$

We can now take any $(\Phi_0, P_0) \in \mathbb{R}^2$ to define a bi-infinite sequence $(\Phi_i, P_i)_{i \in \mathbb{Z}}$ by setting

$$(\Phi_i, P_i) := \phi^i(\Phi_0, P_0), \quad i \in \mathbb{Z}. \quad (1.5.10)$$

By construction this sequence satisfies the system (1.5.9). However, taking for example $(\Phi_0, P_0) = (0.5, 0.7)$ and the cubic nonlinearity (4.1.2) with $a = 0.2$ we soon arrive at $\Phi_{12} = 4.89 \times 10^{11}$. Due to its very large values, this sequence does not correspond with the physical notion of a travelling wave. Therefore, at this point it is not immediately clear that one can actually find a bounded sequence that satisfies (1.5.9).

To prove that such bounded sequences indeed exist, Keener applied results from the field of Symbolic Dynamics, in particular the Moser theorem [71]. This result implies that for every small diffusion d there exist a correspondence between sequences in the set

$$S := \{(\dots, s_{-1}, s_0, s_1, \dots) : s_i \in \{0, 1\}\}$$

and bounded solutions to (1.5.9). Specifically, there exist $x_0 \in [0, a)$ and $x_1 \in (a, 1]$ such that for each $(s_i)_{i \in \mathbb{Z}} \in S$ we can find a sequence $(\Phi_i, P_i)_{i \in \mathbb{Z}} \subset [0, 1]^2$ that satisfies (1.5.9), together with

$$\Phi_i \in [0, x_0), \quad \text{if } s_i = 0, \quad \Phi_i \in (x_1, 1], \quad \text{if } s_i = 1,$$

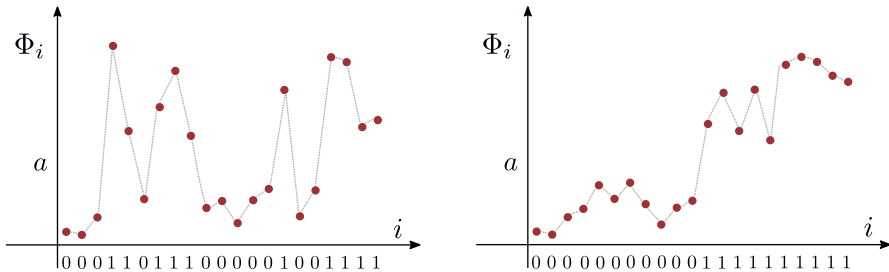


Figure 1.5: Two possible stationary solutions of (1.5.5) and their corresponding sequences $(s_i)_{i \in \mathbb{Z}}$.

see Figure 1.5. To conclude, for small d one can construct a rich variety of solutions in $[0, 1]^2$. Moreover, using the comparison principle, Keener shows that intervals $[0, x_0)$ and $(x_1, 1]$ are invariant for (1.5.2) in the sense that for all $i \in \mathbb{Z}$ we have

$$\begin{aligned} u_i(0) \in [0, x_0) &\implies u_i(t) \in [0, x_0) \text{ for all } t > 0, \\ u_i(0) \in (x_1, 1] &\implies u_i(t) \in (x_1, 1] \text{ for all } t > 0. \end{aligned}$$

Therefore, solutions to the LDE (1.5.3) are blocked from propagating in any direction.

Pinning in systems like (1.5.9) can also be studied from the Dynamical Systems point of view. For example, in [47] the authors characterize pinned fronts as intersection points of stable and unstable manifold of saddle equilibrium points. We describe this construction in the next paragraph.

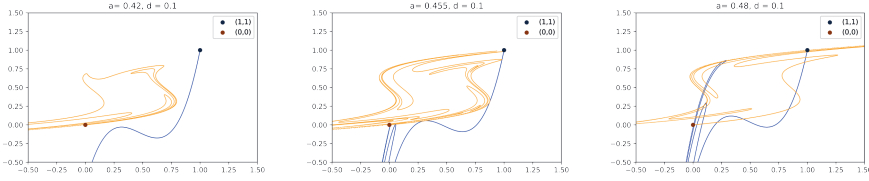
Stable and unstable manifolds Equilibrium points $(\bar{\Phi}, \bar{P})$ of the system (1.5.9) are defined as scalar solutions to

$$\bar{\Phi} = \bar{P}, \quad \bar{\Phi} = 2\bar{\Phi} - \bar{P} - d^{-1}g(\bar{\Phi}; a). \quad (1.5.11)$$

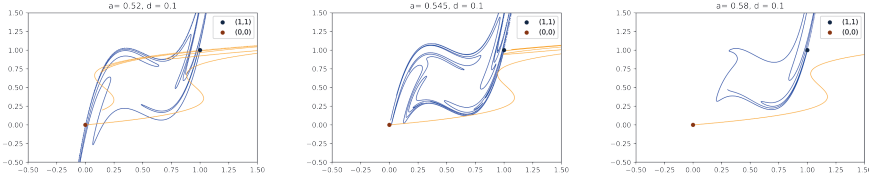
One can verify that $(0, 0)$ and $(1, 1)$ are saddle equilibrium points to which we associate the sets

$$\begin{aligned} W^u(0, 0) &= \{(u, v) : \phi^{-n}(u, v) \rightarrow (0, 0), \text{ as } n \rightarrow \infty\}, \\ W^s(1, 1) &= \{(u, v) : \phi^n(u, v) \rightarrow (1, 1), \text{ as } n \rightarrow \infty\}. \end{aligned}$$

These sets $W^u(0, 0)$ and $W^s(1, 1)$ are called the *stable* and *unstable manifold* of points $(0, 0)$ and $(1, 1)$, respectively. If a point (Φ_0, P_0) lies in the intersection of these two sets then its associated sequence (1.5.10) also belongs to $W^u(0, 0) \cap W^s(1, 1)$ and it satisfies the boundary conditions (1.5.8). We call such solutions *pinned fronts* since they connect two stable points of the nonlinearity g . Provided that g is the cubic function, a result by Qin and Xian from [76] implies that at least two sequences lie the intersection $W^u(0, 0) \cap W^s(1, 1)$. If these manifolds intersect transversely for some parameter a_0 , then these pinned waves persist as we vary a around a_0 , so we obtain pinned fronts in some nonempty interval $[a_-, a_+]$ around a_0 . At $a = a_-$ and $a = a_+$ the manifolds intersect tangentially, and finally, for $a \notin [a_-, a_+]$ the manifolds are disjoint, which means that no pinned fronts exist. To visualize this process, we implemented a numerical algorithm from [41] and we show our results in Figure 1.6.



(a) Manifolds are disjoint, a pinned front does not exist. (b) Manifolds touch in a tangential fashion, $a = a_-$. (c) Manifolds intersect transversely, we have a pinned front.



(d) Manifolds intersect transversely, we have a pinned front. (e) Manifolds touch in a tangential fashion, $a = a_+$. (f) Manifolds are completely separated, a pinned front does not exist.

Figure 1.6: This sequence of panels shows the formation and disappearance of a pinned front as we increase the bistable parameter a . We plot $W^u(0, 0)$ and $W^s(1, 1)$ in orange and blue, respectively. A pinned front exists if these two manifolds intersect. Based on these numerical simulations, for $d = 0.1$ we can find pinned fronts for a approximately in $[0.455, 0.545]$. At the end points of this interval the manifold intersection is tangential.

To conclude this section, we summarize the similarities and some basic differences between the waves on continuous and lattice domains in Table 1.2.

1.6 Infinite k -ary trees

Chapter 4 of this thesis is concerned with the propagation and pinning of waves on infinite k -ary trees \mathcal{T}_k . Infinite k -ary trees are undirected graphs in which the neighbourhood of each node consists of one parent with coordinates $(i - 1, j)$, and k children

$$(i + 1, kj), (i + 1, kj + 1), \dots, (i + 1, kj + k - 1),$$

see Figure 1.7. Assuming that the diffusion parameter d is equal between all nodes, the bistable reaction-diffusion equation takes the form

$$\dot{u}_{i,j} = d \left(\sum_{l=0}^{k-1} u_{i+1, kj+l} - u_{i,j} \right) + d(u_{i-1,j} - u_{i,j}) + g(u_{i,j}; a), \quad (1.6.1)$$

for all $(i, j) \in \mathbb{Z} \times \mathbb{N}_0$. In this thesis we focus on so-called ‘layer’ solutions, i.e., solutions for which we have $u_{i,j}(t) = u_i(t)$ for all (i, j) and $t > 0$. Such solutions

Travelling waves on \mathbb{R} and \mathbb{Z}

Domain	Continuous domain \mathbb{R}	Discrete domain \mathbb{Z}
Type of the equation	a second-order ODE for all $c \in \mathbb{R}$	MFDE for $c \neq 0$ and a difference equation for $c = 0$.
Singular perturbation problem as $c \rightarrow 0$	No, setting $c = 0$ does not change the nature of the equation.	Yes, since the MFDE transforms into a difference equation.
Uniqueness of solutions for $(a, d) \in (0, 1) \times \mathbb{R}_{>0}$	A solution pair (Φ, c) is unique.	A solution pair (Φ, c) is unique only when $c \neq 0$.
Smoothness of solutions	Both Φ and Φ' are in $C(\mathbb{R})$	The wave and its derivative are in $C(\mathbb{R})$ provided that $c \neq 0$.
Pinning	There is no pinning; $c = 0 \iff a = \frac{1}{2}$	Yes; analytical results for $d \ll 1$ and open problem for large d .

Table 1.2: In this table we summarize some similarities and basic differences between the travelling wave solutions of the continuous equation (1.3.1) and the lattice equation (4.1.6).

satisfy the simplified version of (1.6.1), namely

$$\dot{u}_i = d(ku_{i+1} - (k+1)u_i + u_{i-1}) + g(u_i; a). \tag{1.6.2}$$

Searching for a travelling wave solution of the form $u_i(t) = \Phi(i - ct)$ we arrive at the MFDE

$$-c\Phi'(\xi) = d(k\Phi(\xi+1) - (k+1)\Phi(\xi) + \Phi(\xi-1)) + g(\Phi(\xi); a), \tag{1.6.3}$$

coupled with the boundary conditions (1.5.8). Since this MFDE falls under the general framework of Mallet-Paret, there exists a travelling wave solution (Φ, c) for every $k > 0$. For $k = 1$ we recover the standard bistable reaction diffusion equation on \mathbb{Z} . We notice that the future and the past terms in MFDE (1.6.3) are asymmetrical in the parameter k . Indeed, we can also rewrite this equation as a reaction-diffusion equation with a convection term $d(k-1)(\Phi(\xi+1) - \Phi(\xi))$ on the lattice \mathbb{Z} , namely

$$\begin{aligned} -c\Phi'(\xi) = & d(\Phi(\xi+1) - 2\Phi(\xi) + \Phi(\xi-1)) + g(\Phi(\xi); a) \\ & + d(k-1)(\Phi(\xi+1) - \Phi(\xi)). \end{aligned} \tag{1.6.4}$$

For $k \neq 1$, the convection term also contributes to the speed of the wave c and it is expected that the speed c will not be symmetric anymore around the axis $a = 1/2$, also in the case of the standard cubic nonlinearity.

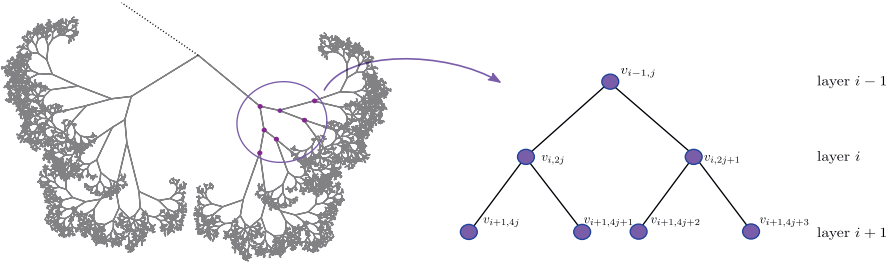


Figure 1.7: Infinite k -ary tree with $k = 2$ and indicated layers.

Motivation and main questions Our work is inspired by the study of Kouvaris, Kori and Mikhailov [62], in which the authors perform a non-rigorous analysis of the bistable reaction-diffusion equation on semi-finite k -ary trees. They discover that the direction of wave propagation largely depends on the branch factor k .

Therefore, our main questions in this work are the following.

- Q1 Do travelling waves on k -ary trees admit both positive and negative speeds?
- Q2 Does the asymmetry in the equation cause a preferred direction for a travelling wave?
- Q3 What is the shape of the pinning region?
- Q4 Can the increase in diffusion parameter d cause the wave to change its direction of propagation for a fixed bistable parameter a and tree parameter k ?

The initial numerical observations indeed suggest that the region in which $c = 0$ is now finite and asymmetric, in contrary to the case $k = 1$, see Figure 1.8.

These numerical findings motivated us to perform a rigorous mathematical analysis to answer the above-mentioned questions. Our methods rely on the construction of two different types of sub-solutions that help us to detect the regions in which we have $c < 0$. Moreover, exploiting certain parameter transformations we can also detect regions in which $c > 0$. We sum up our results into the following answers to our initial questions.

- A1 Yes, for every bistable nonlinearity and every $k \neq 1$, there exists a parameter regime (a, d) close to $a = 0$ for which we have $c < 0$. Similarly, $c > 0$ holds for some parameter regime (a, d) close to $a = 1$.
- A2 For $k > 1$, the wave prefers to retreat on the k -ary tree. In particular, for each bistable parameter $a \in (0, 1)$ there exists a parameter $d^*(a)$ such that the travelling wave solution of (1.6.3) for $d > d^*(a)$ travels with the strictly negative speed $c < 0$ [Theorem 4.2.5 in Chapter 4].
- A3 We show that the pinning region exists for $d \ll 1$. The previous answer implies that the pinning region is finite.
- A4 Yes. For each $k > 1$ and parameter a close to one the wave experiences at least once the following changes as we increase d from 0 to $+\infty$:

pinning ($c = 0$) \rightarrow spreading ($c > 0$) \rightarrow pinning ($c = 0$) \rightarrow retreating ($c < 0$).

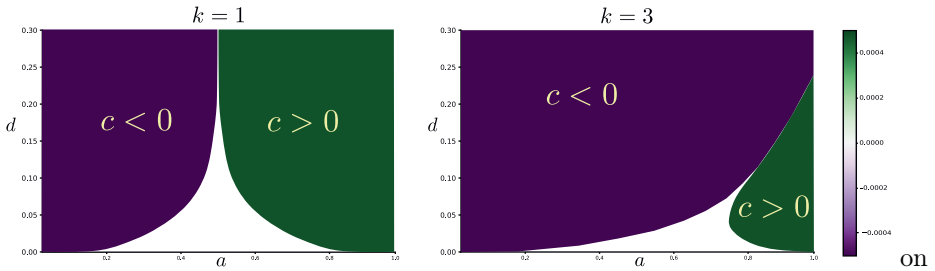


Figure 1.8: Initial numerical observations for the wave propagation on k -ary trees for the standard cubic nonlinearity (1.3.3). For $k = 1$ (left) we have the standard LDE on \mathbb{Z} whose wave solution has no preferred direction. In other words, the speed c is, up to the sign change, symmetrical around the axis $a = \frac{1}{2}$. On the right we show the direction of the wave propagation on the k -ary tree with $k = 3$.

In addition, our methods provide more than abstract existence results. For instance, our results include an analytical description of regions where we surely have $c < 0$, $c = 0$ and $c > 0$ for the standard cubic nonlinearity.

1.7 Two-dimensional lattice \mathbb{Z}^2

In Chapters 2 and 3 of this thesis we study the bistable reaction-diffusion equation on the two-dimensional lattice \mathbb{Z}^2 . For the discrete diffusion operator we take the plus-shaped Laplacian operator that takes into account the four closest neighbours of each point $(i, j) \in \mathbb{Z}^2$, i.e.,

$$[\Delta u_{i,j}] = u_{i+1,j} + u_{i-1,j} + u_{i,j+1} + u_{i,j-1} - 4u_{i,j}, \quad (1.7.1)$$

and set the diffusion coefficient to 1, i.e., $d = 1$. Therefore, the central object of our study in these chapters is the LDE

$$\dot{u}_{i,j} = u_{i+1,j} + u_{i-1,j} + u_{i,j+1} + u_{i,j-1} - 4u_{i,j} + g(u_{i,j}; a), \quad (1.7.2)$$

with $(i, j) \in \mathbb{Z}^2$. The function $g : \mathbb{R} \rightarrow \mathbb{R}$ is a bistable reaction function. We couple this LDE with an initial condition

$$u(0) = u^0 \in \ell^\infty(\mathbb{Z}^2). \quad (1.7.3)$$

Due to the anisotropy of the lattice, wavefront solutions to this LDE experience yet another feature that is uncharacteristic for waves on continuous domains, namely, the wave-pair (Φ, c) depends on the direction of propagation. To elaborate, as we have a two-dimensional lattice, it is natural to search for travelling wave solutions that move in the specific direction $(\sigma_h, \sigma_v) \in \mathbb{R}^2$, with the normalization condition $\sigma_h^2 + \sigma_v^2 = 1$. In particular, we plug the Ansatz

$$u_{i,j}(t) = \Phi(i\sigma_h + j\sigma_v - ct)$$

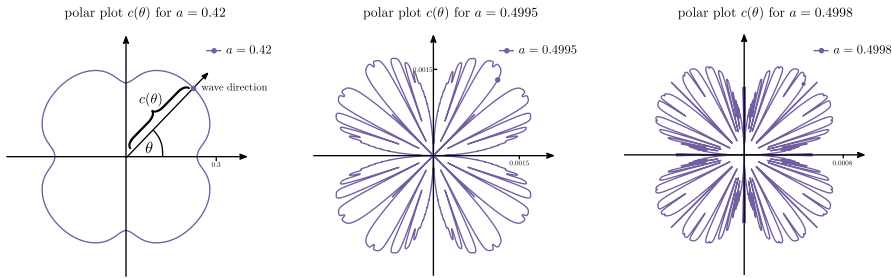


Figure 1.9: These plots depict the directional dependence of speed c on the angle $\theta = \arctan \sigma_v / \sigma_h$ of the wave-propagation for three different values of parameter a . The first image shows the smoothness of the graph $\theta \mapsto c(\theta)$ when far from the pinning region. On the second and third image we see the situation in which the waves propagate in some directions but are pinned in other.

into (1.7.2), which results in the MFDE

$$-c\Phi'(\xi) = \Phi(\xi + \sigma_h) + \Phi(\xi - \sigma_h) + \Phi(\xi + \sigma_v) + \Phi(\xi - \sigma_v) - 4\Phi(\xi) + g(\Phi(\xi); a), \quad (1.7.4)$$

coupled with the boundary conditions

$$\lim_{\xi \rightarrow -\infty} \Phi(\xi) = 0, \quad \lim_{\xi \rightarrow +\infty} \Phi(\xi) = 1.$$

The novelty compared to the previous sections is that the wave-pair solution (c, Φ) now depends also on the chosen direction (σ_h, σ_v) , see Figure 1.9. This phenomenon does not occur for the standard waves on continuous domain \mathbb{R}^n , as the analogous wave Ansatz $u(x, y, t) = \Phi(x\sigma_h + y\sigma_v - ct)$ would again result in the second-order ODE (1.3.1).

1.7.1 Stability of travelling waves on \mathbb{Z}^2

In this work we are interested in the stability and long-term behaviour of the moving waves, far from the pinning regime. For that reason we are not interested in small $d \approx 0$, but we fix $d = 1$. In general, the main stability question (SQ) can be paraphrased as following.

SQ Given an initial condition $u^0 \in X$, where X is a normed space, under which assumptions on u^0 does the solution $u(t)$ of the initial value problem (1.7.2)-(1.7.3) converge in X to the travelling wave solution Φ as $t \rightarrow \infty$?

This question has already been the main topic of two prequel papers [44] and [43]. To demonstrate their results, we assume that $(\sigma_h, \sigma_v) = (1, 0)$ and consider the initial perturbations of the form

$$u_{i,j}^0 = \Phi(i) + v_{i,j}^0. \quad (1.7.5)$$

In [44] the authors assume that v^0 is an arbitrarily big, but localized sequence, i.e.,

$$\lim_{|i|+|j| \rightarrow \infty} v_{i,j}^0 = 0.$$

They show that this assumption is sufficient to guarantee that

$$\sup_{(i,j) \in \mathbb{Z}^2} |u_{i,j}(t) - \Phi(i - ct)| \rightarrow 0, \quad \text{as } t \rightarrow \infty.$$

In their companion paper [43] the authors consider initial perturbations v^0 as elements of the space $\ell^p(\ell^1(\mathbb{Z}); \mathbb{R})$, for any $p \in [1, \infty]$. They prove that there exists $\delta > 0$ such that

$$\|v^0\|_{\ell^p(\mathbb{Z}; \ell^1(\mathbb{Z}))} \leq \delta$$

implies the algebraic convergence of the solution $u(t)$ to the travelling wave solution in $\ell^p(\ell^1(\mathbb{Z}); \mathbb{R})$. Taking $p = \infty$, we see that the absolute value of the initial perturbation necessarily needs to be bounded by a constant δ , and localized only in the j -direction. However, due to technical obstacles, this result is shown exclusively for rational directions, that is, for $(\sigma_h, \sigma_v) \in \mathbb{Z}^2$, whereas [44] handles both rational and irrational directions.

Chapters 2 and 3 of this thesis concern with the stability question of the travelling waves, but now with arbitrarily large perturbations in $\ell^\infty(\mathbb{Z}^2)$. Adapting the framework and methods developed by Matano and Nara in [69] for the bistable reaction-diffusion equation on \mathbb{R}^n , we extend stability results to bounded perturbations that need not to be small or localized. However, to compromise for this generality, we assume that v^0 is a localized perturbation from a sequence that is periodic in the variable j , i.e., the initial perturbation u^0 satisfies the following two conditions (C):

(C₁) We have the spatially uniform bounds when $i \rightarrow \pm\infty$

$$\limsup_{i \rightarrow -\infty} \sup_{(i,j) \in \mathbb{Z}^2} u_{i,j}^0 < a \quad \liminf_{i \rightarrow +\infty} \inf_{(i,j) \in \mathbb{Z}^2} u_{i,j}^0 > a. \quad (1.7.6)$$

(C₂) There exists $P \in \mathbb{Z}$ such that

$$\lim_{|i|+|j| \rightarrow \infty} |u_{i,j+P}^0 - u_{i,j}^0| = 0, \quad (1.7.7)$$

see Figure 2.3 in Chapter 2. We show that these two conditions are enough to guarantee the orbital stability of the travelling wave.

1.8 Graphs and lattices

To conclude this introduction, we provide some insight to shed light on our choices of discrete diffusion operators. For lattices \mathbb{Z} and \mathbb{Z}^2 , these choices can be considered as merely standard discretizations of the continuous Laplace operator. On the other hand, discrete structures such as k -ary trees \mathcal{T}_k have no continuous analogue, and it is not immediately clear how to derive a diffusion operator on such a structure.

1.8.1 Graph Laplacian

To explain the process of a discrete diffusion, let us first consider an undirected graph $G = (V, E)$ with vertices V , edges E and adjacency matrix A , i.e., $A_{I,J} = 1$ if the

nodes I and J are connected and $A_{I,J} = 0$ otherwise. We denote the neighbourhood of the node I by $\mathcal{N}(I)$, i.e., $\mathcal{N}(I) = \{J \in G : A_{I,J} = 1\}$. Moreover, to each node $I \in G$ we assign a function $u_I(t)$. Provided that the rate of diffusion along the edge of two connected nodes is equal to $d > 0$, the rate of change in time of the substance u at the node I is given by

$$\dot{u}_I(t) = d \sum_{J \in \mathcal{N}(I)} (u_J(t) - u_I(t)).$$

This equation is called *the graph heat equation* and the operator

$$[\Delta u]_I = \sum_{J \in \mathcal{N}(I)} (u_J - u_I)$$

is called the discrete Laplace operator or the *graph Laplacian*.

Lattice domains can be considered as special cases of undirected graphs. For example, we can see the integer lattice \mathbb{Z} as a graph with vertices $V = \mathbb{Z}$. Provided that $E = \{\{i, i \pm 1\} : i \in \mathbb{Z}\}$, the discrete Laplace operator reads

$$[\Delta u]_i = (u_{i+1} - u_i) + (u_{i-1} - u_i) = u_{i+1} - 2u_i + u_{i-1}. \quad (1.8.1)$$

It is also possible to consider infinite range-interactions on \mathbb{Z} . For example, in [8], the authors take the discrete Laplacian operator on \mathbb{Z} to be

$$[\Delta u]_i = \sum_{k \in \mathbb{Z}} \alpha_k (u_{i+k} - u_i) \quad (1.8.2)$$

where the coefficients $(\alpha_k)_{k \in \mathbb{Z}}$ satisfy some symmetry and localization conditions, such as $\sum_{k \in \mathbb{Z}} |\alpha_k| k^2 < \infty$ and $\alpha_k = \alpha_{-k}$ for $k \geq 0$. We can see these coefficients as diffusion weights between each edge $\{u_i, u_{i+k}\}$.

For $\Lambda = \mathbb{Z}^2$, the set V is naturally $V = \mathbb{Z}^2$. However, there are many possibilities for the set E , which result in different representations of discrete Laplace operators. For instance, if we take

$$E := \{\{(i, j), (i \pm 1, j)\}, \{(i, j), (i, j \pm 1)\} : (i, j) \in \mathbb{Z}^2\},$$

then we obtain the plus-shaped discrete Laplacian (1.7.1). On the other hand, one could also consider the set

$$E = \{\{(i, j), (i \pm 1, j \pm 1)\}, \{(i, j), (i \mp 1, j \mp 1)\} : (i, j) \in \mathbb{Z}^2\}$$

that gives us the cross-shaped discrete Laplacian Δ^\times , namely

$$[\Delta^\times u]_{i,j} = u_{i+1,j+1} + u_{i-1,j+1} + u_{i-1,j-1} + u_{i+1,j-1} - 4u_{i,j}.$$

For the infinite k -ary tree \mathcal{T}_k , the graph structure is already ingrained in its definition. By assuming that the weights between the nodes are equal, we arrive at the discrete diffusion operator from (1.6.1). However, it would still be interesting to see what happens should the weights between the node and its parent be different than

the weight between the node and its child and how that would change the dynamics between the retreating, pinned and spreading waves.

This freedom of choice of the diffusion operator results in infinite possibilities to model various phenomena with underlying discrete structures using graphs and lattices. As we have seen during the examples of the spatial chaos, pinning, directional-dependency, diffusion-induced propagation-reversal, and many more that we did not even tackle in this introduction, this variety makes lattices an interesting and rich field of research.

1.9 Overview of the thesis

Here we present the content of the chapters in this thesis. Chapters 2 and 3 can be regarded as companion chapters as they both study the bistable LDE on \mathbb{Z}^2 , whereas Chapter 4 concerns the bistable LDE on the infinite k -ary tree \mathcal{T}_k .

Chapter 2 In this chapter we consider the bistable reaction-diffusion equation on the lattice \mathbb{Z}^2 . This equation is also often called *the Allen-Cahn equation*. Our basic assumption is that the initial condition u^0 is a perturbation from the wave that moves in the horizontal direction. In the first part of this work, we do not assume that u^0 is a localized or ‘small’ perturbation from the wave, but that it only satisfies the condition (C1); see (1.7.6). Already this assumption is enough to guarantee that there exists a one-dimensional differential equation which governs the flow of the zero-level surface $\gamma(t)$ of our solution $u(t)$. We call this governing equation a *discrete mean curvature flow* with a drift term. Using the Cole-Hopf transformation, we are able to transform this equation to the discrete heat equation on \mathbb{Z} to show that the zero-level surface $\gamma(t)$ smoothens out over time and that the long-term behaviour of our solution is determined by the travelling wave $\Phi(\cdot - \gamma(t))$. In the second part of this work, by adding the assumption (C2) from (1.7.7) we show that $\gamma(t) \rightarrow ct + \mu$, for some $\mu \in \mathbb{R}$, which ensures the orbital stability of the horizontal travelling wave.

Chapter 3 This chapter is a generalization of our work from Chapter 2 to rational directions on \mathbb{Z}^2 , i.e., now we assume that u^0 is a perturbation of the wave that moves in some direction $(\sigma_h, \sigma_v) \in \mathbb{Z}^2$. The framework is similar to the one in Chapter 2; however, due to the fact that our wave is not aligned with the lattice anymore, we encounter more technical difficulties. One of these difficulties is that the governing equation for the zero-level surface $\gamma(t)$ does not transform via the Cole-Hopf transformation to the discrete heat equation but to a linear lattice equation that has both negative and asymmetrical coefficients. We treat this equation and its decay estimates in detail in Section §3.5, which can also be seen as a section independent of this chapter.

Chapter 4 In this chapter we step away from the travelling waves on the two-dimensional lattice to study a wave-propagation and pinning on infinite k -ary trees. To show the existence of the pinning region that comprises chaotic solutions, we use the Moser Theorem from the field of Symbolic Dynamics. On the other hand, we are also interested in which parameter regimes the moving waves retreat ($c < 0$) or spread

($c > 0$). Therefore, we employ the comparison principle to two types of sub-solutions: steep, step-like profiles that approximate the waves closer to the pinning region, and wide-profiles which show that for $d \gg 0$ the wave always retreats, irrespective of the value of the bistable parameter a .

DYNAMICS OF CURVED TRAVELLING FRONTS FOR
THE DISCRETE ALLEN-CAHN EQUATION ON A
TWO-DIMENSIONAL LATTICE

¹ In this work we consider the discrete Allen-Cahn equation posed on a two - dimensional rectangular lattice. We analyze the large-time behaviour of solutions that start as bounded perturbations to the well-known planar front solution that travels in the horizontal direction. In particular, we construct an asymptotic phase function $\gamma_j(t)$ and show that for each vertical coordinate j the corresponding horizontal slice of the solution converges to the planar front shifted by $\gamma_j(t)$. We exploit the comparison principle to show that the evolution of these phase variables can be approximated by an appropriate discretization of the mean curvature flow with a direction-dependent drift term. This generalizes the results obtained in [69] for the spatially continuous setting. Finally, we prove that the horizontal planar wave is nonlinearly stable with respect to perturbations that are asymptotically periodic in the vertical direction.

2.1 Introduction

Our main aim in this paper is to explore the large time behaviour of the Allen-Cahn lattice differential equation (LDE)

$$\dot{u}_{i,j} = u_{i+1,j} + u_{i-1,j} + u_{i,j+1} + u_{i,j-1} - 4u_{i,j} + g(u_{i,j}; a) \quad (2.1.1)$$

posed on the planar lattice $(i, j) \in \mathbb{Z}^2$. The nonlinearity $g(\cdot; a) \in C^2(\mathbb{R})$ is of bistable type, in the sense that it has two stable equilibria at $u = 0$ and $u = 1$ and one unstable equilibrium at $u = a \in (0, 1)$. The prototypical example is the cubic

$$g_{\text{cub}}(u; a) = u(1 - u)(u - a). \quad (2.1.2)$$

¹The content of this chapter has been published as Mia Jukić, Hermen Jan Hupkes, *Dynamics of curved travelling fronts for the discrete Allen-Cahn equation on a two-dimensional lattice*, Discrete & Continuous Dynamical Systems, see [52].

We are interested in the stability properties of curved versions of the horizontal travelling front

$$u_{i,j}(t) = \Phi(i - ct), \quad \Phi(-\infty) = 0, \quad \Phi(+\infty) = 1 \quad (2.1.3)$$

in the case where $c \neq 0$. In particular, for initial conditions that are j -uniformly ‘front-like’ in the sense

$$\limsup_{i \rightarrow -\infty} \sup_{j \in \mathbb{R}} u_{i,j}(0) < a, \quad \liminf_{i \rightarrow \infty} \inf_{j \in \mathbb{R}} u_{i,j}(0) > a, \quad (2.1.4)$$

we establish the uniform convergence

$$u_{i,j}(t) \rightarrow \Phi(i - \gamma_j(t)), \quad t \rightarrow \infty, \quad (2.1.5)$$

for some appropriately constructed transverse phase variables $\gamma_j(t)$. In addition, we show that the evolution of these phases can be approximated by a discrete version of the mean curvature flow.

After adding further restrictions to (2.1.4), a detailed analysis of this curvature flow allows us to establish the convergence $\gamma_j(t) \rightarrow ct + \mu$. In fact, it turns out that the set of initial conditions covered by this result is significantly broader than the sets considered in earlier work [44, 43]. As a consequence, we widen the known basin of attraction for the planar horizontal wave (2.1.3).

Continuous setting The LDE (2.1.1) can be seen as a discrete analogue of the two-dimensional Allen-Cahn PDE

$$u_t = u_{xx} + u_{yy} + g(u; a). \quad (2.1.6)$$

Our primary interest here is in planar travelling front solutions

$$u(x, y, t) = \Phi(x \cos \theta + y \sin \theta - ct) \quad (2.1.7)$$

that connect the two stable equilibria, in the sense that the waveprofile Φ satisfies

$$\lim_{\xi \rightarrow -\infty} \Phi(\xi) = 0, \quad \lim_{\xi \rightarrow \infty} \Phi(\xi) = 1. \quad (2.1.8)$$

Direct substitution shows that the wave (Φ, c) must satisfy the θ -independent ODE

$$-c\Phi'(\xi) = \Phi''(\xi) + g(\Phi(\xi); a), \quad (2.1.9)$$

reflecting the rotational symmetry of (2.1.6). Indeed, (2.1.9) also arises as the wave ODE for the one-dimensional counterpart

$$u_t = u_{xx} + g(u; a). \quad (2.1.10)$$

of (2.1.6). The existence of solutions to (2.1.9) can be obtained via phase-plane analysis [33] for any parameter $a \in (0, 1)$. Moreover, the pair (Φ, c) is unique up to translations, depends smoothly on the parameter a , and admits the strict monotonicity $\Phi' > 0$.

Let us remark that one can also study (generalized) traveling waves in the setting where g is also allowed to depend on the spatial variables. For example, in [29] the authors construct nonlinearities that depend periodically on x and show that the resulting θ -dependence of the wavespeed can be quite intricate.

Modelling background Reaction-diffusion equations have been used as modelling tools in many different fields. For example, the classical papers [4, 5] use both one- and multi-dimensional versions of such equations to describe the expression of genes throughout a population. Bistable nonlinearities such as (2.1.2) are typically used to model the strong Allee effect - a biological phenomenon which arises in the field of the population dynamics [88]. Indeed, the parameter a can be seen as a type of minimum viability threshold that a population needs to reach in order to grow, in contrast to the standard logistic dynamics. Adding the ability for the population to diffuse throughout its spatial habitat results in systems such as (2.1.6) [87]. In this setting, travelling waves provide a mechanism by which species can invade (or withdraw from) the spatial domain.

In many applications this spatial domain has a discrete structure, in which case it is more natural to consider the LDE (2.1.1). For example, in [64, 58] the authors use this LDE to study populations in patchy landscapes. This allows them to describe and analyze a so-called ‘invasion pinning’ scenario, wherein a species fails to propagate as a direct consequence of the spatial discreteness.

By now, models involving LDEs have appeared in many other scientific and technological fields. For example, they have been used to describe phase transitions in Ising models [9], nerve pulse propagation in myelinated axons [11, 12, 55, 56], calcium channels dynamics [6], crystal growth in materials [15] and wave propagation through semiconductors [17]. For a more extensive list we recommend the surveys [24, 22, 50].

Stability of PDE waves The first stability result for the wave (2.1.7) in the one-dimensional setting of (2.1.10) was established by Fife and McLeod in [34]. In particular, they showed that this wave (and its translates) attracts all solutions u with initial conditions that satisfy

$$\limsup_{x \rightarrow -\infty} u(x, 0) < a, \quad \liminf_{x \rightarrow +\infty} u(x, 0) > a, \quad (2.1.11)$$

together with $u(\cdot, 0) \in [0, 1]$. This latter restriction was later weakened to $u(\cdot, 0) \in L^\infty(\mathbb{R})$ in [32]. Both these proofs rely on the construction of super- and sub-solutions for (2.1.10) in order to exploit the comparison principle for parabolic equations. More recently, similar large-basin stability results have been obtained using variational methods that do not appeal to the comparison principle [36, 78].

In [54], Kapitula established the multidimensional stability of traveling waves in $H^k(\mathbb{R}^n)$, for $n \geq 2$ and $k \geq \lfloor \frac{n+1}{2} \rfloor$. These results were recently extended by Zeng [95], who considered perturbations in $L^\infty(\mathbb{R}^n)$. An alternate stability proof exploiting the comparison principle can be found in the seminal paper [14], where the authors study the interaction of travelling fronts with compact obstacles. Let us also mention the pioneering works [94, 63] which contain the first stability results for $n \geq 4$ together with partial results for $n = 2, 3$.

Based on the techniques developed by Kapitula, Roussier [79] was able to consider ‘asymptotically spherical’ waves and establish their stability under spherically symmetric perturbations. Such solutions behave as

$$u(x, y, t) \rightarrow \Phi\left(\sqrt{x^2 + y^2} - ct - c^{-1} \ln t\right), \quad t \rightarrow \infty \quad (2.1.12)$$

and were first studied by Uchiyama and Jones [51, 89]. Note that the extra time dependence highlights the important role that curvature-driven effects have to play.

Curved PDE fronts Our work in the present paper is inspired heavily by the results for (2.1.6) obtained by Matano and Nara in [69]. They considered bounded initial conditions satisfying the limits

$$\limsup_{x \rightarrow -\infty} \sup_{y \in \mathbb{R}} u_0(x, y) < a, \quad \liminf_{x \rightarrow \infty} \inf_{y \in \mathbb{R}} u_0(x, y) > a, \quad (2.1.13)$$

which form the natural two-dimensional generalization of (2.1.11). They show that eventually horizontal cross-sections of u become sufficiently monotonic to allow a phase $\gamma = \gamma(y, t)$ to be uniquely defined by the requirement

$$u(\gamma(y, t), y, t) = \Phi(0). \quad (2.1.14)$$

These phase variables can be used to characterize the asymptotic behaviour of u . In particular, the authors establish the limit

$$\lim_{t \rightarrow \infty} \sup_{(x, y) \in \mathbb{R}^2} |u(x, y, t) - \Phi(x - \gamma(y, t))| = 0 \quad (2.1.15)$$

and show that - asymptotically - the phase γ closely tracks solutions Γ to the PDE

$$\frac{\Gamma_t}{\sqrt{1 + \Gamma_y^2}} = \frac{\Gamma_{yy}}{(1 + \Gamma_y^2)^{3/2}} + c. \quad (2.1.16)$$

Upon supplementing (2.1.13) with the requirement that the initial condition $u(\cdot, \cdot, 0)$ is uniquely ergodic in the x -direction, a careful analysis of (2.1.16) can be used to show that $\gamma(y, t) \rightarrow ct + \mu$ for some $\mu \in \mathbb{R}$. This can hence be interpreted as a stability result for the planar waves (2.1.7) under a large class of non-localized perturbations. Note however that no information is provided on the rate at which the convergence takes place. Very recently - and simultaneously with our analysis here - Matano, Mori and Nara generalized this approach to consider radially expanding surfaces in anisotropic continuous media [68].

Mean curvature flow In order to interpret the PDE (2.1.16), we consider the interfacial graph $G(t) := \{(\Gamma(y, t), y) : y \in \mathbb{R}\}$. Writing $\nu(y, t)$ for the rightward-pointing normal vector, $V(y, t)$ for the horizontal velocity vector and $H(y, t)$ for the curvature at the point $(\Gamma(y, t), y)$, we obtain

$$\nu = [1 + \Gamma_y^2]^{-1/2}(1, -\Gamma_y), \quad V = (\Gamma_t, 0), \quad H = [1 + \Gamma_y^2]^{-3/2}\Gamma_{yy}. \quad (2.1.17)$$

In particular, (2.1.16) can be written in the form

$$V \cdot \nu = H + c, \quad (2.1.18)$$

which can be interpreted as a mean curvature flow with an additional normal drift of size c . It is no coincidence that this drift does not depend on ν : it reflects the fact that the speed of the planar waves (2.1.7) does not depend on the angle θ .

In a sense, it is not too surprising that the mean curvature flow plays a role in the asymptotic dynamics of wave interfaces. Indeed, one of the main historical reasons for considering the Allen-Cahn PDE is that it actually desingularizes this flow by smoothing out the transition region [1, 27]. However, from a technical point of view, its role in [69] is actually rather minor.

Instead, the main PDE used to capture the behaviour of the phase γ is the non-linear heat equation

$$V_t = V_{yy} + \frac{c}{2}V_y^2 + c. \quad (2.1.19)$$

This PDE can be reformulated as a standard linear heat equation by a Cole-Hopf transformation and hence explicitly solved. These solutions can subsequently be used to construct super- and sub-solutions to (2.1.6) of the form

$$u^\pm(x, y, t) = \Phi \left(\frac{x - V(y, t)}{\sqrt{1 + V_y^2}} \pm q(t) \right) \pm p(t), \quad (2.1.20)$$

in which q and p are small correction terms that allow spatially homogeneous perturbations at $t = 0$ to be traded off for phase-shifts as $t \rightarrow \infty$.

Using the comparison principle, one can use the functions (2.1.20) to show that the phase γ can be approximated asymptotically by V . A second comparison principle argument subsequently shows that V can be used to track the solution Γ of (2.1.16). It therefore plays a crucial role as an intermediary to obtain the desired relation between γ and Γ .

Spatially discrete travelling waves Plugging the travelling wave ansatz

$$\begin{aligned} u_{ij}(t) &= \Phi(i \cos \theta + j \sin \theta - ct), \\ \Phi(-\infty) &= 0, \quad \Phi(+\infty) = 1 \end{aligned} \quad (2.1.21)$$

into the Allen-Cahn LDE (2.1.1), we obtain the functional differential equation of mixed type (MFDE)

$$\begin{aligned} -c\Phi'(\xi) &= \Phi(\xi + \cos \theta) + \Phi(\xi - \cos \theta) + \Phi(\xi + \sin \theta) + \Phi(\xi - \sin \theta) \\ &\quad - 4\Phi(\xi) + g(\Phi(\xi); a). \end{aligned} \quad (2.1.22)$$

The existence of such waves (Φ_θ, c_θ) was first obtained for the horizontal direction $\theta = 0$ [39, 97] and subsequently generalized to arbitrary directions [67]. This θ -dependence is a direct consequence of the anisotropy of the lattice, which breaks the rotational symmetry of the PDE (2.1.6).

A second important difference between (2.1.9) and (2.1.22) is that the character of the latter system depends crucially on the speed c , which depends uniquely but intricately on the parameters (θ, a) . When $c \neq 0$ the associated waveprofile is unique up to translation and satisfies $\Phi' > 0$. When $c = 0$ however, one loses the uniqueness and smoothness of waveprofiles. In addition, monotonic and non-monotonic profiles typically coexist. This behaviour is a direct consequence of the fact that (2.1.22) reduces to a difference equation, posed on a discrete ($\tan \theta \in \mathbb{Q}$) or dense ($\tan \theta \notin \mathbb{Q}$)

subset of \mathbb{R} . The transition between these two regimes is a highly interesting and widely studied topic, focusing on themes such as propagation failure [47, 45, 55], crystallographic pinning [65, 45] and frictionless kink propagation [7, 30]; see [50] for an overview.

For the remainder of the present paper we only consider the case $c \neq 0$ and shift our attention to the stability properties of the associated waves. In one spatial dimension Zinner obtained the first stability result [96], which was followed by the development of a diverse set of tools exploiting either the comparison principle [20], monodromy operators [23] or spatial-temporal Green's functions [10, 82]. The first stability result in two spatial dimensions was obtained in [43] for waves travelling in arbitrary rational ($\tan \theta \in \mathbb{Q}$) directions. Taking $\theta = 0$ here for presentation purposes, the authors consider initial conditions of the form

$$u_{i,j}(0) = \Phi(i) + v_{i,j}^0 \quad (2.1.23)$$

and show that u converges algebraically to the horizontal wave $\Phi(i - ct)$. Here the initial perturbation v^0 is taken to be sufficiently small in $\ell^\infty(\mathbb{Z}; \ell^1(\mathbb{Z}; \mathbb{R}))$. In particular, the perturbation v^0 is only required to be localized in the direction perpendicular to the wave propagation.

The restriction $\tan \theta \in \mathbb{Q}$ was removed in the sequel paper [44], where the initial perturbation v^0 in (2.1.23) can be of arbitrary size as long as it is localized in the sense that

$$\lim_{|i|+|j| \rightarrow \infty} |v_{i,j}^0| = 0. \quad (2.1.24)$$

The proof relies on the construction of explicit sub- and super-solutions to the LDE (2.1.1), generalizing the PDE constructions from [14]. This construction is especially delicate for the cases $\theta \notin \frac{\pi}{4}\mathbb{Z}$, where the disalignment with the lattice directions causes slowly decaying modes that need to be carefully controlled.

Curved LDE fronts In order to avoid the problematic slowly decaying terms discussed above, we restrict ourselves to the horizontal waves (2.1.3) throughout the remainder of the paper. The novelty is that we allow general bounded initial conditions that satisfy the limits (2.1.4). To compare this with the discussion above, we note that this class includes initial conditions of the form

$$u_{i,j}(0) = \Phi(i - \kappa_j) + v_{i,j}^0, \quad (2.1.25)$$

in which κ is an arbitrary bounded sequence and v^0 is allowed to be small in space $\ell^\infty(\mathbb{Z}; \ell^1(\mathbb{Z}; \mathbb{R}))$ or to satisfy the localization condition (2.1.24). In particular, we significantly expand the set of initial conditions that were considered in [43, 44].

Our main aim is to follow the program of [69] that we outlined above as closely as possible. However, the first obstacle already arises when one attempts to define appropriate phase coordinates $\gamma_j(t)$ for $t \gg 1$. Indeed, it no longer makes sense to define the interface of $u(t)$ as the set of points where $u_{i,j}(t) = \Phi(0)$, since this solution set can behave highly erratically due to the discreteness of the spatial variables. To resolve this, we establish an asymptotic monotonicity result in the interfacial region

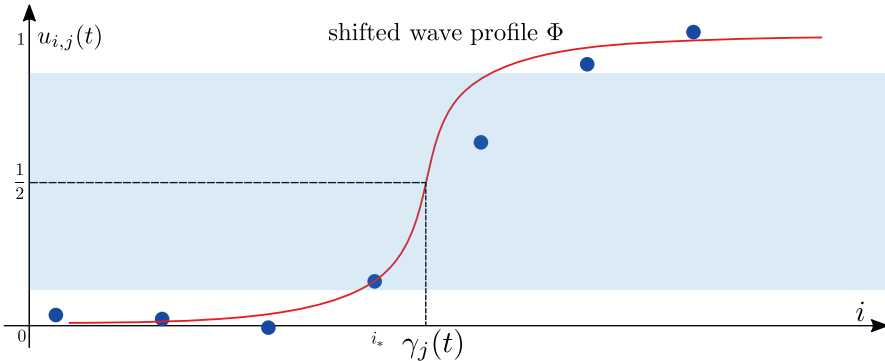


Figure 2.1: In §2.5 we show that for each $j \in \mathbb{Z}$ and $t \gg 0$, the function $i \mapsto u_{i,j}(t)$ is monotonic inside an interfacial region I that is depicted in light blue. The dark blue dots represent the horizontal solution slice $i \mapsto u_{i,j}(t)$. Since u is monotonic inside I , we can find a unique value i_* for which $u_{i_*,j}(t) \leq 1/2 < u_{i_*+1,j}(t)$. We subsequently shift the travelling wave profile Φ in such a way that it matches the solution slice at i_* . The phase $\gamma_j(t)$ is then defined as the argument where this shifted profile equals one half.

where $u_{i,j}(t) \approx \Phi(0)$. This allows us to ‘fill’ the troublesome gaps between lattice points by performing a spatial interpolation based on the shape of Φ ; see Fig. 2.1.

This fundamental problem of not being able to move continuously between lattice points occurs in many other parts of our analysis. For example, we need to construct so-called ω -limit points of solution sequences in order to establish the uniform convergence (2.1.5). In [69] this is achieved by passing to a new coordinate $x' = x - ct$ that ‘freezes’ the wave at the cost of an extra convective term in the PDE (2.1.6). Such a coordinate transformation does not exist in the discrete case, forcing us to use a more involved discontinuous version of this freezing process.

Discrete curvature flow We remark that it is by no means a-priori clear how the mean curvature PDE (2.1.16) should be discretized in order to track the discrete phase coordinates $\gamma_j(t)$. For example, there is more than one reasonable way to define geometric notions such as normal vectors and curvature in discrete settings [26]. On the other hand, the discussion above shows that there may be range of ‘suitable’ choices, as we only desire the tracking to be approximate.

Introducing the convenient notation

$$[\beta_\Gamma]_j = \sqrt{1 + \frac{(\Gamma_{j+1} - \Gamma_j)^2 + (\Gamma_{j-1} - \Gamma_j)^2}{2}},$$

$$[\partial^{(2)}\Gamma]_j = \Gamma_{j+1} + \Gamma_{j-1} - 2\Gamma_j,$$

we will use the standard symmetric discretizations

$$V \cdot \nu \mapsto \beta_\Gamma^{-1} \dot{\Gamma}, \quad H \mapsto \beta_\Gamma^{-3} \partial^{(2)}\Gamma \quad (2.1.26)$$

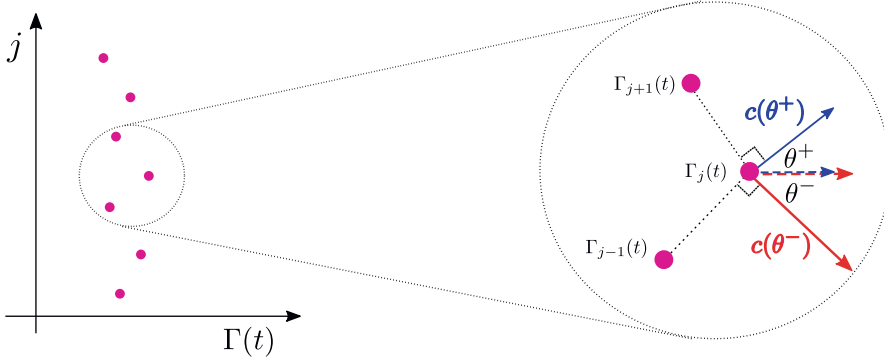


Figure 2.2: The panel on the left represents a graph $j \mapsto \Gamma_j(t)$ at a fixed time t . The right panel zooms in on three nodes of this graph to illustrate the identities (2.1.27) and (2.1.28) that underpin the drift term in our discrete curvature flow.

for the normal velocity and curvature terms in (2.1.18). However, the remaining normal drift term requires more care to account for the direction dependence of the planar front speeds. In particular, it seems natural make the replacement

$$c \mapsto \frac{1}{2}(c_{\theta^+} + c_{\theta^-}), \quad (2.1.27)$$

in which the angles

$$\theta^- = \arctan(\Gamma_j - \Gamma_{j-1}), \quad \theta^+ = \arctan(\Gamma_{j+1} - \Gamma_j) \quad (2.1.28)$$

measure the orientation of the normal vectors for the lower and upper segments of the interface at (Γ_j, j) ; see Fig. 2.2.

In order to make this more explicit, we use the identity $[\partial_\theta c_\theta]_{\theta=0} = 0$ derived in [49, Lem. 2.2] to obtain the expansions

$$c_{\theta^-} \sim c + \frac{1}{2}[\partial_\theta^2 c_\theta]_{\theta=0}(\Gamma_j - \Gamma_{j-1})^2, \quad c_{\theta^+} \sim c + \frac{1}{2}[\partial_\theta^2 c_\theta]_{\theta=0}(\Gamma_{j+1} - \Gamma_j)^2, \quad (2.1.29)$$

which suggests the replacement

$$c \mapsto c + \frac{1}{2}[\partial_\theta^2 c_\theta]_{\theta=0}(\beta_\Gamma^2 - 1). \quad (2.1.30)$$

In order to prevent the quadratic growth in this term, we make the final adjustment

$$c \mapsto c + [\partial_\theta^2 c_\theta]_{\theta=0}(1 - \beta_\Gamma^{-1}), \quad (2.1.31)$$

which agrees with (2.1.30) up to second order in the differences $\Gamma_{j\pm 1} - \Gamma_j$.

All in all, the discrete mean curvature flow that we use in this paper to approximate the phases γ_j can be written as

$$\beta_\Gamma^{-1} \dot{\Gamma} = \beta_\Gamma^{-3} \partial^{(2)} \Gamma + c + [\partial_\theta^2 c_\theta]_{\theta=0}(1 - \beta_\Gamma^{-1}). \quad (2.1.32)$$

While this justification appears to be rather ad-hoc, it turns out that our approximation procedure is not sensitive to $O((\Gamma_{j\pm 1} - \Gamma_j)^3)$ -correction terms. In addition, we explain below how the crucial lower order terms can be recovered by independent technical considerations.

Super- and sub-solutions The technical heart of this paper is formed by our construction of suitable spatially discrete versions of the sub- and super-solutions (2.1.20). The correct generalization of (2.1.19) that preserves the Cole-Hopf structure turns out to be

$$\dot{V}_j = \frac{1}{d} \left(e^{d(V_{j+1} - V_j)} - 2 + e^{d(V_{j-1} - V_j)} \right) + c, \quad (2.1.33)$$

in which we are still free to pick the coefficient d . Indeed, this LDE reduces to the discrete heat equation upon picking $h(t) = e^{d(V - ct)}$.

However, the discrete Laplacian spawns terms proportional to $\Phi''(\beta_V^2 - 1)$ if one simply substitutes a direct discretization of the PDE super-solution (2.1.20) with (2.1.33) into (2.1.1). These terms decay as $O(t^{-1})$ and hence cannot be integrated and absorbed into the phaseshift $q(t)$.

Similar difficulties were also encountered in [44]. The novelty here is that this troublesome behaviour occurs even for the horizontal direction $\theta = 0$, which is completely aligned with the lattice. Inspired by the normal form approach developed in [44], we therefore set out to construct sub- and super-solutions of the form

$$u_{i,j}^\pm(t) = \Phi(i - V_j(t) \pm q(t)) + r(i - V_j(t) \pm q(t))([\beta_V]_j^2 - 1) \pm p(t), \quad (2.1.34)$$

using the extra residual function r to neutralize the slowly decaying terms. Working through the computations, it turns out the relevant condition on the pair (r, d) can be formulated as

$$\mathcal{L}_{\text{tw}} r + d\Phi' = -\Phi'', \quad (2.1.35)$$

in which the Fredholm operator \mathcal{L}_{tw} encodes the linearization of the wave MFDE (2.1.22) around Φ ; see §2.7. Using the Fredholm theory for MFDEs developed in [66, 67] together with the computations in §2.8 and [49, §2], it turns out that d must be given by

$$d = \frac{1}{2}c + \frac{1}{2}[\partial_\theta^2 c_\theta]_{\theta=0} = \frac{1}{2}[\partial_\theta^2 \mathcal{D}(\theta)]_{\theta=0}, \quad (2.1.36)$$

in which the quantity

$$\mathcal{D}(\theta) = \frac{c_\theta}{\cos \theta} \quad (2.1.37)$$

is referred to as the directional dispersion. This quantity measures the horizontal speed of waves travelling in the direction θ , which also plays an important role in the construction of travelling corner solutions to (2.1.1).

Let us emphasize that in the general case $\theta \neq 0$ it is not readily apparent whether the approach developed in this paper can be extended. The main source of the difficulties is the misalignment of the discrete Laplacian, which causes an imbalance between the quadratic convective terms; see e.g. (2.1.29). As a result the Cole-Hopf structure cannot be readily preserved, which is crucial for our analysis here. We believe that this can be corrected by further variable transformations and a more extensive super-solution Ansatz, but leave this subject to future work.

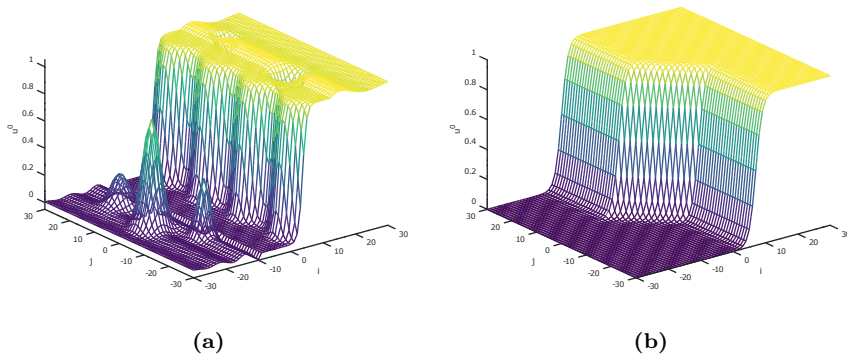


Figure 2.3: Both panels illustrate front-like initial conditions that satisfy (2.1.4) and hence fall within the framework of this paper. Panel a) provides an example of an initial perturbation that converges uniformly to a traveling front. On the contrary, the initial perturbation in b) does not uniformly converge to a traveling planar front, but the evolution of the interface is described asymptotically by (2.1.32).

Stability results As a by-product of our analysis, we are able to extend the stability results obtained previously in [43, 44]. For example, if the phase sequence κ appearing in the initial condition (2.1.25) is periodic (see e.g. Fig. 2.3a), we show that there exists an asymptotic phase $\mu \in \mathbb{R}$ for which we have the convergence $\gamma(t) \rightarrow ct + \mu$ as $t \rightarrow \infty$. In particular, the horizontal planar wave retains its stability under such perturbations, provided we allow for a phase-shift.

In order to prove this result, we first analyze the behaviour of (2.1.1) and (2.1.33) when applied to j -periodic sequences. We subsequently add a localized initial perturbation and show that the effects remain localized in some sense. Since the heat-equation eventually eliminates such localized perturbations, the desired asymptotic convergence persists. We remark that our stability result is slightly less general than its continuous counterpart from [69], since it is not yet clear to us how ergodicity properties can be transferred to our discrete setting.

We emphasize that this stability result does not hold for arbitrary bounded κ in (2.1.25). For example, if there exist κ^- and κ^+ for which we have the limits

$$\lim_{j \rightarrow -\infty} \kappa_j = \kappa^-, \quad \lim_{j \rightarrow +\infty} \kappa_j = \kappa^+ \quad (2.1.38)$$

(see e.g. Fig. 2.3b), then the results in §2.9 imply that for every $t > 0$ we have the convergence

$$u_{i,j}(t) \rightarrow \Phi(i - ct - \kappa^\pm) \quad \text{as } j \rightarrow \pm\infty, \quad (2.1.39)$$

uniformly in i . In particular, the interface $\gamma(t)$ describes the phase transition between κ^- and κ^+ , which is asymptotically captured by (2.1.32).

Organization After formulating our assumptions and main results in §2.2, we transfer the standard ω -limit point constructions for the PDE (2.1.6) to our discrete setting in §2.3. In §2.4 we (partially) generalize the results from [13] concerning

trapped entire solutions to the setting of (2.1.1). In particular, we prove that every entire solution of the Allen-Cahn LDE trapped between two traveling waves is a traveling wave itself. In §2.5 we focus on the large-time behaviour of the solution u and establish the discrete counterpart of (2.1.15). We move on in §2.6 to obtain decay estimates for discrete gradients of solutions to the discrete heat equation. We exploit these in §2.7 to construct super- and sub-solutions, which we use in §2.8 to approximate the phase γ with the solution of the discrete mean curvature flow (2.1.32). Finally, in §2.9 we establish the stability results discussed above for the horizontal planar travelling wave.

Acknowledgments Both authors acknowledge support from the Netherlands Organization for Scientific Research (NWO) (grant 639.032.612).

2.2 Main results

Our principal interest in this paper is the discrete Allen-Cahn equation

$$\dot{u}_{i,j} = (\Delta^+ u)_{i,j} + g(u_{i,j}) \quad (2.2.1)$$

posed on the planar lattice $(i, j) \in \mathbb{Z}^2$. The discrete Laplacian $\Delta^+ : \ell^\infty(\mathbb{Z}^2) \rightarrow \ell^\infty(\mathbb{Z}^2)$ is defined as

$$(\Delta^+ u)_{i,j} = u_{i+1,j} + u_{i,j+1} + u_{i-1,j} + u_{i,j-1} - 4u_{i,j}, \quad (2.2.2)$$

while the nonlinearity is assumed to satisfy the following bistability condition.

(Hg) The nonlinear function $g : \mathbb{R} \rightarrow \mathbb{R}$ is C^2 -smooth and there exists $a \in (0, 1)$ for which we have

$$g(0) = g(a) = g(1) = 0, \quad g'(0) < 0, \quad g'(1) < 0. \quad (2.2.3)$$

In addition, we have the inequalities

$$g > 0 \text{ on } (-\infty, 0) \cup (a, 1), \quad g < 0 \text{ on } (0, a) \cup (1, \infty). \quad (2.2.4)$$

Existence results for planar traveling wave solutions of (2.2.1) were established in [67]. More precisely, if we pick an arbitrary angle $\theta \in [0, 2\pi)$, then (2.2.1) admits a solution of the form

$$u_{ij}(t) = \Phi_\theta(i \cos \theta + j \sin \theta - c_\theta t), \quad (2.2.5)$$

for some wave speed $c_\theta \in \mathbb{R}$ and wave profile $\Phi_\theta : \mathbb{R} \rightarrow \mathbb{R}$ that satisfies the boundary conditions

$$\lim_{\xi \rightarrow -\infty} \Phi_\theta(\xi) = 0, \quad \lim_{\xi \rightarrow +\infty} \Phi_\theta(\xi) = 1. \quad (2.2.6)$$

Substituting the Ansatz (2.2.5) into (2.2.1), we see that the the pair (Φ_θ, c_θ) must satisfy the MFDE

$$\begin{aligned} -c_\theta \Phi'_\theta(\xi) &= \Phi_\theta(\xi + \cos \theta) + \Phi_\theta(\xi + \sin \theta) + \Phi_\theta(\xi - \cos \theta) + \Phi_\theta(\xi - \sin \theta) \\ &\quad - 4\Phi_\theta(\xi) + g(\Phi_\theta(\xi)). \end{aligned} \quad (2.2.7)$$

The results in [67] state that c_θ is unique. In addition, when $c_\theta \neq 0$, the wave profile Φ_θ is unique up to translation and satisfies $\Phi'_\theta > 0$. In this paper, we are interested in planar waves that travel in the horizontal direction $\theta = 0$. Since we rely on smoothness properties of the wave profile, we demand that $c_0 \neq 0$.

(H Φ) There exists a non-zero speed $c \neq 0$ and a wave profile $\Phi \in C^1(\mathbb{R}, \mathbb{R})$ so that the pair (Φ, c) satisfies the boundary conditions (2.2.6) and the MFDE (2.2.7) for the horizontal direction $\theta = 0$. In addition, we have the normalization $\Phi(0) = \frac{1}{2}$.

Our main results concern the Cauchy problem for the Allen-Cahn LDE. In particular, we look for functions

$$u \in C^1([0, \infty); \ell^\infty(\mathbb{Z}^2)) \quad (2.2.8)$$

that satisfy the LDE (2.2.1) for $t > 0$ together with the initial condition

$$u_{i,j}(0) = u_{i,j}^0 \quad (2.2.9)$$

for some $u^0 \in \ell^\infty(\mathbb{Z}^2)$. Observe that the comparison principle together with the bistable structure of g imply that such solutions are unique and exist globally. We impose the following structural condition on u^0 .

(H0) The initial condition $u^0 \in \ell^\infty(\mathbb{Z}^2)$ satisfies the inequalities

$$\limsup_{i \rightarrow -\infty} \sup_{j \in \mathbb{Z}} u_{i,j}^0 < a, \quad \liminf_{i \rightarrow \infty} \inf_{j \in \mathbb{Z}} u_{i,j}^0 > a. \quad (2.2.10)$$

Notice that we do not impose the usual assumption $0 \leq u^0 \leq 1$ or any kind of decay in the spatial limits. As explained in detail in §2.1, this condition is less restrictive than its counterparts from [43, 44] and includes the general class (2.1.25).

2.2.1 Interface formation

Our first goal is to find a link between the solution (2.2.8) of the general Cauchy problem for (2.2.1) and the planar travelling wave (Φ, c) . The result below provides a key tool for this purpose when $t \gg 1$. In particular, it establishes that for each fixed $j \in \mathbb{Z}$, the horizontal slice $i \mapsto u_{ij}(t)$ ‘crosses through’ the value $u = \frac{1}{2}$ in a monotonic fashion.

Proposition 2.2.1 (see §2.5). *There exists a time $T > 0$ such that for every $j \in \mathbb{Z}$ and $t \geq T$ there exists a unique $i_* = i_*(j, t)$ with the property*

$$0 < u_{i_*,j}(t) \leq \frac{1}{2}, \quad u_{i_*+1,j}(t) > \frac{1}{2}. \quad (2.2.11)$$

These functions $i(j, t)$ can be used to define a set of phases $(\gamma_j(t))_{j \in \mathbb{Z}}$ that measure in some sense where the value $u = \frac{1}{2}$ is ‘crossed’. More precisely, we define a function $\gamma : [T, \infty) \rightarrow \ell^\infty(\mathbb{Z})$ that acts as

$$\gamma_j(t) = i_*(j, t) - \Phi^{-1}(u_{i_*(j,t),j}(t)); \quad (2.2.12)$$

see Fig. 2.1. The motivation behind the second term on the right is our desire to recover the traditional phase when u is itself a travelling wave. Indeed, in the special case that

$$u_{i,j}(t) = \Phi(i - ct - \mu)$$

for some $\mu \in \mathbb{R}$, the phase condition $\Phi(0) = \frac{1}{2}$ implies that

$$i_*(j, t) = \lfloor ct + \mu \rfloor.$$

In particular, we obtain

$$\gamma_j(t) = ct + \mu,$$

which allows us to write

$$u_{i,j}(t) = \Phi(i - \gamma_j(t)). \quad (2.2.13)$$

The drawback of this relatively straightforward construction is that the phases $\gamma_j(t)$ will in general admit discontinuities. However, the size of these jumps will tend to zero as $t \rightarrow \infty$, which suffices for our asymptotic purposes.

Our main result here is that this phase description (2.2.13) holds asymptotically for any initial condition u^0 that satisfies (H0). In particular, for large time, the dynamics of the full solution u can be approximated by the behaviour of the phase coordinates $\gamma(t)$.

Theorem 2.2.2 (see §2.5). *Suppose that (Hg), (HΦ) and (H0) are satisfied and consider the solution u of the discrete Allen-Cahn equation (2.2.1) with the initial condition (2.2.9). Then we have the limit*

$$\lim_{t \rightarrow \infty} \sup_{(i,j) \in \mathbb{Z}^2} |u_{i,j}(t) - \Phi(i - \gamma_j(t))| = 0. \quad (2.2.14)$$

2.2.2 Interface evolution

Our second main goal is to uncover the long-term dynamics of the phase γ defined in (2.2.12). In particular, we show that this evolution can be approximated by a discrete version of the mean curvature flow with an appropriate drift term.

In order to formulate this equation, we pick a sequence $\Gamma \in \ell^\infty(\mathbb{Z})$ and introduce the discrete derivatives

$$\begin{aligned} [\partial^+ \Gamma]_j &= \Gamma_{j+1} - \Gamma_j, \\ [\partial^- \Gamma]_j &= \Gamma_j - \Gamma_{j-1}, \\ [\partial^{(2)} \Gamma]_j &= \Gamma_{j+1} - 2\Gamma_j + \Gamma_{j-1}, \end{aligned}$$

together with the sequence

$$[\beta_\Gamma]_j = \sqrt{1 + \frac{1}{2}(\partial^+ \Gamma)_j^2 + \frac{1}{2}(\partial^- \Gamma)_j^2}.$$

As explained in §2.1, the driving force in (2.2.3) below is not a constant as in the PDE case. Instead, it features additional terms that arise due to the underlying anisotropy of the lattice.

Theorem 2.2.3 (see §2.8). *Suppose that (Hg), (HΦ) and (H0) are all satisfied, consider the solution u of the LDE (2.2.1) with the initial condition (2.2.9) and recall the phase γ defined in (2.2.12). Then for every $\epsilon > 0$, there exists $\tau_\epsilon \geq T$ so that for any $\tau \geq \tau_\epsilon$, the solution*

$$\Gamma : [\tau, \infty) \rightarrow \ell^\infty(\mathbb{Z})$$

to the initial value problem

$$\begin{cases} \beta_\Gamma^{-1} \dot{\Gamma} &= \beta_\Gamma^{-3} \partial^{(2)} \Gamma + (c + [\partial_\theta^2 c_\theta]_{\theta=0}) - \beta_\Gamma^{-1} [\partial_\theta^2 c_\theta]_{\theta=0} \\ \Gamma(\tau) &= \gamma(\tau) \end{cases}$$

satisfies the estimate

$$\sup_{t \geq \tau} \|\Gamma(t) - \gamma(t)\|_{\ell^\infty} < \epsilon.$$

Our final result provides more detailed information on the asymptotics of γ in the special case that the initial condition u^0 is a localized perturbation from a front-like background state that is periodic in j . Indeed, this provides sufficient control on (2.2.3) to show that the corresponding solution converges to a planar travelling front. We emphasize that the case $P = 1$ encompasses the stability results from [43, 44], albeit only for horizontal waves.

Theorem 2.2.4 (see §2.9). *Suppose that (Hg), (HΦ) and (H0) are satisfied and consider the solution u of the discrete Allen-Cahn equation (2.2.1) with the initial condition (2.2.9). Suppose furthermore that there exists a sequence $u^{0;\text{per}} \in \ell^\infty(\mathbb{Z}^2)$ so that the following two properties hold.*

(a) *We have the limit*

$$u_{i,j}^0 - u_{i,j}^{0;\text{per}} \rightarrow 0, \quad \text{as } |i| + |j| \rightarrow \infty. \quad (2.2.15)$$

(b) *There exists an integer $P \geq 1$ so that*

$$u_{i,j+P}^{0;\text{per}} = u_{i,j}^{0;\text{per}}, \quad \text{for all } (i,j) \in \mathbb{Z}^2. \quad (2.2.16)$$

Then there exists a constant $\mu \in \mathbb{R}$ for which we have the limit

$$\lim_{t \rightarrow \infty} \sup_{(i,j) \in \mathbb{Z}^2} |u_{i,j}(t) - \Phi(i - ct - \mu)| = 0. \quad (2.2.17)$$

2.3 Omega limit points

The techniques used in [69] relied heavily upon the ability to construct so-called omega limit points. More specifically, consider a solution $u : \mathbb{R}^2 \times [0, \infty) \rightarrow \mathbb{R}$ to the PDE (2.1.6) together with an unbounded sequence $0 < t_1 < t_2 < \dots$ and a set of vertical shifts $(y_k) \subset \mathbb{R}$. One can then establish [69] the existence of an entire solution ω to (2.1.6) for which the convergence

$$u(x + ct_k, y + y_k, t + t_k) \rightarrow \omega(x, y, t) \quad \text{in } C_{\text{loc}}^{2,1}(\mathbb{R}^2 \times \mathbb{R}) \quad (2.3.1)$$

holds as $k \rightarrow \infty$, possibly after passing to a subsequence. This can be achieved efficiently by replacing x with the travelling wave coordinate $x - ct$.

Any direct attempt to generalize this procedure to the LDE setting will fail on account of the fact that $i - ct$ is not necessarily an integer. Indeed, this prevents us from introducing a well-defined co-moving frame. Our approach here to handle this is rather crude: we simply round the horizontal shifts upward towards the nearest integer.

To illustrate this, let us consider the planar wave solution

$$u_{ij}(t) = \Phi(i - ct)$$

together with an unbounded sequence $0 < t_1 < t_2 < \dots$ and a set of vertical shifts $(j_k) \subset \mathbb{Z}$. Possibly taking a subsequence, we obtain the convergence

$$[0, 1] \ni [ct_k] - ct_k \rightarrow \theta_\omega$$

as $k \rightarrow \infty$, which means that

$$u_{i+[ct_k], j+j_k}(t+t_k) = \Phi(i+[ct_k] - ct - ct_k) \rightarrow \Phi(i - ct + \theta_\omega)$$

as $k \rightarrow \infty$. In particular, we do still recover an entire solution, at the price of a small phase-shift that would not occur in the continuous framework. As we will see throughout the following sections, this phase-shift does not cause any qualitative difficulties.

Our main result confirms that our procedure indeed generates ω -limit points. In addition, it states that such limits are trapped between two travelling waves, which turns out to be a crucial point in our analysis. The consequences of this fact will be discussed in greater depth in §2.4.

Proposition 2.3.1. *Suppose that assumptions (Hg), (HΦ) and (H0) are satisfied. Let $u \in C^1([0, \infty); \ell^\infty(\mathbb{Z}^2))$ be a solution of the LDE (2.2.1). Then for any sequence (j_k, t_k) in $\mathbb{Z} \times [0, \infty)$ with $0 < t_1 < t_2 < \dots \rightarrow \infty$, there exists a subsequence (j_{n_k}, t_{n_k}) and a function $\omega \in C^1(\mathbb{R}; \ell^\infty(\mathbb{Z}^2))$ with the following properties.*

(i) *We have the convergence*

$$u_{i+[ct_{n_k}], j+j_{n_k}}(t+t_{n_k}) \rightarrow \omega_{i,j}(t) \quad \text{in } C_{\text{loc}}(\mathbb{Z}^2 \times \mathbb{R}) \quad (2.3.2)$$

as $k \rightarrow \infty$.

(ii) *The limit ω satisfies the discrete Allen-Cahn equation (2.2.1) on $\mathbb{Z}^2 \times \mathbb{R}$.*

(iii) *There exists a constant $\theta \in \mathbb{R}$ such that*

$$\Phi(i - ct - \theta) \leq \omega_{i,j}(t) \leq \Phi(i - ct + \theta), \quad \text{for all } i \in \mathbb{Z} \text{ and } t \in \mathbb{R}. \quad (2.3.3)$$

We refer to such a function ω as an ω -limit point of the solution u . The proof of the bounds (2.3.3) relies on the fact that the LDE (2.2.1) admits a comparison principle; see [44, Prop. 3.1]. In order to exploit this, we introduce the residual

$$\mathcal{J}[u] = \dot{u} - \Delta^+ u - f(u) \quad (2.3.4)$$

and recall that a function

$$u \in C^1([0, \infty); \ell^\infty(\mathbb{Z}^2))$$

is referred to as a sub- or super-solution to the discrete Allen-Cahn equation (2.2.1) if $\mathcal{J}[u]_{i,j}(t) \leq 0$ respectively $\mathcal{J}[u]_{i,j}(t) \geq 0$ holds for all $t \geq 0$ and $(i, j) \in \mathbb{Z}^2$. Our first result describes a standard pair of such solutions, using the well-known principle that uniform perturbations to the travelling wave Φ at $t = 0$ can be traded off for phase-shifts at $t = \infty$.

Lemma 2.3.2. *Assume that (Hg) and (H Φ) are satisfied. Then for any $q_0 \in (0, a)$ and $q_1 \in (0, 1 - a)$, there exist constants $\mu > 0$ and $C \geq 1$ so that the functions*

$$u_{i,j}^+(t) = \Phi(i - ct + Cq_0(1 - e^{-\mu t})) + q_0 e^{-\mu t}, \quad (2.3.5)$$

$$u_{i,j}^-(t) = \Phi(i - ct - Cq_1(1 - e^{-\mu t})) - q_1 e^{-\mu t} \quad (2.3.6)$$

are a super- respectively sub-solution of the discrete Allen-Cahn equation (2.2.1).

Proof. The arguments from Lemma 4.1 in [34] can be copied almost verbatim; see for example [20]. \square

We now turn to the solution u of the LDE (2.2.1) with the initial condition (2.2.9). Using two a-priori estimates we will show that u can eventually be controlled by time translates of u^+ and u^- . By exploiting the divergence $t_k \rightarrow \infty$ of the time-shifts for the ω -limit point, we can subsequently eliminate the uniform additive terms in (2.3.5)-(2.3.6) and recover the phase-shifts in (2.3.3).

Lemma 2.3.3. *Assume that (Hg) and (H0) are satisfied. Pick $q_0 \in (0, a)$ in such a way that the initial condition u^0 satisfies*

$$\limsup_{i \rightarrow -\infty} \sup_{j \in \mathbb{Z}} u_{i,j}^0 < q_0.$$

Then for every $t > 0$ we have the bound

$$\limsup_{i \rightarrow -\infty} \sup_{j \in \mathbb{Z}} u_{i,j}(t) < q_0. \quad (2.3.7)$$

Proof. First, we find a constant $d \in (0, q_0)$ for which

$$\limsup_{i \rightarrow -\infty} \sup_{j \in \mathbb{Z}} u_{i,j}^0 < d. \quad (2.3.8)$$

Next, we pick a constant M in such a way that

$$u_{i,j}^0 \leq d + M e^{i|c|}, \quad \text{for every } (i, j) \in \mathbb{Z}^2. \quad (2.3.9)$$

Writing $K > 0$ for the maximum value of the function g on the interval $[a, 1]$, we choose $\alpha > 0$ sufficiently large to have

$$\alpha|c| - \frac{c^4}{12} \cosh|c| \geq \frac{2K}{a-d}. \quad (2.3.10)$$

We now claim that the j -independent function

$$w_{i,j}(t) = d + Me^{|\alpha|(i+|c|t+\alpha t)} \quad (2.3.11)$$

is a super-solution to (2.2.1). To see this, we compute

$$\begin{aligned} \mathcal{J}[w]_{i,j}(t) &= Me^{|\alpha|(i+|c|t+\alpha t)} \left(c^2 + \alpha|c| - e^{-|c|} - e^{|c|} + 2 \right) - g(w_{i,j}(t)) \\ &= Me^{|\alpha|(i+|c|t+\alpha t)} \left(\alpha|c| - \frac{c^4}{12} \cosh \tilde{c} \right) - g(w_{i,j}(t)) \\ &\geq (w_{i,j}(t) - d) \frac{2K}{a-d} - g(w_{i,j}(t)), \end{aligned}$$

where \tilde{c} is a number between 0 and $|c|$. For $w_{i,j}(t) \in [0, a] \cup [1, \infty)$, we have $g(w_{i,j}(t)) \leq 0$, which immediately gives $\mathcal{J}[w]_{i,j}(t) \geq 0$. On the other hand, for $w_{i,j}(t) \in [a, 1]$ our choice for K yields

$$\mathcal{J}[w]_{i,j}(t) \geq (a-d) \frac{2K}{a-d} - K \geq K > 0.$$

Applying the comparison principle we conclude

$$u_{i,j}(t) \leq w_{i,j}(t) = d + Me^{|\alpha|(i+|c|t+\alpha t)}, \quad (2.3.12)$$

for every $t \geq 0$ and $(i, j) \in \mathbb{Z}^2$. Taking the supremum over $j \in \mathbb{Z}$ and sending i to $-\infty$ we obtain the desired inequality (2.3.7). \square

Lemma 2.3.4. *Suppose that (Hg), (HΦ) and (H0) are satisfied. Let u be the solution of the discrete Allen-Cahn equation (2.2.1) with the initial condition (2.2.9). Then for every $q_0 > 0$ there exists $T > 0$ so that*

$$u_{i,j}(t) \leq 1 + \frac{q_0}{2} \quad (2.3.13)$$

holds for every $t \geq T$ and $(i, j) \in \mathbb{Z}^2$.

Proof. Let \tilde{u} be the solution to the scalar initial value problem

$$\begin{cases} \tilde{u}_t &= g(\tilde{u}), & t > 0 \\ \tilde{u}(0) &= \|u^0\|_{\ell^\infty(\mathbb{Z}^2)}. \end{cases} \quad (2.3.14)$$

Since $g(u) < 0$ for all $u > 1$, there exists $T > 0$ such that $\tilde{u}(t) \leq 1 + \frac{q_0}{2}$ for all $t \geq T$. Exploiting the fact that \tilde{u} is also a spatially homogeneous solution to (2.2.1), the comparison principle yields $u_{i,j}(t) \leq \tilde{u}(t)$ for all $t \geq 0$ and $(i, j) \in \mathbb{Z}^2$. Combining these observations leads directly to (2.3.13). \square

Lemma 2.3.5. *Assume that (Hg), (HΦ) and (H0) are satisfied. Then there exists a time $T > 0$ together with constants*

$$q_0 \in (0, a), \quad q_1 \in (0, 1-a), \quad \theta_0 \in \mathbb{R}, \quad \theta_1 \in \mathbb{R}, \quad \mu > 0, \quad C > 0 \quad (2.3.15)$$

so that the solution u to (2.2.1) with the initial condition (2.2.9) satisfies the estimates

$$u_{i,j}(t) \leq \Phi \left(i + \theta_0 - c(t - T) + Cq_0(1 - e^{-\mu(t-T)}) \right) + q_0 e^{-\mu(t-T)}, \quad (2.3.16)$$

$$u_{i,j}(t) \geq \Phi \left(i - \theta_1 - c(t - T) - Cq_1(1 - e^{-\mu(t-T)}) \right) - q_1 e^{-\mu(t-T)}, \quad (2.3.17)$$

for all $t \geq T$.

Proof. We first choose $q_0 \in (0, a)$ in such a way that

$$\limsup_{i \rightarrow -\infty} \sup_{j \in \mathbb{Z}} u_{i,j}^0 < q_0. \quad (2.3.18)$$

Using Lemma 2.3.4, we obtain $T > 0$ for which

$$u_{i,j}(T) \leq 1 + \frac{q_0}{2} \quad \text{for every } (i, j) \in \mathbb{Z}^2. \quad (2.3.19)$$

On the other hand, Lemma 2.3.3 allows us to find $\vartheta_a \in \mathbb{Z}$ so that

$$u_{i,j}(T) \leq q_0, \quad \text{for } i \leq \vartheta_a \text{ and } j \in \mathbb{Z}. \quad (2.3.20)$$

Finally, in view of the limits (2.2.6) there exists $\vartheta_b \in \mathbb{Z}$ for which

$$\Phi(i) \geq 1 - \frac{q_0}{2}, \quad \text{for every } i \geq \vartheta_b.$$

Combining these inequalities and recalling the definition (2.3.5), we obtain

$$u_{i,j}(T) \leq \Phi(i - \vartheta_a + \vartheta_b) + q_0 = u_{i - \vartheta_a + \vartheta_b}^+(0) \quad (2.3.21)$$

for all $i \in \mathbb{Z}$. The desired upper bound (2.3.16) with $\theta_0 = \vartheta_b - \vartheta_a$ now follows from Lemma 2.3.2 and the comparison principle. The lower bound can be obtained in a similar fashion. \square

Proof of Proposition 2.3.1. Fix an integer $L \in \mathbb{N}$ and consider the functions

$$u^k \in C([-L, L]; \mathbb{R}^{(2L+1) \times (2L+1)})$$

that are defined by

$$u_{i,j}^k(t) = u_{i + \lceil ct_k \rceil, j + j_k}(t + t_k), \quad (i, j, t) \in \{-L, \dots, L\}^2 \times [-L, L]$$

for all sufficiently large k . Lemma 2.3.4 implies that the solution u and hence the functions u^k are globally bounded. Since the derivative \dot{u} satisfies (2.2.1), it follows that \dot{u}^k is also a globally bounded sequence. Hence, Ascoli-Arzelà implies that the sequence u^k is relatively compact. By using a standard diagonalization argument together with (2.2.1), we obtain a subsequence u^{n_k} and a function $\omega : \mathbb{R} \rightarrow \ell^\infty(\mathbb{Z}^2)$ so that

$$\sup_{(i,j,t) \in K} |u_{i,j}^{n_k}(t) - \omega_{i,j}(t)| + |\dot{u}_{i,j}^{n_k}(t) - \dot{\omega}_{i,j}(t)| \rightarrow 0,$$

for every compact $K \subset \mathbb{Z}^2 \times \mathbb{R}$. This immediately implies (i) and (ii). The bounds (2.3.3) follow directly from Lemma 2.3.5. \square

2.4 Trapped entire solutions

The main point of this section is to prove that every entire solution that is trapped between two traveling waves is a traveling wave itself. This is a very useful result when combined with Proposition 2.3.1, since it implies that every ω -limit point of the solution u is a traveling wave. This will turn out to be a crucial tool during our analysis of the large time behaviour of u .

Proposition 2.4.1. *Assume that (Hg) and (H Φ) are satisfied and consider a function $\omega \in C^1(\mathbb{R}; \ell^\infty(\mathbb{Z}^2))$ that satisfies the Allen-Cahn LDE (2.2.1) for all $t \in \mathbb{R}$. Assume furthermore that there exists a constant θ for which the bounds*

$$\Phi(i - ct - \theta) \leq \omega_{i,j}(t) \leq \Phi(i - ct + \theta) \quad (2.4.1)$$

hold for all $(i, j) \in \mathbb{Z}^2$ and $t \in \mathbb{R}$. Then there exists a constant $\theta_0 \in [-\theta, \theta]$ so that

$$\omega_{i,j}(t) = \Phi(i - ct - \theta_0), \quad \text{for all } (i, j) \in \mathbb{Z}^2, t \in \mathbb{R}.$$

This result is a generalization of [13, Thm. 3.1] to the current spatially discrete setting. The main complication lies in the fact that the LDE (2.2.1) is a nonlocal equation, as opposed to the PDE (2.1.6). For example, if a smooth function $f : E \subset \mathbb{R}^2 \rightarrow \mathbb{R}$ attains a local minimum at some point x_0 , then we automatically have $\Delta f(x_0) \geq 0$. This is an important ingredient for the arguments in [13], but fails to hold in our spatially discrete setting.

Indeed, if $v \in \ell^\infty(\mathbb{Z}^2)$ attains a minimum in $E \subset \mathbb{Z}^2$ at some point $(i, j) \in E$, it does not automatically follow that the discrete Laplacian satisfies $(\Delta^+ v)_{i,j} \geq 0$. This conclusion can only be obtained if one can verify that the nearest neighbours of (i, j) are also contained in E . This is the key purpose of our first technical result.

Lemma 2.4.2. *Consider the setting of Proposition 2.4.1 and pick a sufficiently small $\delta > 0$. Choose a pair $(I, J) \in \mathbb{Z}^2$ together with a constant $\sigma \in \mathbb{R}$. Suppose for some $\kappa \in \mathbb{Z}$ that the function*

$$v_{i,j}^\sigma(t) = \omega_{i+I, j+J} \left(t + \frac{I}{c} + \frac{\sigma}{c} \right) \quad (2.4.2)$$

satisfies the inequality

$$v_{i,j}^\sigma(t) \leq \omega_{i,j}(t) \quad (2.4.3)$$

whenever $i - ct \in [\kappa, \kappa + 1]$. Then the following claims holds true.

- (i) If $\omega_{i,j}(t) \geq 1 - \delta$ whenever $i - ct \geq \kappa$, then in fact (2.4.3) holds for all $i - ct \geq \kappa$.
- (ii) If $v_{i,j}^\sigma(t) \leq \delta$ whenever $i - ct \leq \kappa + 1$, then in fact (2.4.3) holds for all $i - ct \leq \kappa + 1$.

Proof. Starting with (i), we define the set

$$E := \{(i, j, t) \in \mathbb{Z}^2 \times \mathbb{R} : i - ct \geq \kappa\}.$$

Since both functions ω and v^σ are globally bounded, the quantity

$$\epsilon^* = \inf \{ \epsilon > 0 : v^\sigma \leq \omega + \epsilon \text{ in } E \}$$

is finite. In addition, by continuity we have

$$v^\sigma \leq \omega + \epsilon^* \quad \text{in } E. \quad (2.4.4)$$

To prove the claim, it suffices to show that $\epsilon^* = 0$. Assuming to the contrary that $\epsilon^* > 0$, we can find sequences $\epsilon_n \nearrow \epsilon^*$ and (i_n, j_n, t_n) in E with the property that

$$\omega_{i_n, j_n}(t_n) + \epsilon_n < v_{i_n, j_n}^\sigma(t_n) \leq \omega_{i_n, j_n}(t_n) + \epsilon^* \quad \text{for each } n \in \mathbb{N}. \quad (2.4.5)$$

Sending $n \rightarrow \infty$ we conclude that

$$\lim_{n \rightarrow \infty} \omega_{i_n, j_n}(t_n) - v_{i_n, j_n}^\sigma(t_n) + \epsilon^* = 0. \quad (2.4.6)$$

Now, notice that the assumption (2.4.1) and the inequality $\epsilon^* > 0$ imply that the sequence $l_n := i_n - ct_n$ is bounded. In addition, our assumption (2.4.3) implies that $l_n > \kappa + 1$. In particular, we can assume that the bounded sequence $i_n - \lceil ct_n \rceil$ is equal to an integer $L \geq \kappa$.

Applying Proposition 3.1 to the function ω and the sequence (j_n, t_n) , we obtain a limiting function ω^∞ for which we have

$$\lim_{n \rightarrow \infty} \omega_{i+\lceil ct_n \rceil, j+j_n}(t+t_n) = \omega_{i,j}^\infty(t), \quad (2.4.7)$$

for each $(i, j, t) \in \mathbb{Z}^2 \times \mathbb{R}$. By construction it also holds that

$$\lim_{n \rightarrow \infty} v_{i+\lceil ct_n \rceil, j+j_n}^\sigma(t+t_n) = \omega_{i+I, j+J}^\infty(t + \frac{I}{c} + \frac{\sigma}{c}). \quad (2.4.8)$$

Next we define the function $z = z_{i,j}(t)$ as

$$z_{i,j}(t) = \omega_{i,j}^\infty(t) - \omega_{i+I, j+J}^\infty(t + \frac{I}{c} + \frac{\sigma}{c}) + \epsilon^*. \quad (2.4.9)$$

For $(i, j, t) \in E$ we have $(i+\lceil ct_n \rceil, j+j_n, t+t_n) \in E$. Combining this with the fact that the inequality (2.4.4) survives the limit (2.4.7), we have $z_{i,j}(t) \geq 0$ in E . By (2.4.6) we obtain $z_{L,0}(0) = 0$. Also, for $i-ct = \kappa$, we have $(i+\lceil ct_n \rceil, j+j_n, t+t_n) \in [\kappa, \kappa+1]$. In particular, we find

$$z_{i,j}(t) \geq \epsilon^* > 0, \quad \text{for } i-ct = \kappa. \quad (2.4.10)$$

Therefore, it must hold that $L \geq \kappa + 1$.

We pick δ to be small enough so that g is non-increasing on $[1-\delta, 1]$. Since $\omega^\infty \in [1-\delta, 1]$ and g is locally Lipschitz continuous on E , there exists $B > 0$ so that

$$\begin{aligned} \dot{z}_{i,j}(t) - (\Delta^+ z)_{i,j}(t) &= g(\omega_{i,j}^\infty(t)) - g(\omega_{i+I, j+J}^\infty(t + \frac{I}{c} + \frac{\sigma}{c})) \\ &\geq g(\omega_{i,j}^\infty(t) + \epsilon^*) - g(\omega_{i+I, j+J}^\infty(t + \frac{I}{c} + \frac{\sigma}{c})) \\ &\geq -Bz_{i,j}(t) \end{aligned} \quad (2.4.11)$$

for all $(i, j, t) \in E$. Since z attains its minimum at the point $(L, 0, 0) \in E$ with $L \geq \kappa + 1$, we have $\dot{z}_{L,0}(0) = 0$. In addition, the inequality $(\Delta^+ z)_{L,0}(0) \geq 0$ holds since all the nearest neighbours of $(L, 0, 0)$ are contained in E . In particular, we compute

$$0 \leq \dot{z}_{L,0}(0) - (\Delta^+ z)_{L,0}(0) + Bz_{L,0}(0) = -(\Delta^+ z)_{L,0}(0) \leq 0. \quad (2.4.12)$$

Therefore, $(\Delta^+ z)(0)_{L,0} = 0$ must hold, which implies that $z_{0,L-1}(0) = 0$.

If $L = \kappa + 1$ then we are done, since $z \geq \epsilon^* > 0$ for $i - ct = \kappa$ which contradicts (2.4.10). On the other hand, if $L - 1 \geq \kappa + 1$ we can iteratively decrease L using this procedure until we reach the desired contradiction. Statement (ii) can be obtained in a similar fashion using $[ct_n]$ instead of $[ct_n]$. \square

Lemma 2.4.3. *Consider the setting of Propostion 2.4.1, fix an arbitrary pair $(I, J) \in \mathbb{Z}^2$ and recall the functions v^σ defined in (2.4.2) Then the quantity*

$$\sigma_* := \inf \{ \sigma \in \mathbb{R} : v^{\tilde{\sigma}} \leq \omega \text{ in } \mathbb{Z}^2 \times \mathbb{R} \text{ for all } \tilde{\sigma} \geq \sigma \} \quad (2.4.13)$$

satisfies $\sigma_* \leq 0$.

Proof. First we show that $\sigma_* < \infty$. Without loss of generality, we may assume that $0 < \delta < 1/2$ holds for the constant defined in Lemma 2.4.2. The inequalities (2.4.1) allow $\kappa \in \mathbb{N}$ such that

$$\begin{aligned} \omega_{i,j}(t) &\geq 1 - \delta, & i - ct &\geq \kappa, \\ \omega_{i,j}(t) &\leq \delta, & i - ct &\leq -\kappa. \end{aligned} \quad (2.4.14)$$

For $\sigma \geq 2\kappa + 1$ and $i - ct \leq \kappa + 1$ one has $i - ct - \sigma \leq -\kappa$. It follows from (2.4.14) that $v^\sigma \leq \delta$ on $i - ct \leq \kappa + 1$. Using $\delta \leq 1 - \delta$ we have $v^\sigma \leq \omega$ on $i - ct \in [\kappa, \kappa + 1]$. Hence, both items (i) and (ii) of Lemma 2.4.2 are satisfied and the bound $v^\sigma \leq \omega$ on \mathbb{R} follows immediately. Since $\sigma \geq 2\kappa + 1$ was arbitrary, we conclude that $\sigma_* \leq 2\kappa + 1$.

Arguing by contradiction, let us assume that $\sigma_* > 0$. Defining the set

$$S = \{-\kappa - 1 \leq i - ct \leq \kappa + 1\}, \quad (2.4.15)$$

we now claim that

$$\inf_S (\omega - v^{\sigma_*}) = 0. \quad (2.4.16)$$

Assume to the contrary that $\inf_S (\omega - v^{\sigma_*}) = K > 0$. Then, using the global Lipschitz continuity of ω , there exists a constant $M > 0$ such that

$$\omega_{i,j}(t) - v_{i,j}^{\sigma_* - \mu}(t) = \omega_{i,j}(t) - v_{i,j}^{\sigma_*}(t) + v_{i,j}^{\sigma_*}(t) - v_{i,j}^{\sigma_* - \mu}(t) \geq K - M\mu \quad (2.4.17)$$

holds for every $\mu \geq 0$ and $(i, j, t) \in S$. Hence, there exists $\mu_0 \in (0, \sigma_*)$ such that $v^{\sigma_* - \mu} \leq \omega$ on S , for all $\mu \in [0, \mu_0]$. Item (i) in Lemma 2.4.2 implies that $v^{\sigma_* - \mu} \leq \omega$ for $i - ct \geq \kappa$ and for all $\mu \in [0, \mu_0]$. Furthermore, since $\sigma_* - \mu \geq 0$, we have $v^{\sigma_* - \mu} \leq \delta$ for $i - ct \leq -\kappa$. Since also $v^{\sigma_* - \mu} \leq \omega$ for $-\kappa - 1 \leq i - ct \leq -\kappa$, item (ii) of Lemma 2.4.2 implies that $v^{\sigma_* - \mu} \leq \omega$ also holds on $i - ct \leq -\kappa$. All together, we have $v^{\sigma_* - \mu} \leq \omega$ on $\mathbb{Z}^2 \times \mathbb{R}$, which contradicts the minimality of σ_* and yields (2.4.16).

We can hence find a sequence (i_n, j_n, t_n) in S such that

$$\omega_{i_n, j_n}(t_n) - v_{i_n, j_n}^{\sigma_*}(t_n) \rightarrow 0 \quad \text{as } n \rightarrow \infty. \quad (2.4.18)$$

Since $i_n - ct_n$ is bounded, we can assume that $i_n - \lceil ct_n \rceil$ is equal to a constant, which we denote by L . As before, we obtain the convergence

$$\lim_{n \rightarrow \infty} \omega_{i+\lceil ct_n \rceil, j+j_n}(t+t_n) = \omega_{i,j}^\infty(t), \quad (2.4.19)$$

where ω^∞ is also an entire solution of the LDE (2.2.1). Hence, the function $z = z_{i,j}(t)$ defined as

$$z_{i,j}(t) := \omega_{i,j}^\infty(t) - \omega_{i+I, j+J}^\infty(t + \frac{I}{c} + \frac{\sigma_*}{c}) \quad (2.4.20)$$

satisfies

$$z_{i,j} \geq 0 \text{ for all } (i, j, t) \in \mathbb{Z}^2 \times \mathbb{R} \quad (2.4.21)$$

and $z_{L,0}(0) = 0$. Using an argument similar to the one in the proof of Lemma 2.4.2, it follows that $z_{i,j}(0) = 0$ for all $(i, j) \in \mathbb{Z}^2$. We then obtain $z \equiv 0$ by the uniqueness of bounded solutions for (2.2.1).

In particular, we have $\omega_{0,0}^\infty(0) = \omega_{kI, kJ}^\infty(kI/c + k\sigma_*/c)$ for all $k \in \mathbb{Z}$. However, we also have the limits

$$\lim_{k \rightarrow -\infty} \omega_{kI, kJ}^\infty(kI/c + k\sigma_*/c) = 1, \quad \lim_{k \rightarrow \infty} \omega_{kI, kJ}^\infty(kI/c + k\sigma_*/c) = 0, \quad (2.4.22)$$

since ω^∞ is trapped between two traveling waves as well. We have hence reached a contradiction and conclude $\sigma_* \leq 0$. \square

Proof of Proposition 2.4.1. From Lemma 2.4.3, we know that

$$\omega_{i,j}(t) \geq \omega_{i+I, j+J}(t + \frac{I}{c}) \quad \text{on } \mathbb{Z}^2 \times \mathbb{R}, \quad (2.4.23)$$

for arbitrary $(I, J) \in \mathbb{Z}^2$. Hence, the function ω depends only on the value of $i - ct$. More precisely, there exists a function ψ such that $\omega_{i,j}(t) = \psi(i - ct)$. The result now follows directly from the fact that solutions to the travelling wave problem (2.2.6)-(2.2.7) for $\theta = 0$ and $c \neq 0$ are unique up to translation. \square

2.5 Large time behaviour of u

The main goal of this section is to study the qualitative large time behaviour of the solution u to our main initial value problem. In particular, we connect this behaviour to the dynamics of the phase γ defined in (2.2.12) and thereby establish Theorem 2.2.2. In addition, we provide an asymptotic flatness result for this phase.

Our first main result concerns the large-time behaviour of the interfacial region

$$I_t = \{(i, j) \in \mathbb{Z}^2 : \Phi(-2) \leq u_{i,j}(t) \leq \Phi(2)\} \quad (2.5.1)$$

where u takes values close to $1/2$. For fixed j and t , we establish that the horizontal coordinate i can not jump in and out from the interface region, which is non-empty. In particular, once the map $i \mapsto u_{i,j}(t)$ enters the interval $[\Phi(-2), \Phi(2)]$ from below, it cannot exit throughout the lower boundary. In addition, it is strictly increasing in i and cannot reenter the interval once it has left through the upper boundary.

Proposition 2.5.1. *Suppose that the assumptions (Hg), (H Φ) and (H0) are satisfied and let u be a solution of the discrete Allen-Cahn equation (2.2.1) with the initial condition (2.2.9). Then there exists a constant $T > 0$ so that the following statements are satisfied.*

(i) *For each $t \geq T$ and $j \in \mathbb{Z}$ there exists $i \in \mathbb{Z}$ for which*

$$\Phi(-2) < u_{i,j}(t) \leq \frac{1}{2}. \quad (2.5.2)$$

(ii) *We have the inequality*

$$\inf_{t \geq T, (i,j) \in I_t} u_{i+1,j}(t) - u_{i,j}(t) > 0. \quad (2.5.3)$$

(iii) *Consider any $t \geq T$ and $(i, j) \in \mathbb{Z}^2$ for which $u_{i,j}(t) \leq \Phi(-2)$ holds. Then we also have $u_{i-1,j}(t) \leq \Phi(-2)$.*

(iv) *Consider any $t \geq T$ and $(i, j) \in \mathbb{Z}^2$ for which $u_{i,j}(t) \geq \Phi(2)$ holds. Then we also have $u_{i+1,j}(t) \geq \Phi(2)$.*

Our second main result shows that the discrete derivative of the phase with respect to j tends to zero. This will turn out to be crucial in order to keep the mean curvature flow under control. We emphasize that this does not necessarily mean that the phase tends to a constant; see (2.1.39).

Proposition 2.5.2. *Consider the setting of Proposition 2.5.1 and recall the phase $\gamma : [T, \infty) \rightarrow \ell^\infty(\mathbb{Z})$ defined in (2.2.12). Then we have the limit*

$$\lim_{t \rightarrow \infty} \sup_{j \in \mathbb{Z}} |\gamma_{j+1}(t) - \gamma_j(t)| = 0.$$

Proof of Proposition 2.2.1. The statement follows directly from Proposition 2.5.1. \square

2.5.1 Proof of Proposition 2.5.1 and Theorem 2.2.2

The key towards establishing Proposition 2.5.1 is to obtain strict monotonicity properties in compact regions that move with the wavespeed c . This is achieved in the following result, which leverages the travelling wave identification obtained in Proposition 2.4.1.

Lemma 2.5.3. *Consider the setting of Proposition 2.5.1 and pick a constant $R > 0$. Then there exists a constant $T > 0$ such that*

$$\inf_{j \in \mathbb{Z}, |i-ct| \leq R, t \geq T} u_{i+1,j}(t) - u_{i,j}(t) > 0. \quad (2.5.4)$$

Proof. Arguing by contradiction, let us assume that there exists a constant $R > 0$ so that

$$\inf_{j \in \mathbb{Z}, |i-ct| \leq R, t \geq T} u_{i+1,j}(t) - u_{i,j}(t) \leq 0$$

holds for every $T > 0$. We can then find a sequence $(t_n, i_n, j_n) \in (0, \infty) \times \mathbb{Z}^2$ with $0 < t_1 < t_2 < \dots \rightarrow \infty$ for which we have the inequalities

$$|i_n - ct_n| \leq R, \quad u_{i_n+1, j_n}(t_n) - u_{i_n, j_n}(t_n) \leq 1/n. \quad (2.5.5)$$

In particular, we may assume that the bounded sequence of integers $i_n - \lceil ct_n \rceil$ is identically equal to some constant $L \in \mathbb{Z}$. Applying Proposition 2.3.1 we obtain the convergence

$$u_{i+\lceil ct_n \rceil, j+j_n}(t+t_n) \rightarrow \omega_{ij}(t) \quad (2.5.6)$$

as $n \rightarrow \infty$, in which ω is an ω -limit point of the function u . In view of Proposition 2.4.1 we have $\omega_{i,j}(t) = \Phi(i - ct - \theta_0)$ for some $\theta_0 \in \mathbb{R}$, which allow us to write

$$\begin{aligned} 1/n &\geq u_{i_n+1, j_n}(t_n) - u_{i_n, j_n}(t_n) \\ &= u_{L+\lceil ct_n \rceil+1, j_n}(t_n) - u_{L+\lceil ct_n \rceil, j_n}(t_n) \\ &\rightarrow \omega_{L+1, 0}(0) - \omega_{L, 0}(0) \\ &= \Phi(L+1 - \theta_0) - \Phi(L - \theta_0) \end{aligned}$$

for $n \rightarrow \infty$. This violates the strict monotonicity $\Phi' > 0$ and hence yields the desired contradiction. \square

Proof of Proposition 2.5.1. We first prove item (iii). Assuming that this statement fails, we can find a sequence (t_k, i_k, j_k) for which we have $0 < t_1 < t_2 < \dots \rightarrow \infty$ together with the inequalities

$$u_{i_k, j_k}(t_k) \leq \Phi(-2), \quad u_{i_k-1, j_k}(t_k) > \Phi(-2). \quad (2.5.7)$$

It follows from Lemma 2.3.5 that the sequence $i_k - ct_k$ is bounded. Arguing as in the proof of Lemma 2.5.3, we can hence again assume that there exists $L \in \mathbb{Z}$ for which we have $L = i_k - \lceil ct_k \rceil$. In addition, we obtain the limits

$$u_{i_k, j_k}(t_k) \rightarrow \omega_{L, 0}(0) \leq \Phi(-2), \quad u_{i_k-1, j_k}(t_k) \rightarrow \omega_{L-1, 0}(0) \geq \Phi(-2). \quad (2.5.8)$$

Here ω is an ω -limit point for u , which must be a travelling wave by Proposition 2.4.1. This again violates the strict monotonicity of Φ . Item (iv) follows analogously.

Turning to (i), we assume that there exists a sequence (t_k, i_k, j_k) with $T \leq t_1 < t_2 < \dots \rightarrow \infty$ together with

$$u_{i_k, j_k}(t_k) \leq \Phi(-2), \quad u_{i_k+1, j_k}(t_k) > \frac{1}{2} = \Phi(0) \quad (2.5.9)$$

and seek a contradiction. Arguing as above, we can find $L \in \mathbb{Z}$ together with an ω -limit point ω for u with

$$\omega_{L, 0} \leq \Phi(-2), \quad \omega_{L+1, 0}(0) \geq \Phi(0), \quad (2.5.10)$$

which violates Proposition 2.4.1.

It remains to establish (ii). Picking $t \geq T$ and $(i, j) \in I_t$, it follows from Lemma 2.3.5 that $i - ct$ is bounded by some constant R that depends only on T . Increasing T if necessary, we can apply Lemma 2.5.3 to obtain the desired bound (2.5.3). \square

Lemma 2.5.4. *Consider the setting of Proposition 2.5.1 and recall the phase $\gamma : [T, \infty) \rightarrow \ell^\infty(\mathbb{Z})$ defined in (2.2.12). Then there exists $T_* \geq T$ and $M > 0$ such that for every $t \geq T_*$ we have*

$$\|\gamma(t) - ct\|_{\ell^\infty} \leq M. \quad (2.5.11)$$

Proof. In view of the definition (2.2.12) it suffices to show that $i_* - ct$ is bounded. Combining Lemma 2.3.5 and (2.2.11) and possibly increasing $T > 0$, we see that

$$\begin{aligned} \Phi(0) \leq u_{i_*(j,t)+1,j}(t) &\leq \Phi\left(i_*(j,t) + 1 + \theta_0 - ct + cT + Cq_0(1 - e^{-\mu(t-T)})\right) \\ &\quad + q_0 e^{-\mu(t-T)} \end{aligned}$$

for all $t \geq T$. Choosing $T_* \geq T$ in such a way that

$$\Phi(0) - q_0 e^{-\mu(T_*-T)} \geq \Phi(-1),$$

we conclude that

$$i_*(j,t) + 1 + \theta_0 - ct + cT + Cq_0(1 - e^{-\mu(t-T)}) > -1, \quad t \geq T_*. \quad (2.5.12)$$

Hence, $i_* - ct$ is bounded from below. An upper bound can be obtained in a similar way. \square

Proof of Theorem 2.2.2. Arguing by contradiction once more, let us assume that there exist $\delta > 0$ together with sequences $(i_k, j_k) \in \mathbb{Z}^2$ and $T \leq t_1 < t_2 < \dots \rightarrow \infty$ for which

$$|\Delta_k| := |u_{i_k, j_k}(t_k) - \Phi(i_k - \gamma_{j_k}(t_k))| \geq \delta. \quad (2.5.13)$$

We first claim that the sequence $i_k - ct_k$ is bounded. To see this, we first use Lemma 2.5.4 to conclude that $\gamma_{j_k}(t_k) - ct_k$ is bounded. Using (2.3.17) we subsequently find

$$\Delta_k \geq \Phi(i_k - ct_k + \alpha_k) - q_1 e^{-\mu(t_k-T)} - \Phi(i_k - ct_k + \beta_k),$$

in which

$$\alpha_k = cT - \theta_1 - Cq_1(1 - e^{-\mu(t_k-T)}), \quad \beta_k = ct_k - \gamma_{j_k}(t_k) \quad (2.5.14)$$

are two bounded sequences. In particular, if $i_k - ct_k$ is unbounded we can use the exponential decay of Φ to achieve $\Delta_k \geq -\delta$ for all large k . A similar argument using (2.3.16) yields $\Delta_k \leq \delta$, which contradicts (2.5.13) and hence establishes our claim.

In particular, we can extract a constant subsequence $i_k - [ct_k] =: L \in \mathbb{Z}$. Passing to a further subsequence, we may also assume that $i_*(j_k, t_k) - [ct_k] =: \tilde{L} \in \mathbb{Z}$. The definition (2.2.12) allows us to write

$$\begin{aligned} \Phi(i_k - \gamma_{j_k}(t_k)) &= \Phi\left(i_k - i_*(j_k, t_k) + \Phi^{-1}\left(u_{i_*(j_k, t_k), j_k}(t_k)\right)\right) \\ &= \Phi\left(i_k - [ct_k] - i_*(j_k, t_k) + [ct_k] + \Phi^{-1}\left(u_{i_*(j_k, t_k), j_k}(t_k)\right)\right) \\ &= \Phi\left(L - \tilde{L} + \Phi^{-1}\left(u_{\tilde{L} + [ct_k], j_k}(t_k)\right)\right). \end{aligned}$$

Applying Proposition 2.3.1, we see that there exists an ω -limit point ω for u for which the limits

$$u_{i_k, j_k}(t_k) \rightarrow \omega_{L,0}(0), \quad u_{\tilde{L} + \lceil ct_k \rceil, j_k}(t_k) \rightarrow \omega_{\tilde{L},0}(0) \quad (2.5.15)$$

hold as $k \rightarrow \infty$. Writing $\omega_{i,j}(t) = \Phi(i - ct - x_0)$ in view of Proposition 2.4.1, we hence find

$$\Delta_k \rightarrow \Phi(L - x_0) - \Phi\left(L - \tilde{L} + \Phi^{-1}(\Phi(\tilde{L} - x_0))\right) = 0 \quad (2.5.16)$$

as $k \rightarrow \infty$, which clearly contradicts (2.5.13). \square

2.5.2 Phase asymptotics

In this subsection we shift our attention to vertical differences of the phase γ , in order to establish Proposition 2.5.2. Our first result resembles Lemma 2.5.3 in the sense that we study the interfacial region of the wave, but in this case we get a flatness result. This can subsequently be used to obtain a bound on the vertical differences of the function i_* defined in (2.2.11), which in view of (2.2.12) allows us to analyze the phase γ .

Lemma 2.5.5. *Consider the setting of Proposition 2.5.1 and pick a constant $R > 0$. Then we have the limit*

$$\lim_{t \rightarrow \infty} \sup_{j \in \mathbb{Z}, |i-ct| \leq R} |u_{i,j+1}(t) - u_{i,j}(t)| = 0.$$

Proof. Assume to the contrary that there exist constants $R > 0$ and $\delta > 0$ together with sequences $(i_k, j_k) \in \mathbb{Z}^2$ and $0 < t_1 < t_2 < \dots \rightarrow \infty$ that satisfy the inequalities

$$|i_k - ct_k| \leq R, \quad |u_{i_k, j_k+1}(t_k) - u_{i_k, j_k}(t_k)| \geq \delta. \quad (2.5.17)$$

As in the proof of the Lemma 2.5.3, we may assume that $i_k - \lceil ct_k \rceil = L \in \mathbb{Z}$ and use Proposition 2.3.1 to conclude the convergence

$$\begin{aligned} u_{i_k, j_k+1}(t + t_k) - u_{i_k, j_k}(t_k) &= u_{L + \lceil ct_k \rceil, j_k+1}(t_k) - u_{L + \lceil ct_k \rceil, j_k}(t_k) \\ &\rightarrow \omega_{L,1}(0) - \omega_{L,0}(0) \\ &= 0, \end{aligned} \quad (2.5.18)$$

in which ω is an ω -limit point of the function u . The last identity follows from Proposition 2.4.1, which states that ω is a planar wave travelling in the horizontal direction. This obviously contradicts (2.5.17) and hence concludes the proof. \square

Lemma 2.5.6. *Consider the setting of Proposition 2.5.1 and recall the function i_* defined by (2.2.11). Then there exists $\tilde{T} > T$ so that*

$$|i_*(j+1, t) - i_*(j, t)| \leq 1 \quad (2.5.19)$$

holds for all $j \in \mathbb{Z}$ and all $t \geq \tilde{T}$.

Proof. If the above claim does not hold, we can find sequences $(i_k, \tilde{i}_k, j_k) \in \mathbb{Z}^3$ and $T < t_1 < t_2 < \dots \rightarrow \infty$ for which the inequality $|i_k - \tilde{i}_k| > 1$ holds, together with

$$\begin{cases} u_{i_k, j_k}(t_k) \leq 1/2, \\ u_{i_k+1, j_k}(t_k) > 1/2, \end{cases} \quad \begin{cases} u_{\tilde{i}_k, j_k+1}(t_k) \leq 1/2, \\ u_{\tilde{i}_k+1, j_k+1}(t_k) > 1/2. \end{cases} \quad (2.5.20)$$

As before, we can assume that $i_k + \lceil ct_k \rceil = L \in \mathbb{Z}$ and $\tilde{i}_k + \lceil ct_k \rceil = \tilde{L} \in \mathbb{Z}$. In addition, we can use Proposition 2.3.1 to construct an ω -limit point ω for u that satisfies the inequalities

$$\begin{cases} \omega_{L,0}(0) \leq 1/2, \\ \omega_{L+1,0}(0) > 1/2, \end{cases} \quad \begin{cases} \omega_{\tilde{L},1}(0) \leq 1/2, \\ \omega_{\tilde{L}+1,1}(0) > 1/2 \end{cases} \quad (2.5.21)$$

on account of (2.5.20). Therefore, Proposition 2.4.1 shows that the bounds

$$L \leq \theta_0 \leq L + 1, \quad \tilde{L} \leq \theta_0 \leq \tilde{L} + 1$$

hold for some $\theta_0 \in \mathbb{R}$. This allows us to conclude that $|L - \tilde{L}| \leq 1$ and obtain the contradiction $|i_k - \tilde{i}_k| \leq 1$. \square

Proof of Proposition 2.5.2. Assume to the contrary that there exists $\delta > 0$ together with subsequences $(j_k) \in \mathbb{Z}$ and $T \leq t_1 < t_2 < \dots \rightarrow \infty$ for which

$$|\gamma_{j_k+1}(t_k) - \gamma_{j_k}(t_k)| \geq \delta. \quad (2.5.22)$$

We now claim that it is possible to pass to a subsequence that has $i(j_k + 1, t_k) \neq i(j_k, t_k)$. Indeed, if actually $i(j_k + 1, t_k) = i(j_k, t_k) = i_k$ holds for all large k , then we can use Lemma 2.5.5 to obtain the contradiction

$$\begin{aligned} \delta &\leq |\gamma_{j_k+1}(t_k) - \gamma_{j_k}(t_k)| = |\Phi^{-1}(u_{i_k, j_k}) - \Phi^{-1}(u_{i_k, j_k+1})| \\ &\leq C|u_{i_k, j_k+1} - u_{i_k, j_k}| \rightarrow 0 \quad \text{as } k \rightarrow \infty. \end{aligned}$$

In particular, Lemma 2.5.6 allows us to assume that $i(j_k + 1, t_k) = i(j_k, t_k) + 1$ without loss of generality. Using the shorthand $i_k = i(j_k, t_k)$, we find

$$|\gamma_{j_k+1}(t) - \gamma_{j_k}(t)| = |1 + \Phi^{-1}(u_{i_k, j_k}) - \Phi^{-1}(u_{i_k+1, j_k+1})|,$$

together with the inequalities

$$\begin{cases} u_{i_k, j_k}(t_k) \leq 1/2, \\ u_{i_k+1, j_k}(t_k) > 1/2, \end{cases} \quad \begin{cases} u_{i_k+1, j_k+1}(t) \leq 1/2, \\ u_{i_k+2, j_k+1}(t) > 1/2. \end{cases}$$

We now proceed in a similar fashion as in the proof of Lemma 2.5.6. In particular, we may assume that $i_k + \lceil ct_k \rceil = L \in \mathbb{Z}$ and use Proposition 2.3.1 to construct an ω -limit point ω for u that satisfies the inequalities

$$\begin{cases} \omega_{L,0}(0) \leq 1/2, \\ \omega_{L+1,0}(0) \geq 1/2, \end{cases} \qquad \begin{cases} \omega_{L+1,1}(0) \leq 1/2, \\ \omega_{L+2,1}(0) \geq 1/2. \end{cases}$$

Again, Proposition 2.4.1 implies that $\omega_{i,j}(t) = \Phi(i - ct - x_0)$, for some $x_0 \in \mathbb{R}$. The independence with respect to j implies that $\omega_{L+1,0}(0) = \omega_{L+1,1}(0) = \frac{1}{2}$ and consequently $x_0 = L + 1$. In particular, we find

$$u_{i_k, j_k}(t_k) \rightarrow \omega_{L,0}(0) = \Phi(-1), \quad u_{i_k+1, j_k+1}(t_k) \rightarrow \omega_{L+1,1}(0) = \Phi(0), \quad (2.5.23)$$

and hence

$$|\gamma_{j_k+1}(t) - \gamma_{j_k}(t)| \rightarrow |1 + \Phi^{-1}(\Phi(-1)) - \Phi^{-1}(\Phi(0))| = 0$$

as $k \rightarrow \infty$, which leads to the desired contradiction with (2.5.22). \square

2.6 Discrete heat equation

In this section we obtain several preliminary estimates for the Cauchy problem

$$\begin{cases} \dot{h}_j(t) = h_{j+1}(t) + h_{j-1}(t) - 2h_j(t), \\ h_j(0) = h_j^0 \end{cases} \quad (2.6.1)$$

$$(2.6.2)$$

associated to the discrete heat equation. These estimates will underpin our analysis of the discrete curvature flow, using a nonlinear Cole-Hopf transformation to pass to a suitable intermediate system.

To set the stage, we recall the well-known fact that the one-dimensional continuous heat equation

$$\begin{cases} H_t = H_{yy}, & y \in \mathbb{R}, t > 0, \\ H(y, 0) = H_0(y), & y \in \mathbb{R}, \end{cases} \quad (2.6.3)$$

admits the explicit solution

$$H(y, t) = \frac{1}{\sqrt{4\pi t}} \int_{\mathbb{R}} e^{-\frac{(y-x)^2}{4t}} H_0(x) dx. \quad (2.6.4)$$

Taking derivatives, one readily obtains the estimates

$$\sup_{y \in \mathbb{R}} |H_y(y, t)| \leq \min\{C \|H_0\|_{L^\infty} t^{-\frac{1}{2}}, \|H_{0,y}\|_{L^\infty}\}, \quad (2.6.5)$$

$$\sup_{y \in \mathbb{R}} |H_{yy}(y, t)| \leq \min\{C \|H_0\|_{L^\infty} t^{-1}, \|H_{0,yy}\|_{L^\infty}\}. \quad (2.6.6)$$

The main result of this section transfers these estimates to the discrete setting (2.6.1). This generalization is actually surprisingly delicate, caused by the fact that supremum norms cannot be readily transferred to Fourier space.

Proposition 2.6.1. *There exists a constant $K > 0$ so that for any $h^0 \in \ell^\infty(\mathbb{Z})$, the solution $h \in C^1([0, \infty); \ell^\infty(\mathbb{Z}))$ to the initial value problem (2.6.1) satisfies the first-difference bound*

$$\|\partial^+ h(t)\|_{\ell^\infty} \leq \min \left\{ \|\partial^+ h^0\|_{\ell^\infty}, K \|h^0\|_{\ell^\infty} \frac{1}{\sqrt{t}} \right\}, \quad (2.6.7)$$

together with the second-difference estimate

$$\|\partial^{(2)} h(t)\|_{\ell^\infty} \leq \min \left\{ \|\partial^{(2)} h^0\|_{\ell^\infty}, K \|h^0\|_{\ell^\infty} \frac{1}{t} \right\} \quad (2.6.8)$$

for all $t > 0$.

Using a suitable Cole-Hopf transformation the linear heat equation (2.6.1) can be transformed to the nonlinear initial value problem

$$\begin{cases} \dot{V} = \frac{1}{d} \left(e^{d\partial^+ V} - 2 + e^{-d\partial^- V} \right) + c, & t > 0 \\ V(0) = V^0, \end{cases} \quad (2.6.9)$$

which will serve as a useful proxy for the discrete curvature flow. In order to exploit the fact that this equation is invariant under spatially homogeneous perturbations, we introduce the deviation seminorm

$$[V]_{\text{dev}} := \|V - V_0\|_{\ell^\infty} \quad (2.6.10)$$

for sequences $V \in \ell^\infty(\mathbb{Z})$.

Corollary 2.6.2. *Fix two constants $c, d \in \mathbb{R}$ with $d \neq 0$. Then there exist positive constants M_{ht} and κ so that for any $V^0 \in \ell^\infty(\mathbb{Z}^2)$, the solution $V : [0, \infty) \rightarrow \ell^\infty(\mathbb{Z}^2)$ to the initial value problem (2.6.9) satisfies the estimates*

$$\|\partial^+ V(t)\|_{\infty} \leq M_{\text{ht}} e^{\kappa [V^0]_{\text{dev}}} \min \left\{ \|\partial^+ V^0\|_{\ell^\infty}, \frac{1}{\sqrt{t}} \right\}, \quad (2.6.11)$$

$$\|\partial^{(2)} V(t)\|_{\infty} \leq M_{\text{ht}} e^{\kappa [V^0]_{\text{dev}}} \min \left\{ \|\partial^+ V^0\|_{\ell^\infty}, \frac{1}{t} \right\}. \quad (2.6.12)$$

2.6.1 Discrete heat kernel

The discrete heat kernel $G : [0, \infty) \rightarrow \ell^\infty(\mathbb{Z})$ is the fundamental solution of the discrete heat equation, in the sense that the function $h = G$ satisfies (2.6.1)-(2.6.2) with the initial condition

$$h_0^0 = 1 \quad \text{and} \quad h_j^0 = 0 \text{ for } j \neq 0.$$

We now recall the characterization

$$I_k(t) = \frac{1}{\pi} \int_0^\pi e^{t \cos \omega} \cos(k\omega) d\omega, \quad k \in \mathbb{Z}, \quad (2.6.13)$$

for the family of modified Bessel functions of the first kind; see e.g. the classical work by Watson [37]. By passing to the Fourier domain, one can readily confirm the well-known identity

$$G_j(t) = e^{-2t} I_j(2t). \quad (2.6.14)$$

We may now formally write

$$h_j(t) = \sum_{k \in \mathbb{Z}} G_k(t) h_{j-k}^0 = e^{-2t} \sum_{k \in \mathbb{Z}} I_k(2t) h_{j-k}^0 \quad (2.6.15)$$

for the solution to the general initial value problem (2.6.1)-(2.6.2). In order to see that this is well-defined for $h^0 \in \ell^\infty(\mathbb{Z})$, one can use the generating function

$$e^{\frac{t}{2}(x+x^{-1})} = \sum_{k=-\infty}^{\infty} I_k(t) x^k \quad (2.6.16)$$

together with the bound $I_k(t) \geq 0$ to conclude that $G(t) \in \ell^1(\mathbb{Z})$. Further useful properties of the functions I_k can be found in the result below.

Lemma 2.6.3. *There exists a constant $C > 0$ so that for any integer $k \geq 0$ we have the bound*

$$I_k(t) \leq C \frac{e^t}{\sqrt{t}}, \quad t > 0, \quad (2.6.17)$$

together with

$$0 < I_k(t) - I_{k+1}(t) \leq C \frac{e^t}{t} \quad t > 0. \quad (2.6.18)$$

Proof. The proof of (2.6.17) can be found in [37], while the lower bound in (2.6.18) is established in [85]; see also [2, Eq. (16)]. Turning to the upper bound in (2.6.18), we remark that $\cos \omega$ is negative for $\omega \in (\pi/2, \pi)$, which allows us to write

$$\begin{aligned} I_k(t) - I_{k+1}(t) &= \frac{2}{\pi} \int_0^\pi e^{t \cos \omega} \sin\left(\frac{2k+1}{2}\omega\right) \sin\left(\frac{\omega}{2}\right) d\omega \\ &= \frac{2}{\pi} \int_0^{\pi/2} e^{t \cos \omega} \sin\left(\frac{2k+1}{2}\omega\right) \sin\left(\frac{\omega}{2}\right) d\omega + O(1) \end{aligned}$$

as $t \rightarrow \infty$. Substituting $u = 2\sqrt{t} \sin(\omega/2)$ we find

$$\begin{aligned} I_k(t) - I_{k+1}(t) &= \frac{1}{t\pi} e^t \int_0^{\sqrt{2t}} e^{-u^2/2} \sin\left((2k+1) \sin^{-1}\left(\frac{u}{2\sqrt{t}}\right)\right) \frac{u}{\sqrt{1-\frac{u^2}{4t}}} du \\ &\quad + O(1) \end{aligned}$$

as $t \rightarrow \infty$. The desired bound now follows from the fact that the integral can be uniformly bounded in t and k . \square

In order to obtain the bounds in Proposition 2.6.1, the convolution (2.6.15) indicates that we need to control the ℓ^1 -norm of the first and second differences of G . The following two results provide the crucial ingredients to achieve this, exploiting telescoping sums. To our surprise, we were unable to find these bounds directly in the literature.

Lemma 2.6.4. *There exists a constant $C > 0$ so that the bound*

$$\sum_{k \in \mathbb{Z}} |I_{k+1}(t) - I_k(t)| \leq C \frac{e^t}{\sqrt{t}} \quad (2.6.19)$$

holds for all $t > 0$.

Proof. We first note that the characterization (2.6.13) implies $I_k(z) = I_{-k}(z)$ for all $k \in \mathbb{Z}$. Using (2.6.18), we can hence use a telescoping series to compute

$$\begin{aligned} \sum_{k \in \mathbb{Z}} |I_{k+1}(t) - I_k(t)| &= 2 \sum_{k \geq 0} I_k(t) - I_{k+1}(t) \\ &= 2I_0(t) - 2 \lim_{N \rightarrow \infty} I_N(t). \end{aligned}$$

The result now follows from (2.6.17) together with the limit $I_N(t) \rightarrow 0$ as $N \rightarrow \infty$. \square

Lemma 2.6.5. *There exists a constant $C > 0$ so that the bound*

$$\sum_{k \in \mathbb{Z}} |I_{k+1}(t) - 2I_k(t) + I_{k-1}(t)| \leq C \frac{e^t}{t} \quad (2.6.20)$$

holds for all $t > 0$.

Proof. We claim that for every $t > 0$ the function

$$\mathbb{Z}_{\geq 0} \ni k \mapsto \nu_k^{(2)}(t) := I_{k+1}(t) - 2I_k(t) + I_{k-1}(t)$$

changes sign exactly once. Note that this allows us to obtain the desired bound (2.6.20) from (2.6.18) by applying a telescoping argument similar to the one used in the proof of Lemma 2.6.4.

Turning to the claim, we recall the notation

$$a_k(t) = \frac{tI'_k(t)}{I_k(t)} = k + t \frac{I_{k+1}(t)}{I_k(t)}$$

from [75] and use the identity $I_{k+1}(t) + I_{k-1}(t) = 2I'_k(t)$ to compute

$$\nu_k^{(2)}(t) = 2I'_k(t) - 2I_k(t) = \frac{2I_k(t)}{t} (a_k(t) - t).$$

The inequality (15) in [73] directly implies that $a_k(t) < a_{k+1}(t)$, for every $t > 0$ and $k \geq 0$. In addition, the lower bound in (2.6.18) implies that

$$a_0(t) - t = t \left(\frac{I_1(t)}{I_0(t)} - 1 \right) < 0,$$

while for $k > t$ we easily conclude $a_k(t) - t \geq k - t > 0$. In particular, $k \mapsto a_k(t) - t$ changes sign precisely once. The claim now follows from the strict positivity $I_k(t) > 0$ for $t > 0$ and $k \geq 0$. \square

2.6.2 Gradient bounds

Using the representation (2.6.15) and the bounds for the discrete heat kernel obtained above, we are now ready to establish Proposition 2.6.1 and Corollary 2.6.2.

Proof of Proposition 2.6.1. In order to establish (2.6.7), we apply a discrete derivative to (2.6.15), which yields

$$(\partial^+ h)_j(t) = e^{-2t} \sum_{k \in \mathbb{Z}} (I_{k+1}(2t) - I_k(2t)) h_{j-k}^0.$$

Applying (2.6.19), we hence find

$$|(\partial^+ h)_j(t)| \leq e^{-2t} \|h^0\|_{\ell^\infty} \sum_{k \in \mathbb{Z}} |I_{k+1}(2t) - I_k(2t)| \leq C \|h^0\|_{\ell^\infty} \frac{1}{\sqrt{t}}. \quad (2.6.21)$$

On the other hand, the inequality $\|\partial^+ h(t)\|_{\ell^\infty} \leq \|\partial^+ h^0\|_{\ell^\infty}$ follows directly from the comparison principle, since $\partial^+ h$ satisfies the discrete heat equation with initial value $\partial^+ h^0$. The second-order bound (2.6.8) can be obtained in a similar fashion by exploiting the estimate (2.6.20). \square

Proof of Corollary 2.6.2. Since the function $\tilde{V} = V - V_0^0$ also satisfies the first line of (2.6.9), we may assume without loss of generality that $V_0^0 = 0$ and hence $[V^0]_{\text{dev}} = \|V^0\|_{\ell^\infty}$. Upon writing

$$h_j(t) = e^{d(V_j(t) - ct)},$$

straightforward calculations show that h satisfies (2.6.1) with the initial condition

$$h_j(0) = e^{dV_j^0},$$

which using the comparison principle implies that

$$h_j(t) \geq e^{-|d|\|V^0\|_{\ell^\infty}}, \quad t \geq 0. \quad (2.6.22)$$

For any $j \in \mathbb{Z}$, the intermediate value theorem allows us to find $h_1^*, h_2^* \in [h_j, h_{j+1}]$ and $h_3^* \in [h_{j-1}, h_j]$ for which we have

$$\partial^+ V_j = \frac{1}{d} \frac{\partial^+ h_j}{h_1^*}, \quad \partial^{(2)} V_j = \frac{1}{d} \left(\frac{\partial^{(2)} h_j}{h_j} - \frac{(\partial^+ h_j)^2}{2(h_2^*)^2} - \frac{(\partial^- h_j)^2}{2(h_3^*)^2} \right). \quad (2.6.23)$$

In particular, (2.6.22) yields the bounds

$$\|\partial^+ V\|_{\ell^\infty} \leq \frac{1}{|d|} e^{|d|\|V^0\|_{\ell^\infty}} \|\partial^+ h\|_{\ell^\infty}, \quad (2.6.24)$$

$$\|\partial^{(2)} V\|_{\ell^\infty} \leq \frac{1}{|d|} \left(e^{|d|\|V^0\|_{\ell^\infty}} \|\partial^{(2)} h\|_{\ell^\infty} + e^{2|d|\|V^0\|_{\ell^\infty}} \|\partial^+ h\|_{\ell^\infty}^2 \right). \quad (2.6.25)$$

In a similar fashion, we obtain

$$\|\partial^+ h^0\|_{\ell^\infty} \leq |d| e^{|d|\|V^0\|_{\ell^\infty}} \|\partial^+ V^0\|_{\ell^\infty}. \quad (2.6.26)$$

Using $\|\partial^{(2)} h^0\|_{\ell^\infty} \leq 2 \|\partial^+ h^0\|_{\ell^\infty}$, the desired estimates (2.6.11)-(2.6.12) can now be established by applying Proposition 2.6.1. \square

2.7 Construction of super- and sub-solutions

In this section we construct refined sub- and super-solutions of (2.2.1) that use the solution V of the nonlinear system (2.6.9) as a type of phase. In particular, we add a transverse j -dependence to the planar sub- and super-solutions (2.3.5)-(2.3.6), which requires some substantial modifications to account for the slowly-decaying resonances that arise in the residuals.

As a preparation, we introduce the linear operator $\mathcal{L}_{\text{tw}} : H^1 \rightarrow L^2$ associated to the linearization of the travelling wave MFDE (2.2.7), which acts as

$$(\mathcal{L}_{\text{tw}}v)(\xi) = cv'(\xi) + v(\xi + 1) - 2v(\xi) + v(\xi - 1) + g'(\Phi(\xi))v(\xi).$$

In addition, we introduce the formal adjoint $\mathcal{L}_{\text{tw}}^{\text{adj}} : H^1 \rightarrow L^2$ that acts as

$$\left(\mathcal{L}_{\text{tw}}^{\text{adj}}w\right)(\xi) = -cw'(\xi) + w(\xi + 1) - 2w(\xi) + w(\xi - 1) + g'(\Phi(\xi))w(\xi).$$

In view of the requirement $c \neq 0$ in $(H\Phi)$, the results in [67] show that there exists a strictly positive function $\psi \in C^1(\mathbb{R}, \mathbb{R})$ for which we have

$$\text{Ker } \mathcal{L}_{\text{tw}}^{\text{adj}} = \text{span}\{\psi\}, \quad \text{Range } \mathcal{L}_{\text{tw}} = \{f \in L^2 : \langle \psi, f \rangle = 0\}, \quad (2.7.1)$$

together with the normalization $\langle \psi, \Phi'_* \rangle = 1$.

We now fix the parameter d in the LDE (2.6.9) by writing

$$d = -\langle \Phi'', \psi \rangle. \quad (2.7.2)$$

The characterization (2.7.1) implies that we can find a solution $r \in H^1$ to the MFDE

$$\mathcal{L}_{\text{tw}}r + d\Phi' = -\Phi'' \quad (2.7.3)$$

that becomes unique upon imposing the normalization $\langle \psi, r \rangle = 0$. Multiplying this residual function by the square gradients

$$[\alpha_V]_j = [\beta_V]_j^2 - 1 = \frac{(V_{j+1} - V_j)^2}{2} + \frac{(V_{j-1} - V_j)^2}{2}$$

gives us the correction terms we need to control the resonances discussed above. In order to account for the possibility that $d = 0$, the actual LDE that we use here is given by

$$\dot{V} = \begin{cases} \frac{1}{d} \left(e^{d\partial^+ V} - 2 + e^{-d\partial^- V} \right) + c & d \neq 0, \\ \partial^{(2)}V + c, & d = 0. \end{cases} \quad (2.7.4)$$

Proposition 2.7.1. *Fix $R > 0$ and suppose that the assumptions (Hg) and $(H\Phi)$ both hold. Then for any $\epsilon > 0$, there exist constants $\delta > 0$, $\nu > 0$ and C^1 -smooth functions*

$$p : [0, \infty) \rightarrow \mathbb{R}, \quad q : [0, \infty) \rightarrow \mathbb{R}$$

so that for any $V^0 \in \ell^\infty(\mathbb{Z})$ with

$$[V^0]_{\text{dev}} < R, \quad \|\partial^+ V^0\|_{\ell^\infty} < \delta$$

the following holds true.

(i) Writing $V : [0, \infty) \rightarrow \ell^\infty(\mathbb{Z})$ for the solution to (2.7.4) with the initial condition $V(0) = V^0$, the functions u^+ and u^- defined by

$$\begin{aligned} u_{i,j}^+(t) &:= \Phi(i - V_j(t) + q(t)) + r(i - V_j(t) + q(t))[\alpha_V]_j + p(t), \\ u_{i,j}^-(t) &:= \Phi(i - V_j(t) - q(t)) + r(i - V_j(t) - q(t))[\alpha_V]_j - p(t) \end{aligned} \quad (2.7.5)$$

are a super- respectively sub-solution of (2.2.1).

(ii) We have $q(0) = 0$ together with the bound $0 \leq q(t) \leq \epsilon$ for all $t \geq 0$.

(iii) We have the bound $0 \leq p(t) \leq \epsilon$ for all $t \geq 0$, together with the initial inequality

$$p(0) - \|r\|_{L^\infty} \delta^2 > \nu > 0. \quad (2.7.6)$$

(iv) The asymptotic behaviour $p(t) = O(t^{-\frac{3}{2}})$ holds for $t \rightarrow \infty$.

In addition, the constants $\nu = \nu(\epsilon)$ satisfy $\lim_{\epsilon \downarrow 0} \nu(\epsilon) = 0$.

In the remainder of this section we set out to establish this result for u^+ , which requires us to understand the residual $\mathcal{J}[u^+]$ introduced in (2.3.4). Upon introducing the notation

$$\xi_{i,j}(t) = i - V_j(t),$$

a short computation allows us to obtain the splitting

$$\mathcal{J}[u^+] = \mathcal{J}_{\text{glb}} + \mathcal{J}_\Phi + \mathcal{J}_r,$$

in which the two expressions

$$\begin{aligned} [\mathcal{J}_\Phi]_{i,j} &= -\Phi'(\xi_{i,j} + q) \dot{V}_j - \Phi(\xi_{i,j+1} + q) - \Phi(\xi_{i+1,j} + q) \\ &\quad - \Phi(\xi_{i+1,j} + q) - \Phi(\xi_{i-1,j} + q) + 4\Phi(\xi_{i,j} + q) - g(\Phi(\xi_{i,j} + q)), \\ [\mathcal{J}_r]_{i,j} &= -r'(\xi_{i,j} + q) \dot{V}_j [\alpha_V]_j \\ &\quad - r(\xi_{i,j+1} + q) [\alpha_V]_{j+1} - r(\xi_{i,j-1} + q) [\alpha_V]_{j-1} \\ &\quad - r(\xi_{i+1,j} + q) [\alpha_V]_j - r(\xi_{i-1,j} + q) [\alpha_V]_j + 4r(\xi_{i,j} + q) [\alpha_V]_j \\ &\quad + r(\xi_{i,j} + q) (\partial^+ V_j \partial^+ \dot{V}_j + \partial^- V_j \partial^- \dot{V}_j) \end{aligned}$$

are naturally related to the defining equations for Φ , r and V , while

$$\mathcal{J}_{\text{glb}} = \dot{q}(\Phi'(\xi + q) + r'(\xi + q)\alpha_V) - g(u^+) + g(\Phi(\xi + q)) + \dot{p}$$

reflects the contributions associated to the dynamics of p and q .

In order to control the quantities \mathcal{J}_Φ and \mathcal{J}_r we introduce the two simplified expressions

$$\begin{aligned} \mathcal{J}_{\Phi;\text{apx}} &= -(d\Phi'(\xi + q) + \Phi''(\xi + q))\alpha_V, \\ \mathcal{J}_{r;\text{apx}} &= \left(d\Phi'(\xi + q) + \Phi''(\xi + q) + g'(\Phi(\xi + q))r(\xi + q) \right) \alpha_V \end{aligned}$$

which will turn out to be useful approximations. Indeed, the two results below provide bounds for the associated remainder terms

$$\mathcal{J}_\Phi = \mathcal{J}_{\Phi;\text{apx}} + \mathcal{R}_\Phi, \quad \mathcal{J}_r = \mathcal{J}_{r;\text{apx}} + \mathcal{R}_r.$$

Lemma 2.7.2. Fix $R > 0$ and suppose that (Hg) and $(H\Phi)$ are satisfied. Then there exists a constant $M > 0$ so that for any $V \in C^1([0, \infty); \ell^\infty)$ that satisfies the LDE (2.7.4) with $[V(0)]_{\text{dev}} < R$ and any pair of functions $p, q \in C([0, \infty); \mathbb{R})$, we have the estimate

$$\|\mathcal{R}_\Phi(t)\|_{\ell^\infty} \leq M \min \left\{ \|\partial^+ V(0)\|_{\ell^\infty}, t^{-\frac{3}{2}} \right\}, \quad t > 0.$$

Proof. Expanding $\Phi(\xi_{i,j\pm 1} + q)$ to third order around $\xi_{i,j} + q$ and evaluating the travelling wave MFDE (2.2.7) at this point, we find

$$\begin{aligned} [\mathcal{J}_\Phi]_{i,j} &= \Phi'(\xi_{i,j} + q) \left(-\dot{V}_j + \partial^{(2)} V_j + c \right) - \Phi''(\xi_{i,j} + q) [\alpha_V]_j \\ &\quad - \frac{1}{2} \int_{\xi_{i,j} + q}^{\xi_{i,j+1} + q} \Phi'''(s) (\xi_{i,j+1} + q - s)^2 ds \\ &\quad - \frac{1}{2} \int_{\xi_{i,j} + q}^{\xi_{i,j-1} + q} \Phi'''(s) (\xi_{i,j-1} + q - s)^2 ds. \end{aligned}$$

Substituting the LDE (2.7.4) and expanding $e^{d\partial^+ V}$ and $e^{-d\partial^- V}$ to third order, we compute

$$\begin{aligned} [\mathcal{J}_\Phi]_{i,j} &= -d\Phi'(\xi_{i,j} + q) [\alpha_V]_j - \Phi''(\xi_{i,j} + q) [\alpha_V]_j \\ &\quad - \frac{1}{2} \int_{\xi_{i,j} - q}^{\xi_{i,j+1} - q} \Phi'''(s) (\xi_{i,j+1} + q - s)^2 ds \\ &\quad - \frac{1}{2} \int_{\xi_{i,j} + q}^{\xi_{i,j-1} + q} \Phi'''(s) (\xi_{i,j-1} + q - s)^2 ds \\ &\quad - \frac{1}{2d} \int_0^{d\partial^+ V} e^s (d\partial^+ V - s)^2 ds + \frac{1}{2d} \int_{-d\partial^- V}^0 e^s (d\partial^- V + s)^2 ds. \end{aligned}$$

Since the first line of this expression corresponds with $\mathcal{J}_{\Phi; \text{apx}}$, the desired estimate follows from Corollary 2.6.2. \square

Lemma 2.7.3. Fix $R > 0$ and suppose that (Hg) and $(H\Phi)$ are satisfied. Then there exists a constant $M > 0$ so that for any $V \in C^1([0, \infty); \ell^\infty)$ that satisfies the LDE (2.7.4) with $[V(0)]_{\text{dev}} < R$ and any pair of functions $p, q \in C([0, \infty); \mathbb{R})$, we have the estimate

$$\|\mathcal{R}_r(t)\|_{\ell^\infty} \leq M \min \left\{ \|\partial^+ V(0)\|_{\ell^\infty}, t^{-\frac{3}{2}} \right\}, \quad t > 0. \quad (2.7.7)$$

Proof. Expanding $r(\xi_{i,j+1} + q)$ and $r(\xi_{i,j-1} + q)$ around $\xi_{i,j} + q$ and evaluating (2.7.3)

at this point, we find

$$\begin{aligned}
[\mathcal{J}_r]_{i,j} &= r'(\xi_{i,j} + q) (-\dot{V}_j + c) [\alpha_V]_j \\
&\quad - [\alpha_V]_{j+1} \int_{\xi_{i,j}+q}^{\xi_{i,j+1}+q} r'(s) ds - [\alpha_V]_{j-1} \int_{\xi_{i,j}+q}^{\xi_{i,j-1}+q} r'(s) ds \\
&\quad - r(\xi_{i,j} + q) \left([\alpha_V]_{j+1} + [\alpha_V]_{j-1} - 2[\alpha_V]_j \right) \\
&\quad + r(\xi_{i,j} + q) (\partial^+ V_j \partial^+ \dot{V}_j + \partial^- V_j \partial^- \dot{V}_j) \\
&\quad + \left(d\Phi'(\xi_{i,j} + q) + \Phi''(\xi_{i,j} + q) + g'(\Phi(\xi_{i,j} + q)) r(\xi_{i,j} + q) \right) [\alpha_V]_j.
\end{aligned}$$

In order to estimate the terms in the third line above, we compute

$$\begin{aligned}
[\alpha_V]_{j+1} - [\alpha_V]_j &= \frac{1}{2} (V_{j+2} - V_{j+1} + V_j - V_{j-1}) (V_{j+2} - V_{j+1} - V_j + V_{j-1}) \\
&= \frac{1}{2} (V_{j+2} - V_{j+1} + V_j - V_{j-1}) \left(\partial^{(2)} V_{j+1} + \partial^{(2)} V_j \right),
\end{aligned} \tag{2.7.8}$$

which can be thought of as a discrete analogue of the identity $\partial_y(\partial_y^2) = 2\partial_y\partial_{yy}$. Substituting (2.7.4) and expanding $e^{d\partial^+V}$ and $e^{-d\partial^-V}$ up to second order, we can again apply Corollary 2.6.2 to obtain the desired estimate. \square

We are now ready to introduce our final approximation

$$\mathcal{J} = \mathcal{J}_{\text{apx}} + \mathcal{R} \tag{2.7.9}$$

by writing

$$\begin{aligned}
\mathcal{J}_{\text{apx}} &= \dot{q}(\Phi(\xi + q) + r'(\xi + q)\alpha_V) + \dot{p} \\
&\quad - p \int_0^1 g'(\Phi(\xi + q) + \tau(p + r(\xi + q)\alpha_V)) d\tau \\
&\quad - pr(\xi + q)\alpha_V \int_0^1 \int_0^\tau g''(\Phi(\xi + q) + s(p + r(\xi + q)\alpha_V)) ds d\tau.
\end{aligned} \tag{2.7.10}$$

We show below that the residual \mathcal{R} satisfies the same bound as \mathcal{R}_Φ and \mathcal{R}_τ . This will allow us to construct appropriate functions p and q and establish Proposition 2.7.1.

Lemma 2.7.4. *Fix $R > 0$ and suppose that (Hg) and (HΦ) are satisfied. Then there exists a constant $M > 0$ so that for any $V \in C^1([0, \infty); \ell^\infty)$ that satisfies the LDE (2.7.4) with $[V(0)]_{\text{dev}} < R$ and any pair of functions $p, q \in C([0, \infty); \mathbb{R})$, we have the estimate*

$$\|\mathcal{R}(t)\|_{\ell^\infty} \leq M \min \left\{ \|\partial^+ V(0)\|_{\ell^\infty}, t^{-\frac{3}{2}} \right\}, \quad t > 0. \tag{2.7.11}$$

Proof. Writing

$$\mathcal{J}_{\text{apx};I} = \mathcal{J}_{\text{glb}} + \mathcal{J}_{\Phi;\text{apx}} + \mathcal{J}_{r;\text{apx}},$$

together with

$$\mathcal{I}_g = g(\Phi(\xi + q)) - g(u^+) + g'(\Phi(\xi + q))r(\xi + q)\alpha_V,$$

we have

$$\mathcal{J}_{\text{app};I} = \dot{q}(\Phi'(\xi + q) + r'(\xi + q)\alpha_V) + \dot{p} + \mathcal{I}_g.$$

Upon rewriting \mathcal{I}_g in the form

$$\begin{aligned} \mathcal{I}_g &= -(p + r(\xi + q)\alpha_V) \int_0^1 g'(\Phi(\xi + q) + \tau(p + r(\xi + q)\alpha_V)) d\tau \\ &\quad + g'(\Phi(\xi + q))r(\xi + q)\alpha_V \\ &= -p \int_0^1 g'(\Phi(\xi + q) + \tau(p + r(\xi + q)\alpha_V)) d\tau \\ &\quad - \alpha_V r(\xi + q)(p + r(\xi + q)\alpha_V) \int_0^1 \int_0^\tau g''(\Phi + s(p + r(\xi + q)\alpha_V)) ds d\tau, \end{aligned}$$

we obtain the splitting (2.7.9) with the residual

$$\mathcal{R} = \mathcal{R}_\Phi + \mathcal{R}_r - r(\xi + q)^2 \alpha_V^2 \int_0^1 \int_0^\tau g''(\Phi + s(p + r(\xi + q)\alpha_V)) ds d\tau.$$

As before, the desired bound now follows from Corollary 2.6.2. \square

Proof of Proposition 2.7.1. Without loss of generality, we assume that the constant M from Lemma 2.7.4 satisfies

$$M \geq \max\{1, \|r\|_{L^\infty}, \|r'\|_{L^\infty}, \sup_{-1 \leq s \leq 2} |g'(s)|, \sup_{-1 \leq s \leq 2} |g''(s)|, M_{\text{ht}} e^{\kappa R}\}.$$

We first pick a constant $m \in (0, 1]$ in such a way that

$$-g'(s) \geq 2m > 0, \quad \text{for } s \in [-\epsilon, 3\epsilon] \cup [1 - 2\epsilon, 1 + 2\epsilon],$$

reducing ϵ if needed. Next, we define the positive constants

$$C_\epsilon := \max\left\{1, \frac{2m + M}{\min_{\Phi \in [\epsilon, 1 - \epsilon]} \Phi'}\right\}, \quad \delta_\epsilon := \frac{\epsilon^3 m^3}{6^3 M^3 C_\epsilon^3}, \quad \nu_\epsilon := \frac{\epsilon^3 m^2}{2 \cdot 6^3 M^2 C_\epsilon^3} = \frac{M \delta_\epsilon}{2m}$$

together with the positive function

$$K_\epsilon : [0, \infty) \rightarrow \mathbb{R}, \quad t \mapsto M \min\left\{\delta_\epsilon, t^{-\frac{3}{2}}\right\}.$$

We now choose functions $p, q \in C^\infty [0, \infty)$ that satisfy

$$K_\epsilon(t) \leq mp(t) \leq 2K_\epsilon(t), \quad m|\dot{p}(t)| \leq 2\tilde{K}_\epsilon(t), \quad q(t) = C_\epsilon \int_0^t p(s) ds,$$

where \tilde{K}_ϵ is defined by

$$\tilde{K}_\epsilon(t) = \begin{cases} 0, & t \leq \delta_\epsilon^{-\frac{2}{3}} \\ \frac{3}{2} M t^{-\frac{5}{2}}, & t > \delta_\epsilon^{-\frac{2}{3}}, \end{cases}$$

which we recognize as the absolute value of weak derivative of the function K_ϵ . The functions p and q are clearly nonnegative, with

$$p(0) - \|r\|_{L^\infty} \delta_\epsilon^2 \geq \frac{M \delta_\epsilon}{m} - M \delta_\epsilon^2 = \frac{M \delta_\epsilon}{m} (1 - \delta_\epsilon m) \geq \frac{M \delta_\epsilon}{m} \left(1 - \frac{1}{6^3}\right) > \nu_\epsilon.$$

Furthermore, we have $p(t) \leq \frac{2M\delta_\epsilon}{m} \leq \epsilon$, together with

$$q(t) \leq \frac{2C_\epsilon}{m} \int_0^\infty K_\epsilon(s) ds \leq \frac{6C_\epsilon}{m} M\delta_\epsilon^{\frac{1}{3}} = \epsilon.$$

In particular, items (ii)-(iv) are satisfied. In addition, using $|\alpha_V| \leq M^2\delta_\epsilon^2$ we obtain the a-priori bound

$$|p(t) + r(\xi_{ij}(t) + q(t))[\alpha_V]_j(t)| \leq \frac{2M\delta_\epsilon}{m} + M^3\delta_\epsilon^2 \leq \epsilon \quad (2.7.12)$$

for all $t \geq 0$ and $(i, j) \in \mathbb{Z}^2$.

Turning to (i), Lemma 2.7.4 implies that it suffices to show that the approximate residual (2.7.10) satisfies $\mathcal{J}_{\text{apx}} \geq K_\epsilon(t)$. Introducing the notation

$$\mathcal{I}_A = \frac{\dot{q}}{p} \Phi'(\xi + q), \quad \mathcal{I}_B = \frac{\dot{q}}{p} r'(\xi + q) \alpha_V, \quad \mathcal{I}_C = \frac{\dot{p}}{p},$$

together with the integral expressions

$$\begin{aligned} \mathcal{I}_D &= - \int_0^1 g' \left(\Phi(\xi + q) + \tau(p + r(\xi + q)\alpha_V) \right) d\tau \\ \mathcal{I}_E &= -r(\xi + q)\alpha_V \int_0^1 \int_0^\tau g'' \left(\Phi(\xi + q) + s(p + r(\xi + q)\alpha_V) \right) ds d\tau, \end{aligned}$$

we see that

$$\mathcal{J}_{\text{apx}} = p(\mathcal{I}_A + \mathcal{I}_B + \mathcal{I}_C + \mathcal{I}_D + \mathcal{I}_E).$$

Using the observation

$$\frac{|\dot{p}(t)|}{p(t)} \leq \begin{cases} 0, & t \leq \delta_\epsilon^{-\frac{2}{3}} \\ 3t^{-1}, & t > \delta_\epsilon^{-\frac{2}{3}}, \end{cases}$$

we obtain the global bounds

$$\begin{aligned} |\mathcal{I}_B| &\leq C_\epsilon M^3 \delta_\epsilon^2 \leq \frac{m}{3}, \\ |\mathcal{I}_C| &\leq 3\delta_\epsilon^{\frac{2}{3}} \leq \frac{m}{3}, \\ |\mathcal{I}_E| &\leq M^2 \delta_\epsilon^2 \leq \frac{m}{3}. \end{aligned}$$

When $\Phi(\xi + q) \in (0, \epsilon] \cup [1 - \epsilon, 1)$, we may use (2.7.12) to obtain the lower bound

$$\mathcal{I}_D \geq 2m.$$

Together with $\mathcal{I}_A \geq 0$, this allows us to conclude

$$\mathcal{J}_{\text{apx}} \geq mp(t) \geq K_\epsilon(t). \quad (2.7.13)$$

On the other hand, when $\Phi(\xi + q) \in [\epsilon, 1 - \epsilon]$, we have

$$|\mathcal{I}_A| \geq C_\epsilon \frac{2m + M}{C_\epsilon} \geq 2m + M, \quad |\mathcal{I}_D| \leq M,$$

which again yields (2.7.13). \square

2.8 Phase approximation

In this section we discuss the relation between the interface γ defined in (2.2.12), solutions of the discrete mean curvature flow

$$\dot{\Gamma} = \frac{\partial^{(2)}\Gamma}{\beta_{\Gamma}^2} + 2d\beta_{\Gamma} + c - 2d, \quad (2.8.1)$$

and solutions of the (nonlinear) heat LDE (2.7.4), both with $d = -\langle \Phi'', \psi \rangle$. In particular, we establish Theorem 2.2.3 in two main steps.

The first step is to show that γ can be well-approximated by V after allowing sufficient time for the interface to 'flatten'. This is achieved using the sub- and super-solutions constructed in §2.7.

Proposition 2.8.1. *Assume that (Hg), (HΦ) and (H0) all hold and let u be a solution of (2.2.1) with the initial condition (2.2.9). Then for every $\epsilon > 0$, there exists a constant $\tau_{\epsilon} > 0$ so that for any $\tau \geq \tau_{\epsilon}$, the solution V of the LDE (2.7.4) with the initial value $V(0) = \gamma(\tau)$ satisfies*

$$\|\gamma(t) - V(t - \tau)\|_{\ell^{\infty}} \leq \epsilon, \quad t \geq \tau. \quad (2.8.2)$$

The second step compares the dynamics of (2.8.1) and (2.7.4) and shows that the solutions V and Γ closely track each other. This is achieved by developing a local comparison principle for (2.8.1) that is valid as long as Γ is sufficiently flat.

Proposition 2.8.2. *Fix $R > 0$. Then for any $\epsilon > 0$ there exists $\delta > 0$ so that any pair $\Gamma, V \in C^1([0, \infty), \ell^{\infty}(\mathbb{Z}, \mathbb{R}))$ that satisfies the assumptions*

- (a) Γ satisfies the mean curvature LDE (2.8.1) on $(0, \infty) \times \mathbb{Z}$;
- (b) V satisfies the heat LDE (2.7.4) on $(0, \infty) \times \mathbb{Z}$;
- (c) $\Gamma(0) = V(0)$, with $\|\partial^+ V(0)\|_{\ell^{\infty}} \leq \delta$ and $[V(0)]_{\text{dev}} \leq R$,

must in fact have

$$\|\Gamma(t) - V(t)\|_{\ell^{\infty}} \leq \epsilon, \quad \text{for all } t \geq 0.$$

2.8.1 Approximating γ by V

The main idea for our proof of Proposition 2.8.1 is to compare the information on γ resulting from the asymptotic description (2.2.14) with the phase information that can be derived from (2.7.5). In particular, we capture the solution u between the sub- and super-solutions constructed in §2.7 and exploit the monotonicity properties of Φ .

Lemma 2.8.3. *Assume that (Hg), (HΦ) and (H0) all hold and let u be a solution of (2.2.1) with the initial condition (2.2.9). Then for every $\epsilon > 0$, there exists a constant $\tau_{\epsilon} > 0$ so that for any $\tau \geq \tau_{\epsilon}$ the solution V of the LDE (2.7.4) with the initial value $V(0) = \gamma(\tau)$ satisfies*

$$\Phi(i - \gamma_j(t)) \leq \Phi(i - V_j(t - \tau)) + \epsilon \quad (2.8.3)$$

for all $(i, j) \in \mathbb{Z}^2$ and $t \geq \tau$.

Proof. Without loss of generality, we assume that $0 < \epsilon < 1$. Recalling the constant ν_ϵ from Proposition 2.7.1, Theorem 2.2.2 and Lemma 2.5.4 allow us to find $\tau_\epsilon > 0$ and $R > 0$ for which the bounds

$$|u_{i,j}(t) - \Phi(i - \gamma_j(t))| \leq \frac{1}{2}\nu_\epsilon, \quad [\gamma(t)]_{\text{dev}} \leq R \quad (2.8.4)$$

hold for all $(i, j) \in \mathbb{Z}^2$ and $t \geq \tau_\epsilon$. We now recall the constant $\delta > 0$ and the functions p and q that arise by applying Proposition 2.7.1 with our pair (ϵ, R) . Decreasing δ if necessary, we may assume that $\epsilon > \delta$. After possibly increasing τ_ϵ , we may use Proposition 2.5.2 to obtain

$$\|\partial^+ \gamma(\tau)\|_{\ell^\infty} \leq \delta.$$

We now recall the super-solution u^+ defined in (2.7.5). Our choice for V together with the bounds (2.7.6) and (2.8.4) imply that

$$u_{i,j}(\tau) \leq \Phi(i - \gamma_j(\tau)) + r(i - \gamma_j(\tau))[\alpha_\gamma]_j(\tau) + p(0) = u_{i,j}^+(\tau).$$

In particular, the comparison principle for LDE (2.2.1) together with the bound (2.8.4) implies that

$$\Phi(i - \gamma_j(t)) \leq u_{i,j}(t) + \frac{1}{2}\nu(\epsilon) \leq u_{i,j}^+(t - \tau) + \frac{1}{2}\nu_\epsilon, \quad t \geq \tau.$$

Corollary 2.6.2 allows us to obtain the uniform bound $\|\alpha_V\|_{\ell^\infty} \leq C_1\delta^2 \leq C_1\epsilon^2$ for some $C_1 > 0$. Recalling items (ii) and (iii) of Proposition 2.7.1, we obtain the bound

$$u_{i,j}^+(t) - \Phi(i - V_j(t)) \leq C_2\epsilon, \quad t \geq 0$$

for some $C_2 > 0$. In particular, we see that

$$\Phi(i - \gamma_j(t)) \leq \Phi(i - V_j(t - \tau)) + \frac{1}{2}\nu_\epsilon + C_2\epsilon, \quad t \geq \tau,$$

from which the statement can readily be obtained. \square

Proof of Proposition 2.8.1. For convenience, we write

$$\sigma = \min_{\xi \in [0,3]} \Phi'(\xi) > 0.$$

Recalling the constant $\tau_\epsilon > 0$ defined in Lemma 2.8.3 and picking $\tau \geq \tau_\epsilon$, we set out to show that

$$V_j(t - \tau) - \gamma_j(t) \leq \sigma^{-1}\epsilon, \quad t \geq \tau.$$

Arguing by contradiction, we plug $i = \lceil V_j(t - \tau) \rceil$ into (2.8.3) and obtain

$$\Phi(\lceil V_j(t - \tau) \rceil - \gamma_j(t)) \leq \Phi(\lceil V_j(t - \tau) \rceil - V_j(t - \tau)) + \epsilon \leq \Phi(1) + \epsilon \leq \Phi(2), \quad (2.8.5)$$

possibly after restricting the size of $\epsilon > 0$. This implies $\sigma^{-1}\epsilon < V_j(t - \tau) - \gamma_j(t) \leq 2$. The first inequality in (2.8.5) now yields the contradiction

$$\begin{aligned} \epsilon &< \sigma(V_j(t - \tau) - \gamma_j(t)) \\ &\leq \Phi(\lceil V_j(t - \tau) \rceil - \gamma_j(t)) - \Phi(\lceil V_j(t - \tau) \rceil - V_j(t - \tau)) \\ &\leq \epsilon, \end{aligned}$$

since both arguments of Φ are contained in the interval $[0, 3]$. An $O(\epsilon)$ lower bound for $V_j(t - \tau) - \gamma_j(t)$ can be obtained in a similar fashion, which allows the proof to be completed. \square

2.8.2 Tracking V with Γ

In this subsection we set out to establish Proposition 2.8.2. The main idea to establish this approximation result is to apply a local comparison principle to the discrete curvature LDE (2.8.1). To this end, we define the residual

$$\mathcal{J}_{\text{dc}}[\Gamma] = \dot{\Gamma} - \frac{\partial^{(2)}\Gamma}{\beta_{\Gamma}^2} - 2d\beta_{\Gamma} - c + 2d \quad (2.8.6)$$

for any $\Gamma \in C^1([0, \infty); \ell^\infty(\mathbb{Z}))$. As usual, we say that Γ is a super- or sub-solution for (2.8.1) if the inequality $\mathcal{J}_{\text{dc}}[\Gamma]_j(t) \geq 0$ respectively $\mathcal{J}_{\text{dc}}[\Gamma]_j(t) \leq 0$ holds for all $j \in \mathbb{Z}$ and $t \geq 0$.

Lemma 2.8.4 (Comparison principle). *Pick a sufficiently small $\delta > 0$ and consider a pair of functions $\Gamma^-, \Gamma^+ \in C^1([0, \infty), \ell^\infty(\mathbb{Z}, \mathbb{R}))$ that satisfy the following assumptions:*

- (a) Γ^- is a subsolution of the LDE (2.8.1);
- (b) Γ^+ is a supersolution of the LDE (2.8.1);
- (c) The inequalities $\|\partial^+\Gamma^-(t)\|_{\ell^\infty} \leq \delta$, and $\|\partial^+\Gamma^+(t)\|_{\ell^\infty} \leq \delta$ hold for every $t \geq 0$;
- (d) $\Gamma_j^-(0) \leq \Gamma_j^+(0)$ holds for every $j \in \mathbb{Z}$.

Then for every $j \in \mathbb{Z}$ and $t \geq 0$ we have the bound

$$\Gamma_j^-(t) \leq \Gamma_j^+(t).$$

Proof. Define the function $W : [0, \infty) \rightarrow \ell^\infty(\mathbb{Z})$ by $W(t) = \Gamma^+(t) - \Gamma^-(t)$. Then W satisfies the differential inequality

$$\dot{W}_j \geq (W_{j+1} - W_j)F(\Gamma^+, \Gamma^-)_j + (W_{j-1} - W_j)G(\Gamma^+, \Gamma^-)_j,$$

in which the functions F and G are defined by

$$F(\Gamma^-, \Gamma^+) = \frac{1}{\beta_{\Gamma^+}^2} + (\partial^+\Gamma^- + \partial^+\Gamma^+) \left(\frac{d}{\beta_{\Gamma^-} + \beta_{\Gamma^+}} - \frac{\partial^{(2)}\Gamma^-}{2\beta_{\Gamma^-}^2\beta_{\Gamma^+}^2} \right),$$

$$G(\Gamma^-, \Gamma^+) = \frac{1}{\beta_{\Gamma^+}^2} - (\partial^-\Gamma^- + \partial^-\Gamma^+) \left(\frac{d}{\beta_{\Gamma^-} + \beta_{\Gamma^+}} - \frac{\partial^{(2)}\Gamma^-}{2\beta_{\Gamma^-}^2\beta_{\Gamma^+}^2} \right).$$

Pick $\delta > 0$ in such a way that $\frac{1}{1 + \delta^2} > \delta(|d| + 2\delta) + \frac{1}{2}$. Notice that this choice and assumption (c) imply that both β_{Γ^-} and β_{Γ^+} are bounded by $\sqrt{1 + \delta^2}$, which in turn implies

$$F(\Gamma^-, \Gamma^+) > \frac{1}{2}, \quad G(\Gamma^-, \Gamma^+) > \frac{1}{2}.$$

In order to prove that $W \geq 0$, we assume to the contrary that there exist $j_* \in \mathbb{Z}$ and t_* such that $W_{j_*}(t_*) = -\vartheta < 0$. Picking $\epsilon > 0$ and $K > 0$ in such a way that $\vartheta = \epsilon e^{2Kt_*}$, we can define

$$T := \sup \{t \geq 0 : W_j(t) > -\epsilon e^{2Kt} \text{ for all } j \in \mathbb{Z}\}.$$

Since $W \in C^1([0, \infty); \ell^\infty(\mathbb{Z}))$ we must have $T \leq t^*$ and

$$\inf_{j \in \mathbb{Z}} W_j(T) = -\epsilon e^{2KT}.$$

Without loss of generality, we may assume that $W_0(T) < -\frac{7}{8}\epsilon e^{2KT}$.

We now choose a sequence $z \in \ell^\infty(\mathbb{Z}, \mathbb{R})$ with the properties

$$z_0 = 1, \quad \lim_{|j| \rightarrow \infty} z_j = 3, \quad 1 \leq z_j \leq 3 \quad \text{and} \quad \|\partial^+ z\|_{\ell^\infty} \leq 1.$$

This allows us to define the function

$$W_j^-(t; \alpha) = -\epsilon \left(\frac{3}{4} + \alpha z_j \right) e^{2Kt},$$

in which $\alpha > 0$ is a parameter. We denote by $\alpha^* \in (\frac{1}{8}, \frac{1}{4}]$ the minimal value of α for which $W_j(t) \geq W_j^-(t; \alpha)$ for all $(j, t) \in \mathbb{Z} \times [0, T]$. In view of the limiting behaviour

$$\lim_{|j| \rightarrow \infty} W_j^-(t; \alpha^*) = -\epsilon \left[\frac{3}{4} + 3\alpha^* \right] e^{2Kt} < -\frac{9}{8}\epsilon e^{2Kt},$$

the minimality of α^* allows us to conclude that there exist $j_0 \in \mathbb{Z}$ and $0 < t_0 \leq T$ such that $W_{j_0}(t_0) = W_{j_0}^-(t_0; \alpha^*)$. As a consequence, we must have

$$\dot{W}_{j_0}(t_0) \leq \dot{W}_{j_0}^-(t_0; \alpha^*).$$

In addition, the definitions of W^- and α^* directly yield the inequalities

$$W_{j_0+1}(t_0) - W_{j_0}(t_0) \geq W_{j_0+1}^-(t_0; \alpha^*) - W_{j_0}^-(t_0; \alpha^*),$$

$$W_{j_0-1}(t_0) - W_{j_0}(t_0) \geq W_{j_0-1}^-(t_0; \alpha^*) - W_{j_0}^-(t_0; \alpha^*).$$

Together with the bounds

$$\dot{W}_{j_0}^-(t_0; \alpha^*) \leq -\frac{7}{4}\epsilon K e^{2Kt_0}, \quad \|\partial^\pm W^-(t_0; \alpha^*)\|_{\ell^\infty} \leq \epsilon e^{2Kt_0},$$

this allows us to compute

$$\begin{aligned} -\frac{7}{4}\epsilon K e^{2Kt_0} &\geq (\partial^+ W)_{j_0}(t_0) F(U, V)_{j_0} - (\partial^- W)_{j_0}(t_0) G(U, V)_{j_0} \\ &\geq \frac{1}{2}(\partial^+ W^-)_{j_0}(t_0; \alpha^*) - \frac{1}{2}(\partial^- W^-)_{j_0}(t_0; \alpha^*) \\ &\geq -\epsilon e^{2Kt_0}. \end{aligned}$$

This leads to the desired contradiction upon choosing $K > 1$ to be sufficiently large. \square

In order to use the comparison principle above to compare V and Γ , we need to obtain uniform bounds on the discrete derivatives ∂^+V and $\partial^+\Gamma$. Corollary 2.6.2 provides such bounds for ∂^+V , but the corresponding estimates for $\partial^+\Gamma$ require some additional technical work.

We pursue this in the results below, establishing a second comparison principle directly for the function $\Upsilon := \partial^+\Gamma$. Indeed, upon introducing the shorthand

$$\Pi[\Upsilon]_j = \sqrt{1 + (\Upsilon_{j+1}^2 + \Upsilon_j^2)}/2$$

and differentiating (2.8.1), a short computation shows that Υ satisfies the LDE

$$\dot{\Upsilon}_j = \frac{\partial^+\Upsilon_j}{\Pi[\Upsilon]_j^2} - \frac{\partial^-\Upsilon_j}{\Pi[\Upsilon]_{j-1}^2} + 2d(\Pi[\Upsilon]_j - \Pi[\Upsilon]_{j-1}). \quad (2.8.7)$$

Lemma 2.8.5. *Pick a sufficiently small $\delta > 0$ and consider a pair of functions Υ^- , $\Upsilon^+ \in C^1([0, \infty), \ell^\infty(\mathbb{Z}))$ that satisfy the following assumptions:*

- (a) Υ^- is a subsolution of the LDE (2.8.7);
- (b) Υ^+ is a supersolution of the LDE (2.8.7);
- (c) The inequalities $\|\Upsilon^-(t)\|_{\ell^\infty} \leq \delta$ and $\|\Upsilon^+(t)\|_{\ell^\infty} \leq \delta$ hold for every $t \geq 0$;
- (d) $\Upsilon_j^-(0) \leq \Upsilon_j^+(0)$ holds for every $j \in \mathbb{Z}$.

Then for every $j \in \mathbb{Z}$ and $t \geq 0$ we have the inequality

$$\Upsilon_j^-(t) \leq \Upsilon_j^+(t).$$

Proof. Defining $Z_j(t) = \Upsilon_j^+(t) - \Upsilon_j^-(t)$, we see that $Z_j(0) \geq 0$ for every $j \in \mathbb{Z}$. Moreover, Z satisfies the differential inequality

$$\dot{Z}_j \geq F(\Upsilon^-, \Upsilon^+)_j(Z_{j+1} - Z_j) + G(\Upsilon^-, \Upsilon^+)_j(Z_{j-1} - Z_j) + H(\Upsilon^-, \Upsilon^+)_j Z_j,$$

in which the functions F , G and H are defined by

$$\begin{aligned} F(\Upsilon^-, \Upsilon^+)_j &= \frac{1}{\Pi[\Upsilon^+]_j^2} + \left(\frac{d(\Upsilon_{j+1}^+ + \Upsilon_{j+1}^-)}{\Pi[\Upsilon^+]_j + \Pi[\Upsilon^-]_j} - \frac{\partial^+\Upsilon_j^-(\Upsilon_{j+1}^+ + \Upsilon_{j+1}^-)}{2\Pi[\Upsilon^+]_j^2\Pi[\Upsilon^-]_j^2} \right), \\ G(\Upsilon^-, \Upsilon^+)_j &= \frac{1}{\Pi[\Upsilon^+]_{j-1}^2} + \left(\frac{\partial^-\Upsilon_j^-(\Upsilon_{j-1}^+ + \Upsilon_{j-1}^-)}{2\Pi[\Upsilon^+]_{j-1}^2\Pi[\Upsilon^-]_{j-1}^2} - \frac{d(\Upsilon_{j-1}^+ + \Upsilon_{j-1}^-)}{\Pi[\Upsilon^+]_{j-1} + \Pi[\Upsilon^-]_{j-1}} \right), \\ H(\Upsilon^-, \Upsilon^+)_j &= \frac{d(\Upsilon_{j+1}^+ + \Upsilon_{j+1}^- + \Upsilon_j^+ + \Upsilon_j^-)}{\Pi[\Upsilon^+]_j + \Pi[\Upsilon^-]_j} - \frac{\partial^+\Upsilon_j^-(\Upsilon_{j+1}^+ + \Upsilon_{j+1}^- + \Upsilon_j^+ + \Upsilon_j^-)}{2\Pi[\Upsilon^+]_j^2\Pi[\Upsilon^-]_j^2} \\ &\quad + \frac{\partial^-\Upsilon_j^-(\Upsilon_j^+ + \Upsilon_j^- + \Upsilon_{j-1}^+ + \Upsilon_{j-1}^-)}{2\Pi[\Upsilon^+]_{j-1}^2\Pi[\Upsilon^-]_{j-1}^2} \\ &\quad - \frac{d(\Upsilon_j^+ + \Upsilon_j^- + \Upsilon_{j-1}^+ + \Upsilon_{j-1}^-)}{\Pi[\Upsilon^+]_{j-1} + \Pi[\Upsilon^-]_{j-1}}. \end{aligned}$$

We again pick $\delta > 0$ in such a way that $\frac{1}{1+\delta^2} > \delta(|d|+2\delta) + \frac{1}{2}$. Notice that this choice and assumption (c) imply that both $\Pi[\Upsilon^-]$ and $\Pi[\Upsilon^+]$ are bounded by $\sqrt{1+\delta^2}$. This in turn yields the bounds

$$F(\Upsilon^-, \Upsilon^+) > 1/2, \quad G(\Upsilon^-, \Upsilon^+) > 1/2, \quad |H(\Upsilon^-, \Upsilon^+)| \leq 4\delta(2\delta + |d|).$$

Applying a similar procedure as in the proof of Lemma 2.8.4 allows us to conclude that $Z_j(t) \geq 0$ for every $j \in \mathbb{Z}$. \square

Lemma 2.8.6. *Fix $T > 0$ and pick a sufficiently small $\delta_0 > 0$. Then for any $\Gamma^0 \in \ell^\infty(\mathbb{Z})$ with $\|\partial^+\Gamma^0\|_{\ell^\infty} \leq \delta_0$, the solution $\Gamma \in C^1([0, T], \ell^\infty(\mathbb{Z}))$ to the mean curvature LDE (2.8.1) with $\Gamma(0) = \Gamma^0$ satisfies*

$$\|\partial^+\Gamma(t)\|_{\ell^\infty} \leq \delta_0, \quad \text{for all } t \in [0, T]. \quad (2.8.8)$$

Proof. Writing $\Upsilon = \partial^+\Gamma$, we can apply Grönwall's inequality to (2.8.7) to find

$$\|\Upsilon(t)\|_{\ell^\infty} \leq K \|\Upsilon(0)\|_{\ell^\infty} e^{bt}, \quad (2.8.9)$$

for some constants $K \geq 1$ and $b > 0$ that are independent of T . Recalling the constant $\delta > 0$ from Lemma 2.8.5, we now choose $\delta_0 > 0$ in such a way that $\delta_0 K e^{bT} \leq \delta$. Applying the comparison principle from Lemma 2.8.5, we conclude that $\|\Upsilon(t)\|_{\ell^\infty} \leq \|\Upsilon(0)\|_{\ell^\infty}$ holds for $t \in [0, T]$. Indeed, the constant function $\|\Upsilon(0)\|_{\ell^\infty}$ also satisfies LDE (2.8.7). \square

Corollary 2.8.7. *Pick $\Gamma^0 \in \ell^\infty(\mathbb{Z})$. Then there exists a unique solution $\Gamma \in C^1([0, \infty), \ell^\infty(\mathbb{Z}))$ of the mean curvature LDE (2.8.1). Moreover, there exists $\delta > 0$ such that the initial bound $\|\partial^+\Gamma^0\|_{\ell^\infty} \leq \delta$, implies that also*

$$\|\partial^+\Gamma(t)\|_{\ell^\infty} \leq \delta, \quad \text{for all } t \geq 0. \quad (2.8.10)$$

Proof. Existence and uniqueness follows from standard arguments. Applying an iterative argument involving Lemma 2.8.6 leads to the uniform bound (2.8.10). \square

Proof of Proposition 2.8.2. Using the fact that V satisfies the LDE (2.7.4), we compute

$$\mathcal{J}_{\text{dc}}[V] = \dot{V} - \frac{\partial^2 V}{\beta_V^2} - 2d\beta_V - c + 2d \quad (2.8.11)$$

$$= \partial^{(2)}V \left(1 - \frac{1}{\beta_V^2}\right) + 2d \left(1 + \frac{1}{2}\alpha_V - \beta_V\right) \quad (2.8.12)$$

$$+ \frac{1}{2d} \int_0^{d\partial^+V} e^s (d\partial^+V - s)^2 ds + \frac{1}{2d} \int_0^{-d\partial^-V} e^s (d\partial^-V + s)^2 ds. \quad (2.8.13)$$

Expanding β_V around 0 and using Corollary 2.6.2, we find a constant $M > 0$ for which

$$\|\mathcal{J}_{\text{dc}}[V]\|_{\ell^\infty} \leq M \min \left\{ \|\partial^+V(0)\|_{\ell^\infty}, t^{-\frac{3}{2}} \right\}.$$

We define the constant $\delta > 0$ and the function $K : [0, \infty) \rightarrow \mathbb{R}$ by

$$\delta = \frac{\epsilon^3}{M^3 6^3}, \quad K(t) = M \min \left\{ \delta, t^{-\frac{3}{2}} \right\}.$$

Possibly reducing $\epsilon > 0$, we may assume that $\delta > 0$ is sufficiently small to satisfy the requirements of Lemma 2.8.4 and Corollary 2.8.7.

Next, we pick a smooth function $q : [0, \infty)$ that satisfies

$$K(t) \leq q(t) \leq 2K(t)$$

and introduce the integral $p(t) = \int_0^t q(s) ds$. It is straightforward to check that $0 \leq p(t) \leq \epsilon$ for every $t \geq 0$. By spatial homogeneity, we have $\mathcal{J}_{\text{dc}}[V + p] = \mathcal{J}_{\text{dc}}[V] + \dot{p}$ and hence

$$\|\mathcal{J}_{\text{dc}}[V + p]\|_{\ell^\infty} \geq 0.$$

In particular, the function $V + p$ is a supersolution of the LDE (2.7.4). Lemma 2.8.4 hence implies

$$\Gamma(t) \leq V(t) + p(t) \leq V(t) + \epsilon.$$

The inequality $V(t) - \epsilon \leq \Gamma(t)$ follows similarly by constructing an appropriate subsolution for the LDE (2.8.1). \square

2.8.3 Proof of Theorem 2.2.3

As a final step, we need to link the parameter $d = -\langle \Psi'', \psi \rangle$ used here and in §2.7 to the expressions in (2.2.3) that involve the wavespeed c and its angular derivatives. To this end, we recall the identity

$$(\partial_\theta^2 c_\theta)|_{\theta=0} = \langle \Phi'(\cdot + 1) - \Phi'(\cdot - 1) - 2\Phi'', \psi \rangle$$

that was obtained in [49]. As expected, this expression vanishes in the continuum limit since

$$\lim_{h \rightarrow 0} \frac{\Phi'(\cdot + h) - \Phi'(\cdot - h)}{h} - 2\Phi'' = 0.$$

Lemma 2.8.8. *Suppose that (Hg) and $(H\Phi)$ both hold. Then the parameter d defined in (2.7.2) satisfies the identity*

$$d = \frac{c}{2} + \frac{(\partial_\theta^2 c_\theta)|_{\theta=0}}{2}. \quad (2.8.14)$$

Proof. Comparing (2.8.14) with (2.7.2) and recalling the characterization (2.7.1) together with the normalization $\langle \Phi', \psi \rangle = 1$, it suffices to show that the function

$$h(\xi) = \Phi'(\xi + 1) - \Phi'(\xi - 1) + c\Phi'(\xi)$$

satisfies $h \in \text{Range}(\mathcal{L}_{\text{tw}})$. To achieve this, we write $\varphi(\xi) = \xi\Phi'(\xi)$ and recall the travelling wave MFDE (2.2.7) to compute

$$\begin{aligned} \mathcal{L}_{\text{tw}}\varphi(\xi) &= c\varphi'(\xi) + \varphi(\xi + 1) + \varphi(\xi - 1) - 2\varphi(\xi) + g'(\Phi(\xi))\varphi(\xi) \\ &= c\Phi'(\xi) + c\xi\Phi''(\xi) + \xi\Phi'(\xi + 1) + \Phi'(\xi + 1) + \xi\Phi'(\xi - 1) - \Phi'(\xi - 1) \\ &\quad - 2\xi\Phi'(\xi) + \xi g'(\Phi(\xi))\Phi'(\xi) \\ &= h(\xi) + \xi \frac{d}{d\xi} \left(c\Phi'(\xi) + \Phi(\xi + 1) + \Phi(\xi - 1) - 2\Phi(\xi) + g(\Phi(\xi)) \right) \\ &= h(\xi), \end{aligned}$$

as desired. \square

Proof of Theorem 2.2.3. The statements follow directly from Propositions 2.8.1-2.8.2 and Lemma 2.8.8. \square

2.9 Stability results

Our goal here is to establish Theorem 2.2.4, our final main result. In particular, we consider the two solutions

$$u : [0, \infty) \rightarrow \ell^\infty(\mathbb{Z}^2), \quad u^{\text{per}} : [0, \infty) \rightarrow \ell^\infty(\mathbb{Z}^2) \quad (2.9.1)$$

to the Allen-Cahn LDE (2.2.1) with the respective initial conditions

$$u(0) = u^0, \quad u^{\text{per}}(0) = u^{0;\text{per}},$$

together with their associated phases

$$\gamma : [T, \infty) \rightarrow \ell^\infty(\mathbb{Z}), \quad \gamma^{\text{per}} : [T, \infty) \rightarrow \ell^\infty(\mathbb{Z}) \quad (2.9.2)$$

that are defined by (2.2.12) for some sufficiently large $T \gg 1$. Since the LDE (2.2.1) is autonomous, the uniqueness of solutions imply that u^{per} and hence the phase γ^{per} inherit the j -periodicity

$$u_{i,j+P}^{\text{per}}(t) = u_{i,j}^{\text{per}}(t), \quad \gamma_{j+P}^{\text{per}}(t) = \gamma_j^{\text{per}}(t)$$

for $t \geq 0$ respectively $t \geq T$.

It is natural to expect that $u_{\cdot,j}(t)$ converges to $u_{\cdot,j}^{\text{per}}(t)$ as $|j| \rightarrow \infty$, which we confirm below in §2.9.1. However, one cannot expect the corresponding result to hold for the phases (2.9.2), on account of the discontinuities that occur. In fact, we obtain the following asymptotic ‘almost-convergence’ result.

Proposition 2.9.1. *Consider the setting of Theorem 2.2.4 and recall the two phase functions (2.9.2). Then for every $\epsilon > 0$ there exists a constant T_ϵ together with a function*

$$J_\epsilon : [T_\epsilon, \infty) \rightarrow \mathbb{Z}_{\geq 0}$$

so that we have the bound

$$|\gamma_j(t) - \gamma_j^{\text{per}}(t)| \leq \epsilon$$

for every $t \geq T_\epsilon$ and $|j| \geq J_\epsilon(t)$.

In order to explore the consequences of the approximation result Proposition 2.8.1, we hence need to understand the evolution of asymptotically almost-periodic initial conditions under (2.7.4). This is achieved in our second main result here. We emphasize that in the special case $P = 1$, the asymptotic phase μ is equal to the value taken by the constant sequence $V^{0;\text{per}}$.

Proposition 2.9.2. *Suppose that the assumptions (Hg) and (HΦ) both hold, fix two constants $R > 0$ and $P \in \mathbb{Z}_{>0}$ and pick a sufficiently large $K > 0$. Then for any $\epsilon > 0$ and $J \in \mathbb{Z}_{\geq 0}$, there exists a time $T_{\epsilon, J} > 0$ so that the following holds true.*

Consider any pair $(V^0, V^{0;\text{per}}) \in \ell^\infty(\mathbb{Z})^2$ that satisfies the conditions

(a) *For all $|j| \geq J$ we have $|V_j^0 - V_j^{0;\text{per}}| \leq \epsilon$.*

(b) *The periodicity $V_{j+P}^{0;\text{per}} = V_j^{0;\text{per}}$ holds for all $j \in \mathbb{Z}$.*

(c) *We have the deviation bounds*

$$[V^{0;\text{per}}]_{\text{dev}} \leq R, \quad [V^0]_{\text{dev}} \leq R.$$

Then there exists an asymptotic phase $\mu \in \mathbb{R}$ so that the solution $V : [0, \infty) \rightarrow \ell^\infty(\mathbb{Z})$ to the LDE (2.7.4) with the initial condition $V(0) = V^0$ satisfies the bound

$$\|V(t) - ct - \mu\|_{\ell^\infty(\mathbb{Z})} \leq K\epsilon, \quad t \geq T_{\epsilon, J}. \quad (2.9.3)$$

Proof of Theorem 2.2.4. Pick $\epsilon > 0$. Recalling the terminology of of Propositions 2.8.1 and 2.9.1, we introduce the constants $\bar{\tau}_\epsilon = \max\{\tau_\epsilon, T_\epsilon\}$ and $\bar{J}_\epsilon = J_\epsilon(\bar{\tau}_\epsilon)$ and write $V^{(\epsilon)}$ for the solution to the LDE (2.7.4) with the initial condition $V^{(\epsilon)}(0) = \gamma(\bar{\tau}_\epsilon)$. Writing μ_ϵ for the phase defined in Proposition 2.9.2, we combine (2.8.2) with (2.9.3) to obtain

$$\begin{aligned} \|\gamma(t + \bar{\tau}_\epsilon) - ct - \mu_\epsilon\|_{\ell^\infty} &\leq \|\gamma(t + \bar{\tau}_\epsilon) - V^{(\epsilon)}(t)\|_{\ell^\infty} + \|V^{(\epsilon)}(t) - ct - \mu_\epsilon\|_{\ell^\infty} \\ &\leq (K + 1)\epsilon, \end{aligned} \quad (2.9.4)$$

for all $t \geq T_{\epsilon, \bar{J}_\epsilon}$.

We now claim that there exists $\mu \in \mathbb{R}$ for which we have the limit

$$\lim_{\epsilon \downarrow 0} (\mu_\epsilon - c\bar{\tau}_\epsilon) = \mu.$$

Indeed, the uniform bound on $\gamma(t) - ct$ obtained in Lemma 2.5.4 allows us to find a convergent subsequence, which using (2.9.4) can be transferred to the full set. Sending $\epsilon \downarrow 0$ we hence obtain

$$\lim_{t \rightarrow \infty} \|\gamma(t) - ct - \mu\|_{\ell^\infty(\mathbb{Z})} = 0,$$

which leads to the desired convergence in view of Theorem 2.2.2. \square

2.9.1 Spatial asymptotics

In this subsection we establish Proposition 2.9.1. As a preparation, we compare the j -asymptotic behaviour of the two solutions (2.9.1). We remark that the arguments in Lemma 2.9.4 below remain valid upon replacing the limits in (2.2.15) and (2.9.5) by their two counterparts $|i| \pm j \rightarrow \infty$, which are one-sided in j . This validates the comments in §2.1 concerning the limit (2.1.39).

Lemma 2.9.3. *Assume that (Hg) is satisfied and consider any $u_A^0 \in \ell^\infty(\mathbb{Z}^2)$. Then for any $\epsilon > 0$ and time $T > 0$, there exists $\delta > 0$ so that for any $u_B^0 \in \ell^\infty(\mathbb{Z}^2)$ that satisfies*

$$\|u_A^0 - u_B^0\|_{\ell^\infty(\mathbb{Z}^2)} \leq \delta,$$

the solutions u_A and u_B of the Allen-Cahn LDE (2.2.1) with the initial conditions $u_A(0) = u_A^0$ and $u_B(0) = u_B^0$ satisfy

$$\|u_A(t) - u_B(t)\|_{\ell^\infty(\mathbb{Z}^2)} \leq \epsilon, \quad t \in [0, T].$$

Proof. This is a standard consequence of the well-posedness of (2.2.1) in $\ell^\infty(\mathbb{Z}^2)$. \square

Lemma 2.9.4. *Consider the setting of Theorem 2.2.4 and recall the two solutions (2.9.1). Then for every $\tau > 0$ we have the spatial limit*

$$u_{i,j}(\tau) - u_{i,j}^{\text{per}}(\tau) \rightarrow 0, \quad \text{as } |i| + |j| \rightarrow \infty. \quad (2.9.5)$$

Proof. In view of symmetry considerations, it suffices to establish the claim for the limit $i+j \rightarrow -\infty$. To this end, we fix an arbitrary $\epsilon > 0$. We write \tilde{u}^{per} for the solution to the LDE (2.7.4) with the initial condition $\tilde{u}^{\text{per}}(0) = u^{0:\text{per}} + \delta$, using Lemma 2.9.3 to pick $\delta > 0$ in such a way that

$$\tilde{u}^{\text{per}}(\tau) \leq u^{\text{per}}(\tau) + \frac{\epsilon}{2}.$$

We subsequently pick $M > 0$ in such a way that

$$u_{i,j}^0 \leq \tilde{u}_{i,j}^{0:\text{per}}(0) + \delta + Me^{|c|(i+j)} = \tilde{u}_{i,j}^{\text{per}}(0) + Me^{|c|(i+j)}$$

holds for every $(i, j) \in \mathbb{Z}^2$.

On account of (H0) and the comparison principle, we can pick $A \geq 1$ in such a way that

$$-A \leq \tilde{u}^{\text{per}}(t) \leq A$$

holds for all $t \in [0, \tau]$. We now write

$$K = \max\{g'(s) : -A \leq s \leq A\} > 0$$

and observe that (Hg) implies that

$$g(s + \beta) \leq g(s) + K\beta \quad (2.9.6)$$

for any $-A \leq s \leq A$ and $\beta \geq 0$.

We now pick $\alpha > 0$ in such a way that

$$\alpha|c| - \frac{c^4}{6} \cosh |c| > K \quad (2.9.7)$$

and claim that the function

$$w_{i,j}(t) = \tilde{u}_{i,j}^{\text{per}}(t) + Me^{c|(i+j+2|c|t+\alpha t)} \quad (2.9.8)$$

is a super-solution to (2.2.1). Indeed, recalling the residual (2.3.4), a short computation yields

$$\begin{aligned} \mathcal{J}[w]_{i,j}(t) &= g(\tilde{u}_{i,j}^{\text{per}}(t)) - g(w_{i,j}(t)) \\ &\quad + Me^{c|(i+j+2|c|t+\alpha t)} \left(2c^2 + \alpha|c| - 2e^{|c|} - 2e^{-|c|} + 4 \right) \\ &= g(\tilde{u}_{i,j}^{\text{per}}(t)) - g(w_{i,j}(t)) + (w_{i,j}(t) - \tilde{u}_{i,j}^{\text{per}}(t)) \left(\alpha|c| - \frac{c^4}{6} \cosh \tilde{c} \right) \end{aligned}$$

for some $\tilde{c} \in [0, |c|]$, which using (2.9.6) and (2.9.7) implies

$$\begin{aligned} \mathcal{J}[w]_{i,j} &\geq (w_{i,j} - \tilde{u}_{i,j}^{\text{per}}) \left(\alpha|c| - \frac{c^4}{6} \cosh \tilde{c} - K \right) \\ &\geq 0. \end{aligned}$$

In particular, the comparison principles allows us to conclude that

$$u_{i,j}(\tau) \leq u_{i,j}^{\text{per}}(\tau) + \frac{\epsilon}{2} + Me^{c|(i+j+2|c|\tau+\alpha\tau)},$$

which implies that there exists $L_\epsilon \gg 1$ so that

$$u_{i,j}(\tau) \leq u_{i,j}^{\text{per}}(\tau) + \epsilon$$

for $i + j \leq -L_\epsilon$. An analogous lower bound can be obtained by exploiting similar sub-solutions, which completes the proof. \square

Proof of Proposition 2.9.1. For any sufficiently large $t \geq 1$ and $(i, j) \in \mathbb{Z}^2$ we may estimate

$$\begin{aligned} \Phi(i - \gamma_j^{\text{per}}(t)) - \Phi(i - \gamma_j(t)) &\leq |\Phi(i - \gamma_j^{\text{per}}(t)) - u_{i,j}^{\text{per}}(t)| + |u_{i,j}(t) - \Phi(i - \gamma_j(t))| \\ &\quad + |u_{i,j}^{\text{per}}(t) - u_{i,j}(t)|. \end{aligned}$$

Applying Theorem 2.2.2 and Lemma 2.9.4, we find a constant $T_\epsilon > 0$ and a function $J_\epsilon : [T_\epsilon, \infty) \rightarrow \mathbb{Z}_{\geq 0}$ for which we have

$$\Phi(i - \gamma_j^{\text{per}}(t)) - \Phi(i - \gamma_j(t)) \leq 3\epsilon \quad (2.9.9)$$

for all $t \geq T_\epsilon$ and $|j| \geq J_\epsilon(t)$. Recalling the constant $M > 0$ from Lemma 2.5.4 and writing

$$\nu = \min\{\Phi'(\xi) : |\xi| \leq M + 1\} > 0,$$

we may substitute $i = \lceil ct \rceil$ into (2.9.9) to obtain

$$\nu|\gamma_j^{\text{per}}(t) - \gamma_j(t)| \leq \Phi(\lceil ct \rceil - \gamma_j^{\text{per}}(t)) - \Phi(\lceil ct \rceil - \gamma_j(t)) \leq 3\epsilon$$

for all $t \geq T_\epsilon$ and $|j| \geq J_\epsilon(t)$. This yields the desired result after some minor re-belling. \square

2.9.2 Phase asymptotics

It remains to establish Proposition 2.9.2. We accomplish this by using the Cole-Hopf transformation discussed in §2.6 to transform (2.7.4) into the linear heat LDE (2.6.1). The bounds in §2.6 readily allow us to analyze solutions with initial conditions that are asymptotically ‘almost-periodic’.

Lemma 2.9.5. *Pick an integer $P \geq 1$ and let $h \in C^1([0, \infty); \ell^\infty(\mathbb{Z}))$ be a solution to the discrete heat equation (2.6.1) with an initial condition $h^0 \in \ell^\infty(\mathbb{Z})$ that satisfies $h_{j+P}^0 = h_j^0$ for all $j \in \mathbb{Z}$. Then upon introducing the average*

$$\bar{h} = \frac{1}{P} \sum_{j=0}^{P-1} h_j^0,$$

we have the limit

$$\lim_{t \rightarrow \infty} \|h(t) - \bar{h}\|_{\ell^\infty} = 0.$$

Proof. Since h inherits the periodicity of h^0 , the function

$$H_j(t) = \frac{1}{P} \sum_{k=0}^{P-1} h_{j+k}(t)$$

is constant with respect to j . Since it also satisfies (2.6.1), we must have $H_j(t) = \bar{h}$. The result now follows from the fact that $\|\partial^+ h(t)\|_{\ell^\infty} \rightarrow 0$ as $t \rightarrow \infty$; see (2.6.7). \square

Proof of Proposition 2.9.2. We first treat the case $d \neq 0$ and write V^{per} for the solution to the nonlinear LDE (2.7.4) with initial condition $V^{\text{per}}(0) = V^{0;\text{per}}$. Without loss of generality, we may assume that $V_0^{0;\text{per}} = 0$. Inspired by the proof of Corollary 2.6.2, we introduce the functions

$$h^{\text{per}}(t) = e^{d(V^{\text{per}}(t)-ct)}, \quad h = e^{d(V(t)-ct)}, \quad q(t) = e^{dV(t)-dV^{\text{per}}(t)} - 1 \quad (2.9.10)$$

and note that h^{per} and h both satisfy the linear heat LDE (2.6.1). By construction, we have

$$h(0) = h^{\text{per}}(0) + h^{\text{per}}(0)q(0),$$

which allows us to write

$$h_j(t) - h_j^{\text{per}}(t) = \sum_{k \in \mathbb{Z}} G_k(t) h_{j-k}^{\text{per}}(0) q_{j-k}(0). \quad (2.9.11)$$

Assuming $0 < \epsilon < 1$ and $R \geq 1$, we see that

$$|V_0^0| \leq R + |V_J| \leq R + \epsilon + V_J^0 \leq 2R + 1 \leq 3R$$

and hence $\|V^0\|_{\ell^\infty} \leq 4R$. This allows us to obtain the global bounds

$$\|h^{\text{per}}(0)\|_{\ell^\infty} \leq e^{|d|R}, \quad \|q(0)\|_{\ell^\infty} \leq e^{5|d|R} + 1,$$

together with the tail bound

$$|q_j(0)| \leq e^{|d|\epsilon} - 1, \quad j \geq |J|.$$

Using (2.9.11), these bounds allow us to obtain the estimate

$$\begin{aligned} \|h(t) - h^{\text{per}}(t)\|_{\ell^\infty} &\leq \sum_{|j-k| \geq J} |G_k(t)|(e^{|d|\epsilon} - 1) + \sum_{|j-k| < J} |G_k(t)|e^{|d|R}(e^{5|d|R} + 1) \\ &\leq (e^{|d|\epsilon} - 1) \|G(t)\|_{\ell^1} + (2J - 1)e^{|d|R}(e^{5|d|R} + 1) \|G(t)\|_{\ell^\infty}. \end{aligned}$$

Since $\|G(t)\|_{\ell^1} = 1$ on account of (2.6.16) and $\|G(t)\|_{\ell^\infty} \leq Ct^{-1/2}$ on account of (2.6.17), we can find a time $T = T(\epsilon, J, d, R)$ so that

$$\|h(t) - h^{\text{per}}(t)\|_{\ell^\infty} \leq 2(e^{|d|\epsilon} - 1)$$

for all $t \geq T$.

After possibly increasing T , we can use Lemma 2.9.5 to conclude

$$\|h(t) - \bar{h}\|_{\ell^\infty} \leq 4(e^{|d|\epsilon} - 1), \quad t \geq T,$$

for some $\bar{h} \in [0, e^{|d|R}]$. Inverting the transformation (2.9.10) hence leads to the desired bound on V with $\mu = \frac{\ln \bar{h}}{d}$. The remaining case $d = 0$ can be treated in the same fashion as above, but now one does not need to use the nonlinear coordinate transformation. \square

CURVATURE-DRIVEN FRONT PROPAGATION
THROUGH PLANAR LATTICES IN OBLIQUE
DIRECTIONS

¹ In this paper we investigate the long-term behaviour of solutions to the discrete Allen-Cahn equation posed on a two-dimensional lattice. We show that front-like initial conditions evolve towards a planar travelling wave modulated by a phaseshift $\gamma_l(t)$ that depends on the coordinate l transverse to the primary direction of propagation. This direction is allowed to be general, but rational, generalizing earlier known results for the horizontal direction. We show that the behaviour of γ can be asymptotically linked to the behaviour of a suitably discretized mean curvature flow. This allows us to show that travelling waves propagating in rational directions are nonlinearly stable with respect to perturbations that are asymptotically periodic in the transverse direction.

3.1 Introduction

The main goal of this paper is to study the behaviour of curved wavefronts under the dynamics of the Allen-Cahn lattice differential equation (LDE)

$$\dot{u}_{i,j} = u_{i+1,j} + u_{i,j+1} + u_{i-1,j} + u_{i,j-1} - 4u_{i,j} + g(u_{i,j}; a), \quad (3.1.1)$$

posed on the planar lattice $(i, j) \in \mathbb{Z}^2$. For concreteness, we consider the standard bistable nonlinearity

$$g(u; a) = u(u - a)(1 - u), \quad a \in (0, 1), \quad (3.1.2)$$

throughout this introduction. We are interested in fronts that move in the rational direction $(\sigma_h, \sigma_v) \in \mathbb{Z}^2$, which motivates the introduction of the parallel and transverse

¹The content of this chapter has been published as Mia Jukić, Hermen Jan Hupkes, *Curvature-driven front propagation through planar lattices in oblique directions*, Communications on Pure & Applied Analysis, see [53].

coordinates

$$n = n(i, j) = i\sigma_h + j\sigma_v, \quad l = l(i, j) = i\sigma_v - j\sigma_h \quad (3.1.3)$$

that we use interchangeably with (i, j) ; see Figure 3.1.

Our main results state that initial conditions that are ‘front-like’ in the rough sense that

$$u_{i,j}(0) < a - \epsilon \quad \text{for } n(i, j) \ll -1, \quad u_{i,j}(0) > a + \epsilon \quad \text{for } n(i, j) \gg 1 \quad (3.1.4)$$

holds for some $\epsilon > 0$, evolve towards an interface of the form

$$u_{i,j}(t) = \Phi(n(i, j) - \gamma_l(i, j)(t)). \quad (3.1.5)$$

Here the special case $\gamma_l(t) = ct$ represents the well-known planar travelling wave solution to (3.1.1) that travels in the direction (σ_h, σ_v) and connects the two stable equilibria

$$\lim_{\xi \rightarrow -\infty} \Phi(\xi) = 0, \quad \lim_{\xi \rightarrow +\infty} \Phi(\xi) = 1. \quad (3.1.6)$$

In general however we show that the dynamics of γ_l can be well-approximated by a discrete mean-curvature flow. This generalizes the results from [52] where we only considered the horizontal direction and extends the known basin of attraction for planar travelling waves beyond the settings considered in [43, 44]. The misalignment of the propagation direction with the underlying lattice causes several mathematical intricacies that we resolve throughout this work.

Modelling background Lattice differential equations arise in numerous problems in which the underlying discrete spatial topology plays an important role. For example, in [11, 12, 55], the authors use LDEs to model *saltatory conduction*, which describes the ‘hopping’ behaviour of action potentials propagating through myelinated nerve axons. In population dynamics, two-dimensional LDEs are used to model the strong Allee effect on patchy landscapes; see [58, 88]. In both of these examples it is necessary to include the spatial heterogeneity of the domain into the model in order to simulate effects such as wave-pinning. Lattice models have also been used in many other fields, such as material science, morphology and statistical mechanics [15, 25, 70, 9]. For a more extensive list of references we refer the reader to the book by Keener and Sneyd [57] or the surveys [50, 60].

Motivation In order to set the stage, we briefly discuss the continuous counterpart of (3.1.1). This is the well-known Allen-Cahn PDE

$$u_t = \kappa [u_{xx} + u_{yy}] + g(u; a), \quad (3.1.7)$$

where we have included a diffusion constant $\kappa > 0$. Planar travelling front solutions of the form

$$u(x, y, t) = \Phi(x \cos \theta + y \sin \theta - ct) \quad (3.1.8)$$

play a key role towards understanding the global behaviour of (3.1.7) [5]. They can be found [33] by solving the travelling wave ODE

$$-c\Phi'(\xi) = \kappa\Phi''(\xi) + g(\Phi(\xi); a), \quad (3.1.9)$$

which does not depend on the direction of propagation $(\cos \theta, \sin \theta)$. In addition, the dependence on the diffusion coefficient κ can be eliminated through the spatial rescaling

$$\xi \mapsto \xi/\sqrt{\kappa}, \quad c \mapsto c/\sqrt{\kappa}. \quad (3.1.10)$$

This was recently exploited by Matano, Mori & Nara in [68], who studied an anisotropic version of (3.1.7) by allowing the diffusion coefficients to depend on ∇u . In terms of the travelling wave ODE (3.1.9), this effectively introduces a direction-dependence $\kappa = \kappa(\theta)$. The spatial rescalings (3.1.10) subsequently point to a natural anisotropic metric that can be used to analyze the long-time evolution of expansion waves. Indeed, for initial conditions u_0 that satisfy

$$\min_{|(x,y)| \leq L} u_0(x, y) > a, \quad \limsup_{|(x,y)| \rightarrow \infty} u_0(x, y) < a \quad (3.1.11)$$

for some $L \gg 1$, the asymptotic behaviour of the level set

$$\Gamma(t) := \{(x, y) \in \mathbb{R}^2 : u(x, y, t) = a\}$$

is well approximated by the boundary of the Wulff shape [18, 74, 93] associated to this metric, expanding at a speed of $c - [ct]^{-1}$. This latter term can be seen as a correction for curvature-driven effects and also appears in the earlier isotropic studies [89, 51, 79]. The key point is that the expanding Wulff shape is a self-similar solution to an anisotropic mean curvature flow that also underpins the large-time behaviour of curved wavefronts.

Returning to our LDE (3.1.1), we emphasize that anisotropic effects are a natural consequence of the broken rotational symmetry, but they cannot be readily transformed away by spatial rescalings such as (3.1.10). Nevertheless, initial numerical experiments such as those in [91] indicate that the Wulff shape also plays an important role in the long-term evolution of initial conditions such as (3.1.11), but that the behaviour near the corners is rather subtle. One of our main longer term goals is to gain a detailed understanding of this expansion mechanism. A key intermediate step that we pursue in this paper is to understand how discretized curvature flows interact with the dynamics of (3.1.1).

Curved PDE fronts

From a technical point of view, our work is chiefly inspired by the results obtained in [69] by Matano and Nara. They considered the Cauchy problem for equation (3.1.7) with an initial condition that roughly satisfies

$$u(x, y, 0) < a - \epsilon \quad \text{for } x \ll -1, \quad u(x, y, 0) > a + \epsilon \quad \text{for } x \gg 1,$$

again with $\epsilon > 0$. The authors show that for $t \gg 1$ the solution u becomes monotone around $\Phi(0) = \frac{1}{2}$, which, via the implicit theorem argument, allows a phase $\gamma(y, t)$ to be defined via the requirement

$$u(\gamma(y, t), y, t) = \Phi(0). \quad (3.1.12)$$

This phase is particularly convenient because it determines the large time behaviour of the solution u via the asymptotic limit

$$\lim_{t \rightarrow \infty} |u(x, y, t) - \Phi(x - \gamma(y, t))| = 0. \quad (3.1.13)$$

Moreover, the authors showed that the phase γ can be closely tracked by solutions θ to the PDE

$$\theta_t = \theta_{yy} + \frac{c}{2}\theta_y^2 + c, \quad (3.1.14)$$

by constructing super- and sub-solutions to (3.1.7) of the form

$$u^\pm(x, y, t) = \Phi \left(\frac{x - \theta(y, t)}{\sqrt{1 + \theta_y^2}} \pm Z(t) \right) \pm z(t), \quad (3.1.15)$$

where Z and z are small correction terms compensating for the initial differences in phase and amplitude. The main advantage of the PDE (3.1.14) is that it transforms into a standard heat equation via the Cole-Hopf transformation, which leads to explicit expressions for the solution.

Describing the phase γ with the dynamics of the PDE (3.1.14) has two main advantages [69]. First, the solution θ approximates solutions of the mean curvature flow with a drift term c , allowing for a physical interpretation of the phase γ . Second, this description can be used to establish convergence results for initial conditions u^0 that are uniquely ergodic, which includes the case that u^0 is periodic or almost-periodic in the transverse direction. These results are hence part of an ever-increasing family of stability results for travelling fronts in dissipative PDEs, which include the classic one-dimensional papers [34, 81] and their higher-dimensional counterparts [54, 94, 63].

Discrete setting Substituting the planar wave Ansatz

$$u_{ij}(t) = \Phi(n(i, j) - ct) \quad (3.1.16)$$

into the LDE (3.1.1), we see that the wave pair (c, Φ) must satisfy the mixed functional differential equation (MFDE)

$$-c\Phi'(\xi) = \Phi(\xi + \sigma_h) + \Phi(\xi - \sigma_h) + \Phi(\xi + \sigma_v) + \Phi(\xi - \sigma_v) - 4\Phi(\xi) + g(\Phi(\xi); a), \quad (3.1.17)$$

which we consider together with the boundary conditions (3.1.6). This MFDE has been well-studied by now and various detailed existence and uniqueness results can be found in the seminal paper [67] and the survey [50]. For now we simply point out the qualitative differences between the $c = 0$ and $c \neq 0$ cases and the explicit dependence on the propagation direction, which can be rather delicate. Indeed, for a single fixed $a \in (0, 1)$ certain directions can support freely travelling waves with smooth profiles, while others only feature pinned step-like profiles [16, 46].

For our purposes in this paper, the main consequence of the spatial discreteness is that it is no longer possible to construct sub- and super-solutions by applying relatively straightforward phase modulations to the profile Φ as in (3.1.15). Indeed, the shifts in (3.1.17) prevent us from simply factorizing out a common factor $\Phi'(\xi)$ from the associated residuals as was possible in the series [68, 69, 14]. Inspired by normal form theory, we circumvent this problem by using a super-solution Ansatz of

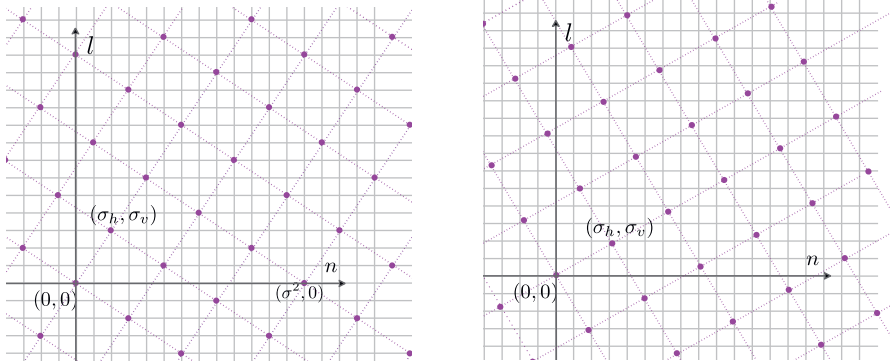


Figure 3.1: Both panels show the sublattice \mathbb{Z}_x^2 obtained after the coordinate transformation (3.1.3), for the rational direction $(\sigma_h, \sigma_v) = (2, 3)$ on the left and the irrational angle $\pi/6$ on the right. We see that the left lattice is a proper subset of \mathbb{Z}^2 . On the right however the purple dots only coincide with \mathbb{Z}^2 at the origin. Moreover, the sets $\{i\sigma_h + j\sigma_v : (i, j) \in \mathbb{Z}^2\}$ and $\{i\sigma_v - j\sigma_h : (i, j) \in \mathbb{Z}^2\}$ are both dense in \mathbb{R} . This feature significantly differentiates the analysis between the rational and irrational directions.

the form

$$\begin{aligned}
 u_{n,l}^+(t) &= \Phi(n - \theta_l(t) + Z(t)) + \sum_{k=-N}^N p_k(n - \theta_l(t) + Z(t))(\theta_{l+k}(t) - \theta_l(t)) \\
 &+ \sum_{k=-N}^N \sum_{k'=-N}^N q_{k,k'}(n - \theta_l(t) + Z(t))(\theta_{l+k}(t) - \theta_l(t))(\theta_{l+k'}(t) - \theta_l(t)) + z(t),
 \end{aligned} \tag{3.1.18}$$

in which $N = 2 \max\{|\sigma_h|, |\sigma_v|\}$. The auxiliary functions (p_k) , and $(q_{k,k'})$ are chosen in such a way that the dangerous slowly decaying terms caused by the lattice anisotropy are cancelled. To achieve this, it is necessary to carefully analyze the spectral stability properties of the underlying planar wave (c, Φ) and exploit the Fredholm theory for linear MFDEs that was developed by Mallet-Paret [66].

The Ansatz (3.1.18) (but with different functions p , q and θ) first appeared in [44] - where it was used to study the evolution of initial conditions of the form

$$u_{i,j}(0) = \Phi(n(i, j)) + v_{i,j}^0, \quad \lim_{|i|+|j| \rightarrow \infty} |v_{i,j}^0| \rightarrow 0.$$

The authors established algebraic decay rates for the convergence

$$u_{ij}(t) \rightarrow \Phi(n(i, j) - ct),$$

hence establishing the stability of the planar wave (3.1.16) under localized perturbations, which form a (restrictive) subset of the general class (3.1.4) considered here.

The main novel aspect compared to [44] is that we need to incorporate nonlinear terms in the evolution of θ in order to capture the curvature-driven interface dynamics resulting from the non-local nature of the perturbations. Indeed, our evolution

equation for θ takes the form

$$\dot{\theta}_l(t) = \frac{1}{d} \sum_{k=-N}^N a_k \left(e^{d(\theta_{l+k}(t) - \theta_l(t))} - 1 \right) + c, \quad (3.1.19)$$

for a set of coefficients (a_k) that is prescribed by the normal form analysis discussed above. For now, we simply mention that the parameter d can be directly expressed in terms of important geometric and spectral quantities associated to the wave (c, Φ) . As we discuss in the sequel, this will allow us to make the connection between (3.1.19) and a discretized mean curvature flow.

As in the continuous case, solutions to (3.1.19) can be used to approximate the behaviour of the phase γ appearing in (3.1.5). This control is sufficiently strong to establish the convergence $\gamma(t) \rightarrow ct + \mu$ for initial conditions of the form

$$u_{i,j}(0) = \Phi(n(i, j) - \kappa_l) + v_{i,j}^0, \quad \lim_{|i|+|j| \rightarrow \infty} |v_{i,j}^0| \rightarrow 0, \quad (3.1.20)$$

where κ_l is an arbitrary periodic sequence. The main significance compared to the earlier results in [43, 44] is that this corresponds to an ‘infinite-energy’ shift in the underlying wave position, during which the periodic wrinkles are flattened out under the flow of (3.1.19).

We believe that the convergence $\gamma(t) \rightarrow ct + \mu$ also holds if for any continuous $\Psi : \ell^\infty \rightarrow \mathbb{R}$ there exists a limit

$$\bar{\Psi} = \lim_{R \rightarrow \infty} \frac{1}{2R+1} \sum_{l=-R}^R \Psi(\kappa_{\cdot+l+k})$$

that is uniform and homogeneous in k . Such sequences κ are referred to as uniquely ergodic, a class that includes almost-periodic sequences. This is discussed in detail by Matano and Nara in [69, §2] and the main ideas can be readily transferred to the present discrete setting. The subtle point is to check in which sense our phase construction preserves this ergodicity, which we do not pursue here due to the technical intricacies involved.

In our earlier work [52] we restricted attention to the horizontal direction

$$(\sigma_h, \sigma_v) = (1, 0),$$

which greatly simplified the analysis of (3.1.18) and (3.1.19). Indeed, we were able to choose $N = 1$, with $a_1 = a_{-1} = 1$ and $p_{-1} = p_1 = 0$, which means that the linear terms reduce to the standard discrete heat equation. Solutions could hence be represented explicitly in terms of modified Bessel functions of the first kind, for which detailed bounds are available in the literature. In addition, the remaining auxiliary functions satisfied the useful identities

$$q_{-1,+1} = q_{+1,-1} = 0, \quad q_{-1,-1} = q_{+1,+1},$$

allowing the quadratic terms in the super-solution residual to be analyzed in a transparent fashion.

For general rational directions, some of the coefficients a_k can become negative, in which case (3.1.19) no longer admits a comparison principle. In addition, we can no longer represent our solutions in terms of special functions for which powerful off-the-shelf estimates are available. We resolve these issues in §3.5-3.6 by developing an approximate comparison principle and using the saddle-point method to extract the necessary decay rates on the Green's function for the linear part of (3.1.19).

Mean curvature flows Matano and Nara proved in [69] that the solution $\theta(t)$ to the PDE (3.1.14) can be approximated by solutions Γ to the PDE

$$\frac{\Gamma_t}{\sqrt{1 + \Gamma_y^2}} = \frac{\Gamma_{yy}}{(1 + \Gamma_y^2)^{3/2}} + c. \quad (3.1.21)$$

This equation is known as a mean curvature flow equation with an additional drift term c . Indeed, writing $\nu(y, t)$ for the rightward-pointing normal vector of the interfacial graph $\{\Gamma(y, t), y\}$, together with $V(y, t)$ for the horizontal velocity vector and $H(y, t)$ for the curvature, we can make the identifications

$$\nu = [1 + \Gamma_y^2]^{-1/2}(1, -\Gamma_y), \quad V = (\Gamma_t, 0), \quad H = [1 + \Gamma_y^2]^{-3/2}\Gamma_{yy}.$$

In particular, (3.1.21) can be written in the form

$$V \cdot \nu = H + c, \quad (3.1.22)$$

which reflects the rotational invariance of the wavespeed c .

In the discrete setting there is no 'canonical' notion of a mean curvature flow due to the absence of a suitable normal vector for the interface (Γ_l, l) . Indeed, for a fixed index $l \in \mathbb{Z}$ one can consider the angle

$$\varphi_{l;k}(\Gamma) = \arctan \frac{\Gamma_l - \Gamma_{l+k}}{k},$$

for any $k \in \mathbb{Z}$, which measures the orientation of the vector that is transverse to the connection between (Γ_l, l) and $(\Gamma_{l+k}, l+k)$; see Figure 3.1. These can all be considered as normal directions in some sense.

However, it is possible and natural to apply appropriate discretization schemes to (3.1.22). In order to take the lattice anisotropy into account, we start by writing c_φ for the wavespeed associated to the planar wave solutions

$$u_{ij}(t) = \Phi_\varphi(n \cos \varphi + l \sin \varphi - c_\varphi t)$$

to (3.1.1) that travel at an *additional* angle of φ relative to our original planar wave (3.1.16). This allows us to define the directional dispersion

$$\mathcal{D}(\varphi) = \frac{c_\varphi}{\cos \varphi},$$

which measures the speed at which level sets of the wave $(c_\varphi, \Phi_\varphi)$ move along the n -direction.

Setting out to discretize the terms in (3.1.22), we first introduce the average

$$[\bar{c}_\Gamma]_l = \frac{1}{2N} \sum_{0 < |k| \leq N} c_{\varphi_{l;k}(\Gamma)}, \quad (3.1.23)$$

where we use $2N$ neighbours in order to account for all the interactions present in (3.1.19). In addition, we introduce the notation

$$[\beta_\Gamma]_l = \sqrt{1 + \sum_{0 < |k| \leq N} \frac{A_k}{k^2} (\Gamma_{l+k} - \Gamma_l)^2}, \quad [\Delta_\Gamma]_l = \sum_{0 < |k| \leq N} \frac{2B_k}{k^2} (\theta_{l+k} - \theta_l), \quad (3.1.24)$$

which depends on two sequences (A_k) and (B_k) . These must satisfy the normalization conditions

$$\sum_{0 < |k| \leq N} A_k = 1, \quad \sum_{0 < |k| \leq N} B_k = 1, \quad \sum_{0 < |k| \leq N} B_k/k = 0 \quad (3.1.25)$$

in order to ensure that β_Γ and Δ_Γ reduce formally to the symbols $\sqrt{1 + \Gamma_y^2}$ and Γ_{yy} in the continuum limit.

These sequences weigh the contributions of each of the normal directions $\varphi_{l;k}$ to the components of our discrete curvature flow, which we formulate as

$$\beta_\Gamma^{-1} \dot{\Gamma} = \kappa_H \beta_\Gamma^{-3} \Delta_\Gamma + \bar{c}_\Gamma. \quad (3.1.26)$$

It turns out that (3.1.26) and (3.1.19) can be matched up to cubic terms if and only if the parameters are chosen as

$$\kappa_H = \frac{1}{2} \sum_{k=-N}^N k^2 a_k, \quad d = \frac{[\partial_\varphi^2 \mathcal{D}(\varphi)]_{\varphi=0}}{2\kappa_H}. \quad (3.1.27)$$

The latter expression precisely matches the choice that comes from the technical considerations that lead to (3.1.19) during the construction of our super-solution (3.1.18). It also plays a key role in the related studies [40, 49] that concern travelling corner solutions in anisotropic media.

Outlook In this paper we have restricted our attention to rational directions, primarily due to the fact that we lose the periodicity of the Fourier transform for irrational directions. In fact, the relevant Fourier symbol becomes quasi-periodic, making it very cumbersome to extract the necessary decay estimates. We are working on further reduction steps to bypass this issue, which could eventually allow us to consider general rounded interfaces. On the other hand, we do believe that the approach developed here is already strong enough to handle further questions such as the stability of the corner solutions constructed in [49] or the propagation of wavefronts through structured networks.

Organization This paper is organized as follows. After stating our main results in §3.2, we discuss the asymptotic formation of interfaces in §3.3 and §3.4 by exploiting

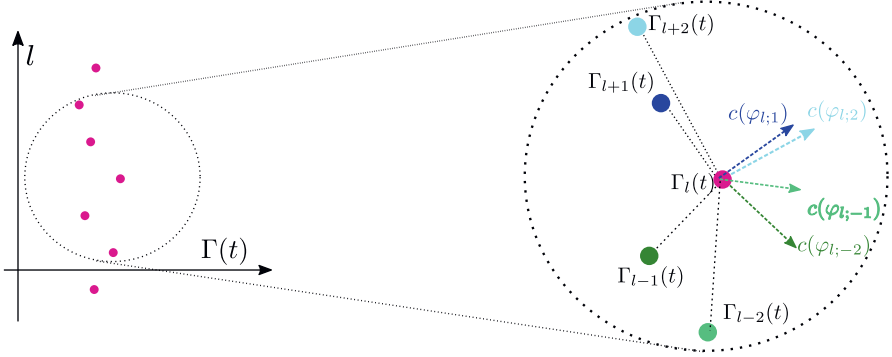


Figure 3.2: Here we provide the geometric motivation behind the definition (3.1.23) for \bar{c}_Γ with $N = 2$. Since there is no uniquely defined normal direction for discrete graphs, we take the average of the velocities associated to the directions transverse to the connecting lines between (Γ_l, l) and $(\Gamma_{l+k}, l+k)$. Here we consider each $0 < |k| \leq 2$.

the properties of ω -limit points. These sections simplify the ideas in [52] and adapt them to the more general setting considered in this paper. We proceed in §3.5 by studying the linearization of our phase LDE (3.1.19). In particular, we use techniques inspired by the saddle-point method to extract our required decay rates and establish a quasi-comparison principle. These are used in §3.6 to incorporate the nonlinear terms in (3.1.19) and build the bridge with the discrete curvature flow (3.1.26). These ingredients allow us to construct sub- and super-solutions for (3.1.1) in §3.7, which are subsequently used in §3.8 to establish our final stability results.

Acknowledgments Both authors acknowledge support from the Netherlands Organization for Scientific Research (NWO) (grant 639.032.612).

3.2 Main results

In this paper we are interested in the discrete Allen-Cahn equation

$$\dot{u}_{i,j}(t) = [\Delta^+ u(t)]_{i,j} + g(u_{i,j}(t)) \quad (3.2.1)$$

posed on the planar lattice \mathbb{Z}^2 . The plus-shaped discrete Laplacian $\Delta^+ : \ell^\infty(\mathbb{Z}^2) \rightarrow \ell^\infty(\mathbb{Z}^2)$ acts as a sum of differences over the nearest neighbors

$$[\Delta^+ u]_{i,j} = u_{i+1,j} + u_{i,j+1} + u_{i-1,j} + u_{i,j-1} - 4u_{i,j}, \quad (3.2.2)$$

while the nonlinear function g satisfies the following standard bistability condition.

(Hg) The nonlinearity $g : \mathbb{R} \rightarrow \mathbb{R}$ is C^3 -smooth and there exists $a \in (0, 1)$ such that

$$g(0) = g(a) = g(1) = 0, \quad g'(0) = g'(1) < 0.$$

In addition, we have the inequalities

$$g(x) > 0 \text{ for } x \in (-\infty, 0) \cup (a, 1), \quad g(x) < 0 \text{ for } x \in (0, a) \cup (1, \infty).$$

In this paper we focus on travelling waves propagating in rational directions. That is, we pick a direction $(\sigma_h, \sigma_v) \in \mathbb{Z}^2$ with $\gcd(\sigma_h, \sigma_v) = 1$ and consider wave-profiles Φ_* that connect the two stable equilibria of the nonlinear function g , while traveling with the speed c_* in the direction (σ_h, σ_v) .

It is convenient to pass to a new (n, l) -coordinate system that is oriented parallel (n) and transverse (l) to the direction of wave-propagation. In particular, we write

$$n = i\sigma_h + j\sigma_v, \quad l = i\sigma_v - j\sigma_h$$

and introduce the notation

$$\mathbb{Z}_\times^2 = \{(n, l) \in \mathbb{Z}^2 : \exists(i, j) \in \mathbb{Z}^2 : n = i\sigma_h + j\sigma_v, l = i\sigma_v - j\sigma_h\} \subset \mathbb{Z}^2$$

for the image of the original grid \mathbb{Z}^2 . Upon introducing the quantities

$$\sigma_* = \sqrt{\sigma_h^2 + \sigma_v^2}, \quad \sigma_\infty = \max\{|\sigma_h|, |\sigma_v|\},$$

we point out the mappings

$$(i + \sigma_h, j + \sigma_v) \mapsto (n + \sigma_*^2, l), \quad (i + \sigma_v, j - \sigma_h) \mapsto (n, l + \sigma_*^2),$$

which implies that for any $(n, l) \in \mathbb{Z}_\times^2$ the point $(n + a\sigma_*^2, l + b\sigma_*^2)$ is also an element of \mathbb{Z}_\times^2 for any $(a, b) \in \mathbb{Z}^2$, see Figure 3.1.

In this new coordinate system the discrete Laplace operator (3.2.2) transforms as

$$[\Delta^\times u]_{n,l} = u_{n+\sigma_h, l+\sigma_v} + u_{n+\sigma_v, l-\sigma_h} + u_{n-\sigma_h, l-\sigma_v} + u_{n-\sigma_v, l+\sigma_h} - 4u_{n,l}. \quad (3.2.3)$$

In particular, the initial value problem that we consider in this paper can be written in the form

$$\dot{u}_{n,l}(t) = [\Delta^\times u(t)]_{n,l} + g(u_{n,l}(t)), \quad (n, l) \in \mathbb{Z}_\times^2, \quad t > 0, \quad (3.2.4)$$

$$u_{n,l}(0) = u_{n,l}^0, \quad (3.2.5)$$

for some initial condition $u^0 \in \ell^\infty(\mathbb{Z}_\times^2)$. Our second assumption imposes a ‘front-like’ property on this initial condition u^0 , see Figure 3.4.

(H0) The initial condition $u^0 \in \ell^\infty(\mathbb{Z}_\times^2)$ satisfies

$$\limsup_{n \rightarrow -\infty} \sup_{l \in \mathbb{Z}: (n,l) \in \mathbb{Z}_\times^2} u_{n,l}^0 < a, \quad \liminf_{n \rightarrow +\infty} \inf_{l \in \mathbb{Z}: (n,l) \in \mathbb{Z}_\times^2} u_{n,l}^0 > a.$$

3.2.1 Travelling waves

A travelling wave solution is any solution of the form

$$u_{n,l}(t) = \Phi_*(n - c_*t) \quad (3.2.6)$$

for some wave-profile Φ_* and speed $c_* \in \mathbb{R}$. Any such pair must necessarily satisfy the MFDE

$$-c_*\Phi'_*(\xi) = \Phi_*(\xi + \sigma_h) + \Phi_*(\xi + \sigma_v) + \Phi_*(\xi - \sigma_h) + \Phi_*(\xi - \sigma_v) - 4\Phi_*(\xi) + g(\Phi_*(\xi)), \quad (3.2.7)$$

which we augment with the boundary conditions

$$\lim_{\xi \rightarrow -\infty} \Phi_*(\xi) = 0, \quad \lim_{\xi \rightarrow \infty} \Phi_*(\xi) = 1. \quad (3.2.8)$$

The existence of such pairs (c_*, Φ_*) was established by Mallet-Paret in [67], both for rational and irrational directions. The wave-speed c_* is unique once the direction (σ_h, σ_v) and the detuning parameter a have been fixed, while the wave-profile Φ_* is monotonically increasing and unique up to translations provided that $c_* \neq 0$. In contrast to the continuous setting, there can be a range of values for a where $c_* = 0$ holds; see [49] for a detailed discussion. The assumption below ensures that we are outside of this so-called pinning regime.

(H Φ) There exists a wave-speed $c_* \neq 0$ and a monotone wave profile Φ_* that satisfy the MFDE (3.2.7) together with the boundary conditions (3.2.8) and the phase normalization $\Phi_*(0) = \frac{1}{2}$.

To examine the stability properties of the wave-pair (Φ_*, c_*) under the dynamics of (3.2.4), one usually starts by considering the linear variational problem

$$\dot{v}_{n,l}(t) = [\Delta^\times v(t)]_{n,l} + g'(\Phi_*(n - c_*t))v_{n,l}(t).$$

Taking the discrete Fourier transform along the transverse direction l , the problem decouples into the set of one-dimensional LDEs

$$\begin{aligned} \dot{v}_n(t) = & e^{i\omega\sigma_v}v_{n+\sigma_h}(t) + e^{-i\omega\sigma_h}v_{n+\sigma_v}(t) + e^{-i\omega\sigma_v}v_{n-\sigma_h}(t) + e^{i\omega\sigma_h}v_{n-\sigma_v}(t) \\ & - 4v_n(t) + g'(\Phi_*(n - c_*t))v_n(t), \end{aligned} \quad (3.2.9)$$

indexed by the frequency variable $\omega \in [-\pi, \pi]$. As shown in [48, §2], there is a close relationship between the Green's function for each of the LDEs (3.2.9) and their associated linear operators

$$\mathcal{L}_\omega : W^{1,\infty}(\mathbb{R}; \mathbb{C}) \rightarrow L^\infty(\mathbb{R}; \mathbb{C}), \quad \omega \in [-\pi, \pi]$$

which act as

$$\begin{aligned} [\mathcal{L}_\omega p](\xi) = & c_*p'(\xi) + e^{i\omega\sigma_v}p(\xi + \sigma_h) + e^{-i\omega\sigma_h}p(\xi + \sigma_v) + e^{-i\omega\sigma_v}p(\xi - \sigma_h) \\ & + e^{i\omega\sigma_h}p(\xi - \sigma_v) - 4p(\xi) + g'(\Phi_*(\xi))p(\xi). \end{aligned} \quad (3.2.10)$$

A special role is reserved for the operator \mathcal{L}_0 , which encodes the linearized behaviour of the wave Φ_* under perturbations that are homogeneous in the transverse direction. We briefly summarize several key Fredholm properties of this operator that were obtained by Mallet-Paret in the seminal paper [66].

Lemma 3.2.1 (see [66]). *Assume that (Hg) and $(H\Phi)$ are satisfied. Then the operator $\mathcal{L}_0 : W^{1,\infty}(\mathbb{R}; \mathbb{C}) \rightarrow L^\infty(\mathbb{R}; \mathbb{C})$ is Fredholm with index zero. It has a one-dimensional kernel spanned by the strictly positive function Φ'_* . In addition, its range admits the characterization*

$$\mathcal{R}(\mathcal{L}_0) = \left\{ f \in L^\infty(\mathbb{R}; \mathbb{R}) : \int_{\mathbb{R}} \psi_*(\xi) f(\xi) d\xi = 0 \right\} \quad (3.2.11)$$

for some strictly positive bounded function² $\psi_* \in C^2(\mathbb{R}; \mathbb{R})$ that we normalize to have

$$\int_{\mathbb{R}} \psi_*(\xi) \Phi'_*(\xi) d\xi = 1.$$

Since clearly $\Phi'_* \notin \mathcal{R}(\mathcal{L}_0)$ we see that $\lambda = 0$ is a simple eigenvalue of the operator \mathcal{L}_0 . The following result states that this property extends to a branch of simple eigenvalues λ_ω for the operators \mathcal{L}_ω with $\omega \approx 0$.

Lemma 3.2.2 (see [43, Prop. 2.2]). *Assume that (Hg) and $(H\Phi)$ are satisfied. Then there exists a constant $0 < \omega_0 \ll 1$ together with pairs*

$$(\lambda_\omega, \phi_\omega) \in \mathbb{C} \times W^{1,\infty}(\mathbb{R}; \mathbb{C}),$$

defined for each $\omega \in (-\omega_0, \omega_0)$, that satisfy the following properties.

(i) *For each $\omega \in (-\omega_0, \omega_0)$ we have the characterization*

$$\text{Ker}(\mathcal{L}_\omega - \lambda_\omega) = \text{span} \{ \phi_\omega \},$$

together with the algebraic simplicity condition

$$\phi_\omega \notin \mathcal{R}(\mathcal{L}_\omega - \lambda_\omega).$$

(ii) *We have $\lambda_0 = 0$, $\phi_0 = \Phi'_*$ and the maps $\omega \mapsto \lambda_\omega$, $\omega \mapsto \phi_\omega$ are analytic.*

(iii) *For each $\omega \in (-\omega_0, \omega_0)$ we have the normalization*

$$\langle \phi_\omega, \psi_* \rangle_{L^2} = 1.$$

Our following assumption states that the map $\omega \mapsto \lambda_\omega$ touches the origin in a quadratic tangency, opening up to the left of the imaginary axis. This is a rather standard condition that was also used in [43] and [44] to show that transverse phase deformations decay at the standard rates prescribed by the heat equation. We remark that Lemma 6.3 in [43] guarantees that this condition is satisfied whenever the propagation direction is close to horizontal or diagonal. Furthermore, numerical experiments in [43, §6] suggest that this extends to all directions where the wavespeed does not vanish.

²In fact, ψ_* spans the kernel of the formal adjoint \mathcal{L}_0^* that arises from \mathcal{L}_0 by flipping the sign of c .

(HS)₁ The branch of eigenvalues $(\lambda_\omega)_{\omega \approx 0}$ satisfies the inequality

$$[\partial_\omega^2 \lambda_\omega]_{\omega=0} < 0.$$

Our final spectral assumption is far less standard and requires some technical preparations. To this end, we introduce the set of shifts

$$(\tau_1, \tau_2, \tau_3, \tau_4) = (\sigma_h, \sigma_v, -\sigma_h, -\sigma_v) \quad (3.2.12)$$

and their associated translation operators T_ν that act as

$$[T_\nu h](\xi) = h(\xi + \tau_\nu), \quad \nu \in \{1, 2, 3, 4\} \quad (3.2.13)$$

for any function $h \in C(\mathbb{R})$. These can be used to define a collection of functions p^\diamond , $p^{\diamond\diamond}$ and $q^{\diamond\diamond}$ that play a key role in §3.7 where we construct sub- and super-solutions for (3.2.4). For our purposes here, we are chiefly interested in the associated coefficients α_p^\diamond , $\alpha_p^{\diamond\diamond}$ and $\alpha_q^{\diamond\diamond}$ that are related to the solvability condition (3.2.11).

Lemma 3.2.3 (see §3.6). *Assume that (Hg) and $(H\Phi)$ both hold. Then for every $\nu, \nu' \in \{1, 2, 3, 4\}$ there exist bounded functions*

$$p_\nu^\diamond, p_{\nu\nu'}^{\diamond\diamond}, q_{\nu\nu'}^{\diamond\diamond} : \mathbb{R} \rightarrow \mathbb{R}$$

that satisfy the identities

$$\begin{aligned} [\mathcal{L}_0 p_\nu^\diamond](\xi) &= [T_\nu \Phi'](\xi) - \alpha_{p;\nu}^\diamond \Phi'(\xi), \\ [\mathcal{L}_0 p_{\nu\nu'}^{\diamond\diamond}](\xi) &= \alpha_{p;\nu}^\diamond p_\nu^\diamond(\xi) - [T_{\nu'} p_\nu^\diamond](\xi) - \alpha_{p;\nu\nu'}^{\diamond\diamond} \Phi'(\xi), \\ [\mathcal{L}_0 q_{\nu\nu'}^{\diamond\diamond}](\xi) &= -\alpha_{p;\nu}^\diamond \frac{d}{d\xi} p_\nu^\diamond(\xi) + [T_{\nu'} \frac{d}{d\xi} p_\nu^\diamond](\xi) - \frac{1}{2} g''(\Phi_*(\xi)) p_\nu^\diamond(\xi) p_{\nu'}^\diamond(\xi) \\ &\quad - \frac{1}{2} \mathbf{1}_{\nu=\nu'} [T_\nu \Phi_*''](\xi) - \alpha_{q;\nu\nu'}^{\diamond\diamond} \Phi'(\xi). \end{aligned} \quad (3.2.14)$$

Here the coefficients $\alpha_{p;\nu}^\diamond$, $\alpha_{p;\nu\nu'}^{\diamond\diamond}$ and $\alpha_{q;\nu\nu'}^{\diamond\diamond}$ are given by

$$\begin{aligned} \alpha_{p;\nu}^\diamond &= \int_{\mathbb{R}} [T_\nu \Phi'](\xi) \psi_*(\xi) d\xi, \\ \alpha_{p;\nu\nu'}^{\diamond\diamond} &= \int_{\mathbb{R}} [\alpha_{p;\nu}^\diamond p_\nu^\diamond(\xi) - [T_{\nu'} p_\nu^\diamond](\xi)] \psi_*(\xi) d\xi, \\ \alpha_{q;\nu\nu'}^{\diamond\diamond} &= \int_{\mathbb{R}} \left(-\alpha_{p;\nu}^\diamond \frac{d}{d\xi} p_\nu^\diamond(\xi) + [T_{\nu'} \frac{d}{d\xi} p_\nu^\diamond](\xi) - \frac{1}{2} g''(\Phi_*(\xi)) p_\nu^\diamond(\xi) p_{\nu'}^\diamond(\xi) \right) \psi_*(\xi) d\xi \\ &\quad - \frac{1}{2} \int_{\mathbb{R}} \mathbf{1}_{\nu=\nu'} [T_\nu \Phi_*''](\xi) \psi_*(\xi) d\xi. \end{aligned} \quad (3.2.15)$$

Moreover, the functions p_ν^\diamond , $p_{\nu\nu'}^{\diamond\diamond}$ and $q_{\nu\nu'}^{\diamond\diamond}$ can be chosen in such a way that

$$\langle p_\nu^\diamond, \psi_* \rangle_{L^2} = 0, \quad \langle p_{\nu\nu'}^{\diamond\diamond}, \psi_* \rangle_{L^2} = 0, \quad \langle q_{\nu\nu'}^{\diamond\diamond}, \psi_* \rangle_{L^2} = 0. \quad (3.2.16)$$

Upon introducing the convenient notation

$$(\sigma_1, \sigma_2, \sigma_3, \sigma_4) = (\sigma_v, -\sigma_h, -\sigma_v, \sigma_h), \quad (3.2.17)$$

we now use the coefficients (3.2.15) to introduce the function $f_{(\sigma_h, \sigma_v)} : [-\pi, \pi] \rightarrow \mathbb{R}$ that acts as

$$\begin{aligned} f_{(\sigma_h, \sigma_v)}(\omega) &= \sum_{\nu=1}^4 \alpha_{p;\nu}^\diamond (\cos(\sigma_\nu \omega) - 1) \\ &+ \sum_{\nu, \nu'=1}^4 \alpha_{p;\nu\nu'}^\diamond \left(\cos((\sigma_\nu + \sigma_{\nu'})\omega) - \cos(\sigma_\nu \omega) - \cos(\sigma_{\nu'} \omega) + 1 \right). \end{aligned} \quad (3.2.18)$$

For the sequel, it is convenient to rewrite this expression in a more compact form. To this end, we write $N = \max_{\nu, \nu' \in \{1, 2, 3, 4\}} \{\sigma_\nu, \sigma_\nu + \sigma_{\nu'}\}$ and introduce the sequence

$$a_k = \sum_{\nu=1}^4 \alpha_{p;\nu}^\diamond \mathbf{1}_{\{k=\sigma_\nu\}} + \sum_{\nu, \nu'=1}^4 \alpha_{p;\nu\nu'}^\diamond (\mathbf{1}_{\{k=\sigma_\nu + \sigma_{\nu'}\}} - \mathbf{1}_{\{k=\sigma_\nu\}} - \mathbf{1}_{\{k=\sigma_{\nu'}\}}), \quad (3.2.19)$$

which allows us to rewrite (3.2.18) as

$$f_{(\sigma_h, \sigma_v)}(\omega) = \sum_{k=-N}^N a_k (\cos(k\omega) - 1). \quad (3.2.20)$$

This function will appear later as the real part of the Fourier symbol associated to the linear dynamics of the transverse phase of the planar wave (c_*, Φ_*) .

In the horizontal case $(\sigma_h, \sigma_v) = (1, 0)$ we can take $N = 1$, $a_{-1} = 1$, $a_1 = 1$ and

$$f_{(1,0)}(\omega) = 2(\cos \omega - 1),$$

but in general the coefficients a_k can be negative. In order to ensure that our phase dynamics can be controlled, our final assumption requires the function f to be strictly negative for all non-zero ω .

(HS)₂ The inequality $f_{(\sigma_h, \sigma_v)}(\omega) < 0$ holds for all $\omega \in [-\pi, \pi] \setminus \{0\}$.

In order to fully appreciate the role of the the coefficients (3.2.15) and the Fourier symbol (3.2.20), it is helpful to link them to geometric properties of (3.2.4). We first note that the pair (c_*, Φ_*) can be perturbed in order to yield waves travelling in directions that are ‘close’ to (σ_h, σ_v) . In particular, we follow the approach from [49] and look for solutions to the Allen-Cahn equation (3.2.4) of the form

$$u_{n,l}(t) = \Phi_\varphi(n \cos \varphi + l \sin \varphi - c_\varphi t), \quad (3.2.21)$$

which travel at an angle φ through the rotated lattice \mathbb{Z}_\times^2 . Inserting this Ansatz into (3.2.4), we find that the pair $(c_\varphi, \Phi_\varphi)$ must satisfy the MFDE

$$\begin{aligned} -c_\varphi \Phi'_\varphi(\xi) &= \Phi_\varphi(\xi + \sigma_h \cos \varphi + \sigma_v \sin \varphi) + \Phi_\varphi(\xi + \sigma_v \cos \varphi - \sigma_h \sin \varphi) \\ &+ \Phi_\varphi(\xi - \sigma_h \cos \varphi - \sigma_v \sin \varphi) + \Phi_\varphi(\xi - \sigma_v \cos \varphi + \sigma_h \sin \varphi) \\ &- 4\Phi_\varphi(\xi) + g(\Phi_\varphi(\xi)). \end{aligned} \quad (3.2.22)$$

Using standard bifurcation arguments one can show that the pair (Φ_*, c_*) can be embedded into a smooth branch of waves $(c_\varphi, \Phi_\varphi)$ for $\varphi \approx 0$.

Lemma 3.2.4 (see [49, Prop. 2.2] and [43, Thm. 2.7]). *Assume that (Hg) and (HΦ) are satisfied. Then there exists a constant $\delta_\varphi > 0$ together with pairs*

$$(c_\varphi, \Phi_\varphi) \in \mathbb{R} \times W^{1,\infty}(\mathbb{R}; \mathbb{R}),$$

defined for every $\varphi \in (-\delta_\varphi, \delta_\varphi)$, such that the following holds true.

- (i) For every $\varphi \in (-\delta_\varphi, \delta_\varphi)$ the pair $(c_\varphi, \Phi_\varphi)$ satisfies the MFDE (3.2.22) together with the boundary conditions (3.2.8).
- (ii) For every $\varphi \in (-\delta_\varphi, \delta_\varphi)$ we have the normalization $\langle \Phi_\varphi - \Phi_*, \psi_* \rangle = 0$.
- (iii) The maps $\varphi \mapsto c_\varphi$ and $\varphi \mapsto \Phi_\varphi$ are C^2 -smooth, with $(c_0, \Phi_0) = (c_*, \Phi_*)$.

Our next result shows that there is a close link between the coefficients (3.2.14), the pairs $(\lambda_\omega, \phi_\omega)$ constructed in Lemma 3.2.3 and the waves $(c_\varphi, \Phi_\varphi)$ described in Lemma 3.2.4. These identities can be stated in a compact fashion by virtue of the choices (3.2.12) and (3.2.17).

Lemma 3.2.5 (see §3.6). *Assume that (Hg) and (HΦ) are satisfied. Then the following identities hold.*

- (i) $c_* = -\sum_{\nu=1}^4 \tau_\nu \alpha_{p;\nu}^\diamond,$
- (ii) $[\partial_\varphi c_\varphi]_{\varphi=0} = -\sum_{\nu=1}^4 \sigma_\nu \alpha_{p;\nu}^\diamond = -\sum_{k=-N}^N a_k k,$
- (iii) $[\partial_\varphi^2 c_\varphi]_{\varphi=0} = -c_* + 2\sum_{\nu=1}^4 \sum_{\nu'=1}^4 \sigma_\nu \sigma_{\nu'} \alpha_{q;\nu\nu'}^\diamond,$
- (iv) $[\partial_\varphi \Phi_\varphi]_{\varphi=0} = -\sum_{\nu=1}^4 \sigma_\nu p_\nu^\diamond,$
- (v) $[\partial_\omega \lambda_\omega]_{\omega=0} = \sum_{\nu=1}^4 \sigma_\nu \alpha_{p;\nu}^\diamond,$
- (vi) $[\partial_\omega^2 \lambda_\omega]_{\omega=0} = -\sum_{\nu=1}^4 \alpha_\nu^\diamond \sigma_\nu^2 - \sum_{\nu,\nu'=1}^4 2\alpha_{p;\nu\nu'}^\diamond \sigma_\nu \sigma_{\nu'} = -\sum_{k=-N}^N a_k k^2.$

Combining item (vi) and (3.2.18), we readily see that

$$f''_{(\sigma_h, \sigma_v)}(0) = [\partial_\omega^2 \lambda_\omega]_{\omega=0}.$$

This identity in combination with (HS)₁ implies that the function $f_{(\sigma_h, \sigma_v)}$ looks like a downwards parabola locally around $\omega = 0$. This information was sufficient to obtain the ‘localized’ stability results in [43] and [44], but our more general setup here requires global information on the function $f_{(\sigma_h, \sigma_v)}$. An important role is reserved for the parameter

$$d = -\frac{\partial_\varphi^2 [c_\varphi / \cos \varphi]_{\varphi=0}}{[\partial_\omega^2 \lambda_\omega]_{\omega=0}} = -\frac{c_* + [\partial_\varphi^2 c_\varphi]_{\varphi=0}}{[\partial_\omega^2 \lambda_\omega]_{\omega=0}} = \frac{2\sum_{\nu=1}^4 \sum_{\nu'=1}^4 \sigma_\nu \sigma_{\nu'} \alpha_{q;\nu\nu'}^\diamond}{\sum_{\nu=1}^4 \alpha_\nu^\diamond \sigma_\nu^2 + \sum_{\nu,\nu'=1}^4 2\alpha_{p;\nu\nu'}^\diamond \sigma_\nu \sigma_{\nu'}}, \quad (3.2.23)$$

which is well-defined on account of assumption (HS)₁. It measures the ratio between the quadratic terms in the directional dispersion $c_\varphi / \cos \varphi$ and the branch of eigenvalues λ_ω . This parameter also played a crucial role throughout the construction of travelling corners for (3.2.1); see [49, Eqs. (7.38) and (7.76)] where it appears as the quadratic coefficient on the center manifold that governs the transverse dynamics.

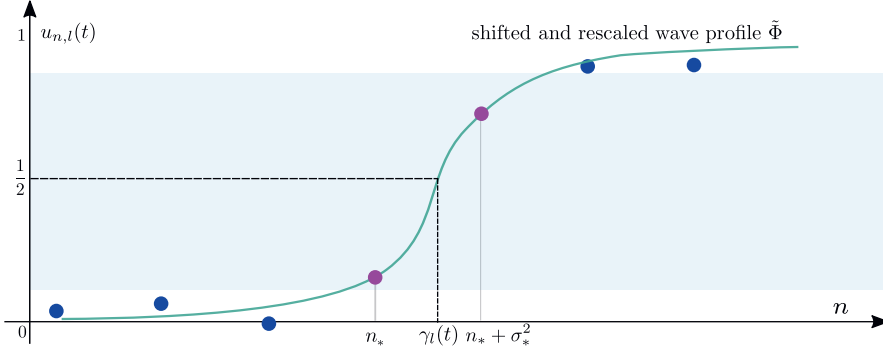


Figure 3.3: In order to construct the phase $\gamma_l(t)$ for a fixed pair (l, t) we first identify an interfacial region around the value $\Phi_*(0) = \frac{1}{2}$ (shaded in blue) where the (discrete) function $n \mapsto u_{n,l}(t)$ is monotone. We subsequently stretch the waveprofile to match the (pink) points $(n_*, u_{n_*,l}(t))$ and $(n_* + \sigma_*^2, u_{n_* + \sigma_*^2, l}(t))$ introduced in (3.2.24).

3.2.2 Interface formation

In this subsection we provide a construction for the set of phases $(\gamma_l(t))_{l \in \mathbb{Z}}$ that should be seen as an *approximation* for the level set $u = \frac{1}{2}$. Indeed, due to the discreteness of the lattice one cannot necessarily find integers $n_*(l, t)$ for which $u_{n_*(l, t), l}(t) = \frac{1}{2}$ holds exactly - even when restricted to large times $t \gg 1$. Instead, we establish the following monotonicity result, which for fixed l and large $t \gg 1$ allows us to capture the ‘crossing’ of u through $\frac{1}{2}$ between $n = n_*(l, t)$ and $n = n_*(l, t) + \sigma_*^2$.

Proposition 3.2.6 (see §3.4). *Suppose that (Hg) , $(H\Phi)$ and $(H0)$ are satisfied. There exists a time $T > 0$ such that for every $l \in \mathbb{Z}$ and $t \geq T$ there exists a unique $n_* = n_*(l, t)$ with the property*

$$0 < u_{n_*, l}(t) \leq \frac{1}{2}, \quad u_{n_* + \sigma_*^2, l}(t) > \frac{1}{2}. \quad (3.2.24)$$

We now use an interpolation argument to construct $\gamma_l(t)$ from the quantities in (3.2.24). The main consideration is that for exact travelling waves $u_{n,l}(t) = \Phi_*(n - c_*t + \mu)$ we wish to recover the standard phase $\gamma_l(t) = c_*t - \mu$, in view of the fact that $\Phi_*(0) = \frac{1}{2}$. To achieve this, we define the phases

$$\theta_l^-(t) = \Phi_*^{-1}(u_{n_*(l, t), l}(t)), \quad \theta_l^+(t) = \Phi_*^{-1}(u_{n_*(l, t) + \sigma_*^2, l}(t))$$

associated to the two values (3.2.24). Upon writing

$$\vartheta_*(l, t) = -\sigma_*^2 \theta_l^-(t) / [\theta_l^+(t) - \theta_l^-(t)], \quad (3.2.25)$$

we note that the linear interpolation

$$\theta_{\text{lin}; l, t}(\xi) = \sigma_*^{-2} \theta_l^+(t) \xi - \sigma_*^{-2} \theta_l^-(t) (\xi - \sigma_*^2)$$

satisfies

$$\theta_{\text{lin}; l, t}(0) = \theta_l^-(t), \quad \theta_{\text{lin}; l, t}(\vartheta_*(l, t)) = 0, \quad \theta_{\text{lin}; l, t}(\sigma_*^2) = \theta_l^+(t).$$

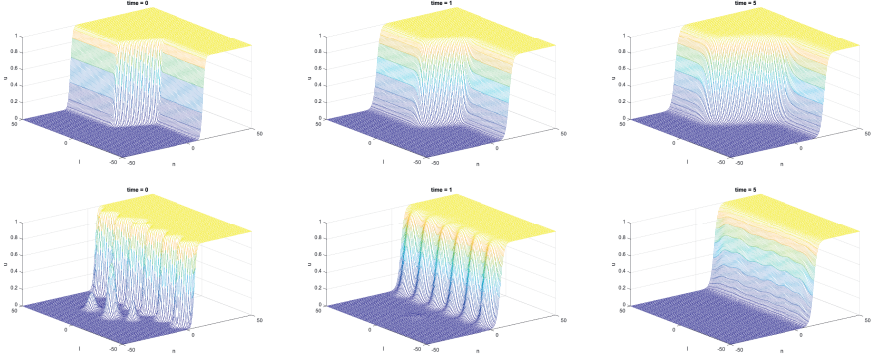


Figure 3.4: Each row represents a time evolution of the solution u to the Allen-Cahn equation (3.1.1) with the cubic nonlinearity (3.1.2). Both initial conditions satisfy (H0), but the bottom row also satisfies the assumptions of Theorem 3.2.10. Proposition 3.2.6 states that u converges to a wavefront travelling in the n -direction with a phase $\gamma_l(t)$, which in the bottom row becomes homogeneous with respect to l on account of (3.2.34).

This motivates the phase-interpolated definition

$$\gamma_l(t) = n_*(l, t) + \vartheta_*(l, t), \quad (3.2.26)$$

which ensures that the ‘stretched’ profile $\tilde{\Phi}(\xi) = \Phi_*(\theta_{\text{lin};l,t}(\xi - n_*(l, t)))$ satisfies

$$\tilde{\Phi}(n_*(l, t)) = u_{n_*(l,t),l}(t), \quad \tilde{\Phi}(\gamma_l(t)) = \frac{1}{2}, \quad \tilde{\Phi}(n_*(l, t) + \sigma_*^2) = u_{n_*(l,t)+\sigma_*^2,l}(t).$$

Notice indeed that for the special case $u_{n,l}(t) = \Phi_*(n - c_*t + \mu)$ we have

$$\theta_l^-(t) = n_*(l, t) - c_*t + \mu, \quad \theta_l^+(t) = n_*(l, t) + \sigma_*^2 - c_*t + \mu,$$

which gives $\vartheta_*(l, t) = -\theta_l^-(t)$ and hence $\gamma_l(t) = c_*t - \mu$, as we desired.

The result below states that our phase indeed tracks the behaviour of u in an asymptotic sense. We emphasize that there are several other choices for the phase that lead to similar results. For example, our previous construction in [52] did not stretch the wave and merely aligned it with u at the point $n_*(l, t)$. Our more refined approach here allows us to streamline our arguments and avoid the discontinuities in $\gamma_l(t)$ that complicated our previous analysis at times.

Proposition 3.2.7 (see §3.4). *Suppose that (Hg), (HΦ) and (H0) are satisfied. Then we have the limit*

$$\lim_{t \rightarrow \infty} \sup_{(n,l) \in \mathbb{Z}_x^2} |u_{n,l}(t) - \Phi_*(n - \gamma_l(t))| = 0. \quad (3.2.27)$$

3.2.3 Interface asymptotics

We are now ready to discuss the main technical results of this paper. These concern the asymptotic behaviour of the phase $\gamma(t)$ that we introduced in (3.2.26), which can be approximated by solutions to the scalar nonlinear LDE

$$\dot{\theta}(t) = \Theta_{\text{ch}}(\theta(t)). \quad (3.2.28)$$

Here the function $\Theta_{\text{ch}} : \ell^\infty(\mathbb{Z}) \rightarrow \ell^\infty(\mathbb{Z})$ acts as

$$[\Theta_{\text{ch}}(\theta)]_l = \begin{cases} \frac{1}{d} \sum_{k=-N}^N a_k \left(e^{d(\theta_{l+k}(t) - \theta_l(t))} - 1 \right) + c_*, & d \neq 0, \\ \sum_{k=-N}^N a_k (\theta_{l+k}(t) - \theta_l(t)) + c_*, & d = 0, \end{cases} \quad (3.2.29)$$

where we have recalled the coefficients (a_k) and parameter d that were introduced in (3.2.19) respectively (3.2.23). The label ‘ch’ refers to the fact that a Cole-Hopf transformation can be used to recast the nonlinear system for $d \neq 0$ into the linear system prescribed for $d = 0$. This reduction is essential for our analysis in §3.6, where we obtain decay rates for solutions to (3.2.28), based on the linear theory that we develop in §3.5.

The decision to use (3.2.29) is hence primarily based on technical considerations. Nevertheless, it is possible to build a bridge back to the discrete curvature flow (3.1.26). To this end, we recall the definitions (3.1.23) and (3.1.24) and introduce the operator $\Theta_{\text{dmc}} : \ell^\infty(\mathbb{Z}) \mapsto \ell^\infty(\mathbb{Z})$ that acts as

$$\Theta_{\text{dmc}}(\theta) = \kappa_H \frac{\Delta\theta}{\beta_\theta^2} + \beta_\theta \bar{c}_\theta, \quad (3.2.30)$$

which depends on the sequences (3.1.25) and the curvature coefficient $\kappa_H > 0$.

The result below shows that Θ_{dmc} can be tailored to agree with Θ_{ch} up to terms that are cubic in the first-differences

$$[\partial\theta]_l = \theta_{l+1} - \theta_l.$$

We will see in §3.6 that such terms decay at a rate of $O(t^{-3/2})$, which in theory is sufficiently fast to be absorbed by our error terms. However, due to the loss of the comparison principle we did not attempt to compare the actual solutions to the respective LDEs as was possible in [52, Prop. 8.2].

Proposition 3.2.8 (see §3.6). *Assume that (Hg) , $(H\Phi)$, $(H0)$, $(HS)_1$, $(HS)_2$ all hold. Assume furthermore that $\kappa_H = -[\partial_\omega^2 \lambda_\omega]_{\omega=0}/2$. Then there exists a unique set of coefficients $(A_k, B_k)_{k=-N}^N$ that satisfy the identities (3.1.25) and allow us to find a constant $K > 0$ for which*

$$\|\Theta_{\text{ch}}(\theta) - \Theta_{\text{dmc}}(\theta)\|_{\ell^\infty} \leq K \|\partial\theta\|_{\ell^\infty}^3 \quad (3.2.31)$$

holds for all sequences $\theta \in \ell^\infty(\mathbb{Z})$ with $\|\partial\theta\|_{\ell^\infty} \leq 1$. On the other hand, such coefficients do not exist if (3.1.27) is violated.

Our main result below makes the asymptotic connection between γ and solutions θ to (3.2.28) fully precise. This allows us to gain detailed control over the long-term dynamics of the phase $\gamma(t)$, which can be used to provide stability results outside the ‘local’ regimes treated in [43] and [44].

Theorem 3.2.9 (see §3.8). *Assume that (Hg) , $(H\Phi)$, $(H0)$, $(HS)_1$, $(HS)_2$ all hold and let u be a solution of (3.2.4) with the initial condition (3.2.5). Then for every $\epsilon > 0$, there exists a constant $\tau_\epsilon > 0$ so that for any $\tau \geq \tau_\epsilon$, the solution θ of LDE (3.2.28) with the initial value $\theta(0) = \gamma(\tau)$ satisfies*

$$\|\gamma(t) - \theta(t - \tau)\|_{\ell^\infty} \leq \epsilon, \quad t \geq \tau. \quad (3.2.32)$$

Our final result should be seen as an example of an asymptotic analysis that is made possible by the phase tracking (3.2.32). In particular, we show that the planar travelling wave (3.2.6) is stable with asymptotic phase under localized perturbations from a front-like background state that is periodic in l , see Figure 3.4. Indeed, such an assumption provides sufficient control on the solution θ to (3.2.28) to establish the uniform convergence $\theta_l \rightarrow c_*t + \mu$. We emphasize that the case $P = 1$ encompasses the stability results from [43] and [44]. The key point is that an asymptotic global phaseshift $\mu \neq 0$ for the case $P \geq 2$ can be seen as an ‘infinite-energy’ shift of the underlying planar wave. In such cases the quadratic terms in (3.2.28) can no longer be absorbed into higher-order residuals as in [43] and [44].

Theorem 3.2.10 (see §3.8). *Assume that (Hg) , $(H\Phi)$, $(H0)$, $(HS)_1$, $(HS)_2$ all hold and let u be a solution of (3.2.4) with the initial condition (3.2.5). Suppose furthermore that there exists a sequence $u^{0;\text{per}} \in \ell^\infty(\mathbb{Z}_\times^2)$ so that the following two properties hold.*

(a) *We have the limit*

$$u_{n,l}^0 - u_{n,l}^{0;\text{per}} \rightarrow 0, \quad \text{as } |n| + |l| \rightarrow \infty. \quad (3.2.33)$$

(b) *There exists an integer $P \geq 1$ so that*

$$u_{n,l+\sigma_*^2 P}^{0;\text{per}} = u_{n,l}^{0;\text{per}} \quad \text{for all } (n,l) \in \mathbb{Z}_\times^2.$$

Then there exists a constant $\mu \in \mathbb{R}$ for which we have the limit

$$\lim_{t \rightarrow \infty} \sup_{(n,l) \in \mathbb{Z}_\times^2} |u_{n,l}(t) - \Phi_*(n - c_*t - \mu)| = 0. \quad (3.2.34)$$

3.2.4 Numerical results

Our goal here is to numerically investigate the condition $(HS)_2$. In order to compensate for the fact that f is locally quadratic around 0, we calculated the values

$$M_{(\sigma_h, \sigma_v)} := \sup_{0 < |\omega| \leq \pi} \frac{f_{(\sigma_h, \sigma_v)}(\omega)}{\omega^2}$$

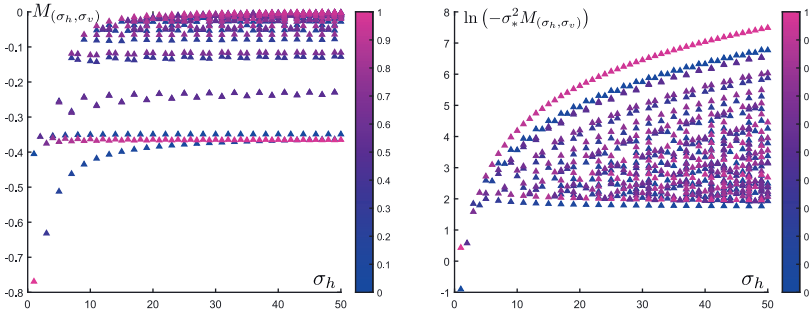


Figure 3.5: These plots represent the outcome of our numerical computations for the values $M_{(\sigma_h, \sigma_v)}$, where we used $g(u; a) = 6u(u - 1)(u - a)$ with $a = 0.45$. For each fixed σ_h (horizontal) we computed these values for each integer $1 \leq \sigma_v \leq \sigma_h$ that has $\gcd(\sigma_h, \sigma_v) = 1$, using the color code to represent the fraction σ_v/σ_h . On the left we see the formation of horizontal bands, suggesting the possibility to take limits along convergent subsequences $(\sigma_v^{(n)}/\sigma_h^{(n)})_{n>0}$; see also Figure 3.6. The σ_v^2 -scaling on the right shows that our condition requiring $M_{(\sigma_h, \sigma_v)}$ to be negative can be confirmed in a robust fashion.

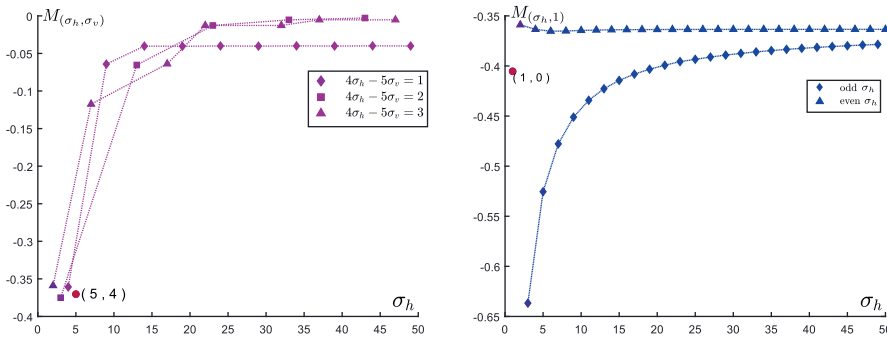


Figure 3.6: These plots track the values of $M_{(\sigma_h, \sigma_v)}$ along several subsequences of fractions σ_v/σ_h that converge to $4/5$ (left) or zero (right). In all cases the limits are strictly above the values $M_{(5,4)}$ (left) and $M_{(1,0)}$ (right) corresponding to the limiting angles, supporting the inequality (3.2.36).

k	1	2	3	4	5	6	7	8	9	10
a_k	0	0.896	0.195	0.068	0.966	0	-0.143	0	0	0.05
a_{-k}	0	0.912	0.0925	0.179	1.005	0	-0.199	0	0	0.03

Table 3.1: Numerically computed values for the coefficients (a_k) defined in (3.2.19) for the propagation direction $(\sigma_h, \sigma_v) = (2, 5)$, with the nonlinearity $g(u; a) = 6u(u - 1)(u - 0.45)$. We computed these coefficients for a large range of angles and used them to calculate the values $M_{(\sigma_h, \sigma_v)}$ depicted in Figures 3.5-3.6.

for a large range of parameters $(\sigma_h, \sigma_v) \in \mathbb{Z}^2$.

As a first step, we numerically solved the coupled set of equations

$$\begin{aligned} -c_* \Phi'_*(\xi) &= \Phi_*(\xi + \sigma_h) + \Phi_*(\xi - \sigma_h) + \Phi_*(\xi + \sigma_v) + \Phi_*(\xi - \sigma_v) - 4\Phi_*(\xi) \\ &\quad + g(\Phi_*(\xi)), \\ c_* \psi'_*(\xi) &= \psi_*(\xi + \sigma_h) + \psi_*(\xi - \sigma_h) + \psi_*(\xi + \sigma_v) + \psi_*(\xi - \sigma_v) - 4\psi_*(\xi) \\ &\quad + g'(\Phi_*(\xi))\psi_*(\xi) \end{aligned}$$

on a domain $[-L, L]$ for some large $L \gg 1$, using the boundary conditions

$$\Phi_*(-L) = 0, \quad \Phi_*(L) = 1, \quad \psi_*(\pm L) = 0.$$

Due to the fact that the solutions are shift-invariant, we also fixed $\Phi(0) = \frac{1}{2}$ and $\psi(0) = 1$. In order to overcome the issue that L needs to be very large when σ_h or σ_v is large, we used the representation

$$\sigma_* = \sqrt{\sigma_h^2 + \sigma_v^2}, \quad (\sigma_h, \sigma_v) = \sigma_*(\cos \zeta_*, \sin \zeta_*)$$

to introduce the rescaled functions

$$\tilde{\Phi}(\xi) := \Phi_*(\xi/\sigma_*), \quad \tilde{\psi}(\xi) := \psi_*(\xi/\sigma_*).$$

These must satisfy the equivalent system of equations

$$\begin{aligned} -\frac{c_*}{\sigma_*} \tilde{\Phi}'(\xi) &= \tilde{\Phi}(\xi + \cos \zeta_*) + \tilde{\Phi}(\xi - \cos \zeta_*) + \tilde{\Phi}(\xi + \sin \zeta_*) + \tilde{\Phi}(\xi - \sin \zeta_*) \\ &\quad + g(\tilde{\Phi}(\xi)) \\ \frac{c_*}{\sigma_*} \tilde{\psi}'(\xi) &= \tilde{\psi}(\xi + \cos \zeta_*) + \tilde{\psi}(\xi - \cos \zeta_*) + \tilde{\psi}(\xi + \sin \zeta_*) + \tilde{\psi}(\xi - \sin \zeta_*) \\ &\quad + g'(\tilde{\Phi}(\xi))\tilde{\psi}(\xi), \end{aligned} \tag{3.2.35}$$

which allowed us to keep L fixed and use a continuation approach to vary the angle ζ_* .

We discretized the domain by dividing the segment $[-L, L]$ into N_L parts of size $\Delta\xi$ for some integer $N_L \gg 1$ and step size $\Delta\xi \ll 1$, discretizing the first derivatives in (3.2.35) by the fourth-order central difference scheme. We proceeded by using a nonlinear system solver to obtain the speed c and the values $(\tilde{\Phi}(\xi_n), \tilde{\psi}(\xi_n))$ in the nodes $\xi_n = -L + n\Delta\xi$, for $n = 0, \dots, N_L$. We subsequently used these values to solve the systems (3.2.14) and compute the coefficients needed to construct the function $f_{(\sigma_h, \sigma_v)}$ defined in (3.2.20). As an example, in Table 3.1 we present the values of (a_k) for the angle of propagation (2, 5), noting that both positive and negative values occur.

Our full results are visualized in Figures 3.5 and 3.6. In all cases the value $M_{(\sigma_h, \sigma_v)}$ was negative, hence validating (HS)₂. In addition, we observed that if we pick a sequence of angles (σ_h^n, σ_v^n) for which we have the convergence

$$\lim_{n \rightarrow \infty} \sigma_v^n / \sigma_h^n = \sigma_v^* / \sigma_h^*$$

for some pair $(\sigma_h^*, \sigma_v^*) \in \mathbb{Z}^2$ not contained in this sequence, then

$$\liminf_{n \rightarrow \infty} M_{(\sigma_h^n, \sigma_v^n)} > M_{(\sigma_h^*, \sigma_v^*)}. \quad (3.2.36)$$

This behaviour closely resembles the crystallographic pinning phenomenon discussed in [46, 65], where the role of M is played by the direction-dependent boundary of the parameters a where the wave is pinned ($c_* = 0$).

3.3 Omega limit points

Both the construction of the phase γ as well as the proof of Proposition 3.2.7 rely heavily on the properties of so-called ω -limit points. Intuitively, these track the long-time behaviour of u after correcting for the velocity of the planar wave. To be more precise, let us consider a sequence in $\mathbb{Z}_\times^2 \times \mathbb{R}$ that is taken from the subset

$$\mathcal{S} = \{(n_k, l_k, t_k)_{k \geq 0} : 0 < t_1 < t_2 < \dots \rightarrow \infty, |n_k - ct_k| \leq M \text{ for some } M > 0\}. \quad (3.3.1)$$

For any solution $u \in C^1([0, \infty), \ell^\infty(\mathbb{Z}_\times^2))$, our goal is to analyze the limiting behaviour of the shifted solutions $u_{n+n_k, l+l_k}(t+t_k)$. In the special case that u is the exact planar wave solution

$$u_{n,l}(t) = \Phi_*(n - c_*t),$$

the fact that the sequence $n_k - c_*t_k$ is bounded allows us to find a constant $\theta_0 \in \mathbb{R}$ for which the convergence

$$u_{n+n_k, l+l_k}(t+t_k) = \Phi_*(n + n_k - c_*t - c_*t_k) \rightarrow \Phi_*(n - c_*t + \theta_0) \quad (3.3.2)$$

holds on some subsequence. The limiting function is hence equal to our planar wave, albeit with a perturbed phase θ_0 .

Our main result here states that the convergence result (3.3.2) continues to hold for a much larger set of solutions of the discrete Allen-Cahn equation (3.2.4). This generalizes our earlier results in [52] where we only considered horizontal directions. Although some minor technical obstacles need to be resolved, the main principles are comparable. In fact, we actually sharpened the setup slightly by avoiding the superfluous usage of the floor and ceiling functions in [52, Prop. 3.1]. This allows for a more efficient and readable analysis here and in the sequel.

Proposition 3.3.1. *Suppose that (Hg), (HΦ) and (H0) hold and let u be a solution of (3.2.4) with the initial condition (3.2.5). Then for any sequence $(n_k, l_k, t_k)_{k \geq 0} \in \mathcal{S}$ there exists a subsequence $(n_{i_k}, l_{i_k}, t_{i_k})_{k \geq 0}$ and a shift $\theta_0 \in \mathbb{R}$ such that*

$$u_{n+n_{i_k}, l+l_{i_k}}(t+t_{i_k}) \rightarrow \Phi_*(n - c_*t + \theta_0) \quad \text{in } C_{\text{loc}}(\mathbb{Z}_\times^2 \times \mathbb{R}).$$

The proof follows directly by combining the two main ingredients that we state below. First, in Proposition 3.3.2, we use Arzela-Ascoli to construct a solution $\omega \in C^1(\mathbb{R}; \ell^\infty(\mathbb{Z}_\times^2))$ to the discrete Allen-Cahn equation (3.2.4) on $\mathbb{Z}_\times^2 \times \mathbb{R}$ as a limit of the sequence $u_{n+n_k, l+l_k}(t+t_k)$. Furthermore, we show that this solution ω lies

between two travelling waves. Proposition 3.3.3 subsequently states that this latter property is sufficient to guarantee that ω is a travelling wave itself. This transfers the comparable ‘Liouville-type’ result in [13] from the continuous to the discrete setting. We note that analogous statements for monostable lattice equations can be found in [38].

Proposition 3.3.2. *Consider the setting of Proposition 3.3.1 and pick a sequence $(n_k, l_k, t_k)_{k \geq 0} \in \mathcal{S}$. Then there exists a subsequence $(n_{i_k}, l_{i_k}, t_{i_k})_{k \geq 0}$ and a function $\omega \in C^1(\mathbb{R}; \ell^\infty(\mathbb{Z}_\times^2))$ that satisfy the following claims.*

(i) *We have the convergence*

$$u_{n+n_{i_k}, l+l_{i_k}}(t+t_{i_k}) \rightarrow \omega_{n,l}(t) \quad \text{in } C_{loc}(\mathbb{Z}_\times^2 \times \mathbb{R}).$$

(ii) *The function ω satisfies the discrete Allen-Cahn equation (3.2.4) on $\mathbb{Z}_\times^2 \times \mathbb{R}$.*

(iii) *There exists a constant $\theta \in \mathbb{R}$ such that*

$$\Phi_*(n - c_*t - \theta) \leq \omega_{n,l}(t) \leq \Phi_*(n - c_*t + \theta), \quad \text{for all } (n, l) \in \mathbb{Z}_\times^2. \quad (3.3.3)$$

Proposition 3.3.3. *Assume that (Hg) and (H Φ) are satisfied and consider a function $\omega \in C^1(\mathbb{R}; \ell^\infty(\mathbb{Z}_\times^2))$ that satisfies the Allen-Cahn LDE (3.2.4) for all $t \in \mathbb{R}$. Assume furthermore that there exists a constant θ for which the bounds*

$$\Phi_*(n - c_*t - \theta) \leq \omega_{n,l}(t) \leq \Phi_*(n - c_*t + \theta) \quad (3.3.4)$$

hold for all $(n, l) \in \mathbb{Z}_\times^2$ and $t \in \mathbb{R}$. Then there exists a constant $\theta_0 \in [-\theta, \theta]$ so that

$$\omega_{n,l}(t) = \Phi_*(n - c_*t + \theta_0), \quad \text{for all } (n, l) \in \mathbb{Z}_\times^2, t \in \mathbb{R}.$$

Proof of Proposition 3.3.1. The claim follows directly from Propositions 3.3.2 and 3.3.3. \square

3.3.1 Construction of ω

Our first result provides preliminary upper and lower bounds for the solution u . It is based upon a standard comparison principle argument that can be traced back to Fife and McLeod [34].

Lemma 3.3.4. *Assume that (Hg), (H Φ) and (H0) are satisfied. Then there exists a time $T > 0$ together with constants*

$$q_1 \in (0, a), \quad q_2 \in (0, 1 - a), \quad \theta_1 \in \mathbb{R}, \quad \theta_2 \in \mathbb{R}, \quad \mu > 0, \quad C > 0$$

so that the solution u to (3.2.4) with the initial condition (3.2.5) satisfies the estimates

$$u_{n,l}(t) \leq \Phi_* \left(n + \theta_1 - c_*(t - T) + Cq_1(1 - e^{-\mu(t-T)}) \right) + q_1 e^{-\mu(t-T)}, \quad \forall t \geq T, \quad (3.3.5)$$

$$u_{n,l}(t) \geq \Phi_* \left(n - \theta_2 - c_*(t - T) - Cq_2(1 - e^{-\mu(t-T)}) \right) - q_2 e^{-\mu(t-T)}, \quad \forall t \geq T. \quad (3.3.6)$$

Proof. The result can be shown by following the procedure outlined in the proof of Lemma 3.5 in [52], using the inequality

$$\alpha|c_*| - 2(\cosh \sigma_h c_* - 1) - 2(\cosh \sigma_v c_* - 1) \geq \frac{2K}{a-d}$$

to replace (3.14) in [52] and modifying the definition (3.16) in [52] to read

$$w_{n,l}(t) = d + Me^{|c_*|(n+\alpha t)}.$$

□

Proof of Proposition 3.3.2. Fix an integer $T \in \mathbb{N}$ and denote by M_T the number of points in \mathbb{Z}_\times^2 that are also contained in the square $[-T, T]^2$, i.e.

$$M_T = \# \{(n, l) \in \mathbb{Z}_\times^2 \cap [-T, T]^2\}.$$

Consider the functions

$$u^k \in C([-T, T]; \mathbb{R}^{M_T \times M_T})$$

that are defined by

$$u_{n,l}^k(t) = u_{n+n_k, l+l_k}(t + t_k)$$

for all sufficiently large k . From Lemma 3.3.4 it follows that the solution u and consequently the functions u^k are globally bounded, which in view of (3.2.4) implies that the same holds for the derivative \dot{u} . The sequence u^k hence satisfies the conditions of the Arzela-Ascoli theorem and is thus relatively compact in $C([-T, T]; \mathbb{R}^{M_T \times M_T})$. Applying (3.2.4) and using a standard diagonalisation argument, we obtain a subsequence u^{i_k} and a function $\omega : \mathbb{R} \rightarrow \ell^\infty(\mathbb{Z}_\times^2)$ for which the convergence

$$\sup_{(n,l,t) \in K} |u_{n,l}^{i_k}(t) - \omega_{n,l}(t)| + |\dot{u}_{n,l}^{i_k}(t) - \dot{\omega}_{n,l}(t)| \rightarrow 0$$

holds for every compact $K \subset \mathbb{Z}_\times^2 \times \mathbb{R}$. This yields items (i) and (ii), while item (iii) follows from Lemma 3.3.4. □

3.3.2 Trapped entire solutions

The main aim of this subsection is to establish Proposition 3.3.3, which states that every entire solution of the discrete Allen-Cahn equation on $\mathbb{Z}_\times^2 \times \mathbb{R}$ trapped between two travelling waves is a travelling wave itself. At the heart of the proof lies a version of the maximum principle for LDEs which we provide below in Lemmas 3.3.5 and 3.3.6. As a preparation, we define the quantities

$$\sigma_\infty := \max\{|\sigma_h|, |\sigma_v|\}, \quad m_* := \sigma_\infty - 1.$$

Lemma 3.3.5. *Pick $\kappa \in \mathbb{R}$ and let $E_\kappa \subset \mathbb{Z}_\times^2 \times \mathbb{R}$ be defined as*

$$E_\kappa = \{(n, l, t) \in \mathbb{Z}_\times^2 \times \mathbb{R} : n - c_* t \geq \kappa\}. \quad (3.3.7)$$

Pick $B \in \mathbb{R}$ and $\epsilon > 0$ and assume that the function $z \in C^1(\mathbb{R}, \ell^\infty(\mathbb{Z}_\times^2))$ satisfies the conditions

- (i) $z_{n,l}(t) \geq 0$ for all $(n, l, t) \in E_\kappa$;
- (ii) $z_{n,l}(t) \geq \epsilon$ for all $(n, l, t) \in E_\kappa$ with $n - c_*t \in [\kappa, \kappa + m_*]$;
- (iii) $\dot{z}_{n,l}(t) - (\Delta^\times z)_{n,l}(t) + Bz_{n,l}(t) \geq 0$ for all $(n, l, t) \in E_\kappa$.

Then, in fact $z_{n,l}(t) > 0$ for all $(n, l, t) \in E_\kappa$.

Proof. Assume to the contrary that there exists $(n_0, l_0, t_0) \in E_\kappa$ for which the equality $z_{n_0, l_0}(t_0) = 0$ holds. Since the function z attains its minimum at this interior point, we know that $\dot{z}_{n_0, l_0}(t_0) = 0$. In addition, assumption (ii) ensures that $(\Delta^\times z)_{n_0, l_0}(t_0) \geq 0$. On the other hand, assumption (iii) gives

$$0 \leq \dot{z}_{n_0, l_0}(t_0) - (\Delta^\times z)_{n_0, l_0}(t_0) + Bz_{n_0, l_0}(t_0) = -(\Delta^\times z)_{n_0, l_0}(t_0) \leq 0.$$

Therefore, the equality $(\Delta^\times z)_{n_0, l_0}(t_0) = 0$ must hold. In particular, we have

$$z_{n_0 - \sigma_h, l - \sigma_v}(t_0) = z_{n_0 + \sigma_h, l + \sigma_v}(t_0) = z_{n_0 - \sigma_v, l + \sigma_h}(t_0) = z_{n_0 + \sigma_v, l - \sigma_h}(t_0) = 0.$$

We note that the inclusion

$$n_0 - \sigma_\infty \in [\kappa, \kappa + m_*]$$

would immediately contradict property (ii). On the other hand, if

$$n_0 - \sigma_\infty \geq \kappa + m_* + 1$$

we can repeat this procedure with $n_0 - \sigma_\infty$ until the desired contradiction is reached. \square

Lemma 3.3.6. *Pick $\kappa \in \mathbb{R}$ and let $F_\kappa \subset \mathbb{Z}_\times^2 \times \mathbb{R}$ be defined as*

$$F_\kappa = \{(n, l, t) \in \mathbb{Z}_\times^2 \times \mathbb{R} : n - c_*t \leq \kappa\}. \quad (3.3.8)$$

Pick $B \in \mathbb{R}$ and $\epsilon > 0$ and assume that the function $z \in C^1(\mathbb{R}, \ell^\infty(\mathbb{Z}_\times^2))$ satisfies the conditions

- (i) $z_{n,l}(t) \geq 0$ for $(n, l, t) \in F_\kappa$;
- (ii) $z_{n,l}(t) \geq \epsilon$ for all $(n, l, t) \in F_\kappa$ with $n - c_*t \in [\kappa - m_*, \kappa]$;
- (iii) $\dot{z}_{n,l}(t) - (\Delta^\times z)_{n,l}(t) + Bz_{n,l}(t) \geq 0$ for all $(n, l, t) \in F_\kappa$.

Then, in fact $z_{n,l}(t) > 0$ on F_κ .

Proof. The proof is almost identical to that of Lemma 3.3.5. \square

Lemma 3.3.7. *Consider the setting of Proposition 3.3.3 and pick a sufficiently small $\delta > 0$. Choose a pair $(N, L) \in \mathbb{Z}_\times^2$ together with a constant $\rho \in \mathbb{R}$. Suppose for some $\kappa \in \mathbb{Z}$ that the function*

$$v_{n,l}^\rho(t) = \omega_{n+N, l+L}(t + N/c_* + \rho/c_*) \quad (3.3.9)$$

satisfies the inequality

$$v_{n,l}^\rho(t) \leq \omega_{n,l}(t) \quad (3.3.10)$$

*whenever $n - c_*t \in [\kappa, \kappa + m_*]$. Then the following claims holds true.*

- (i) If $\omega_{n,l}(t) \geq 1 - \delta$ whenever $n - c_*t \geq \kappa$, then in fact (3.3.10) holds for all $n - c_*t \geq \kappa$.
- (ii) If $v_{n,l}^\rho(t) \leq \delta$ whenever $n - c_*t \leq \kappa + m_*$, then in fact (3.3.10) holds for all $n - c_*t \leq \kappa + m_*$.

Proof. We follow the outline of the proof from [52, §4], which can be seen as a spatially discrete version of [13, §3] where continuous travelling waves were considered. We only establish (i), since (ii) can be obtained in a similar fashion using the set F_κ from Lemma 3.3.6 instead of the set E_κ from Lemma 3.3.5.

Due to the global bounds on the functions ω and v^ρ , the quantity

$$\epsilon^* = \inf \{ \epsilon > 0 : v^\rho \leq \omega + \epsilon \text{ in } E_\kappa \}$$

is finite and by continuity we have

$$v^\rho \leq \omega + \epsilon^* \quad \text{in } E_\kappa. \quad (3.3.11)$$

To prove the claim we must show that $\epsilon^* = 0$.

Assuming to the contrary that $\epsilon^* > 0$, we find sequences $(n_k, l_k, t_k) \in E_\kappa$ and $\epsilon_k \nearrow \epsilon^*$ such that

$$\omega_{n_k, l_k}(t_k) + \epsilon_k < v_{n_k, l_k}^\rho(t_k) \leq \omega_{n_k, l_k}(t_k) + \epsilon^*. \quad (3.3.12)$$

The right inequality above together with the bounds (3.3.4) implies that the sequence $n_k - c_*t_k$ is bounded. Applying a similar construction to that in the proof of Corollary 3.3.2, we obtain a function $\omega^\infty \in C^1(\mathbb{R}; \ell^\infty(\mathbb{Z}_\times^2))$ for which we have the limits

$$\begin{aligned} \lim_{k \rightarrow \infty} \omega_{n+n_k, l+l_k}(t+t_k) &= \omega_{n,l}^\infty(t), \\ \lim_{k \rightarrow \infty} v_{n+n_k, l+l_k}^\rho(t+t_k) &= \omega_{n+N, l+L}^\infty(t + N/c_* + \rho/c_*). \end{aligned} \quad (3.3.13)$$

We define the function $z \in C^1(\mathbb{R}, \ell^\infty(\mathbb{Z}_\times^2))$ by

$$z_{n,l}(t) = \omega_{n,l}^\infty(t) - \omega_{n+N, l+L}^\infty(t) + \epsilon^*$$

and claim that z satisfies conditions (i)-(iii) of Lemma 3.3.5 on the set

$$E_0 = \{ (n, l, t) \in \mathbb{Z}_\times^2 \times \mathbb{R} : n - c_*t \geq 0 \}.$$

To see this, we first note that $n + n_k - c_*t - c_*t_k \geq \kappa$ holds by construction on the set E_0 . Since the inequality (3.3.11) survives the limit (3.3.13), we have $z_{n,l}(t) \geq 0$ on E_0 , verifying (i). Turning to (ii), we note that the inequality (3.3.10) implies that

$$z_{n,l}(t) \geq \epsilon^* > 0, \quad \text{for } n - c_*t \in [0, m_*].$$

To establish (iii), we pick $\delta > 0$ in such a way that the function g is non-increasing on the interval $[1 - \delta, 1]$. Recalling that $\omega^\infty \in [1 - \delta, 1]$ on E_0 and that g is locally Lipschitz, we obtain the bound

$$\begin{aligned} \dot{z}_{n,l}(t) - (\Delta^\times z)_{n,l}(t) &= g(\omega_{n,l}^\infty(t)) - g(\omega_{n+N, l+L}^\infty(t)) \\ &\geq g(\omega_{n,l}^\infty(t) + \epsilon^*) - g(\omega_{n+N, l+L}^\infty(t)) \\ &\geq -Bz_{n,l}(t) \end{aligned}$$

for any $(n, l, t) \in E_0$. We may hence apply Lemma 3.3.5 and conclude that $z > 0$ on E_0 . However, the inequalities (3.3.12) imply that $z_{0,0}(0) = 0$, which is a contradiction. Therefore $\epsilon^* = 0$ must hold, as desired. \square

Lemma 3.3.8. *Consider the setting of Proposition 3.3.3, fix an arbitrary pair $(N, L) \in \mathbb{Z}^2$ and recall the functions v^ρ defined in (3.3.9). Then the quantity*

$$\rho_* := \inf \{ \rho \in \mathbb{R} : v^{\tilde{\rho}} \leq \omega \text{ in } \mathbb{Z}_\times^2 \times \mathbb{R} \text{ for all } \tilde{\rho} \geq \rho \}$$

satisfies $\rho_* \leq 0$.

Proof. One can obtain this result by following the outline presented in the proof of [52, Lemma 4.4]. Instead of [52, Lemma 4.3], one now needs to employ Lemma 3.3.7. \square

Proof of Proposition 3.3.3. From Lemma 3.3.8, it follows that

$$\omega_{n,l}(t) \geq \omega_{n+N,l+L}(t + N/c_*) \quad \text{on } \mathbb{Z}_\times^2 \times \mathbb{R}.$$

Since the pair $(N, L) \in \mathbb{Z}_\times^2$ is arbitrary, we can conclude that the function ω depends only on the difference $n - c_*t$. In particular, there exists a function φ such that $\omega_{n,l}(t) = \varphi(n - c_*t)$. The result now follows directly from the fact that solutions to the travelling wave problem (3.2.7)-(3.2.8) for $c_* \neq 0$ are unique up to translation; see [67]. \square

3.4 Large time behaviour of u

In this section we establish Proposition 3.2.7 by studying the qualitative large time behaviour of the solution u within the interfacial region

$$I_t = \{ (n, l) \in \mathbb{Z}_\times^2 : \Phi_*(-\sigma_*^2 - 1) \leq u_{n,l}(t) \leq \Phi_*(\sigma_*^2 + 1) \},$$

which represents the points at which a solution u is close to $\Phi_*(0) = 1/2$. The boundary values $\Phi_*(-\sigma_*^2 - 1)$ and $\Phi_*(\sigma_*^2 + 1)$ were carefully chosen to ensure that I_t is nonempty for large t , which we show in Proposition 3.4.1. In addition, we show that for a fixed pair (l, t) the map $n \mapsto u_{n,l}(t)$ is monotone within I_t , in the sense that the differences $u_{n+\sigma_*^2,l}(t) - u_{n,l}(t)$ are bounded from below uniformly in time.

In addition to the monotonicity within I_t , the map $n \mapsto u_{n,l}(t)$ cannot exit throughout the lower boundary once it enters the interfacial region from below. Similarly, it cannot reenter the interval once it has left through the upper boundary. All together, these results provide sufficient control in the crucial region away from the stable equilibria zero and one to uniquely define the phase γ by the procedure described in §3.2.2.

The results of this section are a generalization of the results presented in [52, §5], requiring us to take into account several technical differences that arise due to the additional complexities of working with \mathbb{Z}_\times^2 rather than \mathbb{Z}^2 . Moreover, our construction of the phase $\gamma(t)$ here is more refined than the setup in [52], which also causes several modifications to the proofs.

Proposition 3.4.1. *Consider the setting of Proposition 3.2.7. Then there exists $T > 0$ such that the following claims hold true.*

(i) *For each $t \geq T$ and $l \in \mathbb{Z}$ there exists $n_* = n_*(l, t) \in \mathbb{Z}$ for which*

$$\Phi_*(-\sigma_*^2 - 1) < u_{n_*, l}(t) \leq \frac{1}{2}. \quad (3.4.1)$$

(ii) *We have the inequality*

$$\inf_{t \geq T, (n, l) \in I_t} u_{n+\sigma_*^2, l}(t) - u_{n, l}(t) > 0. \quad (3.4.2)$$

(iii) *Consider any $t \geq T$ and $(n, l) \in \mathbb{Z}_\times^2$ for which $u_{n, l}(t) \leq \Phi_*(-\sigma_*^2 - 1)$ holds. Then we also have $u_{n-\sigma_*^2, l}(t) \leq \Phi_*(-\sigma_*^2 - 1)$.*

(iv) *Consider any $t \geq T$ and $(n, l) \in \mathbb{Z}_\times^2$ for which $u_{n, l}(t) \geq \Phi_*(\sigma_*^2 + 1)$ holds. Then we also have $u_{n+\sigma_*^2, l}(t) \geq \Phi_*(\sigma_*^2 + 1)$.*

Proof of Proposition 3.2.6. The statement follows directly from item (i) of Proposition 3.4.1. \square

In the following proposition we provide an asymptotic flatness result for the phase γ . This feature is a crucial property that allows us to construct the super- and sub-solutions that we use in the proof of Theorem 3.2.9 and consequently Theorem 3.2.10.

Proposition 3.4.2. *Consider the setting of the Proposition 3.4.1 and recall the phase $\gamma : [T, \infty) \rightarrow \ell^\infty(\mathbb{Z})$ defined in (3.2.26). Then we have the limit*

$$\limsup_{t \rightarrow \infty} \sup_{l \in \mathbb{Z}} |\gamma_{l+1}(t) - \gamma_l(t)| = 0.$$

3.4.1 Phase construction

In this subsection we prove Proposition 3.4.1, mainly by relying on the convergence results from Proposition 3.3.1. As a preparation, we define the set

$$\mathcal{I}(T, R) := \{(n, l, t) \in \mathbb{Z}_\times^2 \times [T, \infty) : |n - c_* t| \leq R\}$$

for any pair of positive constants T and R and we also remind the reader of the set of sequences \mathcal{S} defined in (3.3.1).

Lemma 3.4.3. *Consider the setting of Proposition 3.4.1 and pick a constant $R > 0$. Then there exists a constant $T > 0$ such that*

$$\inf_{(n, l, t) \in \mathcal{I}(T, R)} u_{n+\sigma_*^2, l}(t) - u_{n, l}(t) > 0.$$

Proof. Assume to the contrary that there exists a constant $R > 0$ such that

$$\inf_{(n, l, t) \in \mathcal{I}(T, R)} u_{n+\sigma_*^2, l}(t) - u_{n, l}(t) \leq 0 \quad (3.4.3)$$

holds for every $T > 0$. That implies that we can find a sequence $(n_k, l_k, t_k)_{k \geq 0} \in \mathcal{S}$ such that

$$u_{n_k + \sigma_*^2, l_k}(t_k) - u_{n_k, l_k}(t_k) \leq \frac{1}{k}. \quad (3.4.4)$$

By virtue of Proposition 3.3.1, we can find $\theta_0 \in \mathbb{R}$ and pass to a subsequence for which we have the convergence

$$u_{n+n_k, l+l_k}(t+t_k) \rightarrow \Phi_*(n - c_*t + \theta_0) \text{ in } C_{\text{loc}}(\mathbb{Z}_x^2 \times \mathbb{R}).$$

Therefore, letting $k \rightarrow \infty$ in (3.4.4) leads to

$$\Phi_*(\sigma_*^2 + \theta_0) - \Phi_*(\theta_0) \leq 0, \quad (3.4.5)$$

which contradicts the monotonicity of the function Φ_* . \square

Proof of Proposition 3.4.1. We first establish (iv). Arguing by contradiction, assume that there exists a sequence $(n_k, l_k, t_k)_{k \geq 0}$, $0 < t_1 < t_2 < \dots \rightarrow \infty$ such that

$$u_{n_k, l_k}(t_k) \geq \Phi_*(\sigma_*^2 + 1) \quad \text{and} \quad u_{n_k + \sigma_*^2, l_k}(t_k) < \Phi_*(\sigma_*^2 + 1). \quad (3.4.6)$$

The bounds in Lemma 3.3.4 imply that the sequence $n_k - c_*t_k$ is bounded by some constant R . We can now apply Lemma 3.4.3 to conclude $u_{n_k + \sigma_*^2, l_k}(t_k) - u_{n_k, l_k}(t_k) > 0$, which contradicts (3.4.6) due to the strict monotonicity of the function Φ_* . Items (i) and (iii) follow in a similar way.

To prove item (ii), we choose a T that satisfies (i), (iii) and (iv) and pick $t \geq T$ together with $(n, l) \in I_t$. Upon further increasing T , Lemma 3.3.4 implies that $n - c_*t$ is bounded by some constant $R > 0$ that only depends on T . Therefore, we have shown that

$$\{(n, l, t) : t \geq T, (n, l) \in I_t\} \subseteq \mathcal{I}(T, R).$$

The desired bound now follows directly from Lemma 3.4.3. \square

Lemma 3.4.4. *Consider the setting of Proposition 3.4.1 and recall the phase $\gamma : [T, \infty) \rightarrow \ell^\infty(\mathbb{Z})$ defined in (3.2.26). Then there exists $T_* \geq T$ such that the difference $n_*(l, t) - c_*t$ is uniformly bounded for $t \geq T_*$ and $l \in \mathbb{Z}$. In particular, we can find a constant $M > 0$ so that*

$$\|\gamma(t) - c_*t\|_{\ell^\infty} \leq M, \quad t \geq T_*.$$

Proof. The proof is analogous to that of Lemma 5.4 in [52]. \square

Proof of Proposition 3.2.7. Arguing by contradiction once more, let us assume that there exists $\delta > 0$ together with sequences $(n_k, l_k) \in \mathbb{Z}_x^2$ and $T \leq t_1 < t_2 < \dots \rightarrow \infty$ for which

$$|\Delta_k| := |u_{n_k, l_k}(t_k) - \Phi_*(n_k - \gamma_{l_k}(t_k))| \geq \delta. \quad (3.4.7)$$

Analogously as in the proof of [52, Thm. 2.2], one can show that $n_k - c_*t_k$ is a bounded sequence. In addition, from Lemma 3.4.4 we also know that $n_*(l_k, t_k) - c_*t_k$ is bounded. Therefore, the sequence $n_*(l_k, t_k) - n_k$ is also bounded, allowing us to

identify it with a constant $m \in \mathbb{Z}$. Applying Proposition 3.3.1 we find $\theta_0 \in \mathbb{R}$ such that the limit

$$u_{n+n_k, l+l_k}(t+t_k) \rightarrow \Phi_*(n - c_*t + \theta_0) \quad (3.4.8)$$

holds for all $(n, l, t) \in \mathbb{Z}_\times^2 \times \mathbb{R}$, after passing to a further subsequence. Recalling the definition (3.2.26), this leads to

$$\begin{aligned} \Phi_*(n_k - \gamma_{l_k}(t_k)) &= \Phi_*(n_k - n_*(l_k, t_k) - \vartheta_*(l_k, t_k)) \\ &= \Phi_*(-m - \vartheta_*(l_k, t_k)). \end{aligned}$$

Due to (3.4.8) and definition (3.2.25) of $\vartheta_*(l, t)$ we obtain the convergence

$$\vartheta_*(l_k, t_k) \rightarrow -\frac{\sigma_*^2 \Phi_*^{-1}(\Phi_*(m + \theta_0))}{\Phi_*^{-1}(\Phi_*(m + \sigma_*^2 + \theta_0)) - \Phi_*^{-1}(\Phi_*(m + \theta_0))} = -m - \theta_0$$

as $k \rightarrow \infty$, which in turn implies that

$$\Phi_*(n_k - \gamma_{l_k}(t_k)) \rightarrow \Phi_*(\theta_0).$$

We hence find that

$$\Delta_k \rightarrow \Phi_*(\theta_0) - \Phi_*(\theta_0) = 0$$

as $k \rightarrow \infty$, which clearly contradicts (3.4.7). \square

3.4.2 Phase asymptotics

In this subsection we establish the asymptotic flatness result for the phase $\gamma(t)$ that was stated in Proposition 3.4.2. A key ingredient is that the first differences of the function $l \mapsto n_*(l, t)$ can be uniformly bounded for large t .

Lemma 3.4.5. *Consider the setting of Proposition 3.4.1. Then there exists a constant $\tilde{T} > T$ so that for every $t \geq \tilde{T}$ and $l \in \mathbb{Z}$ we have*

$$|n_*(l+1, t) - n_*(l, t)| \leq \sigma_*^2.$$

Proof. Assume to the contrary that there exist three sequences $(n_k, \tilde{n}_k, l_k)_{k \geq 0} \subset \mathbb{Z}^3$, $(t_k)_{k \geq 0} \subset (0, \infty)$ with $T < t_1 < t_2 < \dots \rightarrow \infty$ for which

$$|n_k - \tilde{n}_k| > \sigma_*^2 \quad (3.4.9)$$

and

$$\begin{cases} u_{n_k, l_k}(t_k) \leq 1/2, \\ u_{n_k + \sigma_*^2, l_k}(t_k) > 1/2, \end{cases} \quad \begin{cases} u_{\tilde{n}_k, l_k+1}(t_k) \leq 1/2, \\ u_{\tilde{n}_k + \sigma_*^2, l_k+1}(t_k) > 1/2. \end{cases} \quad (3.4.10)$$

Since both sequences $n_*(l_k+1, t_k) - c_*t_k$ and $n_*(l_k, t_k) - c_*t_k$ are bounded, we can assume that their difference is constant and equal to $m \in \mathbb{Z}$, i.e.

$$m = \tilde{n}_k - n_k.$$

With this notation we can apply Proposition 3.3.1 to find a constant $\theta_0 \in \mathbb{R}$ for which

$$\begin{cases} u_{n_k, l_k}(t_k) \rightarrow \Phi_*(\theta_0), \\ u_{n_k + \sigma_*^2, l_k}(t_k) \rightarrow \Phi_*(\theta_0 + \sigma_*^2), \end{cases} \quad \begin{cases} u_{m+n_k, l_k+1}(t_k) \rightarrow \Phi_*(m + \theta_0), \\ u_{m+\sigma_*^2+n_k, l_k+1}(t_k) \rightarrow \Phi_*(m + \theta_0 + \sigma_*^2). \end{cases}$$

Combining these limits with the inequalities (3.4.10) we find that θ_0 necessarily satisfies

$$-\sigma_*^2 \leq \theta_0 \leq 0, \quad -\sigma_*^2 \leq m + \theta_0 \leq 0.$$

This in turn implies that $|m| \leq \sigma_*^2$, contradicting the strict inequality in (3.4.9). \square

Proof of Proposition 3.4.2. Assume to the contrary that there exists $\delta > 0$ together with subsequences $(l_k)_{k \geq 0} \subset \mathbb{Z}$ and $T \leq t_1 < t_2 < \dots \rightarrow \infty$ for which

$$\delta \leq |\gamma_{l_k+1}(t_k) - \gamma_{l_k}(t_k)|. \quad (3.4.11)$$

Lemma 3.4.5 assures us that it is possible to pass to a subsequence that has

$$n_*(l_k + 1, t_k) = n_*(l_k, t_k) + m,$$

for some integer $m \in [0, \sigma_*^2]$. Recalling the definition (3.2.25) for $\vartheta_*(l, t)$, we find

$$\gamma_{l_k+1}(t) - \gamma_{l_k}(t) = m + \vartheta_*(l_k + 1, t_k) - \vartheta_*(l_k, t_k). \quad (3.4.12)$$

We now employ Proposition 3.3.1 to find $\theta_0 \in \mathbb{R}$ such that for all $(n, l, t) \in \mathbb{Z}_\times^2 \times \mathbb{R}$ we have

$$u_{n+n_k, l+l_k}(t+t_k) \rightarrow \Phi_*(n - c_*t + \theta_0), \quad \text{as } k \rightarrow \infty,$$

which further implies that

$$\vartheta_*(l_k, t_k) \rightarrow -\theta_0, \quad \vartheta_*(l_k + 1, t_k) \rightarrow -m - \theta_0.$$

Taking the limit in (3.4.12) we obtain

$$\delta \leq |m - \theta_0 - m + \theta_0| = 0,$$

which is a clear contradiction. \square

3.5 Linearized phase evolution

In this section we consider the lattice differential equation

$$\dot{h}_i(t) = \sum_{k=-N}^N a_k [h_{i+\mu_k}(t) - h_i(t)], \quad t > 0 \quad (3.5.1)$$

with the initial condition

$$h(0) = h^0 \in \ell^\infty(\mathbb{Z}). \quad (3.5.2)$$

In order to highlight the general applicability of our results, we step back here from the specific framework associated to (3.2.28). Instead, we impose the following general assumption on the coefficients $a = (a_k)_{k=-N}^N \subset \mathbb{R}$ and the shifts $\mu = (\mu_k)_{k=-N}^N \subset \mathbb{Z}$.

(h α) The function $f : [-\pi, \pi] \rightarrow \mathbb{R}$ defined by

$$f(\omega) := \sum_{k=-N}^N a_k (\cos(\mu_k \omega) - 1) \quad (3.5.3)$$

is strictly negative on $[-\pi, \pi] \setminus \{0\}$. Furthermore, the constant $\Lambda \in \mathbb{R}$ defined by

$$\Lambda := \sum_{k=-N}^N a_k \mu_k^2 = -f''(0) \quad (3.5.4)$$

satisfies $\Lambda > 0$.

Let us first observe that the assumption (h α) implies that we can find $m > 0$ and $\kappa > 0$ such that

$$f(\omega) \leq -\frac{\Lambda}{2} \omega^2 \quad \text{for } \omega \in [-\kappa, \kappa], \quad (3.5.5)$$

$$f(\omega) < -m \quad \text{for } \omega \in [-\pi, -\kappa] \cup [\kappa, \pi]. \quad (3.5.6)$$

For any $n \in \mathbb{N}_0$ we inductively define the (n)-th discrete derivative $\partial^{(n)} : \ell^\infty(\mathbb{Z}) \rightarrow \ell^\infty(\mathbb{Z})$ by writing

$$[\partial^{(0)}\Gamma]_j := \Gamma_j, \quad [\partial^{(1)}\Gamma]_j := \Gamma_{j+1} - \Gamma_j$$

together with

$$[\partial^{(n)}\Gamma]_j = \left[\partial^{(1)} \left(\partial^{(n-1)}\Gamma \right) \right]_j \quad (3.5.7)$$

for $n > 1$. The first goal of this section is to establish decay estimates of the form

$$\|\partial^{(n)}h(t)\|_{\ell^\infty} \sim O(t^{-\frac{n}{2}}) \quad (3.5.8)$$

for the solution $h(t)$ of the system (3.5.1)-(3.5.2). These rates are consistent with the estimates for solutions of the continuous heat equation $h_t = h_{xx}$, which can be readily obtained by taking x -derivatives of the explicit representation

$$h(x, t) = \frac{1}{\sqrt{4\pi t}} \int_{\mathbb{R}} e^{-\frac{(x-y)^2}{4t}} h(y, 0) dy. \quad (3.5.9)$$

Our goal is to find a solution formula for (3.5.1) equivalent to (3.5.9), in the sense that it takes the form of the convolution between the fundamental solution with the initial condition. By finding such a representation, we can transfer discrete derivatives onto the fundamental solution to establish (3.5.8). Note that related estimates for the fully discrete equivalent of (3.5.1) were obtained in [28, 77].

Theorem 3.5.1 (see §3.5.1). *Assume that condition (h α) holds and pick $n \in \mathbb{N}_0$. Then there exists a constant $C = C(n)$ so that for any $h^0 \in \ell^\infty(\mathbb{Z})$, the n -th discrete derivative of the solution $h \in C^1([0, \infty); \ell^\infty(\mathbb{Z}))$ to the initial value problem (3.5.1)-(3.5.2) satisfies the bound*

$$\left\| \partial^{(n)}h(t) \right\|_{\ell^\infty} \leq C \min \left\{ \left\| \partial^{(n)}h^0 \right\|_{\ell^\infty}, \left\| h^0 \right\|_{\ell^\infty} t^{-\frac{n}{2}} \right\}.$$

The second main result of this section concerns lower and upper bounds for the solution $h(t)$ that are sharper than the ℓ^∞ -bounds in Theorem 3.5.1. In particular, we show that if the initial condition h^0 is bounded away from 0, then the solution $h(t)$ is positive for large time $t \gg 1$. Moreover, under the additional assumption that the first differences of h^0 are flat enough we obtain the same conclusion for all time $t \geq 0$. The key issue is that some of the coefficients (a_k) are allowed to be negative, which causes the usual comparison principle to fail. Indeed, it can (and does) happen that a solution $h(t)$ admits negative values for a short time even if the initial condition is strictly positive.

Proposition 3.5.2 (see §3.5.1). *Consider the setting of Theorem 3.5.1 and pick $\varepsilon > 0$. Then there exists a time $T = T(\varepsilon) > 0$ and $C = C(T, \varepsilon)$ such that for all $t \geq T$ the following properties hold.*

(i) *For any $h^0 \in \ell^\infty(\mathbb{Z})$ that has $h_k^0 \geq 0$ for all $k \in \mathbb{Z}$, we have the bounds*

$$h_k(t) \geq \inf_{j \in \mathbb{Z}} h_j^0 - C \|\partial h^0\|_{\ell^\infty}, \quad k \in \mathbb{Z}, \quad t \in [0, T], \quad (3.5.10)$$

$$h_k(t) \geq \inf_{j \in \mathbb{Z}} h_j^0 - \varepsilon \|h^0\|_{\ell^\infty}, \quad k \in \mathbb{Z}, \quad t \geq T. \quad (3.5.11)$$

(ii) *For any $h^0 \in \ell^\infty(\mathbb{Z})$ that has $h_k^0 \leq 0$ for all $k \in \mathbb{Z}$, we have the bounds*

$$h_k(t) \leq \sup_{j \in \mathbb{Z}} h_j^0 + C \|\partial h^0\|_{\ell^\infty}, \quad k \in \mathbb{Z}, \quad t \in [0, T], \quad (3.5.12)$$

$$h_k(t) \leq \sup_{j \in \mathbb{Z}} h_j^0 + \varepsilon \|h^0\|_{\ell^\infty}, \quad k \in \mathbb{Z}, \quad t \geq T. \quad (3.5.13)$$

3.5.1 Strategy

In order to find an explicit formula for the solution h of the initial problem (3.5.1)-(3.5.2), we note that a spatial Fourier transform leads to the decoupled sets of ODEs

$$\frac{d}{dt} \hat{h}(\omega, t) = \sum_{k=-N}^N a_k (e^{i\mu_k \omega} - 1) \hat{h}(\omega, t)$$

for $\omega \in [-\pi, \pi]$. Introducing the function

$$p(\omega) = \sum_{k=-N}^N a_k \sin(\mu_k \omega), \quad (3.5.14)$$

we hence obtain the convolution formula

$$h_l(t) = \sum_{k \in \mathbb{Z}} h_k^0 M_{l-k}(t), \quad (3.5.15)$$

where the fundamental solution $M(t)$ is defined by

$$M_l(t) = \frac{1}{2\pi} \int_{-\pi}^{\pi} e^{il\omega} e^{t f(\omega) + it p(\omega)} d\omega. \quad (3.5.16)$$

Notice that assumption $(h\alpha)$ ensures that $\|M(t)\|_{\ell^\infty} \leq 1$ for every $t \geq 0$. The following result provides decay estimates for $\partial^{(n)}M(t)$ in $\ell^p(\mathbb{Z})$, which can be used to establish the bounds in Theorem 3.5.1.

Proposition 3.5.3. *Assume that condition $(h\alpha)$ holds and pick $n \in \mathbb{N}_0$ and $p \in [1, \infty]$. Then there exists a positive constant $C = C(n, p)$ such that*

$$\left\| \partial^{(n)}M(t) \right\|_{\ell^p} \leq C \min \left\{ 1, t^{-n/2-1/2+1/(2p)} \right\}.$$

Proof of Theorem 3.5.1. In view of the convolution formula (3.5.15), we have

$$\left\| \partial^{(n)}h(t) \right\|_{\ell^\infty} \leq \|h^0\|_{\ell^\infty} \left\| \partial^{(n)}M(t) \right\|_{\ell^1}.$$

Employing Proposition 3.5.3 with $p = 1$ we obtain a constant $C = C(n)$ for which

$$\left\| \partial^{(n)}h(t) \right\|_{\ell^\infty} \leq C \|h^0\|_{\ell^\infty} t^{-\frac{n}{2}}.$$

On the other hand, by transferring the n -th difference operators to the sequence h^0 , we can write

$$\left\| \partial^{(n)}h(t) \right\|_{\ell^\infty} \leq \left\| \partial^{(n)}h^0 \right\|_{\ell^\infty} \|M(t)\|_{\ell^1} = \left\| \partial^{(n)}h^0 \right\|_{\ell^\infty} \left\| \partial^{(0)}M(t) \right\|_{\ell^1}.$$

Another application of Proposition 3.5.3 with $p = 1$ with $n = 0$ now leads to the desired bound. \square

We establish Proposition 3.5.3 by applying an interpolation argument to the corresponding estimates in $\ell^1(\mathbb{Z})$ and $\ell^\infty(\mathbb{Z})$. To show the latter, we take advantage of the inequality

$$\|\theta\|_{\ell^\infty} \leq \frac{1}{2\pi} \|\hat{\theta}\|_{L^1(-\pi, \pi)},$$

which holds for all $\theta \in \ell^2(\mathbb{Z})$. On the other hand, obtaining $\ell^1(\mathbb{Z})$ -estimates is a challenging process, since we can not directly extract them from the Fourier representation. Instead, we divide the sum into two parts, based on the size of the term $|l/t + a \cdot \mu|$. We note that the constant $-a \cdot \mu = -p'(0)$ is often referred to as the group velocity. It tracks the speed of the ‘center’ of M and - in context of §3.2 - is closely related to $[\partial_\omega \lambda_\omega]_{\omega=0}$ and $[\partial_\varphi c_\varphi]_{\varphi=0}$.

Lemma 3.5.4 (see §3.5.3). *Assume that $(h\alpha)$ is satisfied and pick $n \in \mathbb{N}_0$. Then there exists $C = C(n) > 0$ so that the n -th difference of the sequence $M(t)$ satisfies the bound*

$$\|\partial^n M(t)\|_{\ell^\infty} \leq C \min \left\{ 1, t^{-\frac{n+1}{2}} \right\}. \quad (3.5.17)$$

Lemma 3.5.5 (see §3.5.3). *Consider the setting of Theorem 3.5.1. Then there exist positive constants $K = K(n)$ and $C = C(n)$ such that*

$$\sum_{|l/t+a \cdot \mu| \geq K} |\partial^n M(t)_l| [1 + |l|] \leq C e^{-t}. \quad (3.5.18)$$

Lemma 3.5.6 (see §3.5.4). *Consider the setting of Theorem 3.5.1 and pick $K > 0$. Then there exists $C = C(K, n) > 0$ such that*

$$\sum_{|l/t+a\cdot\mu|\leq K} |[\partial^n M(t)]_l| \leq C \min \{1, t^{-\frac{n}{2}}\}.$$

Proof of Proposition 3.5.3. Employing Lemmas 3.5.5 and 3.5.6 in combination with the fast decay of the exponential, we obtain a constant $C = C(n)$ such that

$$\left\| \partial^{(n)} M(t) \right\|_{\ell^1} \leq C \min \{1, t^{-\frac{n}{2}}\}. \tag{3.5.19}$$

Applying the interpolation inequality

$$\left\| \partial^{(n)} M(t) \right\|_{\ell^p} \leq \left\| \partial^{(n)} M(t) \right\|_{\ell^1}^{1/p} \left\| \partial^{(n)} M(t) \right\|_{\ell^\infty}^{1-1/p}$$

in combination with (3.5.17) and (3.5.19) we arrive at the desired estimate. \square

To prove the lower bounds for solution $h(t)$ that are formulated in Proposition 3.5.2, we first note that

$$\sum_{l \in \mathbb{Z}} M_l(t) = 1, \quad t \geq 0. \tag{3.5.20}$$

Indeed, if $h^0 \equiv 1$, then by uniqueness we must have $h(t) = 1$ for all $t > 0$. Our next task is to extract more detailed information on the spatial distribution of the ‘mass’ of M . In particular, we show that the bulk of this mass is contained in a region that is $O(\sqrt{t})$ wide. By combining our estimates with (3.5.20), the negative components of M can be controlled asymptotically.

Lemma 3.5.7 (see §3.5.4). *Consider the setting of Theorem 3.5.1 and pick positive constants κ and K_* . Then there exist a time $T = T(\kappa, K_*)$ such that for all $t \geq T$ we have*

$$\sum_{|l/t+a\cdot\mu|\leq \frac{K_*}{\sqrt{t}}} |M_l(t)| \leq 1 + \kappa.$$

Lemma 3.5.8 (see §3.5.4). *Consider the setting of Theorem 3.5.1 and pick $\kappa > 0$. Then there exists a constant $K_* > 0$ so that for all $K \geq K_*$ and $t \geq 1$ we have the bound*

$$\sum_{\frac{K}{\sqrt{t}} \leq |l/t+a\cdot\mu| \leq K} |M_l(t)| \leq \kappa.$$

In our next result we show that the kernel $M(t)$ behaves similarly to the Gaussian kernel. In particular, for the continuous kernel we have

$$\frac{1}{\sqrt{t}} \int_{\mathbb{R}} e^{-x^2/t} \frac{|x|}{\sqrt{t}} \sim O(1).$$

To establish the equivalent estimate for the discrete kernel $M(t)$, we have to take into account that the kernel is not symmetric anymore, but that the center of mass ‘travels’ in time with speed $-(a \cdot \mu)t$ (see Figure 3.7).

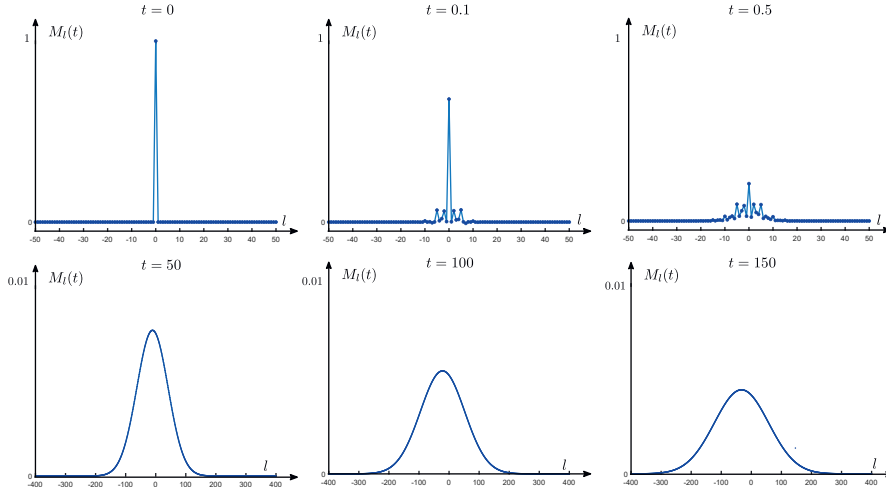


Figure 3.7: These six graphs represent the time evolution of the Green's function $M_l(t)$, which we computed numerically by applying (3.5.16) to the coefficients $(a_k)_{k=-10}^{10}$ appearing in Table 3.1. Observe the negative values for $M_l(t)$ that are clearly visible for $t = 0.1$, together with the leftward movement of the 'center of mass', which travels at the speed $-a \cdot \mu = -0.22$.

Lemma 3.5.9 (see §3.5.4). *Consider the setting of Theorem 3.5.1. There exists a constant C such that for every $t > 0$ we have*

$$\sum_{l \in \mathbb{Z}} |M_l(t)| \frac{|l + (a \cdot \mu)t|}{\sqrt{t}} \leq C.$$

Proof of Proposition 3.5.2. We provide the proof only for (i), noting that item (ii) can be derived analogously. Upon introducing the shorthand

$$x_l^t = \frac{l}{t} + a \cdot \mu,$$

we use Lemmas 3.5.5, 3.5.7 and 3.5.8 to find constants T and K_* so that for all $t \geq T$ we have

$$\sum_{|x_l^t| \leq \frac{K_*}{\sqrt{t}}} |M_l(t)| \leq 1 + \kappa, \quad \sum_{|x_l^t| \geq \frac{K_*}{\sqrt{t}}} |M_l(t)| \leq \kappa. \quad (3.5.21)$$

Combining these inequalities with (3.5.20) we arrive at the bound

$$\sum_{|x_l^t| \leq \frac{K_*}{\sqrt{t}}} M_l(t) = 1 - \sum_{|x_l^t| > \frac{K_*}{\sqrt{t}}} M_l(t) \geq 1 - \sum_{|x_l^t| > \frac{K_*}{\sqrt{t}}} |M_l(t)| \geq 1 - \kappa.$$

Employing Lemma 3.5.7 again, we conclude that

$$-2\kappa \leq \sum_{|x_l^t| \leq \frac{K_*}{\sqrt{t}}} M_l(t) - |M_l(t)| \leq 0,$$

from which we obtain the lower bounds

$$\begin{aligned}
 h_k(t) &= \sum_{l \in \mathbb{Z}} M_l(t) h_{l-k}^0 \\
 &= \sum_{|x_l^t| \leq \frac{\kappa_*}{\sqrt{t}}} |M_l(t)| h_{l-k}^0 + \sum_{|x_l^t| \leq \frac{\kappa_*}{\sqrt{t}}} (M_l(t) - |M_l(t)|) h_{l-k}^0 + \sum_{|x_l^t| > \frac{\kappa}{\sqrt{t}}} M_l(t) h_{l-k}^0 \\
 &\geq (1 - \kappa) \inf_{j \in \mathbb{Z}} h_j^0 - 3\kappa \|h_0\|_\infty \\
 &\geq \inf_{j \in \mathbb{Z}} h_j^0 - 4\kappa \|h_0\|_\infty.
 \end{aligned}$$

The estimate (3.5.11) can now readily be derived by adjusting the constant κ chosen in (3.5.21).

In order to establish (3.5.10) we first compute

$$\begin{aligned}
 h_k(t) &= \sum_{l \in \mathbb{Z}} M_l(t) h_{k-l}^0 = \sum_{l \in \mathbb{Z}} M_l(t) h_k^0 + \sum_{l \in \mathbb{Z}} M_l(t) (h_{k-l}^0 - h_k^0) \\
 &\geq h_k^0 - \|\partial h^0\|_{\ell^\infty} \sum_{l \in \mathbb{Z}} |M_l(t)| |l|.
 \end{aligned}$$

Using Lemma 3.5.9, we can estimate

$$\sum_{l \in \mathbb{Z}} |M_l(t)| |l| \leq C\sqrt{t} + t|a \cdot \mu| \|M(t)\|_{\ell^1}.$$

Lemmas 3.5.5 and 3.5.6 ensure that $\|M(t)\|_{\ell^1}$ is uniformly bounded. We can therefore find $C = C(T)$ such that $\max_{t \in [0, T]} \sum_{l \in \mathbb{Z}} |M_l(t)| |l| \leq C$, which leads to the desired bound (3.5.10). □

3.5.2 Contour deformation

The main difficulty towards proving Lemmas 3.5.5 and 3.5.6 lies in the fact that $[\partial^n M(t)]_l$ depends on the variable l only through the expression $e^{i\omega l}$. By simply taking the absolute value of the integrand in expressions such as (3.5.16), we therefore lose all information on the decay coming from the l -variable. In order to overcome this issue, we pick $\epsilon \in \mathbb{R}$ and denote by Γ_ϵ rectangle consisting of paths

$$\gamma_1 = [-\pi, \pi], \quad \gamma_2 = [\pi, \pi + i\epsilon], \quad \gamma_3 = [\pi + i\epsilon, -\pi + i\epsilon], \quad \gamma_4 = [-\pi + i\epsilon, -\pi].$$

Due to the fact that f and g are 2π -periodic in the real variable, we have

$$\int_{\gamma_2} e^{i\omega} e^{tf(\omega) + itp(\omega)} d\omega = - \int_{\gamma_4} e^{i\omega} e^{tf(\omega) + itp(\omega)} d\omega.$$

Therefore, we obtain

$$0 = \oint_{\Gamma_\epsilon} e^{i\omega} e^{tf(\omega) + itp(\omega)} d\omega = \int_{\gamma_1} e^{i\omega} e^{tf(\omega) + itp(\omega)} d\omega + \int_{\gamma_3} e^{i\omega} e^{tf(\omega) + itp(\omega)} d\omega.$$

Recalling (3.5.16), this allows us to compute

$$M_l(t) = \frac{1}{2\pi} \int_{-\pi+i\epsilon}^{\pi+i\epsilon} e^{il\omega} e^{tf(\omega)+itp(\omega)} d\omega = \frac{1}{2\pi} \int_{-\pi}^{\pi} e^{il(\omega+i\epsilon)} e^{tf(\omega+i\epsilon)+itp(\omega+i\epsilon)} d\omega. \quad (3.5.22)$$

Writing $z = x + iy$ with $x, y \in \mathbb{R}$, we recall the formulas

$$\cos z = \cos x \cosh y - i \sin x \sinh y, \quad \sin z = \sin x \cosh y + i \cos x \sinh y$$

to obtain

$$M_l(t) = \frac{1}{2\pi} e^{-\epsilon l} \int_{-\pi}^{\pi} e^{il\omega} e^{tf(\omega,\epsilon)+itp(\omega,\epsilon)} d\omega, \quad (3.5.23)$$

where the functions $f, p : [-\pi, \pi] \times \mathbb{R} \rightarrow \mathbb{R}$ are now defined by

$$f(\omega, \epsilon) = \sum_{k=-N}^N a_k (\cos(\mu_k \omega) e^{-\mu_k \epsilon} - 1), \quad p(\omega, \epsilon) = \sum_{k=-N}^N a_k \sin(\mu_k \omega) e^{-\mu_k \epsilon},$$

extending the definitions (3.5.3) and (3.5.14).

The main strategy is to choose suitable values for ϵ in order to isolate the relevant decay rates in various (l, t) regimes. Indeed, the representation (3.5.23) does retain sufficient spatial information for our purposes when applying crude estimates to the integrands. To appreciate this, we recall that the Fourier symbol of the difference operator $\partial^{(1)}$ is $e^{i\omega} - 1$ and introduce the real-valued expressions

$$P_l(\epsilon, t, n) = |1 - e^{-\epsilon}|^n e^{-\epsilon l} \int_{-\pi}^{\pi} e^{tf(\epsilon, \omega)} d\omega, \quad (3.5.24)$$

$$R_l(\epsilon, t, n) = e^{-\frac{\epsilon n}{2}} e^{-\epsilon l} \int_{-\pi}^{\pi} |\omega|^n e^{tf(\epsilon, \omega)} d\omega. \quad (3.5.25)$$

The result below shows that their sum can be used to extract the desired bounds on $\partial^n M(t)$. In particular, the problem of estimating the ℓ^1 -norm of the sequence $\partial^n M(t)$ is reduced to finding the corresponding bounds for the ℓ^1 -norm of the sequences $P(\epsilon, t, n)$ and $R(\epsilon, t, n)$.

Lemma 3.5.10. *Consider the setting of Theorem 3.5.1. Then for every $l \in \mathbb{Z}$, $\epsilon \in \mathbb{R}$ and $t \geq 0$ we have*

$$|[\partial^n M(t)]_l| \leq \frac{2^{n/2}}{4\pi} (P_l(\epsilon, t, n) + R_l(\epsilon, t, n)). \quad (3.5.26)$$

Proof. Taking n -th differences in (3.5.23) we obtain the expression

$$[\partial^n M(t)]_l = \frac{1}{2\pi} e^{-\epsilon l} \int_{-\pi}^{\pi} e^{i\omega l} (e^{-\epsilon} e^{i\omega} - 1)^n e^{tf(\omega,\epsilon)+itp(\omega,\epsilon)} d\omega,$$

which leads to the bound

$$|[\partial^n M(t)]_l| \leq \frac{1}{2\pi} e^{-\epsilon l} \int_{-\pi}^{\pi} |e^{-\epsilon} e^{i\omega} - 1|^n e^{tf(\omega,\epsilon)} d\omega. \quad (3.5.27)$$

Next, we compute

$$\begin{aligned} |e^{-\epsilon} e^{i\omega} - 1| &= \sqrt{e^{-2\epsilon} - 2e^{-\epsilon} \cos \omega + 1} \\ &= \sqrt{(1 - e^{-\epsilon})^2 + 2e^{-\epsilon}(1 - \cos \omega)}. \end{aligned}$$

Employing the standard inequality $(a + b)^p \leq 2^{p-1}(a^p + b^p)$ for non-negative real numbers a, b and p together with $1 - \cos \omega \leq \frac{|\omega|^2}{2}$, we obtain the bound

$$|e^{-\epsilon} e^{i\omega} - 1|^n \leq 2^{\frac{n}{2}-1} (|1 - e^{-\epsilon}|^n + e^{-\frac{n\epsilon}{2}} |\omega|^n),$$

from which (3.5.26) readily follows. □

At times, it is convenient to split the exponents in (3.5.24)-(3.5.25) in a slightly different fashion. To this end, we introduce two auxiliary functions $g : \mathbb{Z} \times \mathbb{R} \times (0, \infty) \rightarrow \mathbb{R}$ and $q : \mathbb{R} \times (0, \infty)$ defined by

$$g(l, \epsilon, t) := -\epsilon l + t \sum_{k=-N}^N a_k (e^{-\mu_k \epsilon} - 1), \tag{3.5.28}$$

$$q(\epsilon, \omega) := \sum_{k=-N}^N a_k (\cos(\mu_k \omega) - 1) e^{-\mu_k \epsilon}. \tag{3.5.29}$$

This allows us to rewrite (3.5.24) and (3.5.25) in the form

$$P_l(\epsilon, t, n) = |1 - e^{-\epsilon}|^n e^{g(l, \epsilon, t)} \int_{-\pi}^{\pi} e^{tq(\epsilon, \omega)} d\omega, \tag{3.5.30}$$

$$R_l(\epsilon, t, n) = e^{-\frac{\epsilon n}{2}} e^{g(l, \epsilon, t)} \int_{-\pi}^{\pi} |\omega|^n e^{tq(\epsilon, \omega)} d\omega. \tag{3.5.31}$$

Note that g vanishes for $\epsilon = 0$, while q reduces to f . In the reminder of this subsection we provide several preliminary bounds for q and the integral expressions above.

Lemma 3.5.11. *Pick $n \in \mathbb{N}_0$, introduce two positive constants*

$$C_1 = C_1(n) = \int_{-\infty}^{\infty} u^n e^{-u^2} du, \quad C_2 = C_2(n) = n^{n/2} e^{-n/2} 2^{2-n/2} \tag{3.5.32}$$

and consider the functions

$$s_{n,\nu}(x, t) = |x|^n e^{-\nu t x^2},$$

together with the sequences

$$x_k^t = \frac{k}{t} + b$$

for any $b \in \mathbb{R}$. Then the following claims hold.

(i) For any $t > 0$ and $\nu > 0$ we have

$$\int_{-\infty}^{\infty} s_{n,\nu}(x, t) dx \leq C_1 t^{-\frac{n+1}{2}} \nu^{-\frac{n+1}{2}}.$$

(ii) For any $t > 0$ and $\nu > 0$ the series $\sum_{k \in \mathbb{Z}} s_n(x_k^t, t)$ converges and we have the upper bound

$$\sum_{k \in \mathbb{Z}} s_{n,\nu}(x_k^t, t) \leq C_1 t^{-\frac{n-1}{2}} \nu^{-\frac{n+1}{2}} + C_2 t^{-\frac{n}{2}} \nu^{-\frac{n}{2}}. \quad (3.5.33)$$

(iii) For any $t > 0$, $\nu > 0$ and $K_0 > 0$ we have the tail bound

$$\sum_{|x_k^t| \geq K_0} s_{n,\nu}(x_k^t, t) \leq \left(2 + \frac{2\sqrt{t}}{\sqrt{\nu}}\right) e^{-\nu t K_0^2}. \quad (3.5.34)$$

Proof. Item ((i)) follows directly after substituting $u = \sqrt{\nu t}x$ and observing that for every $n \geq 0$ we have $C_1(n) < \infty$. To prove item ((ii)), we first note that the function $x \mapsto s_{n,\nu}(x, t)$ is symmetric around 0, increasing on the interval $[0, \frac{\sqrt{n}}{\sqrt{2\nu t}}]$ and decreasing on $[\frac{\sqrt{n}}{\sqrt{2\nu t}}, \infty)$. Choosing integers N_1, N_2 and M in such a way that

$$-\frac{\sqrt{n}}{\sqrt{2\nu t}} \in [x_{N_1}^t, x_{N_1+1}^t], \quad \frac{\sqrt{n}}{\sqrt{2\nu t}} \in [x_{N_2}^t, x_{N_2+1}^t], \quad 0 \in [x_M^t, x_{M+1}^t],$$

we can hence write

$$\begin{aligned} \sum_{k \in \mathbb{Z}} s_{n,\nu}(x_k, t) &= \sum_{k=-\infty}^{N_1-1} \frac{1}{x_{k+1}^t - x_k^t} \int_{x_k^t}^{x_{k+1}^t} s_{n,\nu}(x_k^t, t) dx \\ &\quad + \sum_{k=N_1+2}^M \frac{1}{x_k^t - x_{k-1}^t} \int_{x_{k-1}^t}^{x_k^t} s_{n,\nu}(x_k^t, t) dx \\ &\quad + \sum_{k=M+1}^{N_2-1} \frac{1}{x_{k+1}^t - x_k^t} \int_{x_k^t}^{x_{k+1}^t} s_{n,\nu}(x_k^t, t) dx \\ &\quad + \sum_{k=N_2+2}^{\infty} \frac{1}{x_k^t - x_{k-1}^t} \int_{x_{k-1}^t}^{x_k^t} s_{n,\nu}(x_k^t, t) dx \\ &\quad + s_{n,\nu}(x_{N_1}^t, t) + s_{n,\nu}(x_{N_1+1}^t, t) + s_{n,\nu}(x_{N_2}^t, t) + s_{n,\nu}(x_{N_2+1}^t, t). \end{aligned}$$

Noting that $x_{k+1}^t - x_k^t = 1/t$ and recalling ((i)), we find

$$\begin{aligned} \sum_{k \in \mathbb{Z}} s_{n,\nu}(x_k, t) &\leq t \int_{-\infty}^{x_{N_1}^t} s_{n,\nu}(x, t) dx + t \int_{x_{N_2}^t}^{\infty} s_{n,\nu}(x, t) dx + 4s_{n,\nu}(\sqrt{n}/\sqrt{2\nu t}) \\ &\leq C_1 t^{-\frac{n-1}{2}} \nu^{-\frac{n+1}{2}} + C_2 t^{-\frac{n}{2}} \nu^{-\frac{n}{2}}. \end{aligned}$$

This proves (3.5.33), as desired.

For ((iii)), we first choose integers N_1 and N_2 in such a way that

$$-K_0 \in [x_{N_1}^t, x_{N_1+1}^t], \quad K_0 \in [x_{N_2-1}^t, x_{N_2}^t].$$

Using the fact that $x \mapsto s_{0,\nu}(x, t)$ is even and decreasing on $[0, \infty)$, we compute

$$\begin{aligned} \sum_{|x_k^t| \geq K_0}^N s_{0,\nu}(x_k^t, t) &\leq s_{0,\nu}(x_{N_1}^t) + s_{0,\nu}(x_{N_2}^t) + 2t \int_{K_0}^{\infty} e^{-\nu tx^2} dx \\ &\leq 2s_{0,\nu}(K_0) + 2\frac{\sqrt{t}}{\sqrt{\nu}} \int_{\sqrt{\nu t}K_0}^{\infty} e^{-u^2} du. \end{aligned}$$

The desired estimate now follows from the Chernoff bound, which states that $\operatorname{erfc}(x) \leq e^{-x^2}$ holds for all $x > 0$ (see [19, 21]). \square

Lemma 3.5.12. *Consider the setting of Theorem 3.5.1 and pick $0 < \delta < \frac{\Lambda}{2}$. Then there exist positive constants $\bar{\epsilon}$, \bar{m} and $\bar{\kappa}$ such that the following statements hold.*

(i) *For all $\epsilon \in [-\bar{\epsilon}, \bar{\epsilon}]$ we have*

$$q(\epsilon, \omega) \leq -\left(\frac{\Lambda}{2} - \delta\right) \omega^2, \quad \omega \in [-\bar{\kappa}, \bar{\kappa}], \quad (3.5.35)$$

$$q(\epsilon, \omega) \leq -\bar{m}, \quad \omega \in [-\pi, -\bar{\kappa}] \cup [\bar{\kappa}, \pi]. \quad (3.5.36)$$

(ii) *Pick $n \in \mathbb{N}_0$ and recall the constant $C_1 = C_1(n)$ from (3.5.32). Then the estimate*

$$\int_{-\pi}^{\pi} |\omega|^n e^{tq(\epsilon, \omega)} d\omega \leq C_1 t^{-\frac{n+1}{2}} \left(\frac{\Lambda - 2\delta}{2}\right)^{-\frac{n+1}{2}} + \frac{2\pi^{n+1}}{n+1} e^{-\bar{m}t}$$

holds for all $t > 0$ and $\epsilon \in [-\bar{\epsilon}, \bar{\epsilon}]$. In particular, for $n = 0$ we have

$$\int_{-\pi}^{\pi} e^{tq(\epsilon, \omega)} d\omega \leq \frac{\sqrt{2\pi}}{\sqrt{t(\Lambda - 2\delta)}} + 2\pi e^{-\bar{m}t}. \quad (3.5.37)$$

Proof. To prove item ((i)), we start by defining an auxiliary function $\bar{q}(\epsilon, \omega) = q(\epsilon, \omega) + \left(\frac{\Lambda}{2} - \delta\right) \omega^2$, which satisfies

$$\bar{q}(\epsilon, 0) = \bar{q}_{\omega}(\epsilon, 0) = 0, \quad \bar{q}_{\omega\omega}(\epsilon, 0) = -\sum_{k=-N}^N a_k \mu_k^2 e^{-\mu_k \epsilon} + \Lambda - 2\delta. \quad (3.5.38)$$

Recalling the definition (3.5.4) and exploiting continuity, there exists $\bar{\epsilon} > 0$ such that

$$-\sum_{k=-N}^N a_k \mu_k^2 e^{-\mu_k \epsilon} < -\Lambda + \delta, \quad \text{for all } \epsilon \in [-\bar{\epsilon}, \bar{\epsilon}],$$

and consequently

$$\bar{q}_{\omega\omega}(\epsilon, 0) \leq -\delta < 0, \quad \text{for all } \epsilon \in [-\bar{\epsilon}, \bar{\epsilon}].$$

Combining this bound with (3.5.38) allows us to find $\bar{\kappa} > 0$ such that $\bar{q}(\epsilon, \omega) \leq 0$ for all $\omega \in [-\bar{\kappa}, \bar{\kappa}]$ and $\epsilon \in [-\bar{\epsilon}, \bar{\epsilon}]$ which proves (3.5.35). To establish (3.5.36), we note that assumption $(h\alpha)$ implies that there exists a constant $\bar{m} > 0$ such that

$$q(0, \omega) \leq -2\bar{m}, \text{ for } \omega \in [-\pi, -\bar{\kappa}] \cup [\bar{\kappa}, \pi].$$

Therefore, by possibly reducing $\bar{\epsilon}$ we can conclude that for $\epsilon \in [-\bar{\epsilon}, \bar{\epsilon}]$ and $\omega \in [-\pi, -\bar{\kappa}] \cup [\bar{\kappa}, \pi]$ we have $q(\epsilon, \omega) \leq -\bar{m}$, as desired.

To prove item $((ii))$ we use the bounds from (i) to compute

$$\int_{-\pi}^{\pi} |\omega|^n e^{tq(\epsilon, \omega)} d\omega \leq \int_{-\bar{\kappa}}^{\bar{\kappa}} |\omega|^n e^{-\frac{t}{2}(\Lambda - 2\delta)\omega^2} d\omega + 2 \int_{\bar{\kappa}}^{\pi} \omega^n e^{-\bar{m}t} d\omega.$$

We may now employ item $((i))$ from Lemma 3.5.11 with $\nu = \frac{\Lambda - 2\delta}{2}$ and explicitly evaluate the second integral to obtain the desired bound. \square

Corollary 3.5.13. *Consider the setting of Theorem 3.5.1 and pick $n \in N_0$. Then there exist constants $\bar{\epsilon} > 0$ and $C = C(n) > 0$ such that for all $t > 0$ and $\epsilon \in (-\bar{\epsilon}, \bar{\epsilon})$ we have the estimate*

$$\int_{-\pi}^{\pi} |\omega|^n e^{tq(\epsilon, \omega)} d\omega \leq C \min \left\{ 1, t^{-\frac{n+1}{2}} \right\}. \quad (3.5.39)$$

Proof. For $0 < t < 1$ the uniform bound follows from item $((i))$ of Lemma 3.5.12, which implies that $q(\epsilon, \omega) \leq 0$. On the other hand, we may apply item $((ii))$ from the same result with $\delta = \frac{\Lambda}{4}$ to find

$$\int_{-\pi}^{\pi} |\omega|^n e^{tq(\epsilon, \omega)} d\omega \leq C_1 2^{n+1} t^{-\frac{n+1}{2}} \Lambda^{-\frac{n+1}{2}} + \frac{2\pi^{n+1}}{n+1} e^{-\bar{m}t},$$

which can be absorbed into (3.5.39) on account of the fast decay of the exponential. \square

3.5.3 Global and outer bounds

In this subsection we provide the proofs for Lemmas 3.5.4 and 3.5.5. In both cases the arguments proceed in a relatively direct fashion, exploiting the bound (3.5.26).

Proof of Lemma 3.5.4. Picking $\epsilon = 0$, we see that P and g vanish, which in view of (3.5.26) and Corollary 3.5.13 implies the desired bound

$$|[\partial^n M(t)]_l| \leq \frac{2^{n/2}}{2\pi} \int_{-\pi}^{\pi} |\omega|^n e^{tq(0, \omega)} d\omega \leq \frac{2^{n/2} C}{4\pi} \min \left\{ 1, t^{-\frac{n+1}{2}} \right\}.$$

\square

Proof of Lemma 3.5.5. Consider the constant $\bar{\epsilon} > 0$ introduced in Lemma 3.5.12, which guarantees that $q(\bar{\epsilon}, \cdot) \leq 0$ and $q(-\bar{\epsilon}, \cdot) \leq 0$. In view of the bound (3.5.26) and

the representation (3.5.30)-(3.5.31), it suffices to show that there exist $K > |a \cdot \mu|$ and $C > 0$ so that

$$\sum_{l \geq (K-a \cdot \mu)t} (1+l)e^{g(l, \bar{\epsilon}, t)} < Ce^{-t}, \quad \sum_{l \leq -(K-a \cdot \mu)t} (1+|l|)e^{g(l, -\bar{\epsilon}, t)} \leq Ce^{-t}. \quad (3.5.40)$$

Focusing on the former, we pick

$$K > 1 + |a \cdot \mu| + 2\bar{\epsilon}^{-1} \left[2 + \sum_{k=-N}^N |a_k| \right],$$

which allows us to compute

$$\begin{aligned} g(l, \bar{\epsilon}, t) &= -\frac{1}{2}\bar{\epsilon}l - \frac{1}{2}\bar{\epsilon}l + t \sum_{k=-N}^N a_k (e^{-\mu_k \bar{\epsilon}} - 1), \\ &\leq -\frac{1}{2}\bar{\epsilon}l - t \left[\frac{1}{2}\bar{\epsilon}(K - a \cdot \mu) - \sum_{k=-N}^N a_k (e^{-\mu_k \bar{\epsilon}} - 1) \right] \\ &\leq -\frac{1}{2}\bar{\epsilon}l \end{aligned}$$

for all $l \geq (K - a \cdot \mu)t$ and $t > 0$. Using $te^{-t} \leq 1$, this in turn yields

$$\begin{aligned} \sum_{l \geq (K-a \cdot \mu)t} (1+l)e^{g(l, \bar{\epsilon}, t)} &\leq 2 \sum_{l \geq (K-a \cdot \mu)t} l e^{-\frac{1}{2}\bar{\epsilon}l} \\ &\leq 2(1 - e^{-\frac{1}{2}\bar{\epsilon}})^{-2} [(K - a \cdot \mu)t + 1] e^{-\frac{1}{2}(K-a \cdot \mu)\bar{\epsilon}t} \\ &\leq 2(1 - e^{-\frac{1}{2}\bar{\epsilon}})^{-2} (K - a \cdot \mu)(t + 1)e^{-2t} \\ &\leq 4(1 - e^{-\frac{1}{2}\bar{\epsilon}})^{-2} (K - a \cdot \mu)e^{-t}. \end{aligned}$$

Here we used the bound

$$\sum_{l=l_*}^{\infty} l r^l = r \frac{d}{dr} \left(\sum_{l=l_*}^{\infty} r^l \right) = r \frac{d}{dr} \left(\frac{r^{l_*}}{1-r} \right) = \frac{l_* r^{l_*}}{1-r} + \frac{r^{l_*+1}}{(1-r)^2} \leq \frac{(l_* + 1)r^{l_*}}{(1-r)^2}$$

with $r = e^{-\frac{1}{2}\bar{\epsilon}}$ and $l_* = \lfloor (K - a \cdot \mu)t \rfloor$. The second inequality in (3.5.40) can be obtained in a similar fashion. \square

3.5.4 Core bounds

In this subsection we prove Lemmas 3.5.6, 3.5.7 and 3.5.8, which all deal with ℓ^1 -bounds on compact intervals. Recalling the characterization (3.5.30)-(3.5.31), we start by providing useful bounds for the exponent g when $|l/t + a \cdot \mu|$ is bounded. To obtain these estimates, we show that for compact sets of ϵ the function g can be controlled by an upwards parabola in ϵ .

Lemma 3.5.14. *Consider the setting of Theorem 3.5.1 and pick constants $\bar{\epsilon} > 0$ and $K > 0$. Let $\delta > 0$ be any number that satisfies*

$$\delta \geq \max \left\{ \frac{K}{2\bar{\epsilon}} - \frac{\Lambda}{2}, \frac{\bar{\epsilon}}{3}, \frac{1}{3} \sum_{k=-N}^N |a_k \mu_k^3| e^{|\mu_k| \bar{\epsilon}} \right\} \quad (3.5.41)$$

and write

$$\nu_\delta = \frac{1}{2(\Lambda + 2\delta)}. \quad (3.5.42)$$

Then for every pair $(l, t) \in \mathbb{Z} \times (0, \infty)$ with $|l/t + a \cdot \mu| \leq K$, the choice

$$\epsilon^* = \epsilon^*(l, t) = 2\nu_\delta \left(\frac{l}{t} + a \cdot \mu \right) \in [-\bar{\epsilon}, \bar{\epsilon}], \quad (3.5.43)$$

satisfies the inequality

$$g(\epsilon^*, l, t) \leq -\nu_\delta t \left(\frac{l}{t} + a \cdot \mu \right)^2. \quad (3.5.44)$$

Proof. By expanding the function g around $\epsilon = 0$, we obtain

$$g(\epsilon, l, t) = -\epsilon l + \left(-\epsilon a \cdot \mu + \frac{\Lambda}{2} \epsilon^2 - \frac{\epsilon^3}{6} \sum_{k=-N}^N a_k \mu_k^3 e^{-\mu_k \bar{\epsilon}} \right) t$$

for some $\tilde{\epsilon}$ with $|\tilde{\epsilon}| \leq |\epsilon|$, which we rewrite as

$$g(\epsilon, l, t) = -\epsilon l + \left(-\epsilon a \cdot \mu + \left(\frac{\Lambda}{2} + \delta \right) \epsilon^2 \right) t + \epsilon^2 \left(-\delta - \frac{\epsilon}{6} \sum_{k=-N}^N a_k \mu_k^3 e^{-\mu_k \tilde{\epsilon}} \right) t. \quad (3.5.45)$$

For any $\epsilon \in [-\bar{\epsilon}, \bar{\epsilon}]$, $l \in \mathbb{Z}$, $t > 0$ our condition on δ ensures that

$$g(\epsilon, l, t) \leq -\epsilon l + \left(-\epsilon a \cdot \mu + \left(\frac{\Lambda}{2} + \delta \right) \epsilon^2 \right) t = \frac{t}{4\nu_\delta} \left((\epsilon - \epsilon^*)^2 - (\epsilon^*)^2 \right),$$

since the last term in (3.5.45) is negative. It hence suffices to show that $|\epsilon^*| \leq \bar{\epsilon}$, but that follows directly from our assumption on δ . \square

Proof of Lemma 3.5.6. In view of Lemma 3.5.10 it suffices to show that

$$\sum_{|l/t+a \cdot \mu| \leq K} P_l(\epsilon^*, t, n) \leq Ct^{-\frac{n}{2}}, \quad \sum_{|l/t+a \cdot \mu| \leq K} R_l(\epsilon^*, t, n) \leq Ct^{-\frac{n}{2}}, \quad t \geq 1$$

for some constant $C > 0$. Here we make the choice $\epsilon^* = \epsilon^*(l, t)$ as defined by (3.5.43) in Lemma 3.5.14, using the value $\bar{\epsilon} > 0$ that was introduced in Lemma 3.5.12, together with an arbitrary $\delta > 0$ that satisfies (3.5.46). Without loss, we make the further restriction $\bar{\epsilon} < 1$, which allows us to write $|1 - e^{-\epsilon^*}| \leq 2|\epsilon^*|$. We will provide the proof only for P , noting that the estimate for R can be derived analogously.

The bound (3.5.44) allows us to compute

$$P_l(\epsilon^*, t, n) \leq 2^n |\epsilon^*|^n e^{-\nu_\delta t(l/t+a \cdot \mu)^2} \int_{-\pi}^{\pi} e^{tq(\epsilon^*, \omega)} d\omega,$$

which in combination with Corollary 3.5.13 yields

$$\begin{aligned} P_l(\epsilon^*, t, n) &\leq C(n) 2^n t^{-\frac{1}{2}} |\epsilon^*|^n e^{-\nu_\delta t(l/t+a \cdot \mu)^2} \\ &\leq C(n) 4^n t^{-\frac{1}{2}} \nu_\delta^n (l/t + a \cdot \mu)^n e^{-\nu_\delta t(l/t+a \cdot \mu)^2}. \end{aligned}$$

Applying item ((ii)) from Lemma 3.5.11 with $\nu = \nu_\delta$ now yields the desired estimate, upon redefining C . \square

Proof of Lemma 3.5.7. Our goal is to exploit the representations (3.5.10) for $n = 0$ and (3.5.30) to obtain the estimate

$$|M_l(t)| \leq \frac{1}{2\pi} e^{g(l, \epsilon^*, t)} \int_{-\pi}^{\pi} e^{tq(\epsilon^*, \omega)} d\omega,$$

where we again use the values $\epsilon^* = \epsilon^*(l, t)$ defined by (3.5.43) in Lemma 3.5.14, but now picking $0 < \delta < \Lambda/2$ to be small enough to ensure that

$$\sqrt{\frac{\Lambda + 2\delta}{\Lambda - 2\delta}} \leq 1 + \frac{\kappa}{2} \tag{3.5.46}$$

holds. In order to validate the condition (3.5.41) with $K := K_*/\sqrt{T}$, we pick a sufficiently large $T > 0$ and decrease the value of $\bar{\epsilon} > 0$ from Lemma 3.5.12 to ensure that

$$\frac{K_*}{2\sqrt{T}\bar{\epsilon}} - \frac{\Lambda}{2} < 0 < \delta, \quad \frac{\bar{\epsilon}}{3} \sum_{k=-N}^N |a_k \mu_k^3| e^{|\mu_k|\bar{\epsilon}} \leq \delta \tag{3.5.47}$$

both hold. Combining (3.5.37) and (3.5.44) and writing $x_l^t = l/t + a \cdot \mu$, we hence obtain

$$|M_l(t)| \leq \frac{1}{2\pi} e^{-\nu_\delta t(x_l^t)^2} \left[\frac{\sqrt{2\pi}}{\sqrt{t}\sqrt{\Lambda - 2\delta}} + 2\pi e^{-\bar{m}t} \right]$$

whenever $|x_l^t| \leq K_*/\sqrt{t}$ and $t \geq T$. Applying item ((ii)) of Lemma 3.5.11 with $n = 0$ and $\nu = \nu_\delta$, we now compute

$$\begin{aligned} \sum_{|x_l^t| \leq \frac{K_*}{\sqrt{t}}} |M_l(t)| &\leq \frac{1}{2\pi} \left(4 + \sqrt{2t\pi}\sqrt{\Lambda + 2\delta} \right) \left[\frac{\sqrt{2\pi}}{\sqrt{t}\sqrt{\Lambda - 2\delta}} + 2\pi e^{-\bar{m}t} \right] \\ &\leq \sqrt{\frac{\Lambda + 2\delta}{\Lambda - 2\delta}} + \frac{2\sqrt{2}}{\sqrt{\pi t(\Lambda - 2\delta)}} + e^{-\bar{m}t} \left(4 + \sqrt{2t}\sqrt{\pi}\sqrt{\Lambda + 2\delta} \right) \end{aligned} \tag{3.5.48}$$

for all $t \geq T$. The first term is smaller than $1 + \frac{\kappa}{2}$ while the rest can be made smaller than $\frac{\kappa}{2}$ by further increasing T if needed. \square

Lemma 3.5.15. *Consider the setting of Theorem 3.5.1. Then there exist constants $\bar{\epsilon} > 0$ and $C > 0$ such that for any sufficiently large $K > 0$ we have the estimate*

$$|M_l(t)| \leq C \min\{1, t^{-1/2}\} e^{-\bar{\epsilon}t|l/t + a \cdot \mu|^2/(8K)} \tag{3.5.49}$$

whenever $|l/t + a \cdot \mu| \leq K$.

Proof. We first fix $\bar{\epsilon} > 0$ as provided in Corollary 3.5.13 and consider an arbitrary $K > 0$. Writing

$$\delta = \frac{K}{2\bar{\epsilon}} - \frac{\Lambda}{2}, \quad \nu_\delta = \frac{\bar{\epsilon}}{8K}$$

we see that condition (3.5.41) is satisfied provided that K is sufficiently large. Recalling the notation $x_l^t = l/t + a \cdot \mu$, we may again exploit (3.5.10), (3.5.30), (3.5.39) and (3.5.44) to obtain the desired estimate

$$|M_l(t)| \leq \frac{1}{2\pi} e^{g(l, \epsilon^*, t)} \int_{-\pi}^{\pi} e^{tq(\epsilon^*, \omega)} d\omega \leq \frac{C}{2\pi} \min\{1, t^{-1/2}\} e^{-\nu_\delta t(x_l^t)^2}$$

whenever $|x_l^t| \leq K$. \square

Proof of Lemma 3.5.8. Recalling the notation $x_l^t = l/t + a \cdot \mu$, we apply (3.5.34) with $\nu = \frac{\bar{\epsilon}}{8K}$ and $K_0 = K/\sqrt{t}$ to the estimate (3.5.49), which allows us to compute

$$\begin{aligned} \sum_{\frac{K}{\sqrt{t}} \leq |x_l^t| \leq K} |M_l(t)| &\leq C \min\{1, t^{-1/2}\} \sum_{|x_l^t| \geq \frac{K}{\sqrt{t}}} e^{-\nu t (x_l^t)^2} \\ &\leq C \min\{1, t^{-1/2}\} \left[2 + 4 \frac{\sqrt{2Kt}}{\sqrt{\bar{\epsilon}}} \right] e^{-\bar{\epsilon}K/8} \\ &\leq C \left[2 + 4 \frac{\sqrt{2K}}{\sqrt{\bar{\epsilon}}} \right] e^{-\bar{\epsilon}K/8}. \end{aligned}$$

This can be made arbitrarily small by choosing K to be sufficiently large. \square

Proof of Lemma 3.5.9. Writing $x_l^t = l/t + a \cdot \mu$ and taking K as in Lemma 3.5.5, this result shows that it suffices to find a constant $C > 0$ so that

$$\sum_{|x_l^t| \leq K} |M_l(t)| |x_l^t| \leq C t^{-\frac{1}{2}}$$

holds for all $t > 0$. Writing $\nu = \frac{\bar{\epsilon}}{8K}$ and applying the bound (3.5.49) we find

$$\sum_{|x_l^t| \leq K} |M_l(t)| |x_l^t| \leq C \min\{1, t^{-1/2}\} \sum_{|x_l^t| \leq K} |x_l^t| e^{-\nu t (x_l^t)^2}.$$

The desired bound (3.5.4) now follows from an application of (3.5.33) with $n = 1$. \square

3.6 Phase approximation strategies

Throughout this paper, various LDEs of the form $\dot{\theta} = \Theta(\theta)$ are considered, which can all be seen as approximations to the (asymptotic) evolution of the phase $\gamma(t)$ defined in (3.2.26). Our main purpose here is to explore the relationship between the various points of view and to obtain several key decay rates.

We proceed by introducing the standard shift operator $S : \ell^\infty(\mathbb{Z}) \mapsto \ell^\infty(\mathbb{Z})$ that acts as

$$[S\theta]_l = \theta_{l+1}.$$

This allows us to represent the (k) -th discrete derivative (3.5.7) in the convenient form

$$\begin{aligned} \partial^{(k)}\theta &= (S - I)^k \theta = (S^{k-1} + \dots + S + I)(S - I)\theta \\ &= (S^{k-1} + \dots + S + I)\partial\theta. \end{aligned} \tag{3.6.1}$$

Recalling the shifts σ_ν introduced in (3.2.17), we also define the first-difference operators

$$\begin{aligned} \pi_\nu^\diamond \theta &= (S^{\sigma_\nu} - I)\theta, \quad \nu \in \{1, 2, 3, 4\}, \\ \pi_{\nu \oplus \nu'}^\diamond \theta &= (S^{\sigma_\nu + \sigma_{\nu'}} - I)\theta, \quad \nu, \nu' \in \{1, 2, 3, 4\}, \end{aligned} \tag{3.6.2}$$

together with their second-difference counterparts

$$\pi_{\nu\nu'}^{\diamond\diamond} \theta = \pi_{\nu'}^\diamond \pi_\nu^\diamond \theta = (S^{\sigma_{\nu'}} - I)(S^{\sigma_\nu} - I)\theta, \quad \nu, \nu' \in \{1, 2, 3, 4\}. \tag{3.6.3}$$

These can be expanded as first differences by means of the useful identity

$$\pi_{\nu\nu'}^\diamond\theta = \pi_{\nu\oplus\nu'}^\diamond\theta - \pi_\nu^\diamond\theta - \pi_{\nu'}^\diamond\theta. \quad (3.6.4)$$

For convenience, we also introduce the shorthands

$$\pi_{l;\nu}^\diamond\theta = [\pi_\nu^\diamond\theta]_l, \quad \pi_{l;\nu\oplus\nu'}^\diamond\theta = [\pi_{\nu\oplus\nu'}^\diamond\theta]_l, \quad \pi_{l;\nu\nu'}^\diamond\theta = [\pi_{\nu\nu'}^\diamond\theta]_l$$

for $\nu, \nu' \in \{1, 2, 3, 4\}$.

All the nonlinearities that we consider share a common linearization, which using (3.6.4) and the definitions (3.2.19) can be represented in the equivalent forms

$$\begin{aligned} \mathcal{H}_{\text{lin}}[h] &= \sum_{\nu=1}^4 \alpha_{p;\nu}^\diamond \pi_\nu^\diamond h + \sum_{\nu,\nu'=1}^4 \alpha_{p;\nu\nu'}^\diamond \pi_{\nu\nu'}^\diamond h \\ &= \sum_{\nu=1}^4 \alpha_{p;\nu}^\diamond \alpha_{p;\nu}^\diamond \pi_\nu^\diamond h + \sum_{\nu,\nu'=1}^4 \alpha_{p;\nu\nu'}^\diamond (\pi_{\nu\oplus\nu'}^\diamond - \pi_\nu^\diamond - \pi_{\nu'}^\diamond) h \\ &= \sum_{k=-N}^N a_k (S^k - I) h. \end{aligned} \quad (3.6.5)$$

It is important to observe that the assumptions (HS)₁ and (HS)₂ guarantee that condition (h α) in §3.5 is satisfied. In particular, we will be able to exploit all the linear results obtained in that section.

Summation convention To make our notation more concise, we will use the Einstein summation convention whenever this is not likely to lead to ambiguities. This means that any Greek index that appears only on the right hand side of an equation is automatically summed. For example, the first line of (3.6.5) can be simplified as

$$\mathcal{H}_{\text{lin}}[h] = \alpha_{p;\nu}^\diamond \pi_\nu^\diamond h + \alpha_{p;\nu\nu'}^\diamond \pi_{\nu\nu'}^\diamond h. \quad (3.6.6)$$

‘Cole-Hopf’ nonlinearity Θ_{ch} We start by discussing the nonlinearity Θ_{ch} defined by (3.2.15), which for $d \neq 0$ is given by

$$[\Theta_{\text{ch}}(\theta)]_l = \frac{1}{d} \sum_{k=-N}^N a_k \left(e^{d(\theta_{l+k}(t) - \theta_l(t))} - 1 \right) + c_* t. \quad (3.6.7)$$

The key feature is that any solution to

$$\dot{\theta} = \Theta_{\text{ch}}(\theta) \quad (3.6.8)$$

can be used to construct a solution to the linear problem

$$\dot{h}(t) = \mathcal{H}_{\text{lin}}[h(t)] \quad (3.6.9)$$

by applying the Cole-Hopf transform

$$h(t) = e^{d(\theta(t) - c_* t)}. \quad (3.6.10)$$

This can be verified by a straightforward computation. Vice versa, any nonnegative solution to the linear LDE (3.6.10) yields a solution to (3.6.8) by writing

$$\theta(t) = \frac{\log h(t)}{d} + c_* t. \quad (3.6.11)$$

Our first main result uses this correspondence to establish bounds on the discrete derivatives of solutions to (3.6.8). In order to exploit the fact that this LDE is invariant under spatially homogeneous perturbations, we introduce the deviation seminorm

$$[\theta]_{\text{dev}} = \|\theta - \theta_0\|_{\ell^\infty} \quad (3.6.12)$$

for sequences $\theta \in \ell^\infty(\mathbb{Z})$. In view of (3.6.11), it is essential to ensure that h remains positive. This is where Proposition 3.5.2 comes into play, which requires us to impose a flatness condition on the initial condition $\theta(0)$. This was not needed for the corresponding result [52, Cor. 6.2], where the comparison principle could be exploited.

Proposition 3.6.1. *Assume that (Hg) , $(H\Phi)$, $(HS)_1$ and $(HS)_2$ all hold and fix a positive constant $R > 0$. Then there exist constants M and δ such that for any $\theta \in C^1([0, \infty); \ell^\infty(\mathbb{Z}))$ that satisfies the LDE (3.2.28) with $[\theta(0)]_{\text{dev}} < R$ and $\|\partial\theta(0)\|_{\ell^\infty} \leq \delta$, we have the estimates*

$$\left\| \partial^{(k)}\theta(t) \right\|_{\ell^\infty} \leq M \min \left\{ \|\partial\theta^0\|_{\ell^\infty}, t^{-\frac{k}{2}} \right\}, \quad k = 1, 2, 3. \quad (3.6.13)$$

Moreover, for any pair $(m, n) \in \mathbb{Z}^2$ there exists a constant $C = C(m, n, R)$ such that

$$\|n(S^m - I)\theta(t) - m(S^n - I)\theta(t)\|_{\ell^\infty} \leq C \min \left\{ \|\partial\theta^0\|_{\ell^\infty}, t^{-1} \right\}, \quad (3.6.14)$$

$$\|n\partial(S^m - I)\theta(t) - m\partial(S^n - I)\theta(t)\|_{\ell^\infty} \leq C \min \left\{ \|\partial\theta^0\|_{\ell^\infty}, t^{-\frac{3}{2}} \right\}. \quad (3.6.15)$$

‘Comparison’ nonlinearity Θ_{cmp} Upon introducing the quadratic expression

$$[\mathcal{Q}_{\text{cmp}}(\theta)]_l = \alpha_{q; \nu\nu'}^{\diamond\diamond} [\pi_{l; \nu}^{\diamond} \theta] [\pi_{l; \nu'}^{\diamond} \theta], \quad (3.6.16)$$

we are ready to define a new nonlinear function $\Theta_{\text{cmp}} : \ell^\infty(\mathbb{Z}) \rightarrow \ell^\infty(\mathbb{Z})$ that acts as

$$\Theta_{\text{cmp}}(\theta) = \mathcal{H}_{\text{lin}}[\theta] + \mathcal{Q}_{\text{cmp}}(\theta) + c_*. \quad (3.6.17)$$

This function plays an important role in §3.7 where we construct sub- and super solutions for (3.2.1) in order to exploit the comparison principle. Indeed, our choice (3.1.18) will generate terms in the super-solution residual that contain the factor

$$\begin{aligned} \mathcal{R}_\theta(t) &:= \dot{\theta}(t) - \Theta_{\text{cmp}}(\theta(t)) \\ &= \alpha_{p; \nu}^{\diamond} \pi_{\nu}^{\diamond} \theta(t) + \alpha_{p; \nu\nu'}^{\diamond\diamond} \pi_{\nu\nu'}^{\diamond\diamond} \theta(t) + \alpha_{q; \nu\nu'}^{\diamond\diamond} [\pi_{l; \nu}^{\diamond} \theta(t)] [\pi_{l; \nu'}^{\diamond} \theta(t)] + c_*. \end{aligned} \quad (3.6.18)$$

Since this difference does not have a sign that we can exploit, we need to absorb it into our remainder terms. This requires a decay rate of $\mathcal{R}_\theta(t) \sim t^{-3/2}$ or faster.

Obviously, we can achieve $\mathcal{R}_\theta = 0$ by choosing θ appropriately. However, the resulting LDE $\dot{\theta} = \Theta_{\text{cmp}}(\theta)$ is surprisingly hard to analyze due to the presence of the problematic quadratic terms, which precludes us from obtaining the desired $\partial\theta \sim t^{-1/2}$ decay rates in ℓ^∞ (rather than ℓ^2 , which is much easier).

This problem is circumvented by our choice to use (3.6.8) as the evolution for θ . Our second main result provides the necessary bounds on $\mathcal{R}_\theta(t)$ and two other related expressions. The main challenge here is to compare the quadratic terms in Θ_{cmp} and Θ_{ch} . In fact, our choice (3.2.23) for the parameter d is based on the necessity to neutralize the dangerous components that lead to $O(t^{-1})$ behaviour.

Proposition 3.6.2. *Consider the setting of Proposition 3.6.1. There exist constants M and δ such that for any $\theta \in C^1([0, \infty); \ell^\infty(\mathbb{Z}))$ that satisfies the LDE (3.6.8) with $[\theta(0)]_{\text{dev}} < R$ and $\|\partial\theta(0)\|_{\ell^\infty} \leq \delta$, we have the bound*

$$\|\mathcal{R}\theta(t)\|_{\ell^\infty} \leq M \min \left\{ \|\partial\theta(0)\|_{\ell^\infty}, t^{-\frac{3}{2}} \right\} \quad (3.6.19)$$

for all $t > 0$. In addition, for any $\nu \in \{1, 2, 3, 4\}$ and $t > 0$ we have

$$\left\| \pi_\nu^\diamond \dot{\theta}(t) - \sum_{\nu'=1}^4 \alpha_{p;\nu'}^\diamond \pi_{\nu'}^\diamond \theta(t) \right\|_{\ell^\infty} \leq M \min \left\{ \|\partial\theta(0)\|_{\ell^\infty}, t^{-\frac{3}{2}} \right\}, \quad (3.6.20)$$

while for any pair $\nu, \nu' \in \{1, 2, 3, 4\}$ and $t > 0$ we have

$$\left\| \pi_{\nu\nu'}^\diamond \dot{\theta}(t) \right\|_{\ell^\infty} \leq M \min \left\{ \|\partial\theta(0)\|_{\ell^\infty}, t^{-\frac{3}{2}} \right\}. \quad (3.6.21)$$

‘Discrete mean curvature’ nonlinearity Θ_{dmc} Recalling the sequences (A_k) and (B_k) together with the functions β_θ and Δ_θ defined in (3.1.24), we generalize the definition of \bar{c}_θ from (3.1.23) slightly by writing

$$[\tilde{c}_\theta]_l = \sum_{0 < |k| \leq N} C_k c_{\varphi_{l,k}(\theta)} \quad (3.6.22)$$

for a sequence (C_k) that must satisfy

$$\sum_{0 < |k| \leq N} C_k = 1, \quad \sum_{0 < |k| \leq N} k C_k = 0. \quad (3.6.23)$$

The corresponding generalization of the definition (3.2.30) for Θ_{dmc} is now given by

$$\tilde{\Theta}_{\text{dmc}}(\theta) = \kappa_H \frac{\Delta_\theta}{\beta_\theta^2} + \beta_\theta \tilde{c}_\theta, \quad (3.6.24)$$

which reduces to Θ_{dmc} in the special case $C_k = 1/(2N)$.

Our task here is to establish a slight generalization of Proposition 3.2.8 by analyzing the difference of $\tilde{\Theta}_{\text{dmc}}$ with Θ_{ch} . We achieve this by expanding the direction-dependent wavespeeds c_φ introduced in Lemma 3.2.4 in terms of the angle φ . In particular, we provide proofs for the explicit expressions stated in Lemma 3.2.5. This allows us to make the link with the identities (3.1.27) for the parameters κ_H and d .

3.6.1 Coefficient identities

Our results in this section strongly depend on the equivalence of the representations (3.2.23) for the parameter d . Our goal is to establish this equivalence by providing the proofs of Lemma 3.2.3 and Lemma 3.2.5. To set the stage, we recall the set of shifts

$$(\tau_1, \tau_2, \tau_3, \tau_4) = (\sigma_h, \sigma_v, -\sigma_h, -\sigma_v)$$

and their corresponding translation operators

$$[T_\nu h](\xi) = h(\xi + \tau_\nu), \quad \nu \in \{1, 2, 3, 4\}$$

that were defined in (3.2.13). This allows us to recast the direction-dependent travelling wave MFDE (3.2.22) in the convenient form

$$-c_\varphi \Phi'_\varphi(\xi) = \Phi(\xi + \tau_\nu \cos \varphi + \sigma_\nu \sin \varphi) - 4\Phi_\varphi(\xi) + g(\Phi_\varphi(\xi)), \quad (3.6.25)$$

which after linearization around Φ_φ gives rise to the linear operators

$$[\mathcal{L}^\varphi v](\xi) = c_\varphi v'(\xi) + v(\xi + \tau_\nu \cos \varphi + \sigma_\nu \sin \varphi) - 4v(\xi) + g'(\Phi_\varphi(\xi))v(\xi).$$

These should not be confused with their counterparts \mathcal{L}_ω defined in (3.2.10), agreeing only when $\varphi = \omega = 0$.

Proof of Lemma 3.2.3. In view of the definition (3.2.15) and the identity $\langle \Phi'_*, \psi_* \rangle = 1$, we have

$$\langle T_\nu \Phi'_*, \psi_* \rangle - \alpha_{p; \nu}^\diamond \langle \Phi'_*, \psi_* \rangle = \alpha_{p; \nu}^\diamond - \alpha_{p; \nu}^\diamond = 0,$$

for each fixed $\nu \in \{1, 2, 3, 4\}$, which implies that $T_\nu \Phi'_* - \alpha_{p; \nu}^\diamond \Phi'_* \in \mathcal{R}(\mathcal{L}_0)$ by Lemma 3.2.2. In particular, we can find a bounded C^1 -smooth function \bar{p}_ν^\diamond for which

$$\mathcal{L}_0[\bar{p}_\nu^\diamond + b\Phi'_*] = T_\nu \Phi'_* - \alpha_{p; \nu}^\diamond \Phi'_*$$

holds for any $b \in \mathbb{R}$. Setting $b = -\langle \bar{p}_\nu^\diamond, \psi_* \rangle$ we can construct our desired function p_ν^\diamond by writing $p_\nu^\diamond = \bar{p}_\nu^\diamond + b\Phi'_*$. The remaining functions $p_{\nu\nu'}^\diamond$ and $q_{\nu\nu'}^\diamond$ can be constructed analogously. \square

Proof of Lemma 3.2.5. To establish item ((i)), we introduce the function $\chi(\xi) := \xi \Phi'_*(\xi)$ and use the MFDE (3.6.25) at $\varphi = 0$ to compute

$$\begin{aligned} [\mathcal{L}_0 \chi](\xi) &= c_* \Phi'_*(\xi) + c_* \xi \Phi''_*(\xi) + (\xi + \tau_\nu) T_\nu \Phi'_*(\xi) - 4\xi \Phi'_*(\xi) + \xi g'(\Phi_*(\xi)) \Phi'_*(\xi) \\ &= c_* \Phi'_*(\xi) + T_\nu \Phi'_*(\xi) + \xi \frac{d}{d\xi} \left(c_* \Phi'_*(\xi) + \tau_\nu T_\nu \Phi_*(\xi) - 4\Phi_*(\xi) + g(\Phi_*(\xi)) \right) \\ &= c_* \Phi'_*(\xi) + \tau_\nu T_\nu \Phi'_*(\xi). \end{aligned}$$

We integrate this expression against the kernel element ψ_* and recall the definition of $\alpha_{p; \nu}^\diamond$ from Lemma 3.2.3 to obtain $c_* = -\tau_\nu \alpha_{p; \nu}^\diamond$, as claimed.

Turning to the other items, we differentiate the equation (3.6.25) with respect to φ . This yields

$$-[\partial_\varphi c_\varphi] \Phi'_\varphi(\xi) = [\mathcal{L}^\varphi \partial_\varphi \Phi_\varphi](\xi) + \Phi'_\varphi(\xi + \tau_\nu \cos \varphi + \sigma_\nu \sin \varphi) (-\tau_\nu \sin \varphi + \sigma_\nu \cos \varphi), \quad (3.6.26)$$

where we emphasize that differentiations with respect to the angle φ will always be denoted by ∂_φ . Evaluating (3.6.26) in $\varphi = 0$, we obtain

$$-[\partial_\varphi c_\varphi]_{\varphi=0} \Phi'_*(\xi) = [\mathcal{L}_0[\partial_\varphi \Phi_\varphi]_{\varphi=0}](\xi) + \sigma_\nu T_\nu \Phi'_*(\xi).$$

Integrating against the adjoint kernel element ψ_* , we may use the characterization (3.2.11) in combination with Lemma 3.2.3 to arrive at the explicit expression

$$-[\partial_\varphi c_\varphi]_{\varphi=0} = \sigma_\nu \langle T_\nu \Phi'_*, \psi_* \rangle = \sigma_\nu \alpha_{p;\nu}^\diamond$$

stated in (ii). Applying Lemma 3.2.3 once more, we subsequently obtain

$$\mathcal{L}_0[\partial_\varphi \Phi_\varphi]_{\varphi=0} = \sigma_\nu \alpha_{p;\nu}^\diamond \Phi'_* - \sigma_\nu [T_\nu \Phi'_*] = -\mathcal{L}_0(\sigma_\nu p_\nu^\diamond).$$

The Fredholm properties formulated in Lemma 3.2.1 hence imply

$$[\partial_\varphi \Phi_\varphi]_{\varphi=0} = -\sigma_\nu p_\nu^\diamond + b \Phi'_*,$$

where the coefficient b is given by

$$b = \langle [\partial_\varphi \Phi_\varphi]_{\varphi=0}, \psi_* \rangle + \sigma_\nu \langle p_\nu^\diamond, \psi_* \rangle.$$

This vanishes on account of the normalization choices in Lemmas 3.2.2 and 3.2.3, establishing (iv).

A further differentiation of (3.6.26) with respect to φ yields

$$\begin{aligned} -[\partial_\varphi^2 c_\varphi] \Phi'_\varphi(\xi) &= 2[\partial_\varphi c_\varphi] \partial_\varphi \Phi'_\varphi(\xi) + [\mathcal{L}^\varphi \partial_\varphi^2 \Phi_\varphi](\xi) \\ &\quad + 2\partial_\varphi \Phi'_\varphi(\xi + \tau_\nu \cos \varphi + \sigma_\nu \sin \varphi)(-\tau_\nu \sin \varphi + \sigma_\nu \cos \varphi) \\ &\quad + \Phi'_\varphi(\xi + \tau_\nu \cos \varphi + \sigma_\nu \sin \varphi)(-\tau_\nu \cos \varphi - \sigma_\nu \sin \varphi) \quad (3.6.27) \\ &\quad + \Phi''_\varphi(\xi + \tau_\nu \cos \varphi + \sigma_\nu \sin \varphi)(-\tau_\nu \sin \varphi + \sigma_\nu \cos \varphi)^2 \\ &\quad + g''(\Phi_\varphi(\xi))[\partial_\varphi \Phi_\varphi(\xi)]^2. \end{aligned}$$

Evaluating this in $\varphi = 0$ and integrating against the adjoint kernel element ψ_* , we obtain

$$\begin{aligned} -[\partial_\varphi^2 c_\varphi]_{\varphi=0} &= 2[\partial_\varphi c_\varphi]_{\varphi=0} \langle [\partial_\varphi \Phi'_\varphi]_{\varphi=0}, \psi_* \rangle + 2\sigma_\nu \langle T_\nu [\partial_\varphi \Phi'_\varphi]_{\varphi=0}, \psi_* \rangle \\ &\quad - \tau_\nu \langle T_\nu \Phi', \psi_* \rangle + \langle T_\nu \Phi''_*, \psi_* \rangle \sigma_\nu^2 + \langle g''(\Phi_*(\xi)) [\partial_\varphi \Phi_\varphi]_{\varphi=0}^2, \psi_* \rangle. \end{aligned}$$

Substituting the expressions from items (i), (ii) and (iv), we arrive at

$$\begin{aligned} -[\partial_\varphi^2 c_\varphi]_{\varphi=0} &= -2\sigma_\nu \alpha_{p;\nu}^\diamond \langle [\partial_\varphi \Phi'_\varphi]_{\varphi=0}, \psi_* \rangle + 2\sigma_\nu \langle T_\nu [\partial_\varphi \Phi'_\varphi]_{\varphi=0}, \psi_* \rangle + \langle T_\nu \Phi''_*, \psi_* \rangle \sigma_\nu^2 \\ &\quad - \tau_\nu \alpha_{p;\nu}^\diamond + \langle g''(\Phi_*) [\partial_\varphi \Phi_\varphi]_{\varphi=0}^2, \psi_* \rangle \\ &= 2\sigma_\nu \alpha_{p;\nu}^\diamond \langle \sigma_{\nu'} \frac{d}{d\xi} p_{\nu'}^\diamond, \psi_* \rangle - 2\sigma_\nu \sigma_{\nu'} \langle T_\nu \frac{d}{d\xi} p_{\nu'}^\diamond, \psi_* \rangle + \langle T_\nu \Phi''_*, \psi_* \rangle \sigma_\nu^2 \\ &\quad + c_* + \sigma_\nu \sigma_{\nu'} \langle g''(\Phi_*) p_{\nu'}^\diamond p_{\nu'}^\diamond, \psi_* \rangle \\ &= c_* - 2\sigma_\nu \sigma_{\nu'} \alpha_{q;\nu\nu'}^\diamond, \end{aligned}$$

which establishes (iii). Finally, items (v) and (vi) follow directly from Lemma 5.6 in [44] and the definition (3.2.19) for the coefficients (a_k) . \square

3.6.2 Quadratic comparisons

In order to establish the main results of this section we need to carefully examine the structure of the quadratic terms in our nonlinearities. As a preparation, we first confirm that the difference operators (3.6.2) and (3.6.3) can be appropriately bounded by the corresponding discrete derivatives.

Lemma 3.6.3. *There exist a constant $M > 0$ so that for any $\theta \in \ell^\infty(\mathbb{Z})$ and any $\nu, \nu', \nu'' \in \{1, 2, 3, 4\}$ we have the estimates*

$$\|\pi_\nu^\diamond \theta\|_{\ell^\infty} \leq M \|\partial \theta\|_{\ell^\infty}, \quad (3.6.28)$$

$$\|\pi_{\nu\nu'}^\diamond \theta\|_{\ell^\infty} \leq M \left\| \partial^{(2)} \theta \right\|_{\ell^\infty}, \quad (3.6.29)$$

$$\|\pi_\nu^\diamond [\pi_{\nu\nu'}^\diamond \theta(t)]\|_{\ell^\infty} \leq M \left\| \partial^{(3)} \theta \right\|_{\ell^\infty}, \quad (3.6.30)$$

$$\|\pi_\nu^\diamond [\pi_\nu^\diamond [\pi_{\nu\nu'}^\diamond \theta]]\|_{\ell^\infty} \leq M \left\| \partial^{(2)} \theta \right\|_{\ell^\infty} \|\partial \theta\|_{\ell^\infty}. \quad (3.6.31)$$

Proof. The first three bounds follow directly from the fact that the difference operators $\pi_{;\nu}^\diamond$ can all be represented in the form

$$\pi_{;\nu} = S^{-\max\{|\sigma_h|, |\sigma_v|\}} P_\nu(S)(S - I)$$

for appropriate polynomials P_ν . The final bound follows from the product rule

$$(S^n - I)[\theta_1 \theta_2] = [S^n \theta_1](S^n - I)\theta_2 + [(S^n - I)\theta_1]\theta_2$$

which holds for all $\theta_1, \theta_2 \in \ell^\infty(\mathbb{Z})$. \square

We proceed with our analysis by providing an explicit formula for the operators $S^m - I$, which isolates the terms for which only a single discrete derivative ∂ can be factored out. This leads naturally to the crucial bounds (3.6.33), which will allow us to extract additional decay from suitably combined first-difference operators.

Lemma 3.6.4. *For any integer $m \geq 1$ we have the identities*

$$\begin{aligned} (S^m - I) &= (S - I)^2 \sum_{k=0}^{m-2} (m - k - 1) S^k + m(S - I), \\ (S^{-m} - I) &= -(S - I)^2 \sum_{k=0}^{m-2} (m - k - 1) S^{k-m} - mS^{-m}(S - I). \end{aligned} \quad (3.6.32)$$

Proof. We only consider the first identity, noting that the second one follows readily from the computation

$$S^{-m} - I = -S^{-m}(S^m - I).$$

For $m = 1$ the claim follows trivially, while for $m = 2$ we have $(S^2 - I) = (S^2 - 2S + I) + 2(S - I)$. Assuming that (3.6.32) holds for all k up to some $m \geq 2$, we compute

$$\begin{aligned} (S^{m+1} - I) &= S(S^m - I) + (S - I) \\ &= (S - I)^2 \sum_{k=0}^{m-2} (m - k - 1) S^{k+1} + mS(S - I) + (S - I) \\ &= (S - I)^2 \sum_{k=1}^{m-1} (m - k) S^k + mS(S - I) + (S - I). \end{aligned}$$

Adding and subtracting $m(S - I)^2$ results in the desired identity

$$(S^{m+1} - I) = (S - I)^2 \sum_{k=0}^{m-1} (m - k)S^k + (m + 1)(S - I).$$

□

Corollary 3.6.5. *Pick a pair $(m, n) \in \mathbb{Z}^2$. Then there exists a constant $C = C(m, n) > 0$ so that for any $\theta \in \ell^\infty(\mathbb{Z})$ we have the bounds*

$$\begin{aligned} \|n(S^m - I)\theta - m(S^n - I)\theta\|_{\ell^\infty} &\leq C \|\partial^{(2)}\theta\|_{\ell^\infty}, \\ \|n^2[(S^m - I)\theta]^2 - m^2[(S^n - I)\theta]^2\|_{\ell^\infty} &\leq C \|\partial^{(2)}\theta\|_{\ell^\infty} \|\partial\theta\|_{\ell^\infty}, \end{aligned} \quad (3.6.33)$$

where the squares are evaluated in a pointwise fashion.

Proof. To establish the first bound, we assume without loss that $m > 0$ and set out to exploit the identities (3.6.32). The key observation is that all terms featuring an $(S - I)^2$ factor can be absorbed by the stated bound. If also $n > 0$, then the remaining terms involving $(S - I)$ factors cancel. If $n < 0$, then we compute

$$nm(S - I) - mnS^n(S - I) = nm(I - S^n)(S - I),$$

which can be written as a sum of (shifted) second-differences. The second bound now follows directly from the standard factorization $a^2 - b^2 = (a + b)(a - b)$. □

The bounds above can be used to reduce the mixed products appearing in the definition (3.6.16) for \mathcal{Q}_{cmp} as a sum of pure squares. Inspired by (3.6.4) and the identity $2ab = (a + b)^2 - a^2 - b^2$, we introduce the expression

$$\mathcal{Q}_{\text{cmp};I}(\theta) = \frac{1}{2} \alpha_{q;\nu\nu'}^{\otimes} \left([\pi_{\nu \oplus \nu'} \theta]^2 - [\pi_\nu \theta]^2 - [\pi_{\nu'} \theta]^2 \right). \quad (3.6.34)$$

Lemma 3.6.6. *Consider the setting of Proposition 3.6.1. Then there exists $C > 0$ so that for any $\theta \in \ell^\infty(\mathbb{Z})$ we have the bound*

$$\|\mathcal{Q}_{\text{cmp}}(\theta) - \mathcal{Q}_{\text{cmp};I}(\theta)\|_{\ell^\infty} \leq C \|\partial\theta\|_{\ell^\infty} \left\| \partial^{(2)}\theta \right\|_{\ell^\infty}. \quad (3.6.35)$$

Proof. We fix the pair (ν, ν') and use the relation (3.6.4) to write

$$\begin{aligned} [\pi_\nu \theta][\pi_{\nu'} \theta] &= \frac{1}{2} [(\pi_\nu \theta + \pi_{\nu'} \theta)^2 - [\pi_\nu \theta]^2 - [\pi_{\nu'} \theta]^2] \\ &= \frac{1}{2} [(\pi_{\nu \oplus \nu'} \theta - \pi_{\nu\nu'} \theta)^2 - [\pi_\nu \theta]^2 - [\pi_{\nu'} \theta]^2]. \end{aligned}$$

In particular, we see that

$$\mathcal{Q}_{\text{cmp}}(\theta) - \mathcal{Q}_{\text{cmp};I}(\theta) = \frac{1}{2} \alpha_{q;\nu\nu'}^{\otimes} [\pi_{\nu\nu'} \theta] (\pi_{\nu\nu'} \theta - 2\pi_{\nu \oplus \nu'} \theta),$$

from which the bound is immediate by Lemma 3.6.3. □

Turning to Θ_{ch} , we introduce the quadratic expression

$$[\mathcal{Q}_{\text{ch}}(\theta)]_l = \frac{1}{2} \sum_{k=-N}^N a_k (\theta_{l+k} - \theta_l)^2$$

and note that $d\mathcal{Q}_{\text{ch}}(\theta)$ is the second-order term in the Taylor expansion of (3.6.7). Inserting the definitions (3.2.19) for the coefficients (a_k) , we see that

$$\mathcal{Q}_{\text{ch}}(\theta) = \frac{1}{2} \left(\alpha_{p;\nu\nu'}^{\diamond\diamond} ([\pi_{\nu\oplus\nu'}\theta]^2 - [\pi_{\nu}\theta]^2 - [\pi_{\nu'}\theta]^2) + \alpha_{p;\nu}^{\diamond} [\pi_{\nu}\theta]^2 \right), \quad (3.6.36)$$

which closely resembles the structure of (3.6.34). Indeed, in both cases the slowly-decaying terms can be isolated in a transparent fashion, using the coefficients

$$\beta_{\text{cmp}} = \sigma_{\nu}\sigma_{\nu'}\alpha_{q;\nu\nu'}^{\diamond\diamond}, \quad \beta_{\text{ch}} = \sigma_{\nu}\sigma_{\nu'}\alpha_{p;\nu\nu'}^{\diamond\diamond} + \frac{1}{2}\sigma_{\nu}^2\alpha_{p;\nu}^{\diamond}.$$

Lemma 3.6.7. *Consider the setting of Proposition 3.6.1. Then there exists $C > 0$ so that for any $\theta \in \ell^{\infty}(\mathbb{Z})$ we have the bound*

$$\left\| \mathcal{Q}_{\text{cmp};I}(\theta) - \beta_{\text{cmp}}(\partial\theta)^2 \right\|_{\ell^{\infty}} + \left\| \mathcal{Q}_{\text{ch}}(\theta) - \beta_{\text{ch}}(\partial\theta)^2 \right\|_{\ell^{\infty}} \leq C \|\partial\theta\|_{\ell^{\infty}} \left\| \partial^{(2)}\theta \right\|_{\ell^{\infty}}. \quad (3.6.37)$$

Proof. In view of (3.6.33) we have the bound

$$\left\| [\pi_{\nu\oplus\nu'}\theta]^2 - (\sigma_{\nu} + \sigma_{\nu'})^2 [\partial\theta]^2 \right\|_{\ell^{\infty}} + \left\| [\pi_{\nu}\theta]^2 - \sigma_{\nu}^2 [\partial\theta]^2 \right\|_{\ell^{\infty}} \leq C \|\partial\theta\|_{\ell^{\infty}} \left\| \partial^{(2)}\theta \right\|_{\ell^{\infty}},$$

which can be directly applied to the definitions (3.6.34) and (3.6.36) to obtain the desired estimate. \square

Lemma 3.2.5 shows that the ratio

$$\frac{\beta_{\text{cmp}}}{\beta_{\text{ch}}} = \frac{2 \sum_{\nu,\nu'=1}^4 \sigma_{\nu}\sigma_{\nu'}\alpha_{q;\nu\nu'}^{\diamond\diamond}}{\sum_{\nu=1}^4 \sigma_{\nu}^2\alpha_{p;\nu}^{\diamond} + 2 \sum_{\nu,\nu'=1}^4 \sigma_{\nu}\sigma_{\nu'}}$$

is exactly the value of the coefficient d defined in (3.2.23). In particular, combining (3.6.35) and (3.6.37) we see that

$$\left\| \mathcal{Q}_{\text{cmp}}(\theta) - d\mathcal{Q}_{\text{ch}}(\theta) \right\|_{\ell^{\infty}} \leq 3C \|\partial\theta\|_{\ell^{\infty}} \left\| \partial^{(2)}\theta \right\|_{\ell^{\infty}}, \quad (3.6.38)$$

which allows us to establish the following crucial bound.

Corollary 3.6.8. *Consider the setting of Proposition 3.6.1. Then there exists $C > 0$ so that for any $\theta \in \ell^{\infty}(\mathbb{Z})$ we have the bound*

$$\left\| \Theta_{\text{ch}}(\theta) - \Theta_{\text{cmp}}(\theta) \right\|_{\ell^{\infty}} \leq C e^{2N|d|} \|\partial\theta\|_{\ell^{\infty}} \left\| \partial\theta \right\|_{\ell^{\infty}}^3 + C \|\partial\theta\|_{\ell^{\infty}} \left\| \partial^{(2)}\theta \right\|_{\ell^{\infty}}. \quad (3.6.39)$$

Proof. For $d = 0$ we simply have

$$\Theta_{\text{ch}}(\theta) - \Theta_{\text{cmp}}(\theta) = 0.$$

For $d \neq 0$, we note that a Taylor expansion up to third order implies

$$\|\Theta_{\text{ch}}(\theta) - \mathcal{H}_{\text{lin}}[\theta] - d\mathcal{Q}_{\text{ch}}(\theta) - c_*\|_{\ell^\infty} \leq C e^{2N|d|} \|\partial\theta\|_{\ell^\infty} \|\partial\theta\|_{\ell^\infty}^3. \quad (3.6.40)$$

In view of (3.6.38), the desired bound now follows directly from the identity

$$\Theta_{\text{cmp}}(\theta) - \mathcal{H}_{\text{lin}}[\theta] - d\mathcal{Q}_{\text{ch}}(\theta) - c_* = \mathcal{Q}_{\text{cmp}}(\theta) - d\mathcal{Q}_{\text{ch}}(\theta).$$

□

We now turn to our final nonlinearity $\tilde{\Theta}_{\text{dmc}}$ and show that it can be expanded as

$$\begin{aligned} \tilde{\Theta}_{\text{dmc};I}(\theta) &= \sum_{0 < |k| \leq N} \left(\frac{2\kappa_H B_k}{k^2} - C_k \frac{[\partial_\varphi c_\varphi]_{\varphi=0}}{k} \right) (\theta_{l+k} - \theta_l) \\ &+ \sum_{0 < |k| \leq N} \frac{(A_k c_* + C_k [\partial_\varphi^2 c_\varphi]_{\varphi=0})}{2k^2} (\theta_{l+k} - \theta_l)^2 + c_*, \end{aligned} \quad (3.6.41)$$

up to third order in θ . This is more than sufficient to establish Proposition 3.2.8, but also allows the relation between the coefficients to be fully explored by the interested reader. For example, in the setting where $[\partial_\varphi c_\varphi]_{\varphi=0} \neq 0$, it is also possible to prescribe (B_k) and read-off the accompanying values for (A_k, C_k) . In any case, the conclusions of Proposition 3.2.8 are valid for any sequence (C_k) that satisfies (3.6.23).

Lemma 3.6.9. *For any sequence $(A_k, B_k, C_k)_{0 < |k| \leq N}$, there exists a constant $K > 0$ so that we have the bound*

$$\left\| \tilde{\Theta}_{\text{dmc}}(\theta) - \tilde{\Theta}_{\text{dmc};I}(\theta) \right\|_{\ell^\infty} \leq K \|\partial\theta\|_{\ell^\infty}^3. \quad (3.6.42)$$

Proof. Recalling the definitions (3.1.24), we first expand the terms β_θ and $\Delta_\theta/\beta_\theta^2$ as

$$\begin{aligned} [\beta_\theta]_l &= 1 + \sum_{0 < |k| \leq N} \frac{A_k}{2k^2} (\theta_{l+k} - \theta_l)^2 + O(\|\partial\theta\|_{\ell^\infty}^3), \\ \frac{[\Delta_\theta]_l}{[\beta_\theta^2]_l} &= \sum_{0 < |k| \leq N} \frac{2B_k}{k^2} (\theta_{l+k} - \theta_l) + O(\|\partial\theta\|_{\ell^\infty}^3). \end{aligned} \quad (3.6.43)$$

To find a corresponding representation for \tilde{c}_θ we first expand each individual term $c_{\varphi_{l;k}}(\theta)$ as

$$c_{\varphi_{l;k}}(\theta) = c_* + [\partial_\varphi c_\varphi]_{\varphi=0} \varphi_{l;k}(\theta) + \frac{1}{2} [\partial_\varphi^2 c_\varphi]_{\varphi=0} (\varphi_{l;k}(\theta))^2 + O(\varphi_{l;k}(\theta)^3). \quad (3.6.44)$$

Referring to Figure 3.1, we use the explicit formula

$$\tan \varphi_{l;k}(\theta) = -\frac{\theta_{l+k} - \theta_l}{k}$$

together with the expansion $\tan \varphi_{l;k}(\theta) = \varphi_{l;k}(\theta) + O(\varphi_{l;k}(\theta)^3)$ to obtain

$$[\tilde{c}_\theta]_l = c_* - [\partial_\varphi c_\varphi]_{\varphi=0} \sum_{0 < |k| \leq N} \frac{\theta_{l+k} - \theta_l}{k} + \frac{1}{2} [\partial_\varphi^2 c_\varphi]_{\varphi=0} \frac{(\theta_{l+k} - \theta_l)^2}{k^2} + O(\|\partial\theta\|_{\ell^\infty}^3),$$

which yields the desired statement. \square

Proof of Proposition 3.2.8. Recalling that our assumptions imply that $c_* \neq 0$ and $\kappa_H \neq 0$, we may write

$$\begin{aligned} A_k &:= \frac{da_k k^2}{c_*} - \frac{C_k [\partial_\varphi^2 c_\varphi]_{\varphi=0}}{c_*}, \\ B_k &:= \frac{a_k k^2}{2\kappa_H} + \frac{k C_k [\partial_\varphi c_\varphi]_{\varphi=0}}{2\kappa_H} \end{aligned} \tag{3.6.45}$$

for $0 < |k| \leq N$ and use (3.6.41) to conclude

$$\begin{aligned} \tilde{\Theta}_{\text{dmc};\text{I}}(\theta) &= \sum_{k=-N}^N a_k (\theta_{l+k} - \theta_l) + \sum_{k=-N}^N \frac{d}{2} a_k (\theta_{l+k} - \theta_l)^2 + c_* \\ &= \mathcal{H}_{\text{lin}}[\theta] + d\mathcal{Q}_{\text{ch}}(\theta) + c_*. \end{aligned}$$

In particular, the desired bound follows from (3.6.40) and (3.6.42).

It hence remains to check that our coefficients (3.6.45) satisfy the restrictions (3.1.25), which we will achieve under the general conditions (3.6.23). Employing item (vi) of Lemma 3.2.5 we compute

$$\sum_{0 < |k| \leq N} A_k = \frac{-d[\partial_\omega^2 \lambda_\omega]_{\omega=0} - [\partial_\varphi^2 c_\varphi]_{\varphi=0}}{c_*}.$$

This sum is equal to one if and only if the parameter d is chosen as in (3.2.23), which is by straightforward computation equivalent to the definition (3.1.27). In a similar fashion, we may use items (ii) and (vi) of Lemma 3.2.5 to compute

$$\sum_{0 < |k| \leq N} B_k = -\frac{[\partial_\omega^2 \lambda_\omega]_{\omega=0}}{2\kappa_H}, \quad \sum_{0 < |k| \leq N} \frac{B_k}{k} = \left(\sum_{0 < |k| \leq N} \frac{a_k k}{2\kappa_H} \right) + \frac{[\partial_\varphi c_\varphi]_{\varphi=0}}{2\kappa_H} = 0.$$

Setting the first sum equal to one leads to the choice (3.1.27) for κ_H . \square

3.6.3 Cole-Hopf transformation

We have now collected all the ingredients we need to exploit the Cole-Hopf transformation and establish Proposition 3.6.1. The main challenge is to pass difference operators through the relation (3.6.11). Proposition 3.6.2 subsequently follows in a relatively straightforward fashion from the bound (3.6.39).

Proof of Proposition 3.6.1. Since the function $\tilde{\theta}_l(t) = \theta_l(t) - \theta_0(0)$ also satisfies the first line of (3.2.28) and this spatially homogeneous shift is not seen by the difference operators in (3.6.13)-(3.6.15), we may assume without loss that $\theta_0(0) = 0$ and consequently $[\theta(0)]_{\text{dev}} = \|\theta(0)\|_{\ell^\infty} \leq R$. For $d = 0$, we can immediately apply Theorem 3.5.1 to function $h(t) := \theta(t) - c_*t$.

For $d \neq 0$, the initial condition $h(0) = e^{d\theta(0)}$ for the transformed system (3.6.9) satisfies the bounds

$$e^{-|d|R} \leq \inf_{l \in \mathbb{Z}} h_l(0) \leq \sup_{l \in \mathbb{Z}} h_l(0) \leq e^{|d|R}, \quad \|\partial h(0)\|_\infty \leq e^{|d|R} \delta.$$

We can no longer use the comparison principle to extend these bounds to all $t > 0$ as in [52]. Instead, we employ Proposition 3.5.2 with the choice $\varepsilon = e^{-2|d|R}/2$ to find $T = T(R)$ so that

$$\inf_{l \in \mathbb{Z}} h_l(t) \geq e^{-|d|R} - \varepsilon e^{|d|R} = \frac{1}{2} e^{-|d|R}$$

holds for all $t \geq T$. On the other hand, using the constant $C(T, \varepsilon)$ from Proposition 3.5.2 to write

$$\delta = \frac{e^{-2|d|R}}{2C(T, \varepsilon)} = \varepsilon/C(T, \varepsilon),$$

we see that (3.5.10) implies that also

$$\inf_{l \in \mathbb{Z}} h_l(t) \geq e^{-|d|R} - C(T, \varepsilon) e^{|d|R} \delta = \frac{1}{2} e^{-|d|R}$$

for all $0 \leq t \leq T$. This provides a uniform strictly positive lower bound for h that is essential for our estimates below.

Turning to (3.6.13), we pick $l \in \mathbb{Z}$ and use the intermediate value theorem to write

$$[\partial \theta(t)]_l = \frac{1}{d} \frac{[\partial h(t)]_l}{h_l^a(t)},$$

$$[\partial^{(2)} \theta(t)]_l = \frac{1}{d} \left(\frac{[\partial^{(2)} h(t)]_l}{h_l(t)} - \frac{[(S-I)h(t)]_l^2}{h_l^b(t)^2} - \frac{[(S^2-I)h(t)]_l^2}{2h_l^c(t)^2} \right),$$

together with

$$\begin{aligned} [\partial^{(3)} \theta(t)]_l &= \frac{1}{d} \left(\frac{[\partial^{(3)} h(t)]_l}{h_l(t)} + \frac{[(S^3-I)h(t)]_l^2 - 3[(S^2-I)h(t)]_l^2 + 3[(S-I)h(t)]_l^2}{2h_l(t)^2} \right) \\ &+ \frac{1}{d} \left(\frac{[(S^3-I)h(t)]_l^3}{6h_l^d(t)^3} + \frac{[(S^2-I)h(t)]_l^3}{6h_l^e(t)^3} + \frac{[(S-I)h(t)]_l^3}{6h_l^f(t)^3} \right) \end{aligned}$$

where we have the inclusions

$$\begin{aligned} \frac{1}{2} e^{-|d|R} &\leq \min_{n=0,1,2,3} \{h_{l+n}(t)\} \leq h_l^a(t), h_l^b(t), h_l^c(t), h_l^d(t), h_l^e(t), h_l^f(t) \\ &\leq \max_{n=0,1,2,3} \{h_{l+n}(t)\}. \end{aligned}$$

Applying Theorem 3.5.1, the desired bounds for $k = 1, 2$ follow directly, while for $k = 3$ it suffices to show that the term

$$\tilde{h}(t) = [(S^3 - I)h(t)]^2 - 3[(S^2 - I)h(t)]^2 + 3[(S - I)h(t)]^2 \quad (3.6.46)$$

satisfies $\|\tilde{h}(t)\|_{\ell^\infty} \leq Mt^{-3/2}$. In view of the decomposition

$$\tilde{h}(t) = [(S^3 - I)h(t)]^2 - 9[(S - I)h(t)]^2 - 3[(S^2 - I)h(t)]^2 - 4[(S - I)h(t)]^2$$

this follows from (3.6.33) and Theorem 3.5.1. The remaining estimates (3.6.14) and (3.6.15) now follow directly from (3.6.33). \square

Proof of Proposition 3.6.2. The first bound (3.6.19) follows directly by combining (3.6.39) with Proposition 3.6.1. To establish (3.6.20) we fix $\nu \in \{1, 2, 3, 4\}$ and exploit the definition (3.6.18) to compute

$$\begin{aligned} \pi_\nu^\diamond \dot{\theta}(t) - \sum_{\nu'=1}^4 \alpha_{p;\nu'}^\diamond \pi_{\nu'}^\diamond \theta(t) &= \pi_\nu^\diamond \mathcal{R}_\theta(t) + \sum_{\nu', \nu''=1}^4 \alpha_{p;\nu', \nu''}^\diamond \pi_\nu^\diamond [\pi_{\nu', \nu''}^\diamond \theta(t)] \\ &\quad + \sum_{\nu', \nu''=1}^4 \alpha_{q;\nu', \nu''}^\diamond \pi_\nu^\diamond [\pi_{\nu'}^\diamond \theta(t) \pi_{\nu''}^\diamond \theta(t)]. \end{aligned}$$

The desired bound now follows from Lemma 3.6.3 in combination with Proposition 3.6.1. In a similar fashion, the final bound (3.6.20) follows from the observation

$$\begin{aligned} \pi_{\nu\nu'}^\diamond \dot{\theta}(t) &= \pi_{\nu\nu'}^\diamond \mathcal{R}_\theta(t) + \sum_{\nu''=1}^4 \alpha_{p;\nu''}^\diamond \pi_{\nu\nu'}^\diamond [\pi_{\nu''}^\diamond \theta(t)] \\ &\quad + \sum_{\nu''', \nu''=1}^4 \alpha_{p;\nu'', \nu'''}^\diamond \pi_{\nu\nu'}^\diamond [\pi_{\nu''}^\diamond \pi_{\nu'''}^\diamond \theta(t)] \\ &\quad + \sum_{\nu''', \nu''=1}^4 \alpha_{q;\nu'', \nu'''}^\diamond \pi_{\nu\nu'}^\diamond [\pi_{\nu''}^\diamond \theta(t) \pi_{\nu'''}^\diamond \theta(t)]. \end{aligned}$$

\square

3.7 Construction of super- and sub-solutions

The main aim of this section is to construct explicit super- and sub-solutions for the discrete Allen-Cahn equation (3.2.4), using the function θ introduced in Theorem 3.2.9. To be more precise, for any $u \in C^1([0, \infty), \ell^\infty(\mathbb{Z}_\times^2))$ we define the residual

$$\mathcal{J}[u](t) = \dot{u}(t) - [\Delta^\times u(t)] - g(u(t))$$

and say that u is a super- respectively sub-solution for (3.2.4) if the inequality $\mathcal{J}[u]_{n,l}(t) \geq 0$, respectively $\mathcal{J}[u]_{n,l}(t) \leq 0$ holds for all $(n, l) \in \mathbb{Z}_\times^2$ and $t \geq 0$. Our construction utilizes the functions introduced in Lemma 3.2.3 together with the difference operators defined in (3.6.2) and (3.6.3). The main difference compared to our earlier work [52] and the PDE results in [69] is that a significant number of additional terms are needed to control the anisotropic effects caused by the misalignment of our wave with the underlying lattice.

Proposition 3.7.1. *Fix $R > 0$ and suppose that the assumptions (Hg) , $(H\Phi_*)$, $(HS)_1$ and $(HS)_2$ all hold. Then for any $\epsilon > 0$, there exist constants $\delta > 0$, $\nu > 0$ and C^1 -smooth functions*

$$z : [0, \infty) \rightarrow \mathbb{R}, \quad Z : [0, \infty) \rightarrow \mathbb{R}$$

so that for any $\theta^0 \in \ell^\infty(\mathbb{Z})$ with

$$[\theta^0]_{\text{dev}} < R, \quad \|\partial\theta^0\|_{\ell^\infty} < \delta$$

the following holds true.

- (i) Writing $\theta : [0, \infty) \rightarrow \ell^\infty(\mathbb{Z})$ for the solution to (3.2.28) with the initial condition $\theta(0) = \theta^0$, the function u^+ defined by

$$\begin{aligned} u_{n,l}^+(t) &= \Phi_*(n - \theta_l(t) + Z(t)) \\ &\quad + \pi_{l;\nu}^\diamond \theta(t) p_\nu^\diamond (n - \theta_l(t) + Z(t)) + \pi_{l;\nu\nu'}^\diamond \theta(t) p_{\nu\nu'}^\diamond (n - \theta_l(t) + Z(t)) \\ &\quad + \pi_{l;\nu}^\diamond \theta(t) \pi_{l;\nu'}^\diamond \theta(t) q_{\nu\nu'}^\diamond (n - \theta_l(t) + Z(t)) + z(t) \end{aligned} \quad (3.7.1)$$

is a super-solution of (3.2.1), while the function u^- defined by

$$\begin{aligned} u_{n,l}^-(t) &= \Phi_*(n - \theta_l(t) - Z(t)) \\ &\quad + \pi_{l;\nu}^\diamond \theta(t) p_\nu^\diamond (n - \theta_l(t) - Z(t)) + \pi_{l;\nu\nu'}^\diamond \theta(t) p_{\nu\nu'}^\diamond (n - \theta_l(t) - Z(t)) \\ &\quad + \pi_{l;\nu}^\diamond \theta(t) \pi_{l;\nu'}^\diamond \theta(t) q_{\nu\nu'}^\diamond (n - \theta_l(t) - Z(t)) - z(t) \end{aligned} \quad (3.7.2)$$

is a sub-solution of (3.2.1).

- (ii) We have $Z(0) = 0$ together with the bound $0 \leq Z(t) \leq \epsilon$ for all $t \geq 0$.

- (iii) We have the bound $0 \leq z(t) \leq \epsilon$ for all $t \geq 0$, together with the initial inequalities

$$z(0) - \delta \|p_\nu^\diamond\|_{L^\infty} - 2\delta \|p_{\nu\nu'}^\diamond\|_{L^\infty} - \delta^2 \|q_{\nu\nu'}^\diamond\|_{L^\infty} > \nu > 0. \quad (3.7.3)$$

- (iv) The asymptotic behaviour $z(t) = O(t^{-\frac{3}{2}})$ holds for $t \rightarrow \infty$.

In addition, the constants $\nu = \nu(\epsilon)$ satisfy $\lim_{\epsilon \downarrow 0} \nu(\epsilon) = 0$.

3.7.1 Preliminaries

Our proof of Proposition 3.7.1 focuses on the analysis of the super-solution residual $\mathcal{J}[u^+]$, since the sub-solution $\mathcal{J}[u^-]$ can be analyzed completely analogously. We start by splitting the residual into the five components

$$\mathcal{J}[u^+] = \mathcal{J}_\Phi + \mathcal{J}_{p_\nu^\diamond} + \mathcal{J}_{p_{\nu\nu'}^\diamond} + \mathcal{J}_{q_{\nu\nu'}^\diamond} + \mathcal{J}_{\text{glb}}. \quad (3.7.4)$$

The first four are closely related to the functions Φ_* , p_ν^\diamond , $p_{\nu\nu'}^\diamond$, and $q_{\nu\nu'}^\diamond$, respectively, depending on Z only through the variable

$$\xi_{n,l}(t) = n - \theta_l(t) + Z(t).$$

Indeed, we use the definitions

$$\begin{aligned}
[\mathcal{J}_\Phi(t)]_{n,l} &= -\Phi'_*(\xi_{n,l}(t))\dot{\theta}_l(t) - [\Delta^\times \Phi_*(\xi(t))]_{n,l}, \\
[\mathcal{J}_{p_\nu^\diamond}(t)]_{n,l} &= [\pi_{l;\nu}^\diamond \dot{\theta}(t)] p_\nu^\diamond(\xi_{n,l}(t)) - [\pi_{l;\nu}^\diamond \theta(t)] \frac{d}{d\xi} p_\nu^\diamond(\xi_{n,l}(t)) \dot{\theta}_l(t) \\
&\quad - [\Delta^\times [\pi_\nu^\diamond \theta(t)] p_\nu^\diamond(\xi(t))]_{n,l}, \\
[\mathcal{J}_{p_{\nu\nu'}^\diamond}(t)]_{n,l} &= [\pi_{l;\nu\nu'}^\diamond \dot{\theta}(t)] p_{\nu\nu'}^\diamond(\xi_{n,l}(t)) - \dot{\theta}_l(t) [\pi_{l;\nu\nu'}^\diamond \theta(t)], \frac{d}{d\xi} p_{\nu\nu'}^\diamond(\xi_{n,l}(t)) \\
&\quad - [\Delta^\times [\pi_{\nu\nu'}^\diamond \theta(t)] p_{\nu\nu'}^\diamond(\xi(t))]_{n,l}, \\
[\mathcal{J}_{q_{\nu\nu'}^\diamond}(t)]_{n,l} &= [\pi_{l;\nu}^\diamond \dot{\theta}(t)] [\pi_{l;\nu}^\diamond \theta(t)] q_{\nu\nu'}^\diamond(\xi_{n,l}(t)) + [\pi_{l;\nu}^\diamond \theta(t)] [\pi_{l;\nu}^\diamond \dot{\theta}(t)] q_{\nu\nu'}^\diamond(\xi_{n,l}(t)) \\
&\quad - [\pi_{l;\nu}^\diamond \theta(t)] [\pi_{l;\nu}^\diamond \theta(t)] \frac{d}{d\xi} q_{\nu\nu'}^\diamond(\xi_{n,l}(t)) \dot{\theta}_l(t) \\
&\quad - [\Delta^\times [\pi_\nu^\diamond \theta(t)] [\pi_{\nu\nu'}^\diamond \theta(t)] q_{\nu\nu'}^\diamond(\xi(t))]_{n,l}.
\end{aligned} \tag{3.7.5}$$

On the other hand, we group the terms related to the nonlinearity g and the dynamics of the functions Z and z into the global term

$$[\mathcal{J}_{\text{glb}}(t)]_{n,l} = \dot{Z}(t) \left(\Phi'_*(\xi_{n,l}(t)) + B_{n,l}(t) \right) + \dot{z}(t) - g(u_{n,l}^+(t)), \tag{3.7.6}$$

where $B_{n,l}(t)$ denotes the bounded sequence

$$\begin{aligned}
B_{n,l}(t) &:= [\pi_{l;\nu}^\diamond \theta(t)] \frac{d}{d\xi} p_\nu^\diamond(\xi_{n,l}(t)) + [\pi_{l;\nu\nu'}^\diamond \theta(t)] \frac{d}{d\xi} p_{\nu\nu'}^\diamond(\xi_{n,l}(t)) \\
&\quad + [\pi_{l;\nu}^\diamond \theta(t)] [\pi_{l;\nu}^\diamond \theta(t)] \frac{d}{d\xi} q_{\nu\nu'}^\diamond(\xi_{n,l}(t)).
\end{aligned}$$

In the first phase of our analysis we split each of these terms into a useful approximation together with a residual that contains terms that behave asymptotically as $O(t^{-\frac{3}{2}})$. In the second phase we combine these approximations, allowing us to isolate an additional set of higher order terms and extract our final approximation.

3.7.2 Analysis of \mathcal{J}_Φ

Setting out to analyze the term \mathcal{J}_Φ , we introduce the approximation

$$\begin{aligned}
[\mathcal{J}_{\Phi;\text{apx}}(t)]_{n,l} &:= \Phi'_*(\xi_{n,l}(t))(-\dot{\theta}_l(t) + c_*) + g\left(\Phi_*(\xi_{n,l}(t))\right) \\
&\quad + [\pi_{l;\nu}^\diamond \theta(t)] [T_\nu \Phi'_*](\xi_{n,l}(t)) - \frac{1}{2} [\pi_{l;\nu}^\diamond \theta(t)]^2 [T_\nu \Phi''_*](\xi_{n,l}(t))
\end{aligned} \tag{3.7.7}$$

and implicitly define the residual \mathcal{R}_Φ via the splitting

$$\mathcal{J}_\Phi = \mathcal{J}_{\Phi;\text{apx}} + \mathcal{R}_\Phi. \tag{3.7.8}$$

The result below confirms that the expression \mathcal{R}_Φ contains only higher order terms, allowing us to focus on $\mathcal{J}_{\Phi;\text{apx}}$ for our further computations.

Lemma 3.7.2. *Assume the setting of Proposition 3.7.1. There exists constants $M > 0$, $\delta > 0$ so that for any $\theta \in C^1([0, \infty); \ell^\infty)$ that satisfies the LDE (3.2.28) with $[\theta(0)]_{\text{dev}} < R$ and $\|\partial\theta(0)\|_{\ell^\infty} \leq \delta$ and any pair of functions $z, Z \in C([0, \infty); \mathbb{R})$, we have the estimate*

$$\|\mathcal{R}_\Phi(t)\|_{\ell^\infty} \leq M \min \left\{ \|\partial\theta(0)\|_{\ell^\infty}, t^{-\frac{3}{2}} \right\}, \quad t > 0. \quad (3.7.9)$$

Proof. Proceeding from the definition

$$[\Delta^\times \Phi_*(\xi(t))]_{n,l} = [T_\nu \Phi_*](\xi_{n,l+\sigma_\nu}(t)) - 4\Phi_*(\xi_{n,l}(t)), \quad (3.7.10)$$

we expand $[T_\nu \Phi_*](\xi_{n,l+\sigma_\nu}(t))$ around $[T_\nu \Phi](\xi_{n,l}(t))$ to find

$$\begin{aligned} [\Delta^\times \Phi_*(\xi(t))]_{n,l} &= \left([T_\nu \Phi_*](\xi_{n,l}(t)) - 4\Phi_*(\xi_{n,l}(t)) \right) - [\pi_{i;\nu}^\diamond \theta(t)] [T_\nu \Phi_*'](\xi_{n,l}(t)) \\ &\quad + \frac{1}{2} [\pi_{i;\nu}^\diamond \theta(t)]^2 [T_\nu \Phi_*''](\xi_{n,l}(t)) \\ &\quad + \frac{1}{2} \int_0^{-\pi_{i;\nu}^\diamond \theta(t)} [T_\nu \Phi_*'''](\xi_{n,l+\sigma_\nu}(t) - s) s^2 ds. \end{aligned}$$

Inserting this expression into the definition (3.7.5) for \mathcal{J}_Φ , we arrive at

$$\begin{aligned} [\mathcal{J}_\Phi]_{n,l}(t) - [\mathcal{J}_{\Phi;\text{apx}}]_{n,l}(t) &= - \left[c_* \Phi'_*(\xi_{n,l}(t)) + [T_\nu \Phi_*](\xi_{n,l}(t)) - 4\Phi_*(\xi_{n,l}(t)) \right. \\ &\quad \left. + g\left(\Phi_*(\xi_{n,l}(t))\right) \right] \\ &\quad - \frac{1}{2} \int_0^{-\pi_{i;\nu}^\diamond \theta(t)} [T_\nu \Phi_*'''](\xi_{n,l+\sigma_\nu}(t) - s) s^2 ds. \end{aligned}$$

The first two rows vanish due to the MFDE (3.2.7), while the third row satisfies the desired bound (3.7.9) by combination of the estimate (3.6.28) with Proposition 3.6.1. \square

3.7.3 Analysis of $\mathcal{J}_{p_\nu^\diamond}$

In this subsection we fix $\nu \in \{1, 2, 3, 4\}$ and analyze the function $\mathcal{J}_{p_\nu^\diamond}$. In particular, we introduce the expression

$$\begin{aligned} [\mathcal{J}_{p_\nu^\diamond;\text{apx}}]_{n,l}(t) &:= [\pi_{i;\nu}^\diamond \theta(t)] \left[-[\mathcal{L}_0 p_\nu^\diamond](\xi_{n,l}(t)) + g'\left(\Phi_*(\xi_{n,l}(t))\right) p_\nu^\diamond(\xi_{n,l}(t)) \right] \\ &\quad + [\pi_{i;\nu}^\diamond \theta(t)] \left(\alpha_{p;\nu}^\diamond p_{\nu'}^\diamond(\xi_{n,l}(t)) - [T_\nu p_\nu^\diamond](\xi_{n,l}(t)) \right) \\ &\quad + [\pi_{i;\nu}^\diamond \theta(t)] [\pi_{i;\nu}^\diamond \theta(t)] \left(-\alpha_{p;\nu'}^\diamond \frac{d}{d\xi} p_\nu^\diamond(\xi_{n,l}(t)) + \frac{d}{d\xi} [T_\nu p_\nu^\diamond](\xi_{n,l}(t)) \right) \end{aligned} \quad (3.7.11)$$

and set out to obtain bounds for the residual

$$\mathcal{R}_{p_\nu^\diamond} := \mathcal{J}_{p_\nu^\diamond} - \mathcal{J}_{p_\nu^\diamond;\text{apx}}. \quad (3.7.12)$$

Lemma 3.7.3. *Consider the setting of Proposition 3.7.1. Then there exist constants $\delta > 0$ and $M > 0$ so that for any $\theta \in C^1([0, \infty); \ell^\infty)$ that satisfies the LDE (3.2.28) with $[\theta(0)]_{\text{dev}} < R$ and $\|\partial\theta(0)\|_{\ell^\infty} \leq \delta$ and any pair of functions $z, Z \in C([0, \infty); \mathbb{R})$, we have the estimate*

$$\|\mathcal{R}_{p_\nu^\diamond}(t)\|_{\ell^\infty} \leq M \min \left\{ \|\partial\theta(0)\|_{\ell^\infty}, t^{-\frac{3}{2}} \right\}, \quad t > 0. \quad (3.7.13)$$

Proof. For fixed $\nu \in \{1, 2, 3, 4\}$, we rewrite the discrete Laplacian as

$$\Delta^\times [\pi_{i,\nu}^\diamond \theta(t)] p_\nu^\diamond(\xi(t))_{n,l} = [\pi_{i,\nu+\nu'}^\diamond \theta(t)] [T_{\nu'} p_\nu^\diamond]((\xi_{n,l+\sigma_{\nu'}}(t)) - 4[\pi_{i,\nu}^\diamond \theta(t)] p_\nu^\diamond(\xi_{n,l}(t)), \quad (3.7.14)$$

where the first term is summed over the indices $\nu' \in \{1, 2, 3, 4\}$. Using (3.6.4) we rephrase this term as

$$\begin{aligned} [\pi_{i,\nu+\nu'}^\diamond \theta(t)] [T_{\nu'} p_\nu^\diamond]((\xi_{n,l+\sigma_{\nu'}}(t)) &= [\pi_{i,\nu}^\diamond \theta(t)] [T_{\nu'} p_\nu^\diamond] (\xi_{n,l+\sigma_{\nu'}}(t)) \\ &+ [\pi_{i,\nu\nu'}^\diamond \theta(t)] [T_{\nu'} p_\nu^\diamond] (\xi_{n,l+\sigma_{\nu'}}(t)). \end{aligned} \quad (3.7.15)$$

Furthermore, for a fixed pair (ν, ν') we expand $[T_{\nu'} p_\nu^\diamond] (\xi_{n,l+\sigma_{\nu'}}(t))$ around the point $[T_{\nu'} p_\nu^\diamond] (\xi_{n,l}(t))$ to find

$$\begin{aligned} [T_{\nu'} p_\nu^\diamond] (\xi_{n,l+\sigma_{\nu'}}(t)) &= [T_{\nu'} p_\nu^\diamond] (\xi_{n,l}(t)) - [\pi_{i,\nu}^\diamond \theta(t)] \frac{d}{d\xi} [T_{\nu'} p_\nu^\diamond] (\xi_{n,l}(t)) \\ &+ \int_0^{-\pi_{i,\nu}^\diamond \theta(t)} \frac{d^2}{d\xi^2} [T_{\nu'} p_\nu^\diamond] (\xi_{n,l+\sigma_{\nu'}}(t) - s) s ds. \end{aligned}$$

Inserting this expression back into (3.7.15), we obtain

$$\begin{aligned} [\pi_{i,\nu+\nu'}^\diamond \theta(t)] [T_{\nu'} p_\nu^\diamond] ((\xi_{n,l+\sigma_{\nu'}}(t)) &= [\pi_{i,\nu}^\diamond \theta(t)] [T_{\nu'} p_\nu^\diamond] ((\xi_{n,l}(t)) \\ &- [\pi_{i,\nu}^\diamond \theta(t)] [\pi_{i,\nu}^\diamond \theta(t)] \frac{d}{d\xi} [T_{\nu'} p_\nu^\diamond] (\xi_{n,l}(t)) \\ &+ [\pi_{i,\nu\nu'}^\diamond \theta(t)] [T_{\nu'} p_\nu^\diamond] (\xi_{n,l}(t)) + [\tilde{\mathcal{R}}_{p_\nu^\diamond}(t)]_{n,l} \end{aligned}$$

where $\tilde{\mathcal{R}}_{p_\nu^\diamond}$ is defined as

$$\begin{aligned} [\tilde{\mathcal{R}}_{p_\nu^\diamond}(t)]_{n,l} &= ([\pi_{i,\nu}^\diamond \theta(t)] + [\pi_{i,\nu\nu'}^\diamond \theta(t)]) \int_0^{-\pi_{i,\nu}^\diamond \theta(t)} \frac{d^2}{d\xi^2} [T_{\nu'} p_\nu^\diamond] (\xi_{n,l+\sigma_{\nu'}}(t) - u) u du \\ &+ [\pi_{i,\nu\nu'}^\diamond \theta(t)] [\pi_{i,\nu}^\diamond \theta(t)] \frac{d}{d\xi} [T_{\nu'} p_\nu^\diamond] (\xi_{n,l}(t)). \end{aligned}$$

Note that this term satisfies the bound (3.7.13) in view of Proposition 3.6.1 and Lemma 3.6.3.

Comparing (3.7.5) and (3.7.11), the definition (3.7.12) hence yields

$$\begin{aligned}
[\mathcal{R}_{p_\nu^\diamond}(t)]_{n,l} &= \left([\pi_{l;\nu}^\diamond \dot{\theta}(t)] - [\pi_{l;\nu'}^\diamond \theta(t)] \alpha_{p;\nu'}^\diamond \right) p_\nu^\diamond(\xi_{n,l}(t)) \\
&\quad - [\pi_{l;\nu}^\diamond \theta(t)] \left(\dot{\theta}_l(t) - \alpha_{p;\nu'}^\diamond [\pi_{l;\nu'}^\diamond \theta(t)] \right) \frac{d}{d\xi} p_\nu^\diamond(\xi_{n,l}(t)) \\
&\quad - [\pi_{l;\nu}^\diamond \theta(t)] \left[[T_\nu p_\nu^\diamond](\xi_{n,l}(t)) - 4p_\nu^\diamond(\xi_{n,l}(t)) + g'(\Phi_*(\xi_{n,l}(t))) p_\nu^\diamond(\xi_{n,l}(t)) \right] \\
&\quad + [\pi_{l;\nu}^\diamond \theta(t)] [\mathcal{L}_0 p_\nu^\diamond](\xi_{n,l}(t)) \\
&\quad - [\tilde{\mathcal{R}}_{p_\nu^\diamond}(t)]_{n,l}.
\end{aligned}$$

The first row satisfies our estimate (3.7.13) due to the bound (3.6.20) of Proposition 3.6.2. Similarly, for the second row we can apply (3.6.19) in combination with Proposition 3.6.1 and Lemma 3.6.3. The third and fourth rows vanish in view of the definition (3.2.10) for the operator \mathcal{L}_0 , which completes the proof. \square

3.7.4 Analysis of $\mathcal{J}_{p_{\nu\nu'}^\diamond}$ and $\mathcal{J}_{q_{\nu\nu'}^\diamond}$

Throughout this subsection, we fix a pair $(\nu, \nu') \in \{1, 2, 3, 4\}^2$ and study the approximants

$$[\mathcal{J}_{p_{\nu\nu'}^\diamond, \text{apx}}(t)]_{n,l} := [\pi_{\nu\nu'}^\diamond \theta(t)] \left(-[\mathcal{L}_0 p_{\nu\nu'}^\diamond](\xi_{n,l}(t)) + g'(\Phi_*(\xi_{n,l}(t))) p_{\nu\nu'}^\diamond(\xi_{n,l}(t)) \right) \quad (3.7.16)$$

together with

$$\begin{aligned}
[\mathcal{J}_{q_{\nu\nu'}^\diamond, \text{apx}}]_{n,l}(t) &:= [\pi_{l;\nu}^\diamond \theta(t)] [\pi_{l;\nu'}^\diamond \theta(t)] g'(\Phi_*(\xi_{n,l}(t))) q_{\nu\nu'}^\diamond(\xi_{n,l}(t)) \\
&\quad - [\pi_{l;\nu}^\diamond \theta(t)] [\pi_{l;\nu'}^\diamond \theta(t)] [\mathcal{L}_0 q_{\nu\nu'}^\diamond](\xi_{n,l}(t)).
\end{aligned}$$

In particular, we obtain bounds on the residuals

$$\mathcal{R}_{p_{\nu\nu'}^\diamond} := \mathcal{J}_{p_{\nu\nu'}^\diamond} - \mathcal{J}_{p_{\nu\nu'}^\diamond, \text{apx}}, \quad \mathcal{R}_{q_{\nu\nu'}^\diamond} := \mathcal{J}_{q_{\nu\nu'}^\diamond} - \mathcal{J}_{q_{\nu\nu'}^\diamond, \text{apx}}. \quad (3.7.17)$$

Lemma 3.7.4. *Consider the setting of Proposition 3.7.1. Then there exist constants $\delta > 0$ and $M > 0$ so that for any $\theta \in C^1([0, \infty); \ell^\infty(\mathbb{Z}))$ that satisfies the LDE (3.2.28) with $[\theta(0)]_{\text{dev}} < R$ and $\|\partial\theta(0)\|_{\ell^\infty} \leq \delta$ and any pair of functions $z, Z \in C([0, \infty); \mathbb{R})$, we have the estimate*

$$\left\| [\mathcal{R}_{p_{\nu\nu'}^\diamond}(t)] \right\|_{\ell^\infty} \leq M \min \left\{ \|\partial\theta(0)\|_{\ell^\infty}, t^{-\frac{3}{2}} \right\}, \quad t > 0. \quad (3.7.18)$$

Proof. For a fixed pair $(\nu, \nu') \in \{1, 2, 3, 4\}^2$, we write the discrete Laplacian in the form

$$\begin{aligned}
\Delta^\times \left[[\pi_{\nu\nu'}^\diamond \theta(t)] p_{\nu\nu'}^\diamond(\xi(t)) \right]_{n,l} &= \pi_{l+\sigma_{\nu\nu'}}^\diamond \theta(t) [\tau_{\nu\nu'} p_{\nu\nu'}^\diamond](\xi_{n,l+\sigma_{\nu\nu'}}(t)) \\
&\quad - 4\pi_{l;\nu\nu'}^\diamond \theta(t) p_{\nu\nu'}^\diamond(\xi_{n,l}(t)),
\end{aligned}$$

summing the first term over the indices $\nu'' \in \{1, 2, 3, 4\}$. Adding and subtracting $[\pi_{l;\nu\nu'}^\diamond \theta(t)] [\tau_{\nu''} p_{\nu\nu'}^\diamond](\xi_{n,l+\sigma_{\nu''}}(t))$ while also expanding $[\tau_{\nu''} p_{\nu\nu'}^\diamond](\xi_{n,l+\sigma_{\nu''}}(t))$ around

$[\tau_{\nu''} p_{\nu''}^{\diamond\diamond}](\xi_{n,l}(t))$, we obtain

$$\begin{aligned} \Delta^\times \left[[\pi_{\nu''}^{\diamond\diamond} \theta(t)] p_{\nu''}^{\diamond\diamond}(\xi(t)) \right]_{n,l} &= [\pi_{l;\nu''}^{\diamond\diamond} \theta(t)] \left([T_{\nu''} p_{\nu''}^{\diamond\diamond}](\xi_{n,l+\sigma_{\nu''}}(t)) - 4p_{\nu''}^{\diamond\diamond}(\xi_{n,l}(t)) \right) \\ &\quad + [\pi_{l;\nu''}^{\diamond\diamond} \pi_{l;\nu''}^{\diamond\diamond} \theta(t)] [T_{\nu''} p_{\nu''}^{\diamond\diamond}](\xi_{n,l+\sigma_{\nu''}}(t)) \\ &= [\pi_{l;\nu''}^{\diamond\diamond} \theta(t)] \left([T_{\nu''} p_{\nu''}^{\diamond\diamond}](\xi_{n,l}(t)) - 4p_{\nu''}^{\diamond\diamond}(\xi_{n,l}(t)) \right) \\ &\quad + [\tilde{\mathcal{R}}_{p_{\nu''}^{\diamond\diamond}}(t)]_{n,l}. \end{aligned} \tag{3.7.19}$$

Here $\tilde{\mathcal{R}}_{p_{\nu''}^{\diamond\diamond}}(t)$ is equal to

$$\begin{aligned} [\tilde{\mathcal{R}}_{p_{\nu''}^{\diamond\diamond}}(t)]_{n,l} &= [\pi_{l;\nu''}^{\diamond\diamond} \pi_{l;\nu''}^{\diamond\diamond} \theta(t)] [T_{\nu''} p_{\nu''}^{\diamond\diamond}](\xi_{n,l+\sigma_{\nu''}}(t)) \\ &\quad + \pi_{l;\nu''}^{\diamond\diamond} \theta(t) \int_0^{-\pi_{l;\nu''} \theta(t)} \frac{d}{d\xi} [T_{\nu''} p_{\nu''}^{\diamond\diamond}](\xi_{n,l+\sigma_{\nu''}}(t) - u) du, \end{aligned}$$

which satisfies the bound (3.7.18) on account of Proposition 3.6.1 and Lemma 3.6.3.

Combining (3.7.19) with the definitions (3.7.5)₃ and (3.7.16) yields

$$\begin{aligned} [\mathcal{R}_{p_{\nu''}^{\diamond\diamond}}]_{n,l}(t) &= [\pi_{l;\nu''}^{\diamond\diamond} \dot{\theta}(t)] p_{\nu''}^{\diamond\diamond}(\xi_{n,l}(t)) - [\pi_{l;\nu''}^{\diamond\diamond} \theta(t)] \dot{\theta}_l(t) \frac{d}{d\xi} p_{\nu''}^{\diamond\diamond}(\xi_{n,l}(t)) \\ &\quad + [\pi_{l;\nu''}^{\diamond\diamond} \theta(t)] \left(4p_{\nu''}^{\diamond\diamond}(\xi_{n,l}(t)) + [\mathcal{L}_0 p_{\nu''}^{\diamond\diamond}](\xi_{n,l}(t)) - [T_{\nu''} p_{\nu''}^{\diamond\diamond}](\xi_{n,l}(t)) \right) \\ &\quad - [\pi_{l;\nu''}^{\diamond\diamond} \theta(t)] g'(\Phi_*(\xi_{n,l}(t))) p_{\nu''}^{\diamond\diamond}(\xi_{n,l}(t)) \\ &\quad - [\tilde{\mathcal{R}}_{p_{\nu''}^{\diamond\diamond}}]_{n,l}(t). \end{aligned}$$

Exploiting the definition (3.2.10) for the operator \mathcal{L}_0 once more, the second and third row sum to $c_* [\pi_{l;\nu''}^{\diamond\diamond} \theta(t)] \frac{d}{d\xi} p_{\nu''}^{\diamond\diamond}(\xi_{n,l}(t))$. This allows us to write

$$\begin{aligned} [\mathcal{R}_{p_{\nu''}^{\diamond\diamond}}]_{n,l}(t) &= [\pi_{l;\nu''}^{\diamond\diamond} \dot{\theta}(t)] p_{\nu''}^{\diamond\diamond}(\xi_{n,l}(t)) - [\pi_{l;\nu''}^{\diamond\diamond} \theta(t)] \left(\dot{\theta}_l(t) - c_* \right) \frac{d}{d\xi} p_{\nu''}^{\diamond\diamond}(\xi_{n,l}(t)) \\ &\quad - [\tilde{\mathcal{R}}_{p_{\nu''}^{\diamond\diamond}}]_{n,l}(t). \end{aligned}$$

The estimate (3.7.18) now follows from Propositions 3.6.1 and 3.6.2 in combination with Lemma 3.6.3. \square

Lemma 3.7.5. *Consider the setting of Proposition 3.7.1. Then there exist constants $\delta > 0$, $M > 0$ so that for any $\theta \in C^1([0, \infty); \ell^\infty(\mathbb{Z}))$ that satisfies the LDE (3.2.28) with $[\theta(0)]_{\text{dev}} < R$ and $\|\partial\theta(0)\|_{\ell^\infty} \leq \delta$ and any pair of functions $z, Z \in C([0, \infty); \mathbb{R})$, we have the estimate*

$$\left\| [\mathcal{R}_{q_{\nu''}^{\diamond\diamond}}(t)] \right\|_{\ell^\infty} \leq M \min \left\{ \|\partial\theta(0)\|_{\ell^\infty}, t^{-\frac{3}{2}} \right\}, \quad t > 0. \tag{3.7.20}$$

Proof. Proceeding as in Lemma 3.7.4, we first fix a pair $(\nu, \nu') \in \{1, 2, 3, 4\}^2$ and write

$$\begin{aligned} \Delta^\times \left[[\pi_{\nu}^{\diamond\diamond} \theta(t)] [\pi_{\nu'}^{\diamond\diamond} \theta(t)] q_{\nu\nu'}^{\diamond\diamond}(\xi(t)) \right]_{n,l} &= [\pi_{l;\nu}^{\diamond\diamond} \theta(t)] [\pi_{l;\nu'}^{\diamond\diamond} \theta(t)] [T_{\nu''} q_{\nu\nu'}^{\diamond\diamond}](\xi_{n,l}(t)) \\ &\quad - [\pi_{l;\nu}^{\diamond\diamond} \theta(t)] [\pi_{l;\nu'}^{\diamond\diamond} \theta(t)] 4q_{\nu\nu'}^{\diamond\diamond}(\xi_{n,l}(t)) \\ &\quad + [\tilde{\mathcal{R}}_{q_{\nu\nu'}^{\diamond\diamond}}]_{n,l}(t), \end{aligned}$$

Here we sum over $\nu'' \in \{1, 2, 3, 4\}$ and use the expression

$$\begin{aligned} [\tilde{\mathcal{R}}_{q_{\nu\nu'}}^{\diamond\diamond}(t)]_{n,l} &= \pi_{i;\nu''}^{\diamond} [\pi_{i;\nu''}^{\diamond}\theta(t)][\pi_{i;\nu''}^{\diamond}\theta(t)] q_{\nu\nu'}^{\diamond\diamond}(\xi_{n,l}(t)) \\ &\quad + [\pi_{i;\nu''}^{\diamond}\theta(t)][\pi_{i;\nu''}^{\diamond}\theta(t)] \int_0^{-\pi_{i;\nu''}\theta(t)} \frac{d}{d\xi} [T_{\nu''} q_{\nu\nu'}^{\diamond\diamond}](\xi_{n,l+\sigma_{\nu''}} - u) du, \end{aligned}$$

which satisfies the bound (3.7.20) on account of Proposition 3.6.1 and Lemma 3.6.3.

Combining this with the definitions (3.7.5)₄ and (3.7.17), we obtain

$$\begin{aligned} [\mathcal{R}_{q_{\nu\nu'}^{\diamond\diamond}}(t)]_{n,l} &= \left([\pi_{i;\nu}^{\diamond}\dot{\theta}(t)][\pi_{i;\nu}^{\diamond}\theta(t)] + [\pi_{i;\nu}^{\diamond}\theta(t)][\pi_{i;\nu}^{\diamond}\dot{\theta}(t)] \right) q_{\nu\nu'}^{\diamond\diamond}(\xi_{n,l}(t)) \\ &\quad - [\pi_{i;\nu}^{\diamond}\theta(t)][\pi_{i;\nu}^{\diamond}\theta(t)] \dot{\theta}_l(t) \frac{d}{d\xi} q_{\nu\nu'}^{\diamond\diamond}(\xi_{n,l}(t)) \\ &\quad + [\pi_{i;\nu}^{\diamond}\theta(t)][\pi_{i;\nu}^{\diamond}\theta(t)] \left([\mathcal{L}_0 q_{\nu\nu'}^{\diamond\diamond}](\xi_{n,l}(t)) - [T_{\nu''} q_{\nu\nu'}^{\diamond\diamond}](\xi_{n,l}(t)) \right) \\ &\quad + [\pi_{i;\nu}^{\diamond}\theta(t)][\pi_{i;\nu}^{\diamond}\theta(t)] \left(4q_{\nu\nu'}^{\diamond\diamond}(\xi_{n,l}(t)) - g'(\Phi_*(\xi_{n,l}(t))) q_{\nu\nu'}^{\diamond\diamond}(\xi_{n,l}(t)) \right) \\ &\quad - [\tilde{\mathcal{R}}_{q_{\nu\nu'}^{\diamond\diamond}}]_{n,l}(t). \end{aligned}$$

Applying the definition (3.2.10) for the operator \mathcal{L}_0 to simplify the third and fourth row, we arrive at

$$\begin{aligned} [\mathcal{R}_{q_{\nu\nu'}^{\diamond\diamond}}(t)]_{n,l} &= \left([\pi_{i;\nu}^{\diamond}\dot{\theta}(t)][\pi_{i;\nu}^{\diamond}\theta(t)] + [\pi_{i;\nu}^{\diamond}\theta(t)][\pi_{i;\nu}^{\diamond}\dot{\theta}(t)] \right) q_{\nu\nu'}^{\diamond\diamond}(\xi_{n,l}(t)) \\ &\quad - [\pi_{i;\nu}^{\diamond}\theta(t)][\pi_{i;\nu}^{\diamond}\theta(t)] \left(\dot{\theta}_l(t) - c_* \right) \frac{d}{d\xi} q_{\nu\nu'}^{\diamond\diamond}(\xi_{n,l}(t)) \\ &\quad - [\tilde{\mathcal{R}}_{q_{\nu\nu'}^{\diamond\diamond}}]_{n,l}, \end{aligned}$$

The statement now follows from Propositions 3.6.1 and 3.6.2 in combination with Lemma 3.6.3. \square

3.7.5 Final splitting

Defining the aggregate quantities

$$\mathcal{J}_{\text{apx}} = \mathcal{J}_{\Phi;\text{apx}} + \mathcal{J}_{p_{\nu}^{\diamond};\text{apx}} + \mathcal{J}_{p_{\nu\nu'}^{\diamond\diamond};\text{apx}} + \mathcal{J}_{q_{\nu\nu'}^{\diamond\diamond};\text{apx}}, \quad (3.7.21)$$

$$\mathcal{R} = \mathcal{R}_{\Phi} + \mathcal{R}_{p_{\nu}^{\diamond}} + \mathcal{R}_{p_{\nu\nu'}^{\diamond\diamond}} + \mathcal{R}_{q_{\nu\nu'}^{\diamond\diamond}}, \quad (3.7.22)$$

the results in §3.7.2-§3.7.4 provide the decomposition

$$\mathcal{J}[u^+] = \mathcal{J}_{\text{apx}} + \mathcal{J}_{\text{glb}} + \mathcal{R}, \quad (3.7.23)$$

together with the explicit expression

$$\begin{aligned}
[\mathcal{J}_{\text{apx}}(t)]_{n,l} &= \Phi'_*(\xi_{n,l}(t)) \left(-\dot{\theta}_l(t) + c_* \right) \\
&+ [\pi_{l;\nu}^\diamond \theta(t)] \left(-[\mathcal{L}_0 p_\nu^\diamond](\xi_{n,l}(t)) + [\tau_\nu \Phi'_*](\xi_{n,l}(t)) \right) \\
&+ [\pi_{l;\nu\nu'}^\diamond \theta(t)] \left(\alpha_{p;\nu}^\diamond p_{\nu'}^\diamond(\xi_{n,l}(t)) - [T_\nu p_\nu^\diamond](\xi_{n,l}(t)) - [\mathcal{L}_0 p_{\nu\nu'}^\diamond](\xi_{n,l}(t)) \right) \\
&+ [\pi_{l;\nu}^\diamond \theta(t)] [\pi_{l;\nu'}^\diamond \theta(t)] \left(-\alpha_{p;\nu'}^\diamond \frac{d}{d\xi} p_\nu^\diamond(\xi_{n,l}(t)) + \frac{d}{d\xi} [T_{\nu'} p_\nu^\diamond](\xi_{n,l}(t)) \right) \\
&+ [\pi_{l;\nu}^\diamond \theta(t)] [\pi_{l;\nu'}^\diamond \theta(t)] \left(-\frac{1}{2} \mathbf{1}_{\nu=\nu'} [T_\nu \Phi''_*](\xi_{n,l}(t)) - [\mathcal{L}_0 q_{\nu\nu'}^\diamond](\xi_{n,l}(t)) \right) \\
&+ \left(u_{n,l}^+(t) - \Phi_*(\xi_{n,l}(t)) - z(t) \right) g'(\Phi_*(\xi_{n,l}(t))) + g(\Phi_*(\xi_{n,l}(t))).
\end{aligned}$$

Recalling the MFDEs (3.2.14) we can reduce \mathcal{J}_{apx} to

$$\begin{aligned}
[\mathcal{J}_{\text{apx}}(t)]_{n,l} &= \Phi'_*(\xi_{n,l}(t)) (-\dot{\theta}_l(t) + \alpha_{p;\nu}^\diamond \pi_{l;\nu}^\diamond \theta(t) + \alpha_{p;\nu\nu'}^\diamond \pi_{l;\nu\nu'}^\diamond \theta(t) + c_*) \\
&+ \Phi'_*(\xi_{n,l}(t)) \left(\alpha_{q;\nu\nu'}^\diamond [\pi_{l;\nu}^\diamond \theta(t)] [\pi_{l;\nu'}^\diamond \theta(t)] \right) \\
&+ \frac{1}{2} [\pi_{l;\nu}^\diamond \theta(t)] [\pi_{l;\nu'}^\diamond \theta(t)] g''(\Phi_*(\xi_{n,l}(t))) p_\nu^\diamond(\xi_{n,l}(t)) p_{\nu'}^\diamond(\xi_{n,l}(t)) \\
&+ \left(u_{n,l}^+(t) - \Phi_*(\xi_{n,l}(t)) - z(t) \right) g'(\Phi_*(\xi_{n,l}(t))) + g(\Phi_*(\xi_{n,l}(t))).
\end{aligned} \tag{3.7.24}$$

Recalling (3.6.18), the first two rows of (3.7.24) can be recognized as the expression $-\Phi'_*(\xi_{n,l}(t))[\mathcal{R}_\theta(t)]_{n,l}$. Grouping the terms related to the function g in \mathcal{J}_{apx} and \mathcal{J}_{glb} , we introduce the new function

$$\begin{aligned}
[\mathcal{J}_g(t)]_{n,l} &= -g(u_{n,l}^+(t)) + \left(u_{n,l}^+(t) - \Phi_*(\xi_{n,l}(t)) - z(t) \right) g'(\Phi_*(\xi_{n,l}(t))) \\
&+ g(\Phi_*(\xi_{n,l}(t))) \\
&+ \frac{1}{2} [\pi_{l;\nu}^\diamond \theta(t)] [\pi_{l;\nu'}^\diamond \theta(t)] g''(\Phi_*(\xi_{n,l}(t))) p_\nu^\diamond(\xi_{n,l}(t)) p_{\nu'}^\diamond(\xi_{n,l}(t)) \\
&= -g(u_{n,l}^+(t)) + [\mathcal{J}_{\text{apx}}(t)]_{n,l} + \Phi'_*(\xi_{n,l}(t)) [\mathcal{R}_\theta(t)]_{n,l}.
\end{aligned}$$

Together with the residual

$$\begin{aligned}
[\mathcal{R}_{\text{rest}}(t)]_{n,l} &= [\mathcal{J}_{\text{glb}}(t)]_{n,l} + g(u_{n,l}^+(t)) - \Phi'_*(\xi_{n,l}(t)) [\mathcal{R}_\theta(t)]_{n,l} \\
&= \dot{Z}(t) \left(\Phi'_*(\xi_{n,l}(t)) + B_{n,l}(t) \right) + \dot{z}(t) - \Phi'_*(\xi_{n,l}(t)) [\mathcal{R}_\theta(t)]_{n,l}
\end{aligned}$$

this leads to the decomposition

$$\mathcal{J}_{\text{apx}} + \mathcal{J}_{\text{glb}} = \mathcal{J}_g + \mathcal{R}_{\text{rest}}. \tag{3.7.25}$$

Expanding $g(u_{n,l}^+(t))$ around $g(\Phi_*(\xi_{n,l}(t)))$ up to third order, we obtain the further reduction

$$[\mathcal{J}_g(t)]_{n,l} = [G^a(t)]_{n,l} + [G^b(t)]_{n,l} - z(t)g'(\Phi_*(\xi_{n,l}(t))),$$

where we have introduced the expressions

$$\begin{aligned} G_{n,l}^a(t) &= \frac{1}{2}[\pi_{l;\nu}^\diamond \theta(t)][\pi_{l;\nu'}^\diamond \theta(t)]g''(\Phi_*(\xi_{n,l}(t)))p_\nu^\diamond(\xi_{n,l}(t))p_{\nu'}^\diamond(\xi_{n,l}(t)) \\ &\quad - \frac{1}{2}g''(\Phi_*(\xi_{n,l}(t)))\left(u_{n,l}^+(t) - \Phi_*(\xi_{n,l}(t))\right)^2, \\ G_{n,l}^b(t) &= -\frac{1}{6}g'''(s_{n,l}(t))\left(u_{n,l}^+(t) - \Phi_*(\xi_{n,l}(t))\right)^3 \end{aligned}$$

for an appropriate function $s_{n,l}(t) \in [\Phi_*(\xi_{n,l}(t)), u_{n,l}^+(t)]$.

In the following lemma, we formulate an appropriate factorization for these new sequences $G^a(t)$ and $G^b(t)$.

Lemma 3.7.6. *Consider the setting of Proposition 3.7.1. Then there exist constants $\delta > 0$, $M > 0$ so that for any $\theta \in C^1([0, \infty); \ell^\infty)$ that satisfies the LDE (3.2.28) with $[\theta(0)]_{\text{dev}} < R$ and $\|\partial\theta(0)\|_{\ell^\infty} \leq \delta$ and any pair of functions $z, Z \in C([0, \infty); \mathbb{R})$, with $\|z\|_{L^\infty} \leq 1$, the following holds true.*

(i) *For any $t > 0$ there exist sequences $H^a(t)$, $H^b(t)$, $\mathcal{R}^a(t)$ and $\mathcal{R}^b(t)$ in $\ell^\infty(\mathbb{Z}_\times^2)$ such that the identities*

$$G_{n,l}^a(t) = z(t)H_{n,l}^a(t) + \mathcal{R}_{n,l}^a(t), \tag{3.7.26}$$

$$G_{n,l}^b(t) = z(t)H_{n,l}^b(t) + \mathcal{R}_{n,l}^b(t) \tag{3.7.27}$$

hold for all $(n, l) \in \mathbb{Z}_\times^2$.

(ii) *For any $t > 0$ we have the estimate*

$$\max \left\{ \|\mathcal{R}^a(t)\|_{\ell^\infty(\mathbb{Z}_\times^2)}, \|\mathcal{R}^b(t)\|_{\ell^\infty(\mathbb{Z}_\times^2)} \right\} \leq M \min \left\{ \|\partial\theta(0)\|_{\ell^\infty}, t^{-\frac{3}{2}} \right\}. \tag{3.7.28}$$

(iii) *For any $t > 0$ the sequences $H^a(t)$ and $H^b(t)$ satisfy the bound*

$$\max \left\{ \|H^a(t)\|_{\ell^\infty(\mathbb{Z}_\times^2)}, \|H^b(t)\|_{\ell^\infty(\mathbb{Z}_\times^2)} \right\} \leq M(\|z\|_{L^\infty} + \delta).$$

Proof. For convenience, we introduce the shorthand

$$\begin{aligned} K_{n,l}(t) &:= u_{n,l}^+(t) - \Phi_*(\xi_{n,l}(t)) - z(t) \\ &= [\pi_{l;\nu}^\diamond \theta(t)]p_\nu^\diamond(\xi_{n,l}(t)) + [\pi_{l;\nu\nu'}^\diamond \theta(t)]p_{\nu\nu'}^\diamond(\xi_{n,l}(t)) \\ &\quad + [\pi_{l;\nu}^\diamond \theta(t)][\pi_{l;\nu'}^\diamond \theta(t)]q_{\nu\nu'}^\diamond(\xi_{n,l}(t)), \end{aligned}$$

which allows us to rewrite $G_{n,l}^a(t)$ as

$$\begin{aligned} G_{n,l}^a(t) &= \frac{1}{2}g''(\Phi_*(\xi_{n,l}(t)))[\pi_{l;\nu}^\diamond\theta(t)][\pi_{l;\nu'}^\diamond\theta(t)]p_\nu^\diamond(\xi_{n,l}(t))p_{\nu'}^\diamond(\xi_{n,l}(t)) \\ &\quad - \frac{1}{2}g''(\Phi_*(\xi_{n,l}(t)))(K_{n,l}(t) + z(t))^2. \end{aligned}$$

The expression

$$\tilde{\mathcal{R}}_{n,l}^a(t) := [\pi_{l;\nu}^\diamond\theta(t)][\pi_{l;\nu'}^\diamond\theta(t)]p_\nu^\diamond(\xi_{n,l}(t))p_{\nu'}^\diamond(\xi_{n,l}(t)) - (K_{n,l}(t))^2$$

satisfies the estimate (3.7.28) by Proposition 3.6.1 and Lemma 3.6.3, which in turn gives the splitting (3.7.26) upon defining

$$\begin{aligned} H_{n,l}^a(t) &= -\frac{1}{2}g''(\Phi_*(\xi_{n,l}(t)))(z(t) + 2K_{n,l}(t)), \\ \mathcal{R}_{n,l}^a(t) &= \frac{1}{2}g''(\Phi_*(\xi_{n,l}(t)))\tilde{\mathcal{R}}_{n,l}^a(t). \end{aligned} \tag{3.7.29}$$

To obtain the splitting (3.7.27), we first notice that $(K_{n,l}(t))^3$ already satisfies the estimate (3.7.28) by Proposition 3.6.1 and Lemma 3.6.3. In order to establish items (i) and (ii), it therefore suffices to write

$$\begin{aligned} H_{n,l}^b(t) &= \frac{1}{6}g'''(s_{n,l}(t))(z^2(t) + 3K_{n,l}(t)z(t) + 3(K_{n,l}(t))^2), \\ \mathcal{R}_{n,l}^b(t) &= \frac{1}{6}g'''(s_{n,l}(t))(K_{n,l}(t))^3. \end{aligned} \tag{3.7.30}$$

Item (iii) finally follows from the definitions of H^a and H^b and the fact that the functions g'' and g''' are bounded on compact intervals. \square

We are now finally ready to define our final splitting. Setting

$$H(t) = H^a(t) + H^b(t) \tag{3.7.31}$$

we write

$$\mathcal{J}[u^+] = \mathcal{J}_{\text{apx;fin}} + \mathcal{R}_{\text{fin}}, \tag{3.7.32}$$

where the quantities $\mathcal{J}_{\text{apx;fin}}$ and \mathcal{R}_{fin} are defined by

$$\begin{aligned} [\mathcal{J}_{\text{apx;fin}}]_{n,l}(t) &= \dot{Z}(t)\left(\Phi'_*(\xi_{n,l}(t)) + B_{n,l}(t)\right) \\ &\quad + z(t)\left(-g'(\Phi_*(\xi_{n,l}(t))) + H_{n,l}(t)\right) + \dot{z}(t), \end{aligned} \tag{3.7.33}$$

$$\mathcal{R}_{\text{fin}}(t) = \mathcal{J}(t) - \mathcal{J}_{\text{apx;fin}}(t).$$

Lemma 3.7.7. *Consider the setting of Proposition 3.7.1. Then there exist constants $\delta > 0$, $M > 0$ so that for any $\theta \in C^1([0, \infty); \ell^\infty(\mathbb{Z}))$ that satisfies the LDE (3.2.28) with $[\theta(0)]_{\text{dev}} < R$ and $\|\partial\theta(0)\|_{\ell^\infty} < R$ and any pair of functions $z, Z \in C([0, \infty); \mathbb{R})$ with $\|z\|_{L^\infty} \leq 1$, we have the estimate*

$$\|\mathcal{R}_{\text{fin}}(t)\|_{\ell^\infty(\mathbb{Z}_x^2)} \leq M \min \left\{ \|\partial\theta(0)\|_{\ell^\infty}, t^{-\frac{3}{2}} \right\}, \quad t > 0.$$

Proof. Comparing equations (3.7.23), (3.7.25) and (3.7.33) we can explicitly identify $\mathcal{R}_{\text{fin}}(t)$ as

$$[\mathcal{R}_{\text{fin}}(t)]_{n,l} = -\Phi'_*(\xi_{n,l}(t))[\mathcal{R}_\theta(t)]_{n,l} + \mathcal{R}_{n,l}(t) + \mathcal{R}_{n,l}^a(t) + \mathcal{R}_{n,l}^b(t).$$

The statement now follows from Proposition 3.6.2 in combination with the definition (3.7.22) and Lemmas 3.7.2, 3.7.3, 3.7.4, 3.7.5 and 3.7.6. \square

3.7.6 Proof of Proposition 3.7.1

We are now finally ready to prove Proposition 3.7.1. As a first step, we show how to pick all the constants and functions appearing in the statement. Without loss of generality, we assume that the constant M from Lemma 3.7.7 satisfies

$$M \geq \max\{1, 52D, \sup_{s \in [0,1]} |g''(s)|, \sup_{s \in [0,1]} |g'''(s)|\}, \quad (3.7.34)$$

where the constant D is defined by

$$D = \max\{\|p_\nu^\diamond\|_{L^\infty}, \|p_{\nu\nu'}^\diamond\|_{L^\infty}, \|q_{\nu\nu'}^\diamond\|_{L^\infty}, \|p_\nu^\diamond\|'_{L^\infty}, \|p_{\nu\nu'}^\diamond\|'_{L^\infty}, \|q_{\nu\nu'}^\diamond\|'_{L^\infty}\}.$$

We pick a constant $m \in (3\epsilon, \frac{1}{2})$ in such a way that

$$-g'(s) \geq 2m > 0, \text{ for } s \in [-\epsilon, \epsilon] \cup [1 - \epsilon, 1 + \epsilon], \quad (3.7.35)$$

reducing ϵ if needed. Next, we define the positive constants

$$C_\epsilon = \max\{1, \frac{2m + M}{\min_{\Phi_* \in [\epsilon, 1-\epsilon]} \Phi'_*}\}, \quad \delta_\epsilon = \frac{\epsilon^3 m^3}{6^3 M^3 C_\epsilon^3}, \quad \nu_\epsilon = \frac{\epsilon^3 m^2}{3 \cdot 6^3 M^2 C_\epsilon^3} = \frac{M \delta_\epsilon}{3m},$$

together with the positive function

$$K_\epsilon : [0, \infty) \rightarrow \mathbb{R}, \quad t \mapsto M \min\left\{\delta_\epsilon, t^{-\frac{3}{2}}\right\}.$$

We now choose a function $z \in C^\infty([0, \infty); \mathbb{R})$ that satisfies

$$K_\epsilon(t) \leq mz(t) \leq 2K_\epsilon(t), \quad m|\dot{z}(t)| \leq 2\tilde{K}_\epsilon(t),$$

where \tilde{K}_ϵ is defined by

$$\tilde{K}_\epsilon(t) = \begin{cases} 0, & t \leq \delta_\epsilon^{-\frac{2}{3}}, \\ \frac{3}{2}Mt^{-\frac{5}{2}}, & t > \delta_\epsilon^{-\frac{2}{3}}, \end{cases}$$

which we recognize as the absolute value of the weak derivative of the function K_ϵ . In addition, we define the function $Z \in C^\infty[0, \infty)$ by

$$Z(t) = C_\epsilon \int_0^t z(s) ds.$$

Proof of Proposition 3.7.1. The functions z and Z are clearly nonnegative, with

$$\begin{aligned} z(0) - \|p_\nu^\diamond\|_{L^\infty} \delta_\epsilon - 2 \|p_{\nu\nu'}^\diamond\|_{L^\infty} \delta_\epsilon - \|q_{\nu\nu'}^\diamond\|_{L^\infty} \delta_\epsilon^2 &\geq \frac{M\delta_\epsilon}{m} - 52D\delta_\epsilon \\ &\geq \frac{M\delta_\epsilon}{m} (1 - m) \\ &\geq \frac{M\delta_\epsilon}{2m} > \nu_\epsilon. \end{aligned}$$

Furthermore, we have $z(t) \leq \frac{2M\delta_\epsilon}{m} \leq \epsilon$, together with

$$Z(t) \leq \frac{2C_\epsilon}{m} \int_0^\infty K_\epsilon(s) ds \leq \frac{6C_\epsilon}{m} M\delta_\epsilon^{\frac{1}{3}} = \epsilon.$$

In particular, items (ii)-(iv) are satisfied. In addition, using the fact that $z(t) \leq \frac{2M\delta_\epsilon}{m}$ in combination with item (iii) of Lemma 3.7.6, we obtain the crude a-priori bound

$$\|H(t)\|_{\ell^\infty(\mathbb{Z}_\times^2)} \leq \epsilon, \quad \text{for all } t \geq 0. \tag{3.7.36}$$

Turning to (i), Lemma 3.7.7 implies that it suffices to show that the residual (3.7.33) satisfies $\mathcal{J}_{\text{apx;fin}}(t) \geq K_\epsilon(t)$. Introducing the notation

$$\begin{aligned} \mathcal{I}_A(t) &= \frac{\dot{Z}(t)}{z(t)} \Phi'_*(\xi(t)), & \mathcal{I}_B(t) &= \frac{\dot{Z}(t)}{z(t)} B(t), & \mathcal{I}_C(t) &= H(t), \\ \mathcal{I}_D(t) &= -g'(\Phi_*(\xi(t))), & \mathcal{I}_E(t) &= \frac{\dot{z}(t)}{z(t)} \end{aligned}$$

we see that

$$\mathcal{J}_{\text{apx;fin}} = z(\mathcal{I}_A + \mathcal{I}_B + \mathcal{I}_C + \mathcal{I}_D + \mathcal{I}_E).$$

Using the observation

$$\frac{|\dot{z}(t)|}{z(t)} \leq \begin{cases} 0, & t \leq \delta_\epsilon^{-\frac{2}{3}}, \\ 3t^{-1}, & t > \delta_\epsilon^{-\frac{2}{3}}, \end{cases}$$

we obtain the global bounds

$$\begin{aligned} |\mathcal{I}_B(t)| &\leq C_\epsilon M\delta_\epsilon \leq \leq \frac{m}{3}, \\ |\mathcal{I}_C(t)| &\leq \epsilon \leq \frac{m}{3}, \\ |\mathcal{I}_E(t)| &\leq 3\delta_\epsilon^{2/3} \leq \frac{m}{3}. \end{aligned}$$

When $\Phi_*(\xi) \in (0, \epsilon] \cup [1 - \epsilon, 1)$, we may use (3.7.35) to obtain the lower bound

$$\mathcal{I}_D \geq 2m.$$

Together with $\mathcal{I}_A \geq 0$, this allows us to conclude

$$\mathcal{J}_{\text{apx}} \geq mz(t) \geq K_\epsilon(t). \tag{3.7.37}$$

On the other hand, when $\Phi_*(\xi) \in [\epsilon, 1 - \epsilon]$, we have

$$|\mathcal{I}_A| \geq C_\epsilon \frac{2m + M}{C_\epsilon} \geq 2m + M, \quad |\mathcal{I}_D| \leq M,$$

which again yields (3.7.37). In a similar manner one can show that $\mathcal{J}[u^-] \leq 0$. \square

3.8 Phase approximation and stability results

In this section we show that γ can be well-approximated by θ after allowing sufficient time for the interface to ‘flatten’. This is achieved using the sub- and super-solutions constructed in §3.7 and allows us to establish Theorem 3.2.9 and Theorem 3.2.7. In view of the preparatory work in §3.6-3.7 which accounts for the transition from horizontal to general rational propagation directions, we can here simply appeal to the corresponding results in [52, §8-9] to a large extent.

The main idea for our proof of Theorem 3.2.9 is to compare the information on γ resulting from the asymptotic description (3.2.27) with the phase information that can be derived from (3.7.1)-(3.7.2). In particular, we capture the solution u between the sub- and super-solutions constructed in §3.7 and exploit the monotonicity properties of Φ_* .

Lemma 3.8.1. *Assume that (Hg) , $(H\Phi)$, $(H0)$, $(HS)_1$ and $(HS)_2$ all hold and let u be a solution of (3.2.4) with the initial condition (3.2.5). Then for every $\epsilon > 0$, there exists a constant $\tau_\epsilon > 0$ so that for any $\tau \geq \tau_\epsilon$ the solution θ of the LDE (3.2.28) with the initial value $\theta(0) = \gamma(\tau)$ satisfies*

$$|\Phi_*(n - \gamma_l(t)) - \Phi_*(n - \theta_l(t - \tau))| \leq \epsilon \quad (3.8.1)$$

for all $(n, l) \in \mathbb{Z}_\times^2$ and $t \geq \tau$.

Proof. The proof is adapted from [52, Lemma 8.2]. We restrict our attention to the upper bound $\Phi_*(n - \gamma_l(t)) \leq \Phi_*(n - \theta_l(t - \tau)) + \epsilon$, noting that the lower bound follows in the same way.

Without loss of generality, we assume that $0 < \epsilon < 1$. Recalling the constant ν_ϵ from Proposition 3.7.1, Theorem 3.2.7 and Lemma 3.4.4 allow us to find $\tau_\epsilon > 0$ and $R > 0$ for which the bounds

$$|u_{n,l}(t) - \Phi_*(n - \gamma_l(t))| \leq \frac{1}{2}\nu_\epsilon, \quad [\gamma(t)]_{\text{dev}} \leq R \quad (3.8.2)$$

hold for all $(n, l) \in \mathbb{Z}_\times^2$ and $t \geq \tau_\epsilon$. We now recall the constant $\delta > 0$ and the functions z and Z that arise by applying Proposition 3.7.1 with our pair (ϵ, R) . Decreasing δ if necessary, we may assume that $\epsilon > \delta$. After possibly increasing τ_ϵ , we may use Proposition 3.4.2 to obtain

$$\|\partial\gamma(\tau)\|_{\ell^\infty} \leq \delta, \quad \tau \geq \tau_\epsilon.$$

We now recall the super-solution u^+ defined in (3.7.1). Our choice for $\theta(0)$ together with the bounds (3.7.3) and (3.8.2) imply that

$$\begin{aligned}
u_{n,l}(\tau) &\leq \Phi_*(n - \gamma_l(\tau)) + p_\nu^\diamond(n - \gamma_l(\tau))[\pi_{l;\nu}^\diamond \gamma(\tau)] + p_{\nu\nu'}^{\diamond\diamond}(n - \gamma_l(\tau))[\pi_{l;\nu\nu'}^{\diamond\diamond} \gamma(\tau)] \\
&\quad + q_{\nu\nu'}^{\diamond\diamond}(n - \gamma_l(\tau))[\pi_{l;\nu}^\diamond \gamma(\tau)][\pi_{l;\nu'}^\diamond \gamma(\tau)] + z(0) \\
&= u_{n,l}^+(0).
\end{aligned}$$

In particular, the comparison principle for the LDE (3.2.4) together with the bound (3.8.2) implies that

$$\Phi_*(n - \gamma_l(t)) \leq u_{n,l}(t) + \frac{1}{2}\nu(\epsilon) \leq u_{n,l}^+(t - \tau) + \frac{1}{2}\nu_\epsilon, \quad t \geq \tau.$$

On the other hand, Corollary 3.6.1 in combination with (3.7.1) allows us to obtain a constant $C > 0$ for which we have

$$u_{n,l}^+(t) - \Phi_*(n - \theta_l(t)) \leq C\epsilon, \quad t \geq 0.$$

In particular, we see that

$$\Phi_*(n - \gamma_l(t)) \leq \Phi_*(n - \theta_l(t - \tau)) + \frac{1}{2}\nu_\epsilon + C\epsilon, \quad t \geq \tau,$$

from which the statement can readily be obtained. \square

Proof of Theorem 3.2.9 . The result can be obtained by following the proof of Proposition 8.1 in [52]. \square

Proof of Theorem 3.2.10. The proof can be copied almost verbatim from [52, §9] up to the notational changes that we exhibited in the proof of Lemma 3.8.1. \square

PROPAGATION REVERSAL FOR BISTABLE DIFFERENTIAL EQUATIONS ON TREES

¹ We study traveling wave solutions to bistable differential equations on infinite k -ary trees. These graphs directly generalize classical square infinite lattices and our results complement those for bistable lattice equations on \mathbb{Z} . Using comparison principles and explicit lower and upper solutions, we show that wave-solutions are pinned for small diffusion parameters. Upon increasing the diffusion, the wave starts to travel with non-zero speed, in a direction that depends on the detuning parameter. However, once the diffusion is sufficiently strong, the wave propagates in a single direction up the tree irrespective of the detuning parameter. In particular, our results imply that changes to the diffusion parameter can lead to a reversal of the propagation direction.

4.1 Introduction

In this paper we consider travelling wave solutions to the scalar bistable reaction - diffusion - advection lattice differential equation (LDE)

$$\begin{aligned} \dot{u}_i &= d(ku_{i+1} - (k+1)u_i + u_{i-1}) + g(u_i; a) \\ &= d(u_{i+1} - 2u_i + u_{i-1}) + d(k-1)(u_{i+1} - u_i) + g(u_i; a), \quad i \in \mathbb{Z}. \end{aligned} \quad (4.1.1)$$

Here $d > 0$ is a diffusion parameter and the function $g(u; a)$ is a bistable nonlinearity, such as the cubic

$$g(u; a) = u(1-u)(u-a), \quad a \in (0, 1). \quad (4.1.2)$$

As we explain below, the advection parameter $k > 1$ can be interpreted as the branch factor of an infinite tree.

We focus on the travelling front solutions of the form

$$u_i(t) = \Phi(i - ct), \quad \Phi(-\infty) = 0, \quad \Phi(\infty) = 1. \quad (4.1.3)$$

¹The results of this chapter has been submitted as Hermen Jan Hupkes, Mia Jukić, Vladimír Švígler, Petr Stehlík, *Propagation reversal for bistable differential equations on trees*

Our primary concern is how the diffusion strength $d > 0$, the branch factor $k > 1$ and the detuning parameter a influence the sign of the wave-speed c . Our main results can be summed up into the following three points.

- (i) For any sufficiently small $d > 0$, wave pinning occurs in the sense that $c = 0$ for a nonempty range of parameters a (Proposition 4.2.3).
- (ii) As we increase d while keeping k fixed, we have $c < 0$ for all $a \approx 0$ and $c > 0$ for all $a \approx 1$ (Theorem 4.2.6).
- (iii) For all $k > 1$ and $a \in (0, 1)$ there exists a function $d^*(a, k)$ such that $c < 0$ for all $d > d^*(a, k)$ (Theorem 4.2.5).

Consequently, these results show that for $a \approx 1$ we can reverse the speed of the wave from $c > 0$ to $c < 0$ by increasing the diffusion parameter d .

Layer solutions on \mathcal{T}_k Our primary motivation to study (4.1.1) is to further our understanding of reaction-diffusion equations on infinite k -ary trees, see Figure 1.7. An infinite k -ary tree is an (undirected) graph $\mathcal{T}_k = (V, E)$, $k \in \mathbb{N}$ in which the set of vertices is given by $V = \mathbb{Z} \times \mathbb{N}_0$ and the neighbourhood $\mathcal{N}(i, j)$ of each node (i, j) consists of its parent node (in the $(i - 1)$ -th layer) and k children (in the $(i + 1)$ -th layer). We can explicitly characterize the set of edges E as

$$E = \{((i, j), (i + 1, kj + l)) : i \in \mathbb{Z}, j \in \mathbb{N}_0, l \in \{0, k - 1\}\}.$$

Note in particular that \mathcal{T}_1 reduces to independent copies of \mathbb{Z} with nearest-neighbour edges.

Let us now consider the bistable reaction-diffusion system

$$\dot{u}_{i,j}(t) = d[\Delta_k u(t)]_{i,j} + g(u_{i,j}(t); a), \quad (i, j) \in V \quad (4.1.4)$$

posed on the tree \mathcal{T}_k , in which the operator

$$[\Delta_k u]_{i,j} = \sum_{(i',j') \in \mathcal{N}(i,j)} (u_{i',j'} - u_{i,j})$$

is commonly referred to as the graph Laplacian. We restrict our attention to so-called *layer solutions*, which satisfy the equality

$$u_{i,j}(t) = u_i(t)$$

for all $(i, j) \in \mathbb{Z}^2$ and $t \in \mathbb{R}$. This substitution reduces the dynamics of (4.1.4) to that of (4.1.1). In particular, the travelling fronts (4.1.3) can be seen as layered invasion waves for the graph system (4.1.4). From this point of view it appears natural to take $k \in \mathbb{N}$ in (4.1.1), but for our analysis it turns out to be worthwhile to consider $k \in \mathbb{R}_{>0}$.

Propagation through continuous media Taking $k = 1$, our main LDE (4.1.1) can be considered as a spatially discrete approximation of the classical bistable partial differential equation

$$u_t(x, t) = du_{xx}(x, t) + g(u(x, t); a), \quad x \in \mathbb{R}, \quad t > 0. \quad (4.1.5)$$

Indeed, replacing the second derivative $u_{xx}(x, t)$ with the central difference scheme results in the system

$$\dot{u}_i(t) = \frac{d}{h^2}(u_{i+1}(t) - 2u_i(t) + u_{i-1}(t)) + g(u_i(t); a), \quad i \in \mathbb{Z},$$

where $u_i(t) = u(x_i, t)$ and $x_i = ih$. The bistable PDE (4.1.5) has been used to model the spread of genetic traits [4, 35], where it is often referred to as the *heterozygote inferior* case. It has also been proposed as a basic model for the propagation of electrical signals through unmyelinated nerve fibres, also known as the ‘reduced’ Fitzhugh-Nagumo equation [11, 72]. In general, (4.1.5) has played a prototypical role during the development of the theory of travelling waves that connect two stable states of the underlying nonlinearity [34].

Using phase-plane analysis [33], one can show that there exists a travelling wave solution

$$u(x, t) = \Phi(x - ct), \quad \Phi(-\infty) = 0, \quad \Phi(+\infty) = 1$$

of (4.1.5) with

$$\text{sign}(c) = -\text{sign} \left(\int_0^1 g(u; a) du \right).$$

This travelling wave satisfies the second order ODE

$$-c\Phi'(\xi) = \Phi''(\xi) + g(\Phi(\xi); a).$$

In the case of the cubic nonlinearity (4.1.2), there even exists an explicit solution formula for the speed c , namely

$$c = \sqrt{2d} \left(a - \frac{1}{2} \right).$$

From this equation it follows that $c = 0$ if and only if $a = 1/2$. The fact that we have $c = 0$ only at one value of the bistable parameter a is one of the fundamental differences between continuous and discrete differential equations.

Propagation through waves in regular lattices Lattice differential equations are a natural modelling tool when the underlying spatial domain has a discrete structure. Crystals, patchy landscapes and myelinated neurons are all examples of such domains. One can find extensive lists of models and application areas in the book by Keener and Sneyd [55] and the survey [50].

Formally, equation (4.1.1) is a generalization of the classic bistable lattice differential equation (LDE)

$$\dot{u}_i(t) = d(u_{i+1}(t) - 2u_i(t) + u_{i-1}(t)) + g(u_i(t); a), \quad i \in \mathbb{Z}, \quad (4.1.6)$$

which has served as a prototypical example to study key phenomena like pinning and topological chaos. Indeed, it has attracted numerous studies, starting with the threshold propagation results in [11] and [12]. One of the first rigorous studies of propagation failure for (4.1.6) was conducted by Keener in [55], who established that $c = 0$ can hold for a (non-trivial) interval of bistable parameters a . This is in stark contrast to the continuous bistable equation, where a slight change of the detuning parameter a suffices to cause standing waves to move. Keener in [55] applied the Moser theorem [71] to show that for each $a \in (0, 1)$ and sufficiently small diffusion $0 < d \ll 1$ one can construct infinitely many horseshoe maps, with each of them giving rise to a stationary solution of (4.1.6) with values in $[0, 1]$. In addition, he constructed a larger region in the (a, d) plane where wave propagation cannot occur. On the other hand, he also established that pinned waves cannot occur for a in the neighbourhood of zero and one once the diffusion parameter d is sufficiently large.

A general theory for the existence of travelling-wave solutions to a broad class of LDEs that includes (4.1.1) was developed by Mallet-Paret [66, 67], who performed a direct analysis of the mixed functional difference equation (MFDE)

$$-c\Phi'(\xi) = d(k\Phi(\xi + 1) - (k + 1)\Phi(\xi) + \Phi(\xi)) + g(\Phi(\xi); a) \quad (4.1.7)$$

that arises by substituting $u_i(t) = \Phi(i - ct)$. His results guarantee that for each $k > 0$, $a \in (0, 1)$ and $d > 0$ one can find a speed $c \in \mathbb{R}$ and a profile $\Phi : \mathbb{R} \rightarrow \mathbb{R}$ that satisfy (4.1.7). It should be remarked that the first existence result for $k = 1$ was obtained by Zinner in [97] in the regime $d \gg 0$.

Propagation through graphs Trees represent an important class of graphs as they model processes on discrete media with regular branching structures [3, 84, 83, 86]. Our paper is closely connected to a recent study by Kouvaris, Kori and Mikhailov [62], where approximation techniques are used to study propagation and pinning phenomena of waves on arbitrarily large, but finite k -ary trees. The bi-infinite trees that we consider in this paper do not have a root vertex, in order to avoid the technical difficulties caused by adding boundaries to our spatial domain. However, due to the exponential convergence in the tails, we fully expect the travelling waves considered here to play an important organizing role for the dynamics on large but finite k -ary trees. We expect that our results could also be relevant for more general graphs. For example, let us consider the Erdős-Rényi random graph $ER_n(p)$ with n nodes, where the probability of two nodes being connected is given by p [31]. In the sparse regime where $p = k/n$ for some fixed $k > 0$, one can show [90, 80] that the Erdős-Rényi random graph $ER_n(k/n)$ converges locally in probability as $n \rightarrow \infty$ to a Poisson branching process with mean offspring k . We can therefore consider k -ary trees as local approximations of large Erdős-Rényi random graphs. Consequently, wave propagation and pinning in random networks can be directly linked to the related phenomena on trees [61].

Similar ideas were explored very recently in [42] for the monostable Fisher-KPP equation on semi-infinite k -trees with one root. In this study, the authors consider initial conditions that are zero everywhere except at the root vertex and establish the existence of a critical diffusion parameter that separates (linear) spreading through the tree from extinction. Moreover, their numerical simulations suggest that this

conclusion can be transferred in some sense to the dynamics of Erdős-Rényi random graphs.

Comparison principle Turning back to the original equation (4.1.1), we note that our main propagation results rely on the construction of appropriate sub- and super-solutions that push travelling waves to the left ($c < 0$) or right ($c > 0$). We use two different constructions, which yield qualitatively different conclusions.

Our first approach follows the outline from Keener [55] to construct smooth but ‘step-like’ subsolutions. The simple nature of these functions results in a relatively tractable expression for the sub-solution residual \mathcal{J}^- , which we examine thoroughly in §4.5. Via this method we obtain a geometric description for a set \mathcal{D}^- in the (a, d) -plane where the wave speed is guaranteed to be negative. For the cubic nonlinearity, we are able to explicitly compute the boundary of \mathcal{D}^- , thus generalizing and completing the results from [55].

This approach has both advantages and disadvantages. On the one hand, the set \mathcal{D}^- obtained through this method is a-priori bounded in d , unlike the actual region where $c < 0$. On the other hand, this method allows us to exploit a useful symmetry in the system that allows us to invert the sign of the wave speed. In particular, we also obtain a region \mathcal{D}^+ close to $a \approx 1$ where the wave speed is guaranteed to be strictly positive. Moreover, our numerical observations indicate that the lower boundaries of \mathcal{D}^- and \mathcal{D}^+ are closely aligned with the edge of the pinning region. This result can be intuitively explained by the fact that travelling profiles close to the pinning regime are themselves almost step-like; see Figure 4.1. The steep sub-solutions therefore provide a good approximation of the actual wave-profiles.

Our second method relies on a more refined construction of sub-solutions. In particular, we build smooth and wide profiles that agree better with the actual wave-profile Φ in the $d \gg 0$ regime. For every $a \in (0, 1)$ we provide a value $d^*(a)$ so that $d > d^*$ implies $c < 0$, which shows that waves have a preferred direction of propagation. Together, these results allow us to paint a rather complete qualitative picture for general bistable nonlinearities.

Organization This paper is organised as follows. We set the stage and state our main results in §4.2. This section also includes explicit expressions for the propagation and pinning regions for the cubic nonlinearity. In §4.3 we summarize several consequences of the comparison principle that we use throughout the paper. We study the pinning region in §4.4 by establishing the existence of invariant intervals. In §4.5 we construct steep sub-solutions to establish the existence of the region \mathcal{D}^- in which the wave speed is negative. Exploiting a symmetry argument allows us to establish the equivalent results for positive speeds. These two sections adapt the ideas from [55] to the more general setting considered in this work.

We proceed in §4.6 with the construction of wide sub-solutions that work well in the $d \gg 0$ regime. Using the comparison principle we show that $c < 0$ for all $d \gg 0$. Section §4.7 is dedicated to the cubic nonlinearity, as we provide explicit expressions for the boundaries of the sets \mathcal{D}^- and \mathcal{D}^+ . In §4.8 we describe chaotic steady solutions to our initial LDE (4.1.1) by adapting the set-up from [55] and [71]. We conclude the paper with several numerical studies to illustrate the shape of the

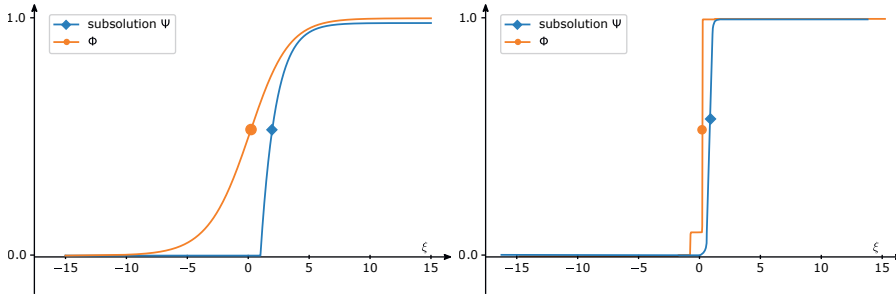


Figure 4.1: These panels display numerically computed traveling waves for $d = 0.5$, $a = 0.1$ and $k = 5$ (left) and $d = 0.002$, $a = 0.2$ and $k = 5$ (right). The travelling speeds of each wave are $c = -1.3084$ and $c = -0.00058$, respectively. In each of these two regimes we use a different technique to construct sub-solutions that rigorously predict the sign of the wavespeed. For $d \gg 0$, we construct wide sub-solutions Ψ (see §4.6), whereas for d small, we use smooth, almost step-like sub-solutions (see §4.5).

pinning and propagation regions in the (a, d) plane, explain the behaviour of the stable and unstable manifolds associated to pinned waves and visualize the reversal of propagation on k -ary trees.

Acknowledgments Mia Jukić and Hermen Jan Hupkes acknowledge support from the Netherlands Organization for Scientific Research (NWO) (grant 639.032.612).

4.2 Main results

The main focus of our study is the reaction-diffusion-advection equation

$$\dot{u}_i(t) = d[\mathcal{A}_k u(t)]_i + g(u_i(t); a), \quad (4.2.1)$$

posed on the one dimensional lattice $i \in \mathbb{Z}$. The discrete diffusion-advection operator $\mathcal{A}_k : \ell^\infty(\mathbb{Z}) \rightarrow \ell^\infty(\mathbb{Z})$ is defined by

$$\mathcal{A}_k u = u_{i-1} - (k+1)u_i + ku_{i+1}. \quad (4.2.2)$$

We require the nonlinearity g to satisfy the following standard bistability assumption.

(Hg) The map $(u, a) \mapsto g(u; a)$ is C^1 -smooth on $\mathbb{R} \times [0, 1]$ and we have

$$g(0; a) = g(a; a) = g(1; a) = 0,$$

$$g'(0; a) < 0, \quad g'(1; a) < 0, \quad g'(a; a) > 0.$$

In addition, we have inequalities

$$g(v; a) > 0 \text{ for } v \in (-\infty, 0) \cup (a, 1), \quad g(v; a) < 0 \text{ for } v \in (0, a) \cup (1, \infty).$$

Throughout this paper we write $g'(v; a) = \partial_v g(v; a)$. At times, we also need to impose the following additional assumptions on g .

(Hg1) For each $a \in (0, 1)$ and $v \in (0, 1)$ we have $\partial_a g(v; a) < 0$.

(Hg2) For each $a \in [0, 1]$, the nonlinearity $g(\cdot; a)$ belongs to $C^2(\mathbb{R})$ and we have $g'(a; a) = 0$ for $a \in \{0, 1\}$, $g''(0; 0) > 0$ and $g''(1; 1) < 0$. Moreover, there exist a_0 and a_1 in $(0, 1)$ such that for each $a \in (0, a_0)$ and $a \in (a_1, 1)$ there exists a unique $v = v(a)$ for which $g''(v; a) = 0$.

Both (Hg1) and (Hg2) are satisfied for the standard cubic nonlinearity (4.1.2), on account of the identities

$$\partial_a g(v; a) = -v(1 - v) < 0, \quad g'(a; a) = -a^2 + a, \quad g''(a; a) = -2a + 1$$

and the fact that $g''(v; a) = 0$ if and only if $v = (a + 1)/3$.

We are specially interested in so-called travelling wave solutions to (4.2.1), which can be written in the form

$$u_i(t) = \Phi(i - ct), \tag{4.2.3}$$

for some speed $c \in \mathbb{R}$ and profile $\Phi : \mathbb{R} \rightarrow \mathbb{R}$. Substituting (4.2.3) into (4.2.1) results in the MFDE

$$-c\Phi'(\xi) = d(k\Phi(\xi + 1) - (k + 1)\Phi(\xi) + \Phi(\xi - 1)) + g(\Phi(\xi); a). \tag{4.2.4}$$

Throughout most of the paper we restrict ourselves to heteroclinic connections that connect the two stable equilibria of the nonlinearity g . Therefore, we also add the boundary conditions

$$\lim_{\xi \rightarrow -\infty} \Phi(\xi) = 0, \quad \lim_{\xi \rightarrow +\infty} \Phi(\xi) = 1. \tag{4.2.5}$$

Equation (4.2.4) is a special case of the general problem considered in [67]. We therefore start by summarizing the key results from [67] that we use in our work. To simplify our notation, we write

$$\mathcal{H} = (0, 1) \times (0, \infty)$$

for the set of parameters (a, d) that we consider.

Proposition 4.2.1. [67, Thm. 2.1] *Suppose that (Hg) holds and pick $(a, d) \in \mathcal{H}$ together with $k > 0$. Then there exist a speed $c = c(a, d, k)$ and a non-decreasing profile $\Phi : \mathbb{R} \rightarrow \mathbb{R}$ that solve (4.2.4) with the boundary conditions (4.2.5). Moreover, $c(a, d, k)$ is uniquely determined and depends C^1 -smoothly on all parameters when $c(a, d, k) \neq 0$. In this case the profile Φ is C^1 -smooth with $\Phi' > 0$ and unique up to translations.*

In the traditional setting where $k = 1$ and g is given by the cubic nonlinearity (4.1.2), one can exploit the identity $g(1 - v; a) = -g(v; 1 - a)$ to obtain the symmetry relation

$$c(a, d, 1) = -c(1 - a, d, 1). \tag{4.2.6}$$

This allows the analysis in [55] to only consider one of the cases $c < 0$ or $c > 0$ and subsequently transfer the results to the other case.

The result below provides a useful generalization of this symmetry relation, which will help to interpret and formulate some of our results. As a preparation, we introduce the transformed parameters

$$\tilde{k} = \frac{1}{k}, \quad \tilde{a} = 1 - a, \quad \tilde{d} = dk, \quad (4.2.7)$$

together with the nonlinearity

$$\tilde{g}(v; \tilde{a}) = -g(1 - v; a). \quad (4.2.8)$$

Since the function \tilde{g} also satisfies (Hg) , Proposition (4.2.1) yields the existence of a transformed speed function \tilde{c} associated to the solutions of (4.2.4)-(4.2.5) with $(\tilde{k}, \tilde{a}, \tilde{d}, \tilde{g})$ instead of (k, a, d, g) .

Lemma 4.2.2. *Suppose that (Hg) holds and pick $(a, d) \in \mathcal{H}$ together with $k > 0$. Then we have*

$$\tilde{c}(\tilde{a}, \tilde{d}, \tilde{k}) = -c(a, d, k). \quad (4.2.9)$$

Proof. Let (c, Φ) be a solution of the MFDE (4.2.4)-(4.2.5) and write $\tilde{\Phi}(\xi) = 1 - \Phi(-\xi)$ together with $\tilde{c} = -c$. A straightforward computation shows that the pair $(\tilde{c}, \tilde{\Phi})$ also satisfies (4.2.4)-(4.2.5), but now with the transformed parameters (4.2.7) and nonlinearity (4.2.8). \square

In our following result we show that for any bistable nonlinearity there exists a nonempty region in the (a, d) plane where waves are pinned, i.e. $c = 0$. We achieve this by showing that there exist two regions with nonempty intersection, one with $c \leq 0$ and the other with $c \geq 0$. To this end, we define two curves $d^- : (0, 1) \rightarrow (0, \infty)$ and $d^+ : (0, 1) \times (0, \infty) \rightarrow (0, \infty)$ by writing

$$d^-(a) := \max_{y \in (a, 1)} \frac{g(y; a)}{y}, \quad d^+(a, k) := \max_{y \in (1-a, 1)} \frac{-g(1-y; a)}{ky}. \quad (4.2.10)$$

We note that the k -dependence of d^+ is directly related to the transformation (4.2.7).

Proposition 4.2.3. *Assume that (Hg) holds and pick $a \in (0, 1)$ together with $k > 0$. Then the following claims hold true.*

(i) *For any $d \in (0, d^+(a, k))$ we have $c(a, d, k) \geq 0$.*

(ii) *For any $d \in (0, d^-(a))$ we have $c(a, d, k) \leq 0$.*

In particular, for any $0 < d < \min\{d^-(a), d^+(a, k)\}$ we have $c(a, d, k) = 0$.

As a follow-up result, we provide more detailed insight into the pinning region. We show that for all sufficiently small $d > 0$ one can construct infinitely many bounded solutions to (4.2.4) with $c = 0$. This system is said to admit ‘spatial chaos’ due to the fact that these solutions can be constructed from arbitrary sequences in $\{0, 1\}$.

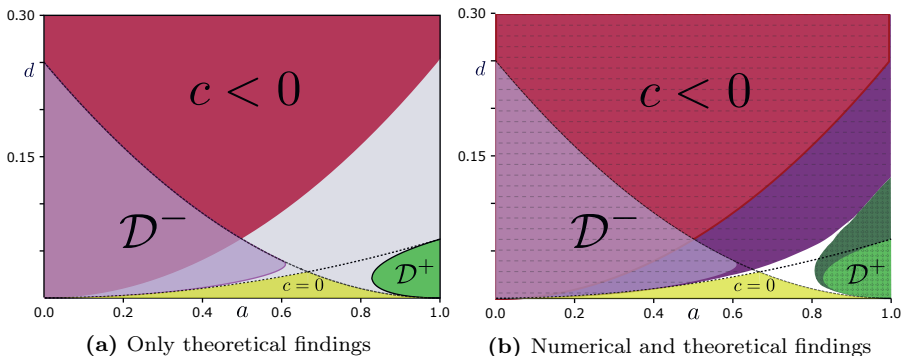


Figure 4.2: The left panel depicts our theoretical findings for $g(v; a) = v(1-v)(v-a)$ and $k = 4$. In the largest region (shown in red) we have $c < 0$ by Theorem 4.2.5. The sets \mathcal{D}^- , in which $c < 0$, and \mathcal{D}^+ with $c > 0$ are given by the exact formula's from Proposition 4.2.9 and Corollary 4.2.10. In the bottom yellow region we have $c = 0$ by Proposition 4.2.3. The right panel compares our theoretical findings with numerically obtained regions where $c < 0$ (purple with $-$ dashes), $c > 0$ (green with $+$ dashes) and $c = 0$ (white).

Proposition 4.2.4. *Assume that (Hg) holds and pick $a \in (0, 1)$ together with $k > 0$. Then there exists $d_0 = d_0(a, k) > 0$ such that for every $0 < d \leq d_0$ and every sequence $(s_i)_{i \in \mathbb{Z}} \subset \{0, 1\}$, there is at least one solution of (4.2.4) that has $c = 0$ together with*

$$\begin{aligned} \Phi(i) &\in [0, a), & \text{if } s_i = 0, \\ \Phi(i) &\in (a, 1], & \text{if } s_i = 1. \end{aligned}$$

The two main results below provide criteria that guarantee the propagation of waves. The first of these provides a quantitative lower bound d^* above which the wave speed is strictly negative. This lower bound is defined for all $k > 1$ and $a \in (0, 1)$, in clear contrast to the symmetry (4.2.6) that occurs for the cubic nonlinearity with $k = 1$. We note that general conditions that guarantee $c > 0$ for $k = 1$ and $a \sim 1$ can be found in [67, Thm. 2.6].

Theorem 4.2.5. *Assume that (Hg) holds. Pick $a \in (0, 1)$ together with $k > 1$ and define the quantity*

$$d^*(a, k) := \left(1 - k^{-1/2}\right)^{-2} d^+(a, k).$$

Then for any $d > d^(a, k)$ we have $c(a, d, k) < 0$.*

Our second main result provides an alternative set of criteria that can guarantee both strictly positive and negative wave speeds. Our numerical results for the cubic nonlinearity (4.1.2) show that the boundary of the associated parameter sets track the edge of the pinning region rather well for a wide range of parameters a ; see Figure 4.2.

The characterization of these sets depend on a geometric construction involving the graph of the nonlinearity g . To describe this construction, we pick parameters

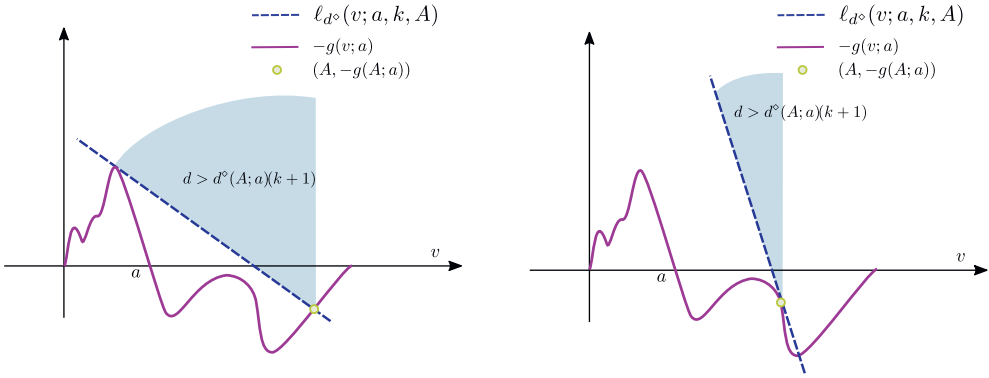


Figure 4.3: In the left panel, the value of $d^\circ = d^\circ(A; a)$ is determined by the tangential intersection of the line and the graph of $-g$ at some point $v \leq A$. In the right panel we have $-d^\circ(A; a)(k + 1) = g'(A; a)$.

$k > 0, a \in (0, 1), A \in (0, 1), d > 0$ and define a linear map $\ell_d(\cdot; a, k, A) : (0, 1) \rightarrow \mathbb{R}$ that acts as

$$\ell_d(v; a, k, A) := d(k + 1)(A - v) - g(A; a). \tag{4.2.11}$$

This linear map intersects the graph of $-g$ at $v = A$ and slopes downward with a steepness that is proportional to d . The smoothness of g now allows us to define

$$d^\circ(A; a) = \inf\{d > 0 : \ell_d(v; a, k, A) \geq -g(v; a), \text{ for all } v \in [0, A]\}, \tag{4.2.12}$$

representing the minimal value of d that is required to ensure that ℓ_d stays above the graph of $-g$ on $[0, A]$; see Figure 4.3.

We now define the set $\mathcal{D}^- \subset \mathcal{H}$ by writing

$$\mathcal{D}^-(g, k) := \left\{ (a, d) \in \mathcal{H} : d^\circ(A; a) < d < \frac{g(A; a)}{A} \text{ for some } A \in (a, 1) \right\}. \tag{4.2.13}$$

We will show that $c < 0$ on \mathcal{D}^- , which is a-priori bounded from above by the function $d^-(a)$ defined in (4.2.10). To tackle the opposite case $c > 0$, we exploit the symmetry (4.2.9) and define the set

$$\mathcal{D}^+(g, k) = \left\{ (a, d) \in \mathcal{H} : (\tilde{a}, \tilde{d}) \in \mathcal{D}^-(\tilde{g}, \tilde{k}) \right\}. \tag{4.2.14}$$

Upon introducing the notation

$$\tilde{d}^\circ(A; a) = \inf\{\tilde{d} > 0 : \tilde{d}(1 + 1/k)(A - v) + g(1 - A; a) \geq g(1 - A; a), \text{ for all } v \in [0, A]\}, \tag{4.2.15}$$

the definition (4.2.14) can be recast in the form

$$\mathcal{D}^+(g, k) = \left\{ (a, d) \in \mathcal{H} : \frac{\tilde{d}^\circ(A; a)}{k} < d < -\frac{g(1 - A; a)}{kA} \text{ for some } A \in (1 - a, 1) \right\},$$

which only involves the original nonlinearity. Notice again that this set is a-priori bounded from above by the function $d^+(a, k)$ defined in (4.2.10).

Theorem 4.2.6. *Assume that (Hg) is satisfied and pick $k > 0$. Then the following claims hold true.*

- (i) *We have $\mathcal{D}^-(g, k) \neq \emptyset$ and $\mathcal{D}^+(g, k) \neq \emptyset$.*
- (ii) *For all $(a, d) \in \mathcal{D}^-(g, k)$ we have $c(a, d, k) < 0$. Equivalently, for all $(a, d) \in \mathcal{D}^+(g, k)$ we have $c(a, d, k) > 0$.*
- (iii) *Assume that (Hg1) holds and pick any $(a, d) \in \overline{\mathcal{D}^-} \cap \mathcal{H}$. Then we have $c(a', d) < 0$ for all $0 < a' < a$. Similarly, pick any $(a, d) \in \overline{\mathcal{D}^+} \cap \mathcal{H}$. Then we have $c(a', d) > 0$ for all $a < a' < 1$.*
- (iv) *Assume that (Hg2) holds. Then there exists $\delta_a \in (0, 1)$ such that*

$$\left(a, \frac{g'(a; a)}{k+1} \right) \in \begin{cases} \mathcal{D}^-(g, k), & \text{for } a \in (0, \delta_a), \\ \mathcal{D}^+(g, k), & \text{for } a \in (1 - \delta_a, 1). \end{cases} \quad (4.2.16)$$

Note that condition (Hg1) implies that we can fully characterize \mathcal{D}^- and \mathcal{D}^+ by finding their right and left boundaries, respectively. In addition, (Hg2) guarantees that the set \mathcal{D}^- extends to the corner $(a, d) = (0, 0)$, while \mathcal{D}^+ extends to $(a, d) = (1, 0)$.

4.2.1 Cubic nonlinearity

In this subsection we apply our techniques to the standard cubic nonlinearity (4.1.2). In particular, we obtain explicit expressions for the curves and regions that appear in our main results. Our first two results describe the functions d^\pm and d_0 that characterize the pinning region and the chaotic behaviour therein. An immediate consequence is that we also have an explicit expression for the curve d^* , above which the wave speed is guaranteed to be negative.

Lemma 4.2.7. *Let g be the standard cubic nonlinearity (4.1.2). Then the explicit expressions for the functions d^- and d^+ defined by (4.2.10) are given by*

$$d^-(a) = \frac{(a-1)^2}{4}, \quad d^+(a, k) = \frac{a^2}{4k}.$$

Proof. This claim follows from a straightforward analysis of quadratic expressions. \square

Proposition 4.2.8. *Let g be the standard cubic nonlinearity (4.1.2) and pick parameters $k > 0$ and $a \in (0, 1)$. Then the following claims hold true.*

- (i) *Pick any $d > 0$ that satisfies*

$$d < \min \left\{ \frac{a^2}{4k}, \frac{(1-a)^2}{4} \right\} = \begin{cases} \frac{a^2}{4k}, & a \leq \frac{1}{1/\sqrt{k}+1}, \\ \frac{(1-a)^2}{4}, & a \geq \frac{1}{1/\sqrt{k}+1}. \end{cases}$$

Then we have $c(a, d, k) = 0$.

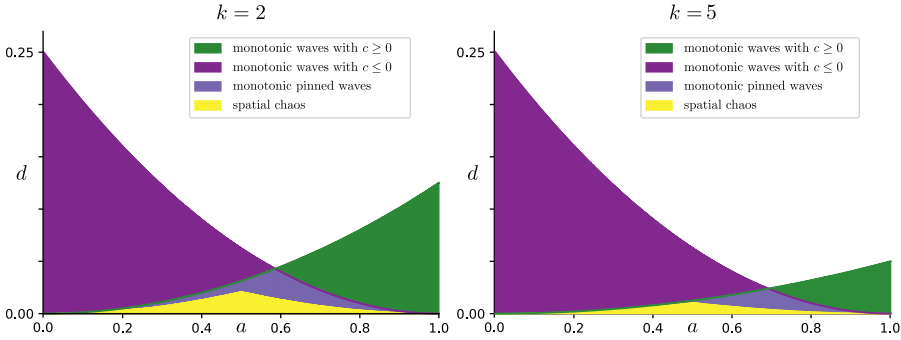


Figure 4.4: These images depict the curves d^- , d^+ and d_0 from Propositions 4.2.3 and 4.2.4 for the standard cubic nonlinearity (4.1.2), with $k = 2$ (left) and $k = 5$ (right). These images already suggest that the pinning region is asymmetric, and that the area in which $c > 0$ decreases as k increases.

(ii) The function d_0 from Proposition 4.2.4 is given by

$$d_0(a, k) := \frac{1}{k + 1} \min \{ kd^+(a, k), d^-(a) \}. \tag{4.2.17}$$

In particular, for any $k > 0$, $a \in (0, 1)$ and $0 < d < d_0(a, k)$ there exist infinitely many bounded solutions to (4.2.4) with $c = 0$.

(iii) Pick any d that satisfies

$$d > \frac{a^2}{4(\sqrt{k} - 1)^2}.$$

Then we have $c(a, d, k) < 0$.

Proof. The proof of items (i) and (iii) follows directly from Proposition 4.2.3 and Theorem 4.2.5 applied to Lemma 4.2.7. For the proof of (ii), see §4.8. \square

We now set out to find explicit expressions for \mathcal{D}^- and \mathcal{D}^+ . Item (iii) of Theorem 4.2.6 shows that it suffices to find the outer boundaries of these sets. To this end, we first define the quantities

$$a_*^-(k) := 1 - \frac{2}{\sqrt{4k + 1} + 1}, \quad a_1^-(k) := \max\{1 - \frac{2}{2\sqrt{k} + 1}, 0\}, \tag{4.2.18}$$

for $k > 0$, together with the curves

$$d_{\min}^-(a, k) := \frac{2a^2k - a + 2k - 2(a+1)\sqrt{k}\sqrt{ka^2 - a(2k+1) + k}}{(4k+1)^2},$$

$$d_{\max}^-(a, k) := \begin{cases} \frac{(1-a)^2}{4}, & \text{if } a \in [0, a_1^-(k)], \\ \frac{2a^2k - a + 2k + 2(a+1)\sqrt{k}\sqrt{ka^2 - a(2k+1) + k}}{(4k+1)^2}, & \text{if } a \in [a_1^-(k), a_*^-(k)], \end{cases}$$

for $k > 0$ and $0 \leq a \leq a_*^-(k)$. Together, these curves define the boundary of \mathcal{D}^- .

Proposition 4.2.9. *[Cubic nonlinearity, negative speed] Pick $k > 0$ and let g be the standard cubic nonlinearity (4.1.2). Then the following claims hold.*

(i) We have $d_{\min}^-, d_{\max}^- \in C([0, a_*^-(k)] \times (0, \infty); \mathbb{R})$ and

$$0 \leq d_{\min}^-(a, k) \leq d_{\max}^-(a, k) \leq d^-(a), \quad \text{for all } a \in [0, a_*^-(k)].$$

(ii) The equality $d_{\max}^-(a_*^-(k)) = d_{\min}^-(a_*^-(k))$ holds.

(iii) The set $\mathcal{D}^-(g, k)$ is bounded precisely by the graphs of d_{\min}^- and d_{\max}^- , namely

$$\mathcal{D}^-(g, k) = \{(a, d) \in \mathcal{H} : a < a_*^-(k), \quad d_{\min}^-(a, k) < d < d_{\max}^-(a, k)\}. \quad (4.2.19)$$

To formulate the equivalent result for the set \mathcal{D}^+ , we again define two values

$$a_*^+(k) = \frac{\sqrt{4k+k^2} - k}{2}, \quad a_1^+(k) = \min\left\{\frac{2\sqrt{k}}{2+\sqrt{k}}, 1\right\} \quad (4.2.20)$$

for $k > 0$, together with two curves

$$d_{\min}^+(a, k) := \frac{2a^2 + a(k-4) + 4 - k - \sqrt{a^2 + ka - k}}{(4+k)^2},$$

$$d_{\max}^+(a, k) := \begin{cases} \frac{a^2}{4k}, & a \in (a_1^+(k), 1), \\ \frac{2a^2 + a(k-4) + 4 - k + \sqrt{a^2 + ka - k}}{(4+k)^2}, & a \in [a_*^+(k), a_1^+(k)], \end{cases}$$

for $k > 0$ and $a_1^+(k) \leq a \leq 1$.

Corollary 4.2.10. *[Cubic nonlinearity, positive speed] Pick $k > 0$ and let g be the standard cubic nonlinearity (4.1.2). Then the following claims hold.*

(i) *We have $d_{\min}^+, d_{\max}^+ \in C([a_*^+(k), 1] \times (0, \infty); \mathbb{R})$ and*

$$0 \leq d_{\min}^+(a, k) \leq d_{\max}^+(a, k) \leq d^+(a, k), \quad \text{for all } a \in [0, a_*^+(k)].$$

(ii) *The equality $d_{\max}^+(a_*^+(k)) = d_{\min}^+(a_*^+(k))$ holds.*

(iii) *The set \mathcal{D}^+ is bounded precisely by the graphs of d_{\min}^+ and d_{\max}^+ , namely*

$$\mathcal{D}^+(g, k) = \{(a, d) \in \mathcal{H} : a > a_*^+(k), d_{\min}^+(a, k) < d < d_{\max}^+(a, k)\}. \quad (4.2.21)$$

Proof. This result follows directly from Proposition 4.2.9 and Lemma 4.2.2 by noting that

$$a_*^+(k) = 1 - a_*^- \left(\frac{1}{k} \right), \quad a_1^+(k) = 1 - a_1^- \left(\frac{1}{k} \right),$$

together with

$$d_{\min}^+(a, k) = \frac{d_{\min}^-(1 - a, 1/k)}{k}, \quad d_{\max}^+(a, k) = \frac{d_{\max}^-(1 - a, 1/k)}{k}.$$

□

4.3 Comparison principles

The main tool that we use in this paper to analyze the LDE (4.2.1) is the well-known comparison principle, which is formulated in the first result below. We will exploit this principle in a standard fashion to show that solutions with monotonic initial conditions remain monotonic. In addition, we show how the sign of the wave speed $c(a, d, k)$ defined in Proposition 4.2.1 can be controlled by constructing appropriate sub and super-solutions.

Lemma 4.3.1. *Let $u, v \in C^1([0, \infty); \ell^\infty(\mathbb{Z}))$ be such that*

$$\begin{aligned} \dot{u}_i(t) &\geq d[\mathcal{A}_k u(t)]_i + g(u_i(t); a), \\ \dot{v}_i(t) &\leq d[\mathcal{A}_k v(t)]_i + g(v_i(t); a) \end{aligned} \quad (4.3.1)$$

and $u_i(0) \geq v_i(0)$ for all $i \in \mathbb{Z}$. Then $u_i(t) \geq v_i(t)$ for $t > 0$ and all $i \in \mathbb{Z}$.

Proof. The statement is the reformulation of [20, Lemma 1] with $j = \infty$ and

$$\mathcal{N}_i u(t) = \dot{u}_i(t) - d[\mathcal{A}_k u(t)]_i - g(u_i(t); a).$$

□

Lemma 4.3.2. *Assume that the assumption (Hg) holds and pick a non-decreasing sequence $u^0 \in \ell^\infty(\mathbb{Z})$. Then the solution $u(t)$ to the LDE (4.2.1) with $u(0) = u^0$ is also a non-decreasing sequence for all $t > 0$.*

Proof. Define the function $v(t)$ with $v_i(t) = u_{i+1}(t)$. Then this function also satisfies the LDE (4.2.1) and we have $u_i^0 \leq v_i^0$ for each $i \in \mathbb{Z}$. By Lemma 4.3.1 this implies $u_i(t) \leq v_i(t)$ for all $i \in \mathbb{Z}$ and $t > 0$. \square

In order to translate the inequalities (4.3.1) to the context of travelling waves, we introduce the operators $\mathcal{I}_{a,d,g,k} : \mathbb{R} \times C^1(\mathbb{R}) \rightarrow C(\mathbb{R})$ that act as

$$\begin{aligned} \mathcal{I}_{a,d,g,k}[c, \Phi](\xi) := & -c\Phi'(\xi) - d(\Phi(\xi - 1) - (k + 1)\Phi(\xi) + k\Phi(\xi + 1)) \\ & - g(\Phi(\xi); a). \end{aligned} \tag{4.3.2}$$

This can be interpreted as the residual of the travelling-wave equation (4.2.4), i.e., $\mathcal{I}_{a,d,g,k}[c, \Phi] = 0$ if and only if the pair (c, Φ) solves (4.2.4).

Corollary 4.3.3. *Pick $k > 0$, a pair $(a, d) \in \mathcal{H}$ and a function g that satisfies (Hg). Let the pair (c, Φ) be a solution of (4.2.4)-(4.2.5). Assume that there exist a constant $\bar{c} < 0$ (resp. $\bar{c} > 0$) and a function $\Psi \in C^1(\mathbb{R})$ that satisfies the properties*

- (i) $\sup_{\xi \in \mathbb{R}} \Psi(\xi) > 0$,
- (ii) $\Psi(\xi) \leq \Phi(\xi)$ (resp. $\Psi(\xi) \geq \Phi(\xi)$) for all $\xi \in \mathbb{R}$.
- (iii) $\mathcal{I}_{a,d,g,k}[\bar{c}, \Psi](\xi) \leq 0$ (resp. $\mathcal{I}_{a,d,g,k}[\bar{c}, \Psi](\xi) \geq 0$) for all $\xi \in \mathbb{R}$.

Then we have $c < 0$ (resp. $c > 0$).

Proof. Without loss of generality, we consider the case $\bar{c} < 0$. Let us define two time-dependent sequences, $v_i(t) := \Psi(i - \bar{c}t)$ and $u_i(t) := \Phi(i - ct)$, for $i \in \mathbb{Z}$. We assume that the profile Ψ is shifted in such manner that $v_i(0) \leq u_i(0)$ for all $i \in \mathbb{Z}$. Therefore, the assumptions of Lemma 4.3.1 are satisfied and we have

$$\Psi(i - \bar{c}t) \leq \Phi(i - ct) \tag{4.3.3}$$

for all $i \in \mathbb{Z}$ and $t > 0$. To show that $c < 0$, we assume to the contrary that $c \geq 0$. Let $\xi_0 \in \mathbb{R}$ be such that $\Psi(\xi_0) = M > 0$. Due to the shift-invariance of the MFDE (4.3.3), we can shift both Ψ and Φ to have $\xi_0 = 0$. In addition, we can find $i_1 \in \mathbb{Z}$ for which $\Phi(i_1) < M/2$. Monotonicity of the profile Φ implies that $i_1 < 0$. Writing $i_1 = \bar{c}t_1$, we now have $v_{i_1}(t_1) = \Psi(i_1 - \bar{c}t) = \Psi(0) = M$. On the other hand, we have $u_{i_1}(t_1) = \Phi(i_1 - ct_1) \leq \Phi(i_1) < M/2$, which clearly contradicts (4.3.3). The case with reversed inequalities can be proved similarly. \square

4.4 Pinned monotonic waves

In this section we follow the approach from [55] to establish Proposition 4.2.3. The series of Lemmas 4.4.1, 4.4.2 and 4.4.3 yield the existence of two invariant intervals $(x_1, 1]$ and $[0, y_2)$ for the LDE (4.2.1). More precisely, choosing $(a, d) \in \mathcal{H}$ with $d < d^-(a)$, we have $u_i(t) \in (x_1, 1]$ provided that $u_i^0 \in (x_1, 1]$. This feature blocks propagation to the right since travelling waves are known to be strictly monotonic [67]. On the other hand, the interval $[0, y_2)$ is invariant for the LDE (4.2.1) when $d < d^+(a, k)$, which blocks propagation to the left.

Lemma 4.4.1. *Consider the setting of Proposition 4.2.3. Pick any $a \in (0, 1)$ and $d < d^-(a)$. Then there exist two points x_1, x_2 , with $a < x_1 < x_2 < 1$ such that*

$$dy - g(y; a) < 0, \quad y \in (x_1, x_2). \quad (4.4.1)$$

Proof. Let us take $d < d^-(a)$. By definition of d^- , there exists $x_0 \in (a, 1)$ such that

$$d < \frac{g(x_0; a)}{x_0}.$$

The strict inequality ensures that there exists an interval (x_1, x_2) around x_0 such that (4.4.1) holds. \square

Lemma 4.4.2. *Consider the setting of Proposition 4.2.3. Pick any $a \in (0, 1)$ and $d < d^+(a, k)$. Then there exist two points y_1, y_2 with $1 - a < y_1 < y_2 < 1$ such that*

$$dky + g(1 - y; a) < 0, \quad y \in (y_1, y_2).$$

Proof. The proof is analogous to that of Lemma 4.4.1. \square

Lemma 4.4.3. *Assume that (Hg) holds and pick a pair $(a, d) \in \mathcal{H}$ together with a non-decreasing sequence $u^0 \in \ell^\infty(\mathbb{Z})$ that has $0 \leq u_i^0 \leq 1$ for all $i \in \mathbb{Z}$. Let $u(t)$ be the solution to the LDE (4.2.1) with $u(0) = u^0$. Then the following claims hold.*

(i) *If $d < d^+(a, k)$ and $u_i^0 \in [0, y_2)$ for some $i \in \mathbb{Z}$, then $u_i(t) \in [0, y_2)$ for all $t > 0$.*

(ii) *If $d < d^-(a)$ and $u_i^0 \in (x_1, 1]$ for some $i \in \mathbb{Z}$, then $u_i(t) \in (x_1, 1]$ for all $t > 0$.*

Proof. By the comparison principle we have $u_i(t) \in [0, 1]$ for all $t > 0$. By Lemma 4.3.2 we also know that $u_i(t)$ is a monotonic sequence for all $t > 0$. Assume that $u_i^0 \in [0, y_2)$ and that there exists $t > 0$ such that $u_i(t) \geq y_2$. A continuity argument ensures that there exists $t_0 > 0$ such that $u_i(t_0) \in (y_1, y_2)$ and $\dot{u}_i(t_0) \geq 0$. However, by Lemma 4.4.2, we have

$$\begin{aligned} \dot{u}_i(t_0) &= d(u_{i-1}(t_0) - u_i(t_0) + k(u_{i+1}(t_0) - u_i(t_0))) + g(u_i(t); a) \\ &\leq d(k(1 - u_i(t_0))) + g(u_i(t); a) < 0, \end{aligned}$$

which contradicts our assumption $\dot{u}_i(t_0) \geq 0$. This proves item (i). Item (ii) follows similarly. \square

Proof of Proposition 4.2.3. In view of Proposition 4.2.1, we can find a solution (Φ, c) to (4.2.4)-(4.2.5). Setting

$$u_i^0 := \Phi(i),$$

we see that u^0 is a non-decreasing sequence connecting 0 and 1. Let $I_1 \in \mathbb{Z}$ be such that

$$\Phi(i) < y_2, \quad i \leq I_1.$$

Assume now that $0 < d < d^+(a, k)$. By item (i) of Lemma 4.4.3 the associated wave solution $u_i(t) = \Phi(i - ct)$ has $u_i(t) < y_2$ for all $t > 0$ and $i \leq I_1$, which implies $c \geq 0$. Item (ii) follows analogously. \square

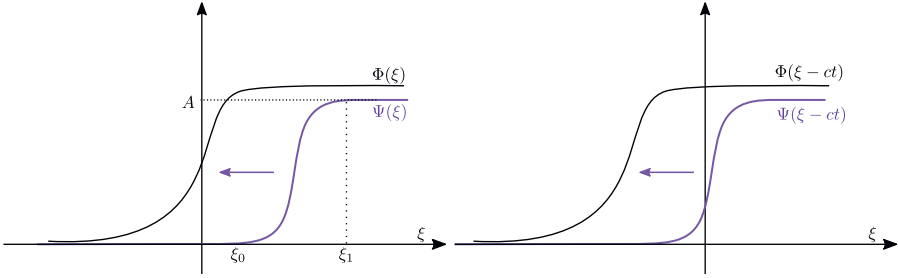


Figure 4.5: These images show how a sub-solution with negative speed causes the wave to move to the left. At $t = 0$ we have $\Psi(\xi) \leq \Phi(\xi)$. The wave profile Φ must also travel with negative speed to ensure that the correct ordering is preserved for $t > 0$.

4.5 Small d regime

The main goal of this section is to establish Theorem 4.2.6 by constructing appropriate sub-solutions. In light of the a-priori upper bounds for the regions \mathcal{D}^- and \mathcal{D}^+ , we consider this the ‘small d ’-regime. The geometric interpretation that we develop here will allow us to find explicit characterizations for these sets in §4.7 in the special case that g is the standard cubic nonlinearity (4.1.2).

Following the approach developed by Keener [55], we fix $a \in (0, 1)$ and $A \in (a, 1)$ and set out to construct a smooth but steep sub-solution Ψ that connects zero to A , see Figure 4.5. We first show that the corresponding sub-solution residual can be controlled by the expression

$$\mathcal{J}^-(a, d, A, g, k) := \max_{v \in [0, A]} (d(k+1)v - dkA - g(v; a)), \tag{4.5.1}$$

which forces $c(a, d, k) < 0$ whenever it is negative.

Lemma 4.5.1. *Consider the setting of Theorem 4.2.6. Pick $(a, d) \in \mathcal{H}$ and suppose that there exists $A \in (a, 1)$ with the property $\mathcal{J}^-(a, d, A, g, k) < 0$. Then we have $c(a, d, k) < 0$.*

Proof. The strict inequality $A < 1$ allows us to choose ξ_0 and ξ_1 so that

$$\Phi(\xi_0) > A \quad \text{and} \quad 0 < \xi_1 - \xi_0 < 1.$$

We use ξ_0 and ξ_1 to define a smooth function $\Psi : \mathbb{R} \rightarrow \mathbb{R}$ that satisfies

$$\Psi(\xi) = \begin{cases} 0, & \xi \leq \xi_0 \\ A, & \xi \geq \xi_1 \end{cases} \tag{4.5.2}$$

and is strictly increasing for $\xi_0 < \xi < \xi_1$. We will show that there exists $\bar{c} < 0$ such that

$$\mathcal{I}_{a, d, g, k}(\bar{c}, \Psi) \leq 0,$$

which yields $c(a, d, k) < 0$ using Corollary 4.3.3.

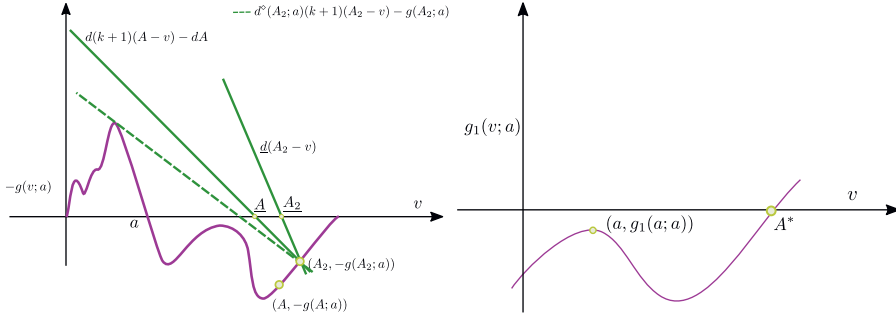


Figure 4.6: The left panel provides a geometric proof for Proposition 4.5.2. The right panel depicts the function g_1 defined by (4.5.5) which has a unique local maximum on $(0, A^*)$ at $v = a$.

To this end, we define

$$\epsilon := \min_{v \in [0, A]} g(v; a) + d(kA - (k+1)v) > 0, \tag{4.5.3}$$

which allows us to choose $\bar{c} < 0$ in such a way that

$$|\bar{c}\Psi'(\xi)| \leq \epsilon.$$

For $\xi < \xi_0$ we have $\Psi'(\xi) = 0$ and

$$\mathcal{I}_{a,d,g,k}(\bar{c}, \Psi) \leq -dk\Psi(\xi + 1) \leq 0.$$

If $\xi > \xi_1$ we again have $\Psi'(\xi) = 0$ and

$$\mathcal{I}_{a,d,g,k}(\bar{c}, \Psi) \leq dA - g(A; a) < 0.$$

For $\xi \in [\xi_0, \xi_1]$ we have $\Psi(\xi) \in [0, A]$, $\Psi(\xi - 1) = 0$ and $\Psi(\xi + 1) = A$, which gives

$$\mathcal{I}_{a,d,g,k}(\bar{c}, \Psi) \leq \epsilon - d(kA - (k+1)\Psi(\xi)) - g(\Psi(\xi); a) \leq 0,$$

as desired. □

A key ingredient towards establishing Theorem 4.2.6 is to find an explicit relation between the set \mathcal{D}^- and the expression \mathcal{J}^- . This is achieved in the following result, using a geometric construction that is illustrated in Figure 4.6.

Proposition 4.5.2. *Consider the setting of Theorem 4.2.6. Then the following two statements are equivalent.*

- (i) We have $(a, d) \in \mathcal{D}^-(g, k)$.
- (ii) There exists $A \in (a, 1)$ for which $\mathcal{J}^-(a, d, A, g, k) < 0$.

Proof. Assuming (i), there exists $A \in (a, 1)$ so that for all $v \in [0, A]$ we have $d(k + 1)(A - v) - g(A; a) \geq -g(v; a)$. Since also $dA < g(A; a)$, this implies that

$$\begin{aligned} \mathcal{J}^-(a, d, A, g, k) &= d(k + 1)(v - A) + dA - g(v; a) \\ &< d(k + 1)(v - A) - g(A; a) - g(v; a) \leq 0. \end{aligned}$$

To establish the opposite inclusion, we assume (ii) and write $\underline{A} = \frac{k}{k+1}A$. The line through $(\underline{A}, 0)$ with slope $-d(k + 1)$ intersects the graph of $-g$ at some point $v = A_2 > A$, see Figure 4.6 (left). We automatically have $d > d_\diamond(A_2; a)$ by definition of $d_\diamond(A_2; a)$, so it suffices to show that $d < g(A_2; a)/A_2$.

To this end, we write $\underline{A}_2 = \frac{k}{k+1}A_2$ and point out that the slope of the line connecting the points $(\underline{A}_2, 0)$ and $(A_2, -g(A_2; a))$ is given by $\underline{d} = -\frac{g(A_2; a)}{A_2}(k + 1)$. Since we have $\underline{A}_2 > \underline{A}$, the inequality $-d(k + 1) > -\underline{d}$ must also hold, which immediately implies $d < g(A_2; a)/A_2$. \square

We now continue with two essential observations concerning the quantities d^\diamond and \mathcal{J}^- . These will allow us to conclude that \mathcal{D}^- is non-empty and - when (Hg1) holds - free of holes.

Lemma 4.5.3. *Consider the setting of Theorem 4.2.6. There exist $0 < A^* < 1$ and $a_- > 0$ such that for all $a \in (0, a_-)$ we have*

$$d^\diamond(A^*; a) < \frac{g(A^*; a)}{A^*}. \tag{4.5.4}$$

Proof. We first note that it suffices to find $0 < A^* < 1$ for which (4.5.4) holds at $a = 0$. Indeed, $g(A; a)/A$ and $d^\diamond(A; a)$ are continuous with respect to both their arguments, the latter since it is the supremum of a difference quotient on a compact interval that depends continuously on these arguments.

To show this, we define

$$\epsilon = \frac{k}{8(k + 1)}$$

and use the fact that $g'(1; 0) < 0$ to pick $A_* \in (1/2, 1)$ in such a way that the line connecting the points $(A_*, -g(A_*; 0))$ and $(\epsilon, 0)$ is above the graph of $-g(\cdot; 0)$ on $[0, A]$. The slope of this line is given by $d_\epsilon = -\frac{g(A_*; 0)}{A_* - \epsilon}$, which using the fact that $kA - (k + 1)\epsilon > 0$ implies

$$d^\diamond(A_*; 0) \leq d_\epsilon/(k + 1) = \frac{g(A_*; 0)}{(k + 1)(A_* - \epsilon)} < g(A_*; 0)/A_*,$$

as desired. \square

Lemma 4.5.4. *Consider the setting of Theorem 4.2.6 and assume furthermore that (Hg1) is satisfied. Pick $(a, d) \in \overline{\mathcal{D}^-} \cap \mathcal{H}$ and $\underline{a} \in (0, a)$. Then we have $(\underline{a}, d) \in \mathcal{D}^-$.*

Proof. By Proposition 4.5.2 we have

$$\mathcal{D}^-(g, k) = \bigcup_{a \in (0, 1)} \bigcup_{A \in (a, 1)} \{(a, d) \in \mathcal{H} : \mathcal{J}^-(a, d, A, g, k) < 0\}.$$

Let us now pick $(a, d) \in \overline{\mathcal{D}^-} \cap \mathcal{H}$. The continuity of \mathcal{J}^- with respect to A implies that $\mathcal{J}^-(a, d, A, g, k) \leq 0$ holds for some $A \in (a, 1]$. Note that $A = a$ is excluded here since $\mathcal{J}^- = da$ for $A = a$.

For $\bar{a} < a$, the assumption (Hg1) implies that

$$g(v; \bar{a}) + d(kA - (k + 1)v) > g(v; a) + d(kA - (k + 1)v) \geq 0, \quad v \in (0, A],$$

while for $v = 0$ we have $g(0; \bar{a}) + dkA = dkA > 0$. Therefore, $\mathcal{J}^-(\bar{a}, d, A, g, k) < 0$ holds. □

In the following lemma we explore how the extra condition (Hg2) leads to the explicit inclusion $(a, g'(a; a)/(k + 1)) \in \mathcal{D}^-(g, k)$ for $a \approx 0$. In particular, translated into the language of d° , the first item implies that $g'(a; a)/(k + 1) > d^\circ(A; a)$ for any $A \in (a, 1)$. The second item then ensures that there exists A such that $d^\circ(A; a) < g(A; a)/A$.

Lemma 4.5.5. *Pick $k > 0$ and assume that the nonlinearity g satisfies (Hg) and (Hg2). Then there exist a constant $\delta_a \in (0, 1)$ such that for all $a \in (0, \delta_a)$ we have*

(i) $g''(a; a) > 0,$

(ii) $0 < \frac{g'(a; a)}{k + 1} < \max_{A \in [a + \frac{2a}{k}, 1]} \frac{g(A; a)}{A}.$

Proof. Due to the assumption (Hg), the function

$$D_-(a) = \max_{A \in [a + \frac{2a}{k}, 1]} \frac{g(A; a)}{A}$$

is well defined, positive and decreasing for $a \leq 1/(k + 2)$. In particular, we have $D_-(0) > 0$. The assumption (Hg2) ensures that $0 = g'(0, 0) < D_-(0)(k + 1)$. Now the existence of δ_a and the claim of item (ii) follow from the continuity properties of the nonlinearity g and the function D_- . The inequality $g''(a; a) > 0$ for $a \in (0, \delta_a)$ follows again from (Hg2) by reducing δ_a if necessary. □

Proof of Theorem 4.2.6. Item (i) follows directly from Lemma 4.5.3. To show item (ii), we first employ Proposition 4.5.2 in combination with Lemma 4.5.1 to conclude that $c < 0$ in \mathcal{D}^- . The result $c > 0$ in \mathcal{D}^+ now follows from Lemma 4.2.2.

Item (iii) for \mathcal{D}^- is a direct consequence of Lemma 4.5.4 and Proposition 4.5.2. To show the equivalent result for \mathcal{D}^+ , we assume that $(a, d) \in \mathcal{D}^+$ and take $\bar{a} > a$. In view of the definition (4.2.14) for \mathcal{D}^+ , we have $(1 - a, dk) \in \mathcal{D}^-(\tilde{g}, 1/k)$ and consequently $(1 - \bar{a}, dk) \in \mathcal{D}^-(\tilde{g}, 1/k)$. In particular, this implies $(\bar{a}, d) \in \mathcal{D}^+$.

To show item (iv), we take δ_a from Lemma 4.5.5 and implicitly define the quantity $A^* \geq a + 2a/k$ by writing

$$\frac{g(A^*; a)}{A^*} = \max_{A \in [a + 2a/k, 1]} \frac{g(A; a)}{A}.$$

For $d = d(a) := g'(a; a)/(k + 1)$, the function $g_1(v; a)$ defined by

$$g_1(v; a) = -g(v; a) - d(kA^* - (k + 1)v) \tag{4.5.5}$$

satisfies $g_1(0; a) < 0$ and $g_1(A^*; a) = -g(A^*; a) + d^* A^* < 0$ by Lemma 4.5.5. Moreover, its unique local maximum or inflection point is achieved at $v = a$ since

$$g_1'(a; a) = -g'(a; a) + (k + 1)d = 0 \quad \text{and} \quad g_1''(a; a) = -g''(a; a) < 0.$$

The value in the local minimum is $g_1(a; a) = -d(kA^* - (k + 1)a) \geq -ad/k > 0$. Therefore, we have $\mathcal{J}^-(a, d, A^*, g, k) < 0$, which implies $c(a, d, k) < 0$ by Lemma 4.5.1 and Proposition 4.5.2.

To show that $(a, d(a)) \in \mathcal{D}^+$ for $a \approx 1$, where $d(a) = g'(a; a)/(k + 1)$ it suffices to show that $(\tilde{a}, \tilde{d}(\tilde{a})) \in \mathcal{D}^-(\tilde{g}, 1/k)$. We note now that the nonlinearity \tilde{g} also satisfies (Hg) and $(Hg2)$. Therefore, by repeating the procedure above, we have

$$\tilde{d}(\tilde{a}) = \tilde{g}'(\tilde{a}; \tilde{a})/(\tilde{k} + 1) \in \mathcal{D}^-(\tilde{g}, \tilde{k}).$$

Translating back to our original coordinates we obtain

$$d(a) = \frac{\tilde{d}(\tilde{a})}{k} = \frac{g'(a; a)}{k + 1} \in \mathcal{D}^+(g, k).$$

□

4.6 Large d regime

In this subsection we prove Theorem 4.2.5 by constructing a second class of subsolutions Ψ to which we can apply Corollary 4.3.3. To start, we denote

$$\mathcal{A}_k[\Phi](\xi) := \Phi(\xi - 1) - (k + 1)\Phi(\xi) + k\Phi(\xi + 1),$$

which allows us to rewrite (4.3.2) as

$$\mathcal{I}_{a,d,g,k}[c, \Phi] = -c\Phi' - d\mathcal{A}_k[\Phi] - g(\Phi; a).$$

The operator

$$\mathcal{A}_1[\Phi] = \Phi(\xi + 1) - 2\Phi(\xi) + \Phi(\xi - 1)$$

can be understood as a discrete version of the second derivative of a smooth function. Moreover, $\Phi''(\xi) \leq 0$ (≥ 0) for all $\xi \in \mathbb{R}$ implies $\mathcal{A}_1[\Phi](\xi) \leq 0$ (≥ 0) for all $\xi \in \mathbb{R}$. We remark that the reverse implication does not hold (consider for example the function $(2x)^4 - (2x)^2$). Since the term $\mathcal{A}_k[\Psi]$ appears with a negative sign in the residual expression $\mathcal{I}_{a,d,g,k}$, our goal is to construct a simple subsolution Ψ with a strictly positive sign of $\mathcal{A}_k[\Psi]$. By choosing $d > 0$ large enough the contribution of $d\mathcal{A}_k[\Psi]$ can then be used to overcome the impact of the nonlinearity g .

We approach the construction of the profile Ψ in a stepwise fashion. First of all, for $l \in \mathbb{R}$ and $A > 0$ we define the function $\kappa_{l;A} : \mathbb{R} \rightarrow \mathbb{R}$ by writing

$$\kappa_{l;A}(\xi) = A(1 - l^{-\xi}). \tag{4.6.1}$$

One can directly compute that $\kappa_{l;A}$ is strictly increasing with

$$\mathcal{A}_k[\kappa_{l;A}] = Al^{-\xi}(k - l)(1 - \frac{1}{l}). \tag{4.6.2}$$

We therefore have $\mathcal{A}_k[\kappa_{l;A}] > 0$ if and only if $l \in (1, k)$. Our first goal is to maximize the the expression $l \mapsto (k - l)(1 - 1/l)$, as that minimizes the expression $\mathcal{I}_{a,d,g,k}[c, \kappa_{l;A}]$.

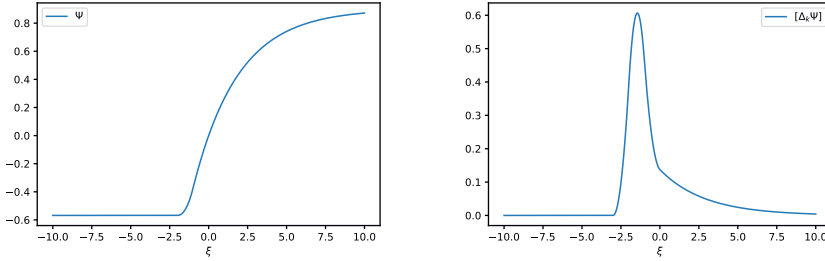


Figure 4.7: These images illustrate the function Ψ defined by (4.6.4) and its discrete Laplacian $\mathcal{A}_k\Psi$, for $k = 2$ and $A = 0.9$.

Lemma 4.6.1. *Pick $k > 1$. Then the maximum of the function $l \mapsto (k - l)(1 - 1/l)$ for $l \in (1, k)$ is achieved at $l = \sqrt{k}$ and its value is given by*

$$f(k) := (k - \sqrt{k})(1 - \frac{1}{\sqrt{k}}) = (1 - \sqrt{k})^2. \tag{4.6.3}$$

Proof. Denoting $Q(l) = (k - l)(1 - 1/l)$, a straightforward computation shows that $Q'(l) = 0 \iff l = \sqrt{k}$. Moreover, we have $Q(1) = Q(k) = 0$. Therefore, the maximum is achieved at $l = \sqrt{k}$. \square

In view of Lemma 4.6.1, we always take $l = \sqrt{k}$ in what follows and set

$$\kappa_A(\xi) := \kappa_{\sqrt{k};A}(\xi).$$

We now write $\delta = \frac{A(\sqrt{k}-1)^2}{2}$ and choose a smooth function $\Psi_A : \mathbb{R} \rightarrow [\kappa_A(-1) - \delta, A)$ that satisfies

$$\Psi_A(\xi) = \begin{cases} \kappa_A(-1) - \delta, & \xi \ll -1, \\ \kappa_A(\xi), & \xi > -1, \end{cases} \tag{4.6.4}$$

together with the flatness assumption

$$|\Psi'_A(\xi)| \leq \frac{A\sqrt{k} \log k}{2} = \kappa'_A(-1),$$

see Figure 4.6. The function Ψ_A represents a smooth bounded version of κ_A that by construction satisfies $\mathcal{A}_k[\Psi](\xi) = \mathcal{A}_k[\kappa_A](\xi)$ for $\xi \geq 0$. Moreover, a straightforward calculation shows that $\mathcal{A}_k[\Psi]$ is strictly positive for $\xi \geq -1$. In particular, we have the following result.

Lemma 4.6.2. *Pick $k > 1$. Then there exists $M \geq 0$ so that $\mathcal{A}_k[\Psi_A]$ satisfies the lower bounds*

$$\mathcal{A}_k[\Psi_A](\xi) \geq \begin{cases} A(\sqrt{k} - 1)^2 k^{-\xi/2}, & \xi \geq 0 \\ \frac{A(\sqrt{k} - 1)^2}{2}, & \xi \in [-1, 0) \\ -M, & \xi \in (-\infty - 1). \end{cases} \tag{4.6.5}$$

Proof. For $\xi \geq 0$ we have $\mathcal{A}_k[\Psi_A](\xi) = \mathcal{A}_k[\kappa_{\sqrt{k};A}](\xi)$, which by (4.6.2) is equal to $A(\sqrt{k} - 1)^2 k^{-\xi/2}$. For $\xi \in [-1, 0]$ we use the bound $k^{-\xi/2} \geq 1$ to find

$$\begin{aligned} \mathcal{A}_k[\kappa_{\sqrt{k};A}](\xi) &\geq kA(1 - k^{-\xi/2-1/2}) - (k+1)A(1 - k^{-\xi/2}) + A(1 - \sqrt{k}) - \delta \\ &= Ak^{-\xi/2}(-\sqrt{k} + k + 1) - A\sqrt{k} - \delta \\ &\geq A(\sqrt{k} - 1)^2 - \delta \\ &\geq \frac{A(\sqrt{k} - 1)^2}{2} \end{aligned}$$

by our choice of δ . Finally, for $\xi \in (-\infty, -1]$, we define

$$M := \sup_{\xi \in (-\infty, -1)} |\mathcal{A}_k[\Psi_A](\xi)|,$$

which is finite since Ψ_A is a bounded function. □

For $\xi \in [-1, \infty)$ the strict positivity of $\mathcal{A}_k[\Psi_A](\xi)$ allows us to obtain the desired sign of the subsolution residual in that region. On the other hand, for $\xi \in (-\infty, -1]$, we will control the residual by appropriately adjusting our nonlinearity. To this end, we impose the following auxiliary condition on g .

(Hg_{d;A}) For all $v \leq A(1 - \sqrt{k})$ we have the bound

$$g(v; a) \geq -v \frac{\log k}{2A} + dM. \tag{4.6.6}$$

Since the wave-solutions of the MFDE (4.2.4) do not ‘see’ the region outside $[0, 1]$, we will show that we can replace the original nonlinearity g with its modified version.

To conclude this set-up, for $a \in (0, 1)$, $k > 1$ and $A \in (a, 1]$, we define the function $d^*(a, k, A)$ with

$$\begin{aligned} d^*(a, k, A) &= \max_{x \in (0,1]} -\frac{g(A(1-x); a)}{Af(k)x} = \max_{x \in [1-\frac{a}{A}, 1]} -\frac{g(A(1-x); a)}{Af(k)x} \\ &= \max_{y \in [0, a]} -\frac{g(y; a)}{f(k)(A-y)}, \end{aligned} \tag{4.6.7}$$

and we note that

$$d^*(a, k, A) \geq d^*(a, k, 1) = d^*(a, k). \tag{4.6.8}$$

Proposition 4.6.3. *Consider the setting of Theorem 4.2.5. Pick $A \in (a, 1)$ and $d > d^*(a, k, A)$ and assume that g additionally satisfies (Hg_{d;A}). Then there exist $\bar{c} < 0$ such that for all $\xi \in \mathbb{R}$ we have*

$$\mathcal{I}_{a,d,g,k}[\bar{c}, \Psi_A](\xi) \leq 0.$$

Proof of Theorem 4.2.5. We first note that the function $d^*(a, k, A)$ is continuous in all parameters as a maximum of a smooth function over a compact set. Therefore,

$d > d^*(a, k) = d^*(a, k, 1)$ implies that there exists $A \in (a, 1)$ such that $d > d^*(a, k, A)$. We now define a modified nonlinearity $g_{d;A} : \mathbb{R} \rightarrow \mathbb{R}$ that satisfies

$$g_{d;A}(v; a) = \begin{cases} g(v; a), & v \geq 0, \\ -v \frac{\log k}{2A} + dM, & v \leq A(1 - \sqrt{k}), \end{cases} \quad (4.6.9)$$

with a smooth connection between $v = A(1 - \sqrt{k})$ and $v = 0$. It is crucial to notice that the non-decreasing solution (Φ, c) MFDE (4.2.4)-(4.2.5) also satisfies (4.2.4) with $g_{d;A}$ instead of g , since $g = g_{d;A}$ for $v \in [0, 1]$. Moreover, since $\Psi_A < A < 1$, we can find $\sigma \in \mathbb{R}$ so that $\Psi_A \leq \Phi(\cdot + \sigma)$. Therefore, by Proposition 4.6.3 and Corollary 4.3.3 we have $c < 0$. \square

4.6.1 Proof of Proposition 4.6.3

In this subsection we prove Proposition 4.6.3 by discussing the two regions $\xi \geq 0$ and $\xi \leq 0$ separately in the two lemmas below.

Lemma 4.6.4. *Consider the setting of Proposition 4.6.3. Then there exist $\epsilon > 0$ and $c^* < 0$ such that for all $c \in (c^*, 0)$ and $\xi \geq 0$ we have*

$$\mathcal{I}_{a,d,g,k}[c, \Psi_A](\xi) < -\epsilon k^{-\xi/2} \leq 0.$$

Proof. Recalling the notation $f(k) = (\sqrt{k} - 1)^2$, writing

$$\epsilon = Af(k)(d - d^*(a, k, A)) > 0$$

and picking $\xi \geq 0$, a direct computation shows that

$$\begin{aligned} \mathcal{I}_{a,d,g,k}[c, \Psi_A](\xi) &= -\frac{cA \log k}{2} k^{-\xi/2} - dAf(k)k^{-\xi/2} - g(A(1 - k^{-\xi/2}); a) \\ &= k^{-\xi/2} Af(k) \left(-\frac{c \log k}{2f(k)} - d - \frac{g(A(1 - k^{-\xi/2}); a)}{Af(k)k^{-\xi/2}} \right). \end{aligned}$$

In view of the definition (4.6.7), we hence obtain

$$\mathcal{I}_{a,d,g,k}[c, \Psi_A](\xi) \leq k^{-\xi/2} \left(-\frac{cA \log k}{2} - \epsilon \right).$$

Choosing $c^* < 0$ in such a way that $-c^*A \log k/2 < \epsilon/2$ yields the desired conclusion. \square

Lemma 4.6.5. *Consider the setting of Proposition 4.6.3. Then there exist $\epsilon > 0$ and $c^* < 0$ such that for all $c \in (c^*, 0)$ and $\xi \leq 0$ we have*

$$\mathcal{I}_{a,d,g,k}[c, \Psi_A](\xi) < -\epsilon.$$

Proof. Let us first consider $\xi \in (-\infty, -1)$, in which case we have $k^{-\xi/2} \in (\sqrt{k}, \infty)$ and consequently $A(1 - k^{-\xi/2}) \in (-\infty, A(1 - \sqrt{k}))$. By assumption $(Hg_{d;A})$ we have

$$g(A(1 - k^{-\xi/2}); a) = -\frac{\log k}{2}(1 - k^{-\xi/2}) + dM \geq \frac{\sqrt{k} - 1}{2} \log k + dM.$$

Using this bound together with Lemma 4.6.2 we obtain the inequality

$$\begin{aligned} \mathcal{I}_{a,d,g,k}[c, \Psi](\xi) &\leq -cA\sqrt{k}\frac{\log k}{2} + dM - g\left(A(1 - k^{-\xi/2}); a\right) \\ &\leq -\frac{\log k}{2}\left(-c\sqrt{k} + \sqrt{k} - 1\right). \end{aligned}$$

By choosing $c < 0$ to be sufficiently close to 0 we can achieve

$$\mathcal{I}_{a,d,g,k}[c, \Psi](\xi) \leq -\frac{\log k(\sqrt{k} - 1)}{4}.$$

On the other hand, for $\xi \in (-1, 0)$ we have $-g(A(1 - k^{-\xi/2})) \leq 0$ and

$$\mathcal{A}_k[\Psi](\xi) \geq A(\sqrt{k} - 1)^2/2$$

by Lemma 4.6.2. Therefore, by choosing $c < 0$ to be sufficiently close to 0, we obtain

$$\mathcal{I}_{a,d,g,k}[c, \Psi_A](\xi) \leq -cA\sqrt{k}\frac{\log k}{2} - \frac{dA}{2}(\sqrt{k} - 1)^2 < -\epsilon$$

for some $\epsilon > 0$. □

Proof of Proposition 4.6.3. The claim follows directly from Lemmas 4.6.4 and 4.6.5 □

4.7 Cubic nonlinearity

The aim of this section is to prove Proposition 4.2.9, which explicitly describes the region \mathcal{D}^- for the standard cubic nonlinearity

$$g(v; a) = v(1 - v)(v - a). \tag{4.7.1}$$

We achieve this by finding explicit expressions for the slope d° defined in (4.2.12). The definition of $d^\circ(A; a)$ and consequently of $\mathcal{A}(a)$ directly depends on the convexity regions of our cubic nonlinearity. Namely, there exists a unique inflection point $v_i = v_i(a)$ on the interval $(0, 1)$ such that g is convex on $(0, v_i)$ and concave on $(v_i, 1)$. A straightforward computation shows that

$$v_i(a) = \frac{a + 1}{3}.$$

Lemma 4.7.1. *Let g be the standard cubic nonlinearity (4.7.1). Pick any $a \in (0, 1)$ and $A \in (v_i, 1)$. Then the linear function*

$$v \mapsto d^\circ(k + 1)(A - v) - g(A; a)$$

touches the nonlinearity $v \mapsto -g(v; a)$ tangentially at some touching point u_{tp} ; see Fig 4.3 (left). Moreover, we have

$$u_{tp} = \frac{1}{2}(1 + a - A) \in \left(\frac{a}{2}, v_i\right), \tag{4.7.2}$$

$$d^\circ(A; a) = \frac{-3A^2 + 2(a + 1)A + (a - 1)^2}{4(k + 1)} > 0. \tag{4.7.3}$$

Proof. In order to find $d^\circ(A; a)$ and the touching point u_{tp} for $A \in (v_i, 1)$ we exploit the idea used by Keener in [55] for $k = 1$ and match the coefficients of two cubic polynomials. In particular, we write

$$g(v; a) + d^\circ(k + 1)(A - v) - g(A; a) = (v - u_{tp})^2(A - v). \tag{4.7.4}$$

The polynomial on the right-hand-side is always positive on $[0, A]$. Moreover, if we show that $u_{tp} < A$, then $d^\circ(k + 1)$ is indeed the smallest possible slope such that the line $d^\circ(k + 1)(A - v) - g(A; a)$ stays above the graph of $-g$ for $v \in [0, A]$. However, this inequality follows easily from $A > v_i$ which implies that $u_{tp} < v_i < A$. \square

Lemma 4.7.2. *Pick $a \in (0, \frac{1}{2})$ and $A \in (a, v_i)$. Then we have*

$$d^\circ(A; a) = g'(A; a)/(k + 1). \tag{4.7.5}$$

Proof. The choice $a < \frac{1}{2}$ implies that the function $-g$ is concave on $(0, v_i)$. This implies that the line with the smallest slope that stays above the graph of $-g$ on the interval $(0, A) \subset (0, v_i)$ is indeed given by $d^\circ(k + 1)(A - v) - g(A; a)$ for $d^\circ = g'(A; a)/(k + 1)$. \square

Recall the definition (4.2.13) and pick $a \in (0, 1)$. We denote by $\mathcal{A}(a)$ the set of admissible parameters A , namely

$$A \in \mathcal{A}(a) \iff d^\circ(A; a) \leq \frac{g(A; a)}{A}. \tag{4.7.6}$$

On account of Lemmas 4.7.1 and 4.7.2, we have to separately consider the two cases $A \in (a, v_i)$ and $A \in (v_i, 1)$ in our study of $d^\circ(A; a)$. We therefore define two subsets of $\mathcal{A}(a)$, namely

$$\mathcal{A}_1(a) = (a, v_i) \cap \mathcal{A}(a), \quad \mathcal{A}_2(a) = [v_i, 1) \cap \mathcal{A}(a).$$

A key point in our analysis is that the contribution from the parameters $A \in (a, v_i)$ can be safely neglected. In particular, we have the following result.

Lemma 4.7.3 (see §4.7.1). *Let g be the standard cubic nonlinearity (4.7.1). Then we have the identities*

$$\min_{A \in \mathcal{A}(a)} d^\circ(A; a) = \min_{A \in \mathcal{A}_2(a)} d^\circ(A; a), \tag{4.7.7}$$

$$\max_{A \in \mathcal{A}(a)} \frac{g(A; a)}{A} = \max_{A \in \mathcal{A}_2(a)} \frac{g(A; a)}{A}. \tag{4.7.8}$$

In the following lemma we further characterize the set $\mathcal{A}_2(a)$. In particular, we show that there exists an upper bound on a for which $\mathcal{A}_2(a)$ is not an empty set.

Lemma 4.7.4. *Let g be the standard cubic nonlinearity (4.7.1). Pick any parameter $a \in (0, 1)$ and recall the value $a_*^-(k)$ defined by (4.2.18). Then the following claims hold.*

(i) *If $a > a_*^-(k)$ then*

$$\mathcal{A}_2(a) = \emptyset.$$

(ii) *If $a \leq a_*^-(k)$ then*

$$\mathcal{A}_2(a) = [v_i, 1) \cap [A_2^-(a), A_2^+(a)],$$

where $A_2^-(a)$ and $A_2^+(a)$ are defined by

$$A_2^-(a) = \frac{(1+a)(1+2k) - 2\sqrt{k^2(a-1)^2 - ka}}{4k+1},$$

$$A_2^+(a) = \frac{(1+a)(1+2k) + 2\sqrt{k^2(a-1)^2 - ka}}{4k+1}.$$

Moreover, we have the inequalities

$$A_2^+(a) \geq \frac{a+1}{2}, \quad A_2^+(a) \in (1-a, 1). \tag{4.7.9}$$

Proof. Pick $A \in [v_i, 1)$. By Lemma 4.7.1, we have $A \in \mathcal{A}_2(a)$ if and only if

$$\frac{-3A^2 + 2(a+1)A + (a-1)^2}{4(k+1)} \leq (1-A)(A-a). \tag{4.7.10}$$

This quadratic inequality has solutions if and only if $A \in [A_2^-(a), A_2^+(a)]$, which are well defined for

$$k^2(a-1)^2 - ka \geq 0,$$

which is equivalent to $a \leq a_*^-(k)$. On the other hand, for $a > a_*^-(k)$ there is no solution to (4.7.10), establishing (i).

The inequality $A_2^+(a) > (1+a)/2$ follows directly from

$$A_2^+(a) \geq \frac{(1+a)(1+2k)}{4k+1} = \frac{(1+a)}{2} + \frac{(1+a)}{2(4k+1)} > \frac{(1+a)}{2}.$$

To show $A_2^+(a) > 1-a$, we write

$$A_2^+(a) - (1-a) = 2 \frac{a(1+3k) - k + \sqrt{k^2(1-a)^2 - ka}}{1+4k}.$$

For $a \geq k/(1+3k)$ the numerator is immediately positive. To examine the case $a < k/(1+3k)$ we define the quadratic expression $\mathcal{Q}_1(a, k)$ by

$$\mathcal{Q}_1(a, k) = k^2(1-a)^2 - ka - (a+3ka-k)^2 = a(k+4k^2 - (1+6k+8k^2)a).$$

This is strictly positive for $0 < a \leq \frac{k}{1+3k}$, since $\mathcal{Q}_1(0, k) = 0$ and

$$\mathcal{Q}_1\left(\frac{k}{1+3k}, k\right) = \frac{k}{1+3k} \frac{k^2(1+4k)}{1+3k} = \frac{k^3(1+4k)}{(1+3k)^2} > 0.$$

To establish our final inequality $A_2^+(a) < 1$, we note that

$$1 - A_2^+(a) = \frac{2k - (1+2k)a - 2\sqrt{k^2(1-a)^2 - ka}}{1+4k}. \tag{4.7.11}$$

Upon writing

$$\mathcal{Q}_2(a, k) = (2k - (1+2k)a)^2 - 4(k^2(1-a)^2 - ka) = (1+4k)a^2,$$

we see that (4.7.11) is indeed strictly positive. □

Lemma 4.7.5. *Let g be the standard cubic nonlinearity (4.7.1). Pick $k > 0$ together with $a \in (0, a_*(k))$ and recall the constant $a_1^-(k)$ defined by (4.2.18). Then we have*

$$\max_{A \in \mathcal{A}_2(a)} \frac{g(A; a)}{A} = \begin{cases} \frac{(1-a)^2}{4}, & \text{if } a \in (0, a_1^-(k)], \\ \frac{g(A_2^-(a); a)}{A_2^-(a)}, & \text{if } a \in [a_1^-(k), a_*(k)). \end{cases}$$

Proof. Let us first define $A_{\max} = \frac{a+1}{2}$. A standard analysis shows that

$$\max_{A \in (0,1)} g(A; a)/A = g(A_{\max}; a)/A_{\max}.$$

By Lemma 4.7.4 we have

$$\max_{A \in \mathcal{A}_2(a)} \frac{g(A; a)}{A} = \begin{cases} \frac{g(A_{\max}; a)}{A_{\max}}, & A_2^-(a) \leq A_{\max}, \\ \frac{g(A_2^-(a); a)}{A_2^-(a)}, & A_2^-(a) \geq A_{\max}. \end{cases}$$

We claim that for $a \in (0, 1)$ we have

$$A_2^-(a) \leq A_{\max}(a) \iff a \in (0, a_1^-(k)). \tag{4.7.12}$$

Indeed, the inequality on the left can be written as

$$\frac{(1+a)(1+2k) - 2\sqrt{k^2(a-1)^2 - ka}}{4k+1} \leq \frac{1+a}{2},$$

which reduces to

$$a^2(4k-1) - 2a(4k+1) + 4k-1 \geq 0. \tag{4.7.13}$$

If $k > 1/4$ then this expression is positive for

$$a \leq 1 - \frac{4\sqrt{k}-2}{4k-1} = 1 - \frac{2}{2\sqrt{k}+1} \quad \text{and} \quad a \geq 1 + \frac{2}{2\sqrt{k}-1}.$$

We recognize that the first value is exactly equal to $a_1^-(k)$, while the second value is greater than 1 and therefore not of interest. For $k \leq 1/4$ there is no solution of (4.7.13) in the set of positive numbers. □

Lemma 4.7.6. *Let g be the standard cubic nonlinearity (4.7.1) and pick any $a \in (0, a_*(k))$. Then we have*

$$\min_{A \in \mathcal{A}_2^+(a)} d^\circ(A; a) = \frac{g(A_2^+(a); a)}{A_2^+(a)}.$$

Proof. The graph of $d^\circ(A; a)$ is a downwards parabola, positive on some superset of $(0, 1)$, with the maximum at $A = v_i \leq A_2^+(a) < 1$. Therefore, the minimum is attained at the right boundary $A_2^+(a)$. \square

Proof of Proposition 4.2.9. Direct computation yields

$$\begin{aligned} \frac{g(A_2^-(a); a)}{A_2^-(a)} &= \frac{2a^2k - a + 2k + 2(a+1)\sqrt{k}\sqrt{ka^2 - a(2k+1)} + k}{(4k+1)^2}, \\ \frac{g(A_2^+(a); a)}{A_2^+(a)} &= \frac{2a^2k - a + 2k - 2(a+1)\sqrt{k}\sqrt{ka^2 - a(2k+1)} + k}{(4k+1)^2}. \end{aligned}$$

Applying Lemmas 4.7.3, 4.7.5 and 4.7.6 now guarantees that the upper and lower boundary of the set \mathcal{D}^- are given by d_{\max} and d_{\min} . The fact that the cubic nonlinearity satisfies (Hg1) ensures that the whole set \mathcal{D}^- is given as the area between these curves, establishing (iii). Items (i) and (ii) follow directly from the construction of d_{\max} and d_{\min} . \square

4.7.1 Proof of Lemma 4.7.3

In this section we complete our analysis of the cubic nonlinearity by establishing Lemma 4.7.3. In addition to the points $a_*(k)$ and $a_1^-(k)$ defined by (4.2.18), we introduce a third value that plays an important role in this section, namely

$$a_2(k) := \min \left\{ 0, 1 - \frac{2\sqrt{k+4}}{\sqrt{k+4} + 3\sqrt{k}} \right\}. \quad (4.7.14)$$

In the following lemma we show that these three points are always ordered, irrespective of $k > 0$.

Lemma 4.7.7. *For every $k > 0$ we have the ordering*

$$a_2(k) \leq a_1^-(k) < a_*(k). \quad (4.7.15)$$

Proof. Our first observation is that for $k > 0$ we have

$$\begin{aligned} a_1^-(k) > 0 &\iff k > \frac{1}{4}, \\ a_2(k) > 0 &\iff k > \frac{1}{2}, \\ a_*(k) > 0 &\iff k > 0. \end{aligned}$$

Therefore, for $k \leq \frac{1}{2}$ the ordering $a_2(k) \leq a_1^-(k)$ trivially holds. For $k > \frac{1}{2}$, the inequality $a_2(k) \leq a_1^-(k)$ is equivalent to

$$\frac{1}{2\sqrt{k}+1} \leq \frac{\sqrt{k+4}}{\sqrt{k+4}+3\sqrt{k}},$$

which is in turn equivalent to

$$\sqrt{k} \left(2\sqrt{k+4} - 3 \right) \geq 0.$$

This holds for all $k > 0$. To show $a_1^-(k) \leq a_*^-(k)$ we apply the bound $\sqrt{4k+1} \geq 2\sqrt{k}$ to the denominator of $a_*^-(k)$. This concludes the proof. \square

Lemma 4.7.8. *Let g be the standard cubic nonlinearity (4.7.1). Pick $k > 0$ and $a \in (0, \frac{1}{2})$. Then we have*

$$\mathcal{A}_1(a) \neq \emptyset \iff a \in (0, a_2(k)).$$

Proof. In view of Lemma 4.7.2, we have $d^\diamond(A; a) \leq g(A; a)/A$ if and only if

$$\frac{g'(A; a)}{k+1} \leq \frac{g(A; a)}{A}, \quad (4.7.16)$$

which can be rewritten as

$$f(A; a) := A^2(k-2) + A(1-k)(a+1) + ka \leq 0.$$

To examine this quadratic function, we first note that $f(a; a) = a(1-a) > 0$ and $f(1; a) = a-1 < 0$. By showing that

$$\bar{f}(a) := f(v_i; a) = f\left(\frac{a+1}{3}; a\right) > 0 \iff a > a_2(k),$$

it follows that f must also be positive on (a, v_i) . Consequently, there exists no $A \in (a, v_i)$ such that $\bar{f}(A) \leq 0$. To establish this claim, we compute

$$\bar{f}(a) = \frac{1}{9} \left((1-2k)a^2 + (2+5k)a + 1 - 2k \right). \quad (4.7.17)$$

For $k > 1/2$, the graph of the mapping $a \mapsto \bar{f}(a)$ is a downward orientated parabola with two roots, the smaller of which is given exactly by $a_2(k)$. Moreover, we can directly check that the expression $\bar{f}(1/2)$ is equal to $0.25 > 0$. Therefore, for all $a \in (a_2(k), 1/2)$ we have $\bar{f}(a) > 0$. For $k \leq 1/2$, all roots of $a \mapsto \bar{f}(a)$ are nonpositive, which implies that $\mathcal{A}_1(a)$ is an empty set for all $a \in (0, \frac{1}{2})$. \square

Lemma 4.7.9. *Let g be the standard cubic nonlinearity (4.7.1). Pick any $a \in (0, a_*^-(k))$. Then we have*

$$\max_{A \in \mathcal{A}_1(a)} \frac{g(A; a)}{A} \leq \max_{A \in \mathcal{A}_2(a)} \frac{g(A; a)}{A}.$$

Proof. If $a > a_2(k)$ the claim trivially holds since $\mathcal{A}_1(a) = \emptyset$. If $a \leq a_2(k)$ then we automatically have $a \leq a_1^-(k)$ due to Lemma 4.7.9. By Lemma 4.7.5 the maximum of $g(A; a)/A$ is attained on $(0, a_1^-(k)]$ as A_{\max} belongs to $\mathcal{A}_2(a)$. Therefore, the contribution from the values of $A \in \mathcal{A}_1(a)$ cannot exceed this maximum. \square

Lemma 4.7.10. *Let g be the standard cubic nonlinearity (4.7.1). Pick any $a \in (0, a_*^-(k))$. Then we have*

$$\min_{A \in \mathcal{A}_1(a)} d^\circ(A; a) \geq \min_{A \in \mathcal{A}_2(a)} d^\circ(A; a).$$

Proof. If $a \geq a_2(k)$ the claim trivially holds since $\mathcal{A}_1(a) = \emptyset$. We therefore assume $a \in (0, a_2(k))$ and recall from Lemma 4.7.6 that

$$\min_{A \in \mathcal{A}_2(a)} d^\circ(A; a) = \frac{g(A_2^+(a))}{A_2^+(a)}.$$

By Lemma 4.7.4 we also know that $A_2^+(a) > 1 - a$, which in turn gives

$$u_{tp}(A_2^+(a)) < a. \tag{4.7.18}$$

Assume now to the contrary that there exists $A \in \mathcal{A}_1(a) \subset (v_i, a)$ for which

$$\frac{g(A_2^+(a); a)}{A_2^+(a)} > \frac{g'(A; a)}{k + 1}. \tag{4.7.19}$$

Since $-g$ is concave on (v_i, a) the linear map $g'(A; a)(A - v) - g(A; a)$ crosses the v -axis at some point $\hat{A} > a$. However, (4.7.18) automatically implies that $d^\circ(A_2^+(a); a) \leq g'(A; a)/(k+1)$, which clearly contradicts (4.7.19) and hence establishes our claim. \square

Proof of Lemma 4.7.3. The claim follows directly from Lemmas 4.7.9 and 4.7.10. \square

4.8 Spatial chaos

To prove Proposition 4.2.4, we follow the outline from [55] and adapt the Moser theorem from [71]. We first note that the solutions of the MFDE (4.2.4) with $c = 0$ are equivalent to steady-state solutions of (4.2.1), i.e., sequences $(u_i)_{i \in \mathbb{Z}}$ that satisfy the difference equation

$$d(u_{i-1} - (k + 1)u_i + ku_{i+1}) + g(u_i; a) = 0. \tag{4.8.1}$$

To find a solution to (4.8.1), we introduce a new sequence $(v_i)_{i \in \mathbb{Z}}$ by setting $v_i := u_{i-1}$. This allows to rewrite (4.8.1) as the two-dimensional recursion relation

$$\begin{cases} v_{i+1} &= u_i, \\ u_{i+1} &= \frac{k + 1}{k}u_i - \frac{v_i}{k} - \frac{g(u_i; a)}{kd}, \end{cases} \tag{4.8.2}$$

for $i \in \mathbb{Z}$. Writing $\phi : \mathbb{R}^2 \rightarrow \mathbb{R}^2$ for the map

$$\phi(u, v) := \left(\frac{k+1}{k}u - \frac{1}{k}v - \frac{g(u; a)}{kd}, u \right), \quad (4.8.3)$$

we notice that solving (4.8.2) is equivalent to constructing a sequence $(u_i, v_i)_{i \in \mathbb{Z}}$ in \mathbb{R}^2 that has

$$\phi(u_i, v_i) = (u_{i+1}, v_{i+1}). \quad (4.8.4)$$

The inverse of the mapping ϕ is given by

$$\phi^{-1}(\tilde{u}, \tilde{v}) = \left(\tilde{v}, (k+1)\tilde{v} - k\tilde{u} - \frac{1}{d}g(\tilde{v}; a) \right) \quad (4.8.5)$$

and a straightforward calculation shows that ϕ and ϕ^{-1} are further related by the identity

$$\phi^{-1} = R_k \phi R_k,$$

where R_k is given by

$$R_k = \begin{pmatrix} 0 & 1 \\ k & 0 \end{pmatrix}.$$

In the special case $k = 1$, this matrix represent reflection through the line $v = u$.

4.8.1 The Moser theorem

We first define a few notions that we use throughout this section. We call a curve $v = v(u)$ a *horizontal curve* if $0 \leq v(u) \leq 1$ for $0 \leq u \leq 1$. Analogously, we call a curve $u = u(v)$ a *vertical curve* if $0 \leq u(v) \leq 1$ for $0 \leq v \leq 1$. For two disjoint horizontal curves $0 \leq v_1(u) < v_2(u) \leq 1$ we call the set

$$U = \{(u, v) : 0 \leq u \leq 1 : v_1(u) \leq v \leq v_2(u)\}$$

a *horizontal strip*. Similarly, we define a *vertical strip* as an area V lying between disjoint vertical curves $0 \leq u_1(v) < u_2(v) \leq 1$, namely

$$V = \{(u, v) : 0 \leq v \leq 1 : u_1(v) \leq u \leq u_2(v)\}.$$

We also introduce the space \mathcal{S} containing all bi-infinite sequences with elements in $\{0, 1\}$, i.e.,

$$\mathcal{S} := \{(\dots, s_{-2}, s_{-1}, s_0, s_1, s_2, \dots) : s_i \in \{0, 1\}\}.$$

This space \mathcal{S} when endowed with an appropriate topology makes a topological space [71], on which we define the forward shift $\sigma : \mathcal{S} \rightarrow \mathcal{S}$ by

$$[\sigma(s)]_i = s_{i+1}.$$

Theorem 4.8.1. [71, Moser] Suppose for $n \in \{0, 1\}$ that U_n, V_n are disjoint horizontal and vertical, respectively, strips in $Q := [0, 1]^2$ that additionally satisfy

- (i) $\phi(V_n) = U_n$, $n \in \{0, 1\}$.

(ii) The vertical boundaries of V_n are mapped to vertical boundaries of U_n and the horizontal boundaries of V_n are mapped to horizontal boundaries of U_n .

Then there exist a function $\tau : \mathcal{S} \mapsto \mathcal{Q}$ such that

$$\phi\tau = \tau\sigma.$$

In addition, the function τ satisfies

$$\phi^i\tau(s) \in U_{s_i}, \quad s \in \mathcal{S}, \quad i \in \mathbb{Z}.$$

Stated informally, one says that ϕ possesses the shift σ on sequences of elements of $\{0, 1\}$ as a subsystem. The main consequence of the Moser theorem is that for every sequence $s \in \mathcal{S}$ we can find a sequence $(u_i, v_i)_{i \in \mathbb{Z}}$ satisfying (4.8.4) with $(u_i, v_i) \in U_{s_i}$ for every $i \in \mathbb{Z}$. To achieve this, we simply set $(u_0, v_0) := \tau(s)$ and $(u_i, v_i) := \phi^i(u_0, v_0)$.

Construction of horizontal and vertical strips Let us define a function h that acts as

$$h(v; a, d) = (k+1)v - \frac{1}{d}g(v; a). \quad (4.8.6)$$

To construct the strips U_n and V_n , for $n = 0, 1$, we need to ensure that the parameter d is small enough so that the following assumption holds.

(Hd) There exist points y_0 and y_1 , satisfying $0 < y_0 < a$ and $a < y_1 < 1$ such that

$$\begin{aligned} h(y_0; a, d) &> k+1, \\ h(y_1; a, d) &< 0, \\ h'(v; a, d) &> 0, \quad v \in (0, y_0) \cup (y_1, 1). \end{aligned}$$

Lemma 4.8.2. *Assume that conditions (Hg) and (Hd) hold. Then there exist horizontal strips U_0, U_1 , and vertical strips V_0, V_1 that satisfy the assumptions of Theorem 4.8.1.*

Proof of Proposition 4.2.4. It suffices to show that the function h defined by (4.8.6) satisfies condition (Hd) for all sufficiently small $d > 0$. Indeed, we can then combine the Moser Theorem and Lemma 4.8.2 to obtain the desired conclusion.

On the interval $(0, a)$ we have

$$h(v; a, d) - (k+1) = (k+1)(v-1) - \frac{1}{d}g(v; a) \geq -(k+1) - \frac{1}{d}g(v; a).$$

We now choose $\delta > 0$ in such a way that the function $v \mapsto g(x; a)$ is strictly negative and decreasing on $(0, \delta)$. By choosing d small enough we can therefore achieve $h(\delta; a, d) - (k+1) > 0$. This shows that we can choose $y_0 = \delta$. The point y_1 can be found analogously. \square

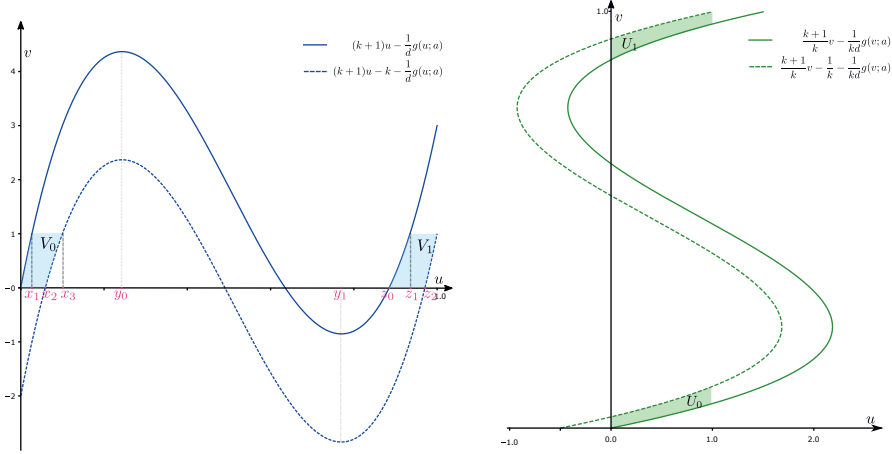


Figure 4.8: The sets $V_n, U_n, n = 0, 1$ for $k = 2, d = 0.014$ and the cubic nonlinearity $g(u; a) = u(1 - u)(u - a)$ with $a = 0.52$.

Lemma 4.8.3. *Assume that conditions (Hg) and (Hd) hold. Then there exist six points $(x_i)_{i=1}^3$ and $(z_i)_{i=0}^2$ that satisfy the identities*

$$\begin{aligned} h(x_1; a, d) &= 1, & h(x_2; a, d) &= k, & h(x_3; a, d) &= k + 1, \\ h(z_0; a, d) &= 0, & h(z_1; a, d) &= 1, & h(z_2; a, d) &= k, \end{aligned}$$

together with the identities

$$0 < x_1 < x_2 < x_3 < y_0 < a < y_1 < z_0 < z_1 < z_2 < 1.$$

Proof. The existence of x_1, x_2 and x_3 follow directly from assumption (Hd). In addition, we have $h(1; a, d) = k + 1$ and $h(y_1; a, d) < 0$. Again, the monotonicity assumption ensures that we can find points $z_0 < z_1 < z_2 < 1$ that satisfy the claim. \square

Proof of Lemma 4.8.2. We define the curves u_1 and u_2 by writing

$$\begin{aligned} u_1 &:= \left\{ (u, v) \in \mathbb{R}^2 : 0 \leq u \leq x_1, v = (k + 1)u - \frac{1}{d}g(u; a) \right\} \\ &= \phi^{-1}\{(0, \tilde{v}) : 0 \leq \tilde{v} \leq x_1\}, \\ u_2 &:= \left\{ (u, v) \in \mathbb{R}^2 : x_2 \leq u \leq x_3, v = (k + 1)u - k - \frac{1}{d}g(u; a) \right\} \\ &= \phi^{-1}\{(1, \tilde{v}) : x_2 \leq \tilde{v} \leq x_3\}. \end{aligned}$$

Using the definition of the points x_1, x_2 and x_3 , we see that the curve u_1 connects the points $(0, 0)$ and $(x_1, 1)$, while the curve u_2 connects the points $(x_2, 0)$ and $(x_3, 1)$. Due to the monotonicity of the mapping $u \mapsto (k + 1)u - \frac{1}{d}g(u; a)$ on $[0, y_0]$, both of these curves can be represented as graphs $u_1(v)$ and $u_2(v)$ for $v \in [0, 1]$. This proves that these are indeed vertical curves. We now define the set V_0 as the area lying between those two curves, and we set $U_0 := \phi(V_0)$.

It remains to show that U_0 is a horizontal strip. The horizontal boundaries of V_0 , characterized by $\{(u, 0) : 0 \leq u \leq x_2\}$ and $\{(u, 1) : x_1 \leq u \leq x_3\}$, respectively, are mapped by ϕ to the curves

$$\begin{aligned} v_1 &:= \left\{ \left(\frac{k+1}{k}u - \frac{g(u; a)}{kd}, u \right) : 0 \leq u \leq x_2 \right\}, \\ v_2 &:= \left\{ \left(\frac{k+1}{k}u - \frac{1}{k} - \frac{g(u; a)}{kd}, u \right) : x_1 \leq u \leq x_3 \right\}. \end{aligned}$$

The curve v_1 connects the point $(0, 0)$ with $(1, x_2)$ whereas the curve v_2 connects the point $(0, x_1)$ with $(1, x_3)$ and both of these curves are monotonically increasing, implying that they are horizontal strips.

Finally, the left vertical boundary u_1 of V_0 is by definition mapped to the set $\{(0, \tilde{v}) : 0 \leq \tilde{v} \leq x_1\}$, while the right vertical boundary u_2 of V_0 is mapped to the set $\{(1, \tilde{v}) : x_2 \leq \tilde{v} \leq x_3\}$. This shows that U_0 is indeed a horizontal strip, with V_0 and U_0 satisfying item (ii).

To construct the set V_1 , we define the curves u_3 and u_4 by writing

$$\begin{aligned} u_3 &:= \left\{ (u, v) \in \mathbb{R}^2 : z_0 \leq u \leq z_1, v = (k+1)u - \frac{1}{d}g(u; a) \right\} \\ &= \phi^{-1}\{(0, \tilde{v}) : z_0 \leq \tilde{v} \leq z_1\}, \\ u_4 &:= \left\{ (u, v) \in \mathbb{R}^2 : z_2 \leq u \leq 1, v = (k+1)u - k - \frac{1}{d}g(u; a) \right\} \\ &= \phi^{-1}\{(1, \tilde{v}) : z_2 \leq \tilde{v} \leq 1\}. \end{aligned}$$

Straightforward checks show that the curve u_3 connects the points $(z_0, 0)$ and $(z_1, 1)$, while the curve u_4 connects the points $(z_2, 0)$ and $(1, 1)$. The map

$$u \mapsto (k+1)u - \frac{1}{d}g(u; a)$$

is increasing on $[y_1, 1]$ so both of these curves can be represented as graphs $u_3(v)$ and $u_4(v)$ for $v \in [0, 1]$. We define the set V_1 as the area lying between these two curves and we set $U_1 := \phi(V_1)$.

The function ϕ maps the horizontal boundaries of V_1 , characterized by the sets

$$\{(u, 0) : z_0 \leq u \leq z_2\} \text{ and } \{(u, 1) : z_1 \leq u \leq 1\},$$

to the curves

$$\begin{aligned} v_3 &:= \left\{ \left(\frac{k+1}{k}u - \frac{g(u; a)}{kd}, u \right) : z_0 \leq u \leq z_2 \right\}, \\ v_4 &:= \left\{ \left(\frac{k+1}{k}u - \frac{1}{k} - \frac{g(u; a)}{kd}, u \right) : z_1 \leq u \leq 1 \right\}. \end{aligned}$$

The curve v_3 connects the point $(0, z_0)$ with $(1, z_2)$ and curve v_4 connects the point $(0, z_1)$ with $(1, 1)$. Both of these curves are monotonically increasing.

As before, the left boundary u_3 of V_1 is mapped to $\{(0, \tilde{v}) : z_0 \leq \tilde{v} \leq z_2\}$, while the right boundary u_4 of V_1 is mapped to the set $\{(1, \tilde{v}) : z_2 \leq \tilde{v} \leq 1\}$. This finally proves that U_1 is a horizontal strip, with V_1 and U_1 satisfying item (ii). \square

In our final result we give the explicit formula for the curve $d_0(a, k)$ for the standard cubic linearity (4.1.2).

Lemma 4.8.4. *Consider the setting of Proposition 4.2.4, let g be the standard cubic nonlinearity and define the function d_0 by (4.2.17). Then for any $0 < d < d_0(a, k)$ condition (Hd) holds.*

Proof. One can check that for $d > 0$ the quadratic inequalities

$$\begin{aligned} d(k+1)(v-1) - v(1-v)(v-a) &> 0, \\ d(k+1)v - v(1-v)(v-a) &< 0 \end{aligned}$$

have a solution in the set of real numbers if and only if $0 < d < d_0(a, k)$. \square

4.9 Numerics

In this final section we showcase some results of our numerical experiments.

Example 4.9.1. (Propagation direction) In order to validate our theoretical findings for the standard cubic nonlinearity (4.1.2), we numerically solved the MFDE (4.2.4) on a domain $[-L, L]$ for some large $L \gg 1$ with boundary conditions $\Phi(-L) = 0$, $\Phi(L) = 1$. For fixed $(a, d) \in \mathcal{H}$, we divided our domain into $N_L \gg 1$ segments. Upon writing $\Delta x = 2L/N_L$ we have N_L unknown variables - a speed c and $N_L - 1$ spatial points

$$(\Phi_1, \dots, \Phi_{N_L-1}),$$

where each point Φ_i approximates the value of $\Phi(-L + i\Delta x)$. It is important to note that N_L is chosen in such a manner that $1/\Delta x = I_0 \in \mathbb{N}$.

Moreover, we discretized the first derivatives in (4.2.4) by the fourth order central difference scheme. The complete discretization scheme then takes the form

$$\begin{aligned} 0 = - \frac{c(8\Phi_{i+1} - 8\Phi_{i-1} - \Phi_{i+2} + \Phi_{i-2})}{12\Delta x} \\ - d(k\Phi_{i+I_0} - (k+1)\Phi_i + \Phi_{i-I_0}) - g(\Phi_i; a) \end{aligned} \tag{4.9.1}$$

for $i = 1, \dots, N_L-1$, to which we also add the boundary conditions $\Phi_i = 0$ for all $i \leq 0$ and $\Phi_i = 1$ for all $i \geq L$. Adding the requirement

$$\Phi_{\lfloor N_L/2 \rfloor} - 1/2 = 0, \tag{4.9.2}$$

to compensate for the shift-invariance, we rewrite this problem in the compact form as

$$F(c, \Phi_1, \dots, \Phi_{N_L-2}, \Phi_{N_L-1}) = 0, \tag{4.9.3}$$

where the function $F : \mathbb{R}^{N_L} \rightarrow \mathbb{R}^{N_L}$ is derived from (4.9.1)-(4.9.2).

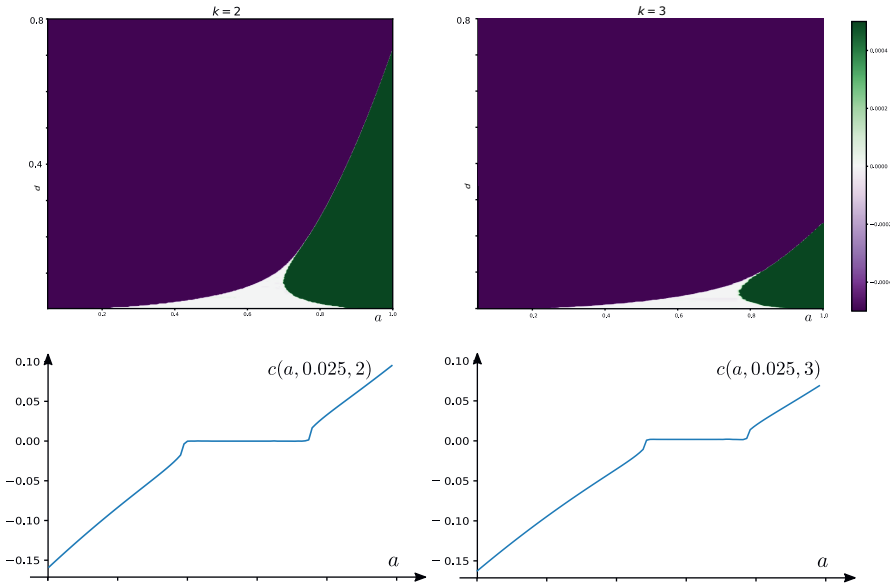


Figure 4.9: The images in the first row show a colormap of the numerical speed c obtained as a solution to the fixed point problem (4.9.3), for $k = 2$ (left) and $k = 3$ (right). The strong contrast between dark purple and white, and between white and dark green depict the steep jump between the values $|c| \gg 0$ and $|c| \approx 0$. In the second row we plot the mapping $a \mapsto c(a, 0.025, k)$ to visualize the pinning interval for $d = 0.025$.

To this fixed point scheme we applied a nonlinear fixed-point solver using the Python programming language. We present our results in Figure 4.9 using a colormap representation, i.e., to each value of the numerical speed c we assign a color from dark purple and dark green. The dark purple area represents the values $c < -0.004$ and in the dark green areas we have $c > 0.004$.

Since numerical computations never provide exact values, it is not straightforward to determine when the speed of the wave is exactly equal to 0. Nevertheless, as the value of a increases from 0 to 1, keeping d fixed, one can observe that at some $a = a_-$ a harsh jump occurs between the values $|c| \gg 0$, and $c \approx 0$. That is, the absolute value of the speed does not follow a smooth path but suddenly drops from values of the order 10^{-2} to values of the order 10^{-6} or even lower. Similarly, for some $a = a_+$ the numerical speed suddenly rises from the low-order values back to the smooth trajectory. In view of the fact that c is a smooth, monotonic function with respect to the detuning parameter a whenever $c \neq 0$, we simply set $c = 0$ in this region $[a_-, a_+]$. In Figure 4.9, the numerical pinning region is depicted in white. We observe that the ‘cone’ in which $c = 0$ becomes smaller as we increase k , which is in line with our theoretical results.

Example 4.9.2 (Manifold computations). In order to improve our understanding of the mechanism behind the evolution of standing waves that connect 0 and 1, we

study the equilibrium points $(0, 0)$ and $(1, 1)$ of the mapping (4.8.4). An eigenvalue analysis of matrices $D\phi(0, 0)$ and $D\phi(1, 1)$ shows that both equilibria are saddle-points. Consequently, we implemented the numerical methods developed in [41] to compute the unstable manifold

$$W^u(0, 0) = \{(u, v) \in \mathbb{R}^2 : (\phi^{-1})^n(u, v) \rightarrow (0, 0) \text{ as } n \rightarrow \infty\}$$

and the stable manifold $W^s(1, 1)$

$$W^s(1, 1) = \{(u, v) \in \mathbb{R}^2 : \phi^n(u, v) \rightarrow (1, 1) \text{ as } n \rightarrow \infty\}.$$

If these two manifolds intersect, there exists a standing wave solution to (4.8.1) that consists of the points (u_i, u_{i+1}) that lie in the intersection. As described in [47], these manifolds can intersect in a number of ways. If they intersect transversely, then the standing wave persists as we vary the parameter a , until we reach the boundary points a_- and a_+ at which the intersection is tangential, see Figure 4.10.

The main motivation for our numerical experiments is to investigate the pinning region from Figure 4.9. Namely, we are interested to see if the cone where $c = 0$ touches the $a = 1$ axis at one exactly point, or if there is a range of parameters d for which $c = 0$. The results in Figure 4.9.2 suggest that the cone in which $c = 0$ does not touch the vertical $a = 1$ axis at only point, but for an open range of parameters d .

Example 4.9.3 (Propagation reversal). In our final example we illustrate the diffusion driven propagation reversal on an example with nonconstant diffusion given by

$$d(t) = \begin{cases} .001 & t \leq 100, \\ .001 + \frac{1}{1500}(t - 100) & t > 100, \end{cases} \tag{4.9.4}$$

illustrated in the top left panel of Figure 4.12. We consider the bistable differential equation (4.1.1) on the binary tree \mathcal{T}_2

$$\begin{cases} \dot{u}_i(t) = d(t)(2u_{i+1}(t) - 3u_i(t) + u_{i-1}(t)) + g(u_i(t); .72), \\ u_i(0) = 0 \text{ if } i < 0, \\ u_i(0) = 1 \text{ if } i \geq 0, \end{cases} \tag{4.9.5}$$

with the standard cubic nonlinearity (4.1.2) with fixed $a = .72$. In particular, as we increase the diffusion parameter d we expect the wave Φ to go through four phases: pinning for small d , i.e., $c = 0$; spreading through the k -ary tree ($c > 0$); pinning again; and finally wave retreat, i.e., $c < 0$ for large d . Our expectations are numerically confirmed and we show our results in the bottom four panels of Figure 4.12. We note that the wave direction aligns with the results from the numerical investigations from Example 4.9.1.

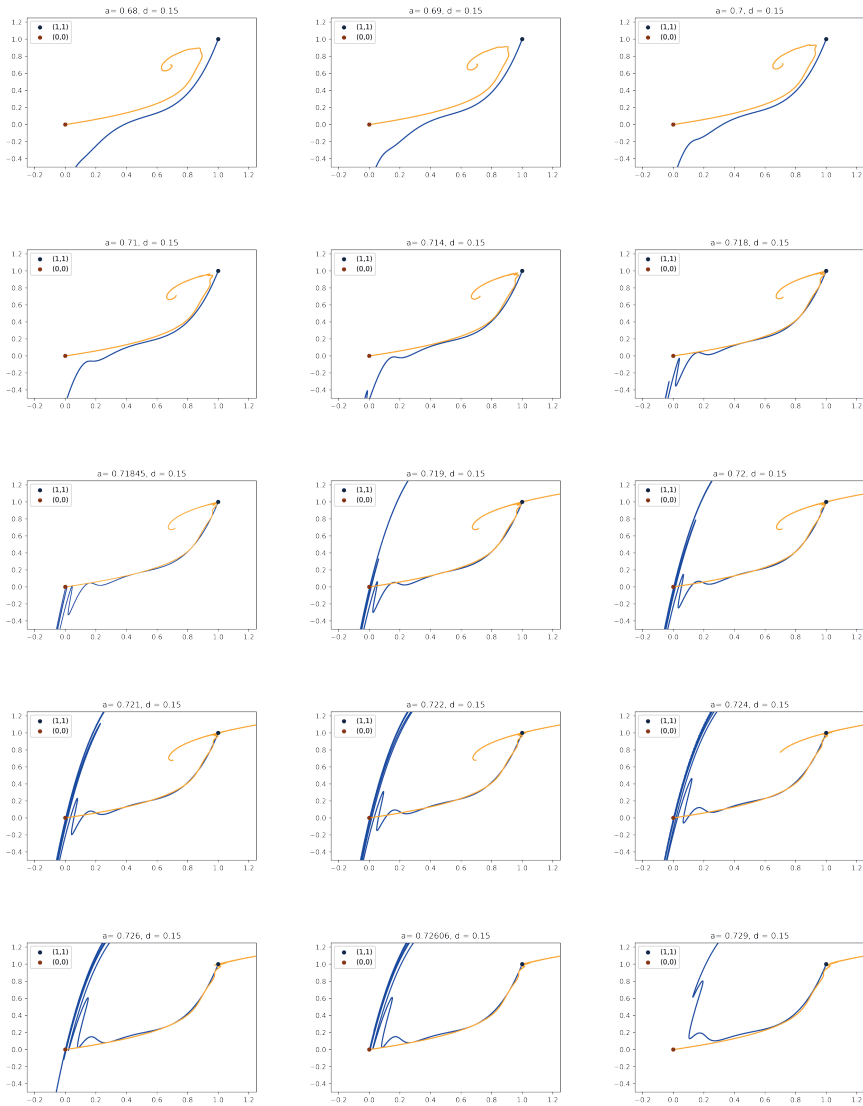


Figure 4.10: This series of images depicts the formation of standing waves for the standard cubic nonlinearity (4.7.1) with $k = 2$, $d = 0.15$ and several parameters $a \in (0.68, 0.729)$. We draw two manifolds - the stable manifold of $(1, 1)$ depicted in blue color, and the unstable manifold of $(0, 0)$ shown in orange. We observe that for $a \in (0.71845, 0.72606)$ these two manifolds intersect transversely. At the two boundary values the manifolds intersect tangentially.

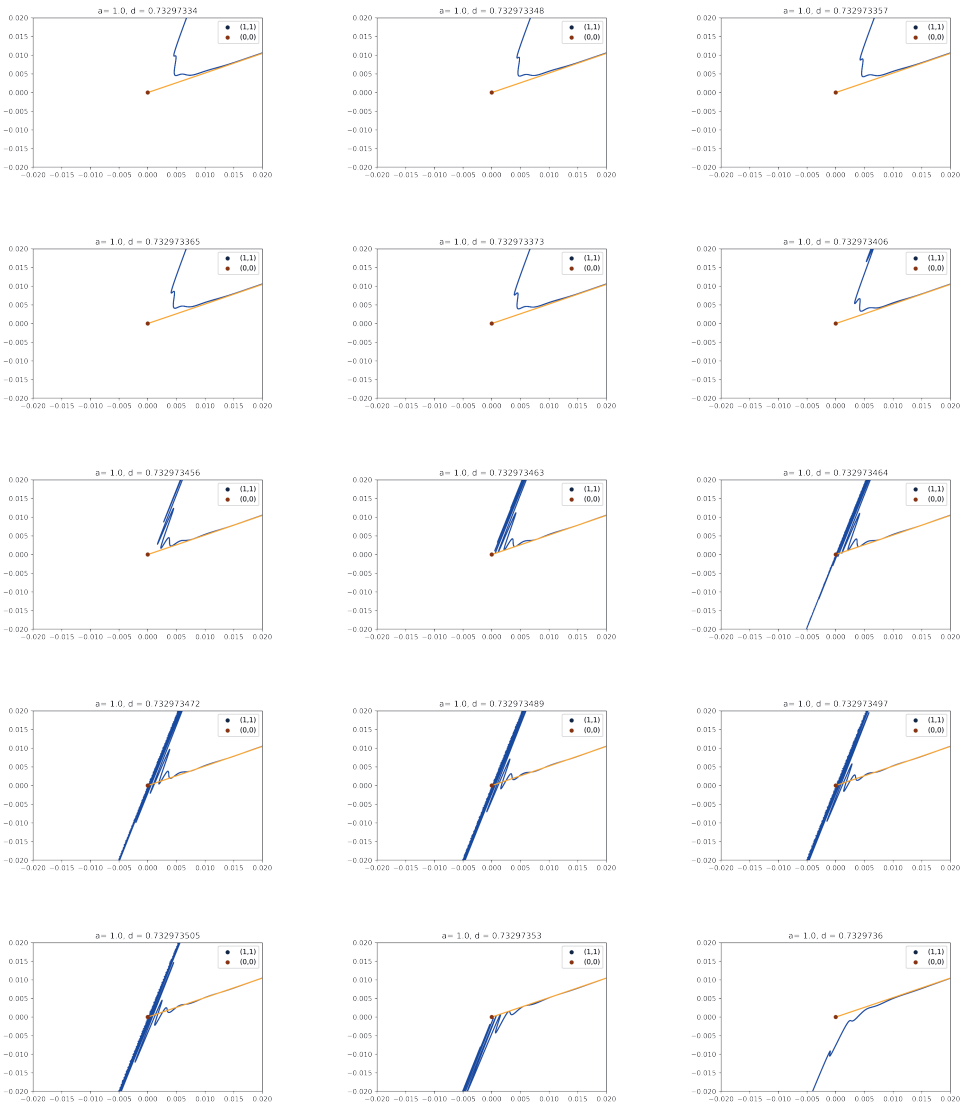


Figure 4.11: This series of images depicts the formation of standing waves for the standard cubic nonlinearity (4.7.1) with $k = 2$, $a = 1$. We provide a zoom of the two manifolds discussed in Figure 4.10 close to the point $(0, 0)$ and we vary the parameter d . The images suggest that we have standing waves for a nontrivial open range of parameters d as $a = 1$.

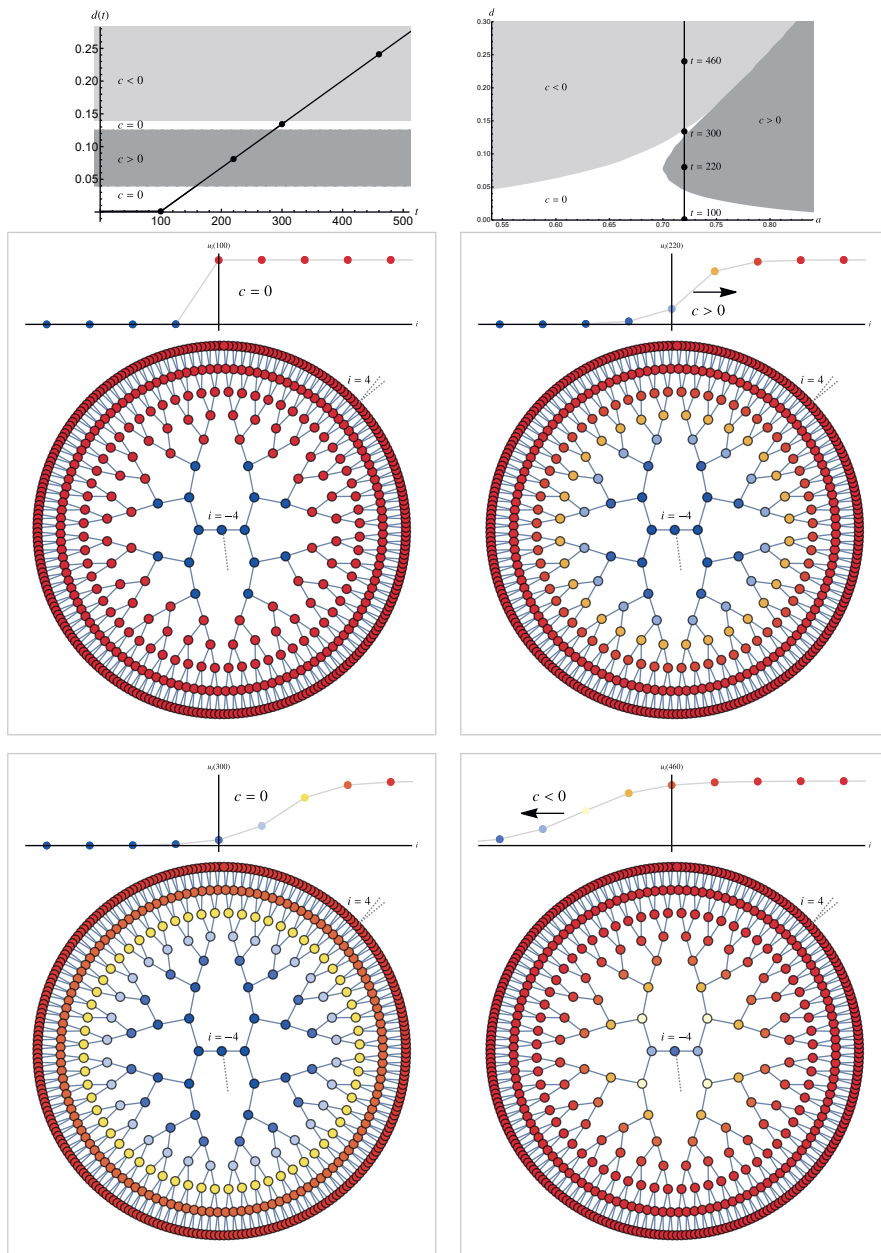


Figure 4.12: Illustration of the diffusion-driven propagation reversal discussed in Ex. 4.9.3. The top panels show the nonconstant time-dependent diffusion $d(t)$ given by (4.9.4) (left) and its trajectory through the (a, d) plane (right). The top panels in each frame below display the solutions $u_i(t)$ of (4.9.5) at $t = 100, 220, 300$ and 460 . The bottom panels in each frame depict the corresponding solutions of equation (4.1.4) on the binary tree \mathcal{T}_2 . Only layers with $i = -4, -3, \dots, 3, 4$ are visualised.

BIBLIOGRAPHY

- [1] Samuel M. Allen and John W. Cahn. A microscopic theory for antiphase boundary motion and its application to antiphase domain coarsening. *Acta Metallurgica*, 27(6):1085 – 1095, 1979.
- [2] Donald E Amos. Computation of modified bessel functions and their ratios. *Mathematics of Computation*, 28(125):239–251, 1974.
- [3] Alex Arenas, Albert Díaz-Guilera, and Roger Guimera. Communication in networks with hierarchical branching. *Physical review letters*, 86(14):3196, 2001.
- [4] D. G. Aronson and Hans F. Weinberger. Nonlinear diffusion in population genetics, combustion, and nerve pulse propagation. 1975.
- [5] Donald G Aronson and Hans F Weinberger. Multidimensional nonlinear diffusion arising in population genetics. *Advances in Mathematics*, 30(1):33–76, 1978.
- [6] Markus Bär, Martin Falcke, Herbert Levine, and Lev S Tsimring. Discrete stochastic modeling of calcium channel dynamics. *Physical Review Letters*, 84(24):5664, 2000.
- [7] IV Barashenkov, OF Oxtoby, and Dmitry E Pelinovsky. Translationally invariant discrete kinks from one-dimensional maps. *Physical Review E*, 72(3):035602, 2005.
- [8] Peter W. Bates, Xinfu Chen, and Adam J. J. Chmaj. Traveling waves of bistable dynamics on a lattice. *SIAM J. Math. Anal.*, 35(2):520–546, 2003.
- [9] Peter W Bates and Adam Chmaj. A discrete convolution model for phase transitions. *Archive for Rational Mechanics and Analysis*, 150(4):281–368, 1999.
- [10] M. Beck, B. Sandstede, and K. Zumbrun. Nonlinear stability of time-periodic viscous shocks. *Archive for rational mechanics and analysis*, 196(3):1011–1076, 2010.
- [11] Jonathan Bell. Some threshold results for models of myelinated nerves. *Mathematical Biosciences*, 54(3-4):181–190, 1981.

- [12] Jonathan Bell and Chris Cosner. Threshold behavior and propagation for non-linear differential-difference systems motivated by modeling myelinated axons. *Quarterly of Applied Mathematics*, 42(1):1–14, 1984.
- [13] Henri Berestycki and François Hamel. Generalized travelling waves for reaction-diffusion equations. *Contemporary Mathematics*, 446:101–124, 2007.
- [14] Henri Berestycki, Hiroshi Matano, and François Hamel. Bistable traveling waves around an obstacle. *Communications on Pure and Applied Mathematics: A Journal Issued by the Courant Institute of Mathematical Sciences*, 62(6):729–788, 2009.
- [15] John W Cahn. Theory of crystal growth and interface motion in crystalline materials. *Acta metallurgica*, 8(8):554–562, 1960.
- [16] John W. Cahn, John Mallet-Paret, and Erik S. Van Vleck. Traveling wave solutions for systems of ODEs on a two-dimensional spatial lattice. *SIAM J. Appl. Math.*, 59(2):455–493, 1999.
- [17] A Carpio, LL Bonilla, and G Dell’Acqua. Motion of wave fronts in semiconductor superlattices. *Physical Review E*, 64(3):036204, 2001.
- [18] Raphaël Cerf. *The Wulff Crystal in Ising and Percolation Models: Ecole D’Eté de Probabilités de Saint-Flour XXXIV-2004*. Springer, 2006.
- [19] Seok-Ho Chang, Pamela C Cosman, and Laurence B Milstein. Chernoff-type bounds for the gaussian error function. *IEEE Transactions on Communications*, 59(11):2939–2944, 2011.
- [20] X. Chen, J. S. Guo, and C. C. Wu. Traveling Waves in Discrete Periodic Media for Bistable Dynamics. *Arch. Ration. Mech. Anal.*, 189:189–236, 2008.
- [21] Marco Chiani and Davide Dardari. Improved exponential bounds and approximation for the q-function with application to average error probability computation. In *Global Telecommunications Conference, 2002. GLOBECOM’02. IEEE*, volume 2, pages 1399–1402. IEEE, 2002.
- [22] S-N Chow and John Mallet-Paret. Pattern formation and spatial chaos in lattice dynamical systems. i. *IEEE Transactions on Circuits and Systems I: Fundamental Theory and Applications*, 42(10):746–751, 1995.
- [23] Shui-Nee Chow, John Mallet-Paret, and Wenxian Shen. Traveling waves in lattice dynamical systems. *J. Differential Equations*, 149(2):248–291, 1998.
- [24] Shui-Nee Chow, John Mallet-Paret, and Erik S Van Vleck. Dynamics of lattice differential equations. *International Journal of Bifurcation and Chaos*, 6(09):1605–1621, 1996.
- [25] H. Cook, D. D. Fontaine, and J. E. Hilliard. A model for diffusion on cubic lattices and its application to the early stages of ordering. *Acta Metallurgica*, 17:765–773, 1969.

- [26] Keenan Crane. Discrete differential geometry: An applied introduction. *Notices of the AMS, Communication*, pages 1153–1159, 2018.
- [27] Klaus Deckelnick, Gerhard Dziuk, and Charles M Elliott. Computation of geometric partial differential equations and mean curvature flow. *Acta numerica*, 14:139–232, 2005.
- [28] Persi Diaconis and Laurent Saloff-Coste. Convolution powers of complex functions on. *Mathematische Nachrichten*, 287(10):1106–1130, 2014.
- [29] Weiwei Ding and Thomas Giletti. Admissible speeds in spatially periodic bistable reaction-diffusion equations. *arXiv preprint arXiv:2006.05118*, 2020.
- [30] S. V. Dmitriev, P. G. Kevrekidis, and N. Yoshikawa. Discrete Klein–Gordon Models with Static Kinks Free of the Peierls–Nabarro Potential. *J. Phys. A.*, 38:7617–7627, 2005.
- [31] A. Erdős, P.; Rényi. On random graphs i. *Publ. Math. Debrecen*, 6:290–297, 1959.
- [32] Paul C Fife. Long time behavior of solutions of bistable nonlinear diffusion equations. *Archive for Rational Mechanics and Analysis*, 70(1):31–36, 1979.
- [33] Paul C Fife. *Mathematical aspects of reacting and diffusing systems*, volume 28. Springer Science & Business Media, 2013.
- [34] Paul C Fife and J Bryce McLeod. The approach of solutions of nonlinear diffusion equations to travelling front solutions. *Archive for Rational Mechanics and Analysis*, 65(4):335–361, 1977.
- [35] Ronald Aylmer Fisher. The wave of advance of advantageous genes. *Annals of eugenics*, 7(4):355–369, 1937.
- [36] Thierry Gallay, Emmanuel Risler, et al. A variational proof of global stability for bistable travelling waves. *Differential and integral equations*, 20(8):901–926, 2007.
- [37] G.N.Watson. *A Treatise On The Theory of Bessel Functions*. Merchant Books, 1922.
- [38] Jong-Shenq Guo and François Hamel. Front propagation for discrete periodic monostable equations. *Mathematische Annalen*, 335(3):489–525, 2006.
- [39] D. Hankerson and B. Zinner. Wavefronts for a cooperative tridiagonal system of differential equations. *Journal of Dynamics and Differential Equations*, 5(2):359–373, Apr 1993.
- [40] Mariana Haragus and Arnd Scheel. Almost Planar Waves in Anisotropic Media. *Communications in Partial Differential Equations*, 31(5):791–815, 2006.
- [41] Dana Hobson. An efficient method for computing invariant manifolds of planar maps. *Journal of Computational Physics*, 104(1):14–22, 1993.

- [42] Aaron Hoffman and Matt Holzer. Invasion fronts on graphs: The fisher-kpp equation on homogeneous trees and erdős-rényi graphs. *Discrete & Continuous Dynamical Systems - B*, 24(2):671–694, 2019.
- [43] Aaron Hoffman, H Hupkes, and E Van Vleck. Multi-dimensional stability of waves travelling through rectangular lattices in rational directions. *Transactions of the American Mathematical Society*, 367(12):8757–8808, 2015.
- [44] Aaron Hoffman, Hermen Hupkes, and E Van Vleck. *Entire solutions for bistable lattice differential equations with obstacles*, volume 250. American Mathematical Society, 2017.
- [45] Aaron Hoffman and John Mallet-Paret. Universality of crystallographic pinning. *J. Dynam. Differential Equations*, 22(2):79–119, 2010.
- [46] Aaron Hoffman and John Mallet-Paret. Universality of crystallographic pinning. *Journal of Dynamics and Differential Equations*, 22(2):79–119, 2010.
- [47] H Hupkes, D Pelinovsky, and Björn Sandstede. Propagation failure in the discrete nagumo equation. *Proceedings of the American Mathematical Society*, 139(10):3537–3551, 2011.
- [48] H. J. Hupkes and B. Sandstede. Stability of pulse solutions for the discrete FitzHugh-Nagumo system. *Trans. Amer. Math. Soc.*, 365(1):251–301, 2013.
- [49] Hermen Jan Hupkes and Leonardo Morelli. Travelling corners for spatially discrete reaction-diffusion system. *Communications on Pure and Applied Analysis*, 2019.
- [50] Hermen Jan Hupkes, Leonardo Morelli, Willem M Schouten-Straatman, and Erik S Van Vleck. Traveling waves and pattern formation for spatially discrete bistable reaction-diffusion equations. In *International Conference on Difference Equations and Applications*, pages 55–112. Springer, 2018.
- [51] Christopher KRT Jones. Spherically symmetric solutions of a reaction-diffusion equation. *Journal of Differential Equations*, 49(1):142–169, 1983.
- [52] Mia Jukić and Hermen Jan Hupkes. Dynamics of curved travelling fronts for the discrete allen-cahn equation on a two-dimensional lattice. *Discrete & Continuous Dynamical Systems-A*, 2019.
- [53] Mia Jukic and Hermen Jan Hupkes. Curvature-driven front propagation through planar lattices in oblique directions. *Communications on Pure & Applied Analysis*, 2022.
- [54] Todd Kapitula. Multidimensional stability of planar travelling waves. *Transactions of the American Mathematical Society*, 349(1):257–269, 1997.
- [55] James P Keener. Propagation and its failure in coupled systems of discrete excitable cells. *SIAM Journal on Applied Mathematics*, 47(3):556–572, 1987.

- [56] James P Keener. The effects of discrete gap junction coupling on propagation in myocardium. *Journal of theoretical biology*, 148(1):49–82, 1991.
- [57] James P Keener and James Sneyd. *Mathematical physiology*, volume 1. Springer, 1998.
- [58] Timothy H Keitt, Mark A Lewis, and Robert D Holt. Allee effects, invasion pinning, and species' borders. *The American Naturalist*, 157(2):203–216, 2001.
- [59] William Ogilvy Kermack and Anderson G McKendrick. A contribution to the mathematical theory of epidemics. *Proceedings of the royal society of london. Series A, Containing papers of a mathematical and physical character*, 115(772):700–721, 1927.
- [60] Panayotis G Kevrekidis. Non-linear waves in lattices: past, present, future. *IMA Journal of Applied Mathematics*, 76(3):389–423, 2011.
- [61] Hiroshi Kori and Alexander S. Mikhailov. Strong effects of network architecture in the entrainment of coupled oscillator systems. *Physical Review E*, 74(6):066115, dec 2006.
- [62] Nikos E. Kouvaris, Hiroshi Kori, and Alexander S. Mikhailov. Traveling and pinned fronts in bistable reaction-diffusion systems on networks. *PLoS ONE*, 7(9):e45029, sep 2012.
- [63] C. D. Levermore and J. X. Xin. Multidimensional Stability of Travelling Waves in a Bistable Reaction-Diffusion Equation, II. *Comm. PDE*, 17:1901–1924, 1992.
- [64] Simon A Levin. Population dynamic models in heterogeneous environments. *Annual review of ecology and systematics*, 7(1):287–310, 1976.
- [65] J. Mallet-Paret. *Crystallographic Pinning: Direction Dependent Pinning in Lattice Differential Equations*. Citeseer, 2001.
- [66] John Mallet-Paret. The fredholm alternative for functional differential equations of mixed type. *Journal of Dynamics and Differential Equations*, 11(1):1–47, Jan 1999.
- [67] John Mallet-Paret. The global structure of traveling waves in spatially discrete dynamical systems. *Journal of Dynamics and Differential Equations*, 11(1):49–127, 1999.
- [68] Hiroshi Matano, Yoichiro Mori, and Mitsunori Nara. Asymptotic behavior of spreading fronts in the anisotropic allen–cahn equation on rn. In *Annales de l'Institut Henri Poincaré C, Analyse non linéaire*, volume 36, pages 585–626. Elsevier, 2019.
- [69] Hiroshi Matano and Mitsunori Nara. Large time behavior of disturbed planar fronts in the allen–cahn equation. *Journal of Differential Equations*, 251(12):3522–3557, 2011.

- [70] Roeland MH Merks, Yves Van de Peer, Dirk Inzé, and Gerrit TS Beemster. Canalization without flux sensors: a traveling-wave hypothesis. *Trends in plant science*, 12(9):384–390, 2007.
- [71] Jurgen Moser. *Stable and random motions in dynamical systems*. Princeton university press, 2016.
- [72] J. Nagumo, S. Arimoto, and S. Yoshizawa. An active pulse transmission line simulating nerve axon. *Proceedings of the IRE*, 50(10):2061–2070, 1962.
- [73] Edward Neuman. Inequalities involving modified bessel functions of the first kind. *Journal of mathematical analysis and applications*, 171(2):532–536, 1992.
- [74] Stanley Osher and Barry Merriman. The wulff shape as the asymptotic limit of a growing crystalline interface. *Asian Journal of Mathematics*, 1(3):560–571, 1997.
- [75] B. V. Pal'tsev. Two-sided bounds uniform in the real argument and the index for modified bessel functions. *Mathematical Notes*, 65(5):571–581, May 1999.
- [76] W.-X. Qin and X. Xiao. Homoclinic Orbits and Localized Solutions in Nonlinear Schrödinger Lattices. *Nonlinearity*, 20:2305–2317, 2007.
- [77] Evan Randles and Laurent Saloff-Coste. On the convolution powers of complex functions on \mathbb{Z} . *Journal of Fourier Analysis and Applications*, 21(4):754–798, 2015.
- [78] Emmanuel Risler. Global convergence toward traveling fronts in nonlinear parabolic systems with a gradient structure. In *Annales de l'Institut Henri Poincaré (C) Non Linear Analysis*, volume 25, pages 381–424. Elsevier, 2008.
- [79] Violaine Roussier. Stability of radially symmetric travelling waves in reaction–diffusion equations. In *Annales de l'Institut Henri Poincaré (C) Non Linear Analysis*, volume 21, pages 341–379. Elsevier, 2004.
- [80] J. F. F. Mendes S. N. Dorogovtsev. *Evolution of Networks: From Biological Nets to the Internet and WWW*. OXFORD UNIV PR, January 2014.
- [81] DH Sattinger. Weighted norms for the stability of traveling waves. *Journal of Differential Equations*, 25(1):130–144, 1977.
- [82] W. M. Schouten-Straatman and H. J. Hupkes. Nonlinear Stability of Pulse Solutions for the Discrete Fitzhugh-Nagumo equation with Infinite-Range Interactions. *Discrete and Continuous Dynamical Systems A*, 39(9), 2019.
- [83] Fanni Sélley, Ádám Besenyei, Istvan Z. Kiss, and Péter L. Simon. Dynamic control of modern, network-based epidemic models. *SIAM J. Appl. Dyn. Syst.*, 14(1):168–187, 2015.
- [84] Antonín Slavík. Lotka-Volterra competition model on graphs. *SIAM J. Appl. Dyn. Syst.*, 19(2):725–762, 2020.

- [85] R. P. Soni. On an inequality for modified bessel functions. *Journal of Mathematics and Physics*, 44(1-4):406–407, 1965.
- [86] P. Stehlík. Exponential number of stationary solutions for Nagumo equations on graphs. *J. Math. Anal. Appl.*, 455(2):1749–1764, 2017.
- [87] Gui-Quan Sun. Mathematical modeling of population dynamics with allee effect. *Nonlinear Dynamics*, 85(1):1–12, Jul 2016.
- [88] Caz M Taylor and Alan Hastings. Allee effects in biological invasions. *Ecology Letters*, 8(8):895–908, 2005.
- [89] Kōhei Uchiyama. Asymptotic behavior of solutions of reaction-diffusion equations with varying drift coefficients. *Archive for Rational Mechanics and Analysis*, 90(4):291–311, 1985.
- [90] Remco Van Der Hofstad. *Random Graphs and Complex Networks: Volume 1*, volume 43. Cambridge university press, 2016.
- [91] B. van Hal. Travelling Waves in Discrete Spatial Domains. *Bachelor Thesis*, 2017.
- [92] Pierre-François Verhulst. Notice sur la loi que la population suit dans son accroissement. *Corresp. Math. Phys.*, 10:113–126, 1838.
- [93] G Wul. Achen on the question of the speed of growth and dissolution of the crystal. *Z. Crystallogr.*, 34:449–530, 1901.
- [94] J. X. Xin. Multidimensional Stability of Travelling Waves in a Bistable Reaction-Diffusion Equation, I. *Comm. PDE*, 17:1889–1900, 1992.
- [95] Huihui Zeng. Stability of planar travelling waves for bistable reaction–diffusion equations in multiple dimensions. *Applicable Analysis*, 93(3):653–664, 2014.
- [96] Bertram Zinner. Stability of traveling wavefronts for the discrete nagumo equation. *SIAM journal on mathematical analysis*, 22(4):1016–1020, 1991.
- [97] Bertram Zinner. Existence of traveling wavefront solutions for the discrete nagumo equation. *Journal of differential equations*, 96(1):1–27, 1992.

SAMENVATTING

In dit proefschrift bestuderen we bistabiele reactie-diffusievergelijkingen op multidimensionale roosterdomeinen, zoals k -voudige bomen en \mathbb{Z}^2 . De kracht van reactie-diffusievergelijkingen is dat ze met hun intuïtieve en relatief eenvoudige vorm met succes verschillende natuurlijke en sociale fenomenen kunnen modelleren. Een van de belangrijkste kenmerken van reactie-diffusievergelijkingen is dat ze speciale oplossingen toelaten, zogenaamde ‘lopende golven’, die we kunnen omschrijven als vaste profielen $\Phi : \mathbb{R} \rightarrow \mathbb{R}$ welke zich in een bepaalde richting bewegen met een vaste snelheid c . Afhankelijk van hun vorm kunnen we golven grofweg in drie categorieën verdelen:

- pulsen of solitonen, die kunnen worden omschreven als lokale verstoringen
- periodieke pulsen (golftreinen)
- golffronten die twee constante toestanden verbinden

In dit proefschrift richten we ons op het laatste type golf en bestuderen we hun existentie, propagatie en lange-termijn gedrag op twee soorten discrete domeinen - het twee- dimensionaal rooster \mathbb{Z}^2 en oneindige bomen.

Hoofdstuk 1 bevat een overzicht van het proefschrift. In het overzicht gaan we onder meer in op verschillen tussen lopende golven op continue domeinen en op roosterdomeinen. Specifieke aandacht besteden we verder aan het fenomeen van ‘pinning’, ook wel ‘propagation failure’ genoemd.

In Hoofdstuk 2 beschouwen we de bistabiele reactie-diffusievergelijking op het rooster \mathbb{Z}^2 . Deze vergelijking wordt ook vaak *de Allen-Cahn vergelijking* genoemd. Onze basisaanname is dat de begintoestand u^0 een verstoring is van de golf Φ die zich in horizontale richting beweegt. In het eerste deel van dit werk nemen we niet aan dat u^0 een gelokaliseerde of ‘kleine’ verstoring van de golf is, maar dat het alleen voldoet aan de zwakkere voorwaarde (C1) geformuleerd in (1.7.6). Deze aanname is al voldoende om te garanderen dat er een eendimensionale differentiaalvergelijking bestaat die het gedrag van het *nulniveau-oppervlak* $\gamma(t)$ van onze oplossing $u(t)$ regelt. We noemen deze differentiaalvergelijking een *discrete mean curvature flow* met een driftterm. Met behulp van de Cole-Hopf-transformatie zijn we in staat om deze vergelijking om te zetten in de discrete warmtevergelijking op \mathbb{Z} om aan te tonen

dat het nulniveau-oppervlak $\gamma(t)$ na verloop van tijd gladder wordt en dat het langetermijn gedrag van onze oplossing wordt bepaald door de lopende golf $\Phi(\cdot - \gamma(t))$. In het tweede deel van dit hoofdstuk laten we zien dat $\gamma(t)$ convergeert naar $ct + \mu$, voor zekere $\mu \in \mathbb{R}$, wat de orbitale stabiliteit van de horizontale lopende golf aantoont.

Hoofdstuk 3 is een generalisatie van ons werk van hoofdstuk 2 naar rationale richtingen op \mathbb{Z}^2 , d.w.z. we nemen nu aan dat u^0 een verstoring is van de golf die in een bepaalde richting $(\sigma_h, \sigma_v) \in \mathbb{Z}^2$ beweegt. De setting is vergelijkbaar met dat in hoofdstuk 2. Echter, vanwege het feit dat onze golf niet meer parallel is aan het rooster, komen we meer technische problemen tegen. Een van deze problemen is dat de heersende vergelijking voor het nulniveau-oppervlak $\gamma(t)$ niet via de Cole-Hopf-transformatie transformeert naar de discrete warmtevergelijking, maar naar een lineaire rooster-vergelijking die zowel negatieve als asymmetrische coëfficiënten heeft. We behandelen deze vergelijking en zijn vervalschattingen in detail in §3.5.

In Hoofdstuk 4 verlaten we het tweedimensionale rooster om golfvoortplanting en het gebrek daaraan te bestuderen op oneindige k -voudige bomen. Om het bestaan van het pinning-gebied dat chaotische oplossingen omvat aan te tonen, gebruiken we de stelling van Moser uit het veld van de symbolische dynamiek. Aan de andere kant zijn we ook geïnteresseerd in welke parameterregimes de bewegende golven zich terugtrekken ($c < 0$) of juist verspreiden ($c > 0$). Daarom passen we het vergelijkingsprincipe toe met twee soorten suboplossingen: steile, stapvormige profielen die de golven dichter bij het pinninggebied benaderen, en brede profielen die laten zien dat voor $d \gg 0$ de golf zich altijd terugtrekt, ongeacht de waarde van de bistabiele parameter a .

ACKNOWLEDGEMENTS

Dear Hermen Jan, it has been a privilege to have you as a supervisor. I have always admired you as a mathematician and as a mentor as you never stay out of ideas on how to proceed with projects. Your door has always been open for me, and I could always share my problems and achievements with you. Thank you for encouraging me to attend conferences and present our results, even when I was very early in my career. This trust you placed in me helped me considerably to gain confidence in my skills. Also, I am very grateful that you let me explore my interests, and that I had your support to work on the side-projects that I found important, such as attending Math Meets Industry workshops or volunteering for the EWM. Thank you for being a wonderful, considerate mentor and a guide to me.

I would also like to express my gratitude to the members of the dissertation committee for accepting the invitation and their time in reading and evaluating my thesis.

I am especially thankful to everyone in the Analysis group for welcoming me into the community. I enjoyed our seminars, discussions and conferences that we attended together. In particular, I would like to thank my promotor Arjen Doelman for his continuous support and guidance. Dear Vivi, thank you for encouraging me to attend Math Meets Industry meetings and for your friendly and helpful advice whenever I needed it. Dear Martina, you have been very supportive of me and my career and I always enjoyed listening to your lectures and talks. Dear Frits, thank you for helping me to organize our internal seminars by suggesting exciting and diverse speakers.

I am also very grateful to my collaborators Petr Stehlík and Vladimír Švígler for initiating our project on k -ary trees. Our discussions have been very valuable for me and I learned a lot during our collaboration.

For me, the MI has been more than a workplace. It has been a source of joy, numerous discussions, a place where I met so many wonderful and enthusiastic people that helped me on my journey to completing this thesis.

Dear Liza, you have been with me since the beginning of my journey. We shared so many happy moments in our offices, and I always knew that I can confide in you. I have always admired your persistence, humour and indomitable spirit. You are a true friend to me.

Dear Amine, Benthén, Daoyi, Lasse and Vera, thank you for your company in the last years, and especially during the corona lockdown. Because of you, the MI has been a happy and safe place for me, even if online and at 1.5 m distance. To

paraphrase J.K. Rowling: “There are some things you can’t share without ending up liking each other, and living through the pandemic is one of them.”

Dear Rosa, Vera, Margriet and Bart, I enjoyed organizing the PhD Colloquium with you. I am very grateful that we managed to frequently organize these meetings during the pandemic.

To my EWM family, thank you for embracing me into your team. Dear Carina, thank you for your guidance and trust with the projects within the EWM. I must especially extend my gratitude to Prof. Dr. Maria G. Westdickenberg and Prof. Dr. Rebecca Waldecker for their constant enthusiasm and kind words which encouraged me so much during the corona pandemics.

Dear Sanne and Mar, I learned so much from you during the organization of our PhD event. I sincerely hope we will organize many future workshops together.

To my Dutch study group - Marleen, Divya and Thomas, it has been a pleasure to learn Dutch from you and with you. Beste Marleen, bedankt voor al je goede zorgen, vooral tijdens de corona-lockdown. Bedankt voor alle bijeenkomsten die je hebt georganiseerd en voor het verbeteren van mijn Nederlands. Ik hoop dat we nog veel samen gaan wandelen naar het Polderpark.

To my friends in Croatia - Ivana, Helena, Monika, Matko, Matea and Toni, thank you for not forgetting me when I moved to the Netherlands. Thank you for staying in touch, for meeting with me when I am in Zagreb and for your visits to the Netherlands.

To my godparents Lidija and Vlado, thank you for taking care of me ever since my childhood. You held me in your arms during my baptism, and never let me down since.

Mom, you have always been my greatest supporter. When I moved abroad, you understood my reasons and supported me the whole time, always encouraging me and giving me the strength to go on. I never had a feeling that we are 1000 km apart, but that we are closer than ever before. All of my achievements belong to you too.

Mikola, you are woven into every word of this thesis. You celebrated my every lemma, and patiently helped me to prepare for all of my talks. Because of you I am a better mathematician and a better person in every way possible, and I can not thank you enough for that. I am immensely grateful that our PhD journeys intertwined and that some invisible string brought us both to Trieste where we met on the way to the Galileo Guesthouse. I am looking forward to the life we will build together!

CURRICULUM VITAE

Mia Jukić was born in Zagreb, Croatia, on April 24, 1993. From 2007 to 2011 she attended the gymnasium programme at Vladimir Prelog Science School. Afterwards she enrolled in the Bachelor's Mathematics programme at the Faculty of Science in Zagreb, which she completed in 2014. In the same year, she started a master's degree in Applied Mathematics, which she finished in September 2016 *summa cum laude*. In the summer of 2016, Mia participated in the Guest Student Programme at the Jülich Supercomputing Centre (JSC), Germany. There she worked on the project *Gray-Scott simulations with SDC and DUNE* under the supervision of Dr. Robert Speck.

In February 2018, she moved to Leiden, the Netherlands, to work as a PhD researcher in the Analysis and Dynamical Systems group under the supervision of Dr. Hermen Jan Hupkes. Mia has been an active member of the mathematical community throughout these four years. She organised the *NDNS+ PhD Days* in 2019, as well as the workshop *A PhD, is that for me?* in February 2022. Since the summer of 2020, Mia has volunteered for the European Women in Mathematics (EWM) organization as their website and social media content editor.

Mia's thesis *Travelling waves on trees and square lattices* comprises results from three research projects, two about travelling waves on two-dimensional lattices and one on wave-propagation on k -ary trees. Mia regularly presented her research at various workshops, conferences, and seminars in the Netherlands, Germany, Spain, and the USA. In July 2019, she won the Best Poster Award at the *Equadiff Conference* for her poster *Curved Traveling Fronts on a Lattice*.

